Distribution Category:
Physics—General
(UC-34)

ANL-81-79

ANL--81-79

DE82 021147

ARGONNE NATIONAL LABORATORY
9700 South Cass Avenue
Argonne, Illinois 60439

PHYSICS DIVISION ANNUAL REVIEW

1 APRIL 1980—31 MARCH 1981

John P. Schiffer
Division Director

June 1982

Preceding Annual Reviews

ANL-78-66	1977—1978
ANL-79-40	1978—1979
ANL-80-94	1979—1980

FOREWORD

The Physics Division Annual Review presents a broad but necessarily incomplete view of the research activity within the Division for the year ending March 1981. The reproduction of this document was delayed by one year.

At the back of this report a complete list of publications along with the Divisional roster can be found.

TABLE OF CONTENTS

	Page
NUCLEAR PHYSICS RESEARCH	1
INTRODUCTION	1
I. MEDIUM-ENERGY PHYSICS	3
INTRODUCTION	3
A. STUDY OF PION REACTION MECHANISMS	5
a. Pion Absorption Mechanism on Nuclei	5
b. Comparison of Pion and Photon Induced Reactions on ^{12}C	6
c. Inclusive Inelastic Pion Measurements	6
d. Study of the Pion Absorption Mechanism Through the $A(\pi,p)X$ Reaction at T_π = 500 MeV	8
e. The Isospin Dependence of Pion Absorption on a Pair of Nucleons	8
f. Inclusive π^+ Scattering from ^4He	9
g. Survey of Inclusive Pion Scattering Near the Δ_{33} Resonance	9
h. Large Acceptance Spectrometer (LAS)	12
i. Fermi-Gas Model for π-Nucleus Inclusive Scattering	13
B. HIGH-RESOLUTION STUDIES AND NUCLEAR STRUCTURE	14
a. Scattering of Pions by Complex Nuclei	14
b. Determination of Neutron Radii from Pion Scattering	15
c. Excitation of High-Spin Particle-Hole States in ^{28}Si	15
d. Inelastic Pion Scattering from ^{10}B and ^{11}B	16
e. Inelastic Pion Scattering from ^{14}N	16
f. Excitation of High-Spin Particle-Hole States in ^{54}Fe and ^{58}Ni	18
g. Discrete States from Pion Double-Charge-Exchange on Heavy Nuclei	19
h. Study of the $^4He(\pi^-,\pi^+)$ Reaction at Small Angles	19
C. TWO-NUCLEON PHYSICS WITH PIONS AND ELECTRONS	20
a. Deuteron Polarimeter Development	20

		Page
	b. Measurement of the Angular Distribution of Tensor Polarization in π-d Elastic Scattering	20
	c. Tensor Polarization in Electron-Deuteron Elastic Scattering	23
II.	HEAVY-ION RESEARCH AT THE TANDEM AND SUPERCONDUCTING LINAC ACCELERATOR	25
	INTRODUCTION	25
	A. RESONANT STRUCTURE IN HEAVY-ION REACTIONS	27
	a. Resonance Strength to States at High Excitation Energy in ^{28}Si Populated Via the $^{24}Mg(^{16}O,^{12}C)^{28}Si^*$ Reaction	27
	b. Resonant Behavior in the 0° Excitation Function of $^{24}Mg(^{16}O,^{12}C)^{28}Si$ at Linac Energies	27
	c. Measurement of Back-Angle Cross Sections in ^{16}O Induced Alpha Transfer on ^{24}Mg	30
	B. FUSION CROSS SECTIONS	32
	a. Fusion of $^{16}O + ^{24,26}Mg$ at Linac Energies	32
	b. Distribution of Evaporation Residue Strength in the Fusion of $^{18}O + ^{24}Mg$ and $^{16}O + ^{26}Mg$	33
	c. Search for Structure in the Fusion Excitation Function of $^{16}O + ^{24}Mg$	34
	d. The Fusion of $^{24}Mg + ^{24}Mg$	35
	e. Measurement of Compound Nucleus K x-Ray Production Cross Sections for $^{37}Cl + ^{124}Sn$ and $^{32}S + ^{116,120,124}Sn$	37
	C. HIGH ANGULAR MOMENTUM STATES IN NUCLEI	39
	a. High-Spin Yrast Levels of $^{148,149,150,151,152}Dy$	39
	b. Yrast Levels in ^{154}Dy	41
	c. Search for a Very High Spin Isomer in ^{152}Er	42
	d. Study of Continuum γ-Ray Spectra of $^{151,152}Dy$	43
	e. Systematics of Continuum States in Dy and Er Nuclei	45
	f. Lifetimes of Continuum States	46
	g. The $(\pi h_{11/2})^3$ Spectrum in the Three Valence Proton Nucleus $^{149}_{67}Ho_{82}$	47
	h. Yrast Spectroscopy of the N=83 Nucleus ^{150}Ho	49
	D. REACTION MECHANISMS AND DISTRIBUTIONS OF REACTION STRENGTHS	52
	a. Single-Nucleon Transfer Reactions Induced on ^{48}Ca by ^{12}C Beams at $E_{lab}(^{12}C)$ = 45 MeV	52

		Page
	b. Energy Dependence of Inelastic Scattering and Transfer Reactions of ^{16}O on ^{48}Ca	53
	c. Excitation Functions of Heavy-Ion Induced Fusion-Fission with ^{58}Ni Beams	53
	d. Fragmentation of ^{18}O Projectiles at 141 MeV	55
	e. Mechanism of Heavy-Ion Reactions at 7.5 to 20 MeV/amu: Singles and Coincidence Measurements of Light and Projectile-like Ejectiles	57
	f. A Possible New Technique for the Measurement of Quadrupole Moments of Short-lived Excited States	58
E.	EQUIPMENT DEVELOPMENT	62
	a. Installation of Beam Lines in the Linac Experimental Area	62
	b. 65-in. Scattering Chamber in New Target Area	62
	c. The Split-Pole Magnetic Spectrograph in the Linac Experimental Area	63
	d. A Position-Sensitive, Large Ionization-Chamber Heavy-Ion Gas Detector	64
	e. Measurement of Fusion Cross Sections in Heavy Systems with an Electrostatic Deflector	64
	f. γ-Ray Facility	66
	g. Nuclear Target Making and Development	67
III.	CHARGED-PARTICLE RESEARCH	69
	INTRODUCTION	69
A.	CHARGED-PARTICLE RESEARCH AT THE DYNAMITRON	70
1.	WEAK INTERACTIONS	70
	a. Parity Violation in the 5.1-MeV J=2 Doublet of ^{10}B	70
	b. Beta Spectrum Measurements	73
	c. Search for Parity Violation in ^{6}Li	75
	d. Test of the Isobaric Multiplet Mass Equation from β-Delayed Proton Decay of ^{24}Si	76
2.	REACTIONS USING LIGHT NUCLEI	76
	a. Nuclear Reactions of Light Ions with ^{6}Li at Low Energies	76
	b. The $^{7}Li(d,p)^{8}Li$ and $^{7}Be(p,\gamma)^{8}B$ Reactions	77
	c. $^{3}He(\alpha,\gamma)^{7}Be$	79
	d. Calculations of the Solar Neutrino Flux	79

	Page
e. Search for Superheavy Hydrogen	80
3. NEAR FUTURE RESEARCH AT THE DYNAMITRON	81
B. CHARGED-PARTICLE RESEARCH AT THE TANDEM ACCELERATOR	83
1. $f_{7/2}$ NUCLEI	83
The Gamma Decay of States in ^{47}Cr	83
2. STUDY OF RADIOACTIVE NUCLEI	84
a. Decay of ^{72m}Br	84
b. Mass and Low-Lying Levels of ^{106}In	85
c. Helium-Jet Recoil Transfer System	85
d. On-Line Laser Spectroscopy at the Argonne Superconducting Linac	86
3. ACCELERATOR MASS SPECTROMETRY	90
a. The Half-Life of ^{32}Si	90
b. The Measurement of Nuclear Cross Sections	92
c. On the Detection of ^{7}Be	93
d. Accelerator Mass Spectrometry of ^{59}Ni and Fe Isotopes at the Superconducting Linac	95
e. An Overview on Long-lived Radioisotopes	100
4. NEAR FUTURE RESEARCH AT THE TANDEM ACCELERATOR	103
IV. NEUTRON AND PHOTONUCLEAR PHYSICS	105
INTRODUCTION	105
A. NEUTRON RESEARCH	106
Measurement of the Electric Dipole Moment of the Neutron	106
B. PHOTONUCLEAR PHYSICS	108
a. Photodisintegration of the Deuteron	108
b. Doorway Resonances in ^{29}Si	110
c. Isospin Splitting of the Giant Dipole Resonance in ^{60}Ni	110
d. Photon Scattering by the Giant-Dipole Resonance in Vibrational Nuclei	112
V. THEORETICAL PHYSICS	113
INTRODUCTION	113
A. HEAVY-ION DIRECT-REACTION THEORY	114
A Program for Coupled-Channels Calculations of Heavy-Ion Inelastic Scattering	114

		Page
B.	NUCLEAR SHELL THEORY AND NUCLEAR STRUCTURE	116
	a. Pion Excitation of States of Non-normal Parity by Inelastic Scattering	116
	b. Parity Mixing in ^{10}B	118
	c. Theory of the Nuclear Shell Model	118
	d. Nuclear Structure Studies of ^{149}Ho and ^{150}Ho	118
	e. Expected $(h_{11/2})^n$ States in the Nuclei $^{150}_{68}Er_{82}$, $^{151}_{69}Tm_{82}$, and $^{152}_{70}Yb_{82}$	119
	f. 10^- States in ^{90}Zr	119
	g. $^{18}O(t,p)^{20}O$ Reaction	120
	h. Study of Pion Double-Charge-Exchange (π^+,π^-) Reactions from Oxygen Isotopes	120
	i. Test of Interacting Boson Model by Pion Scattering	121
C.	NUCLEAR MATTER AND NUCLEAR FORCES	122
	a. Nuclear Matter Calculations with the Paris Potential	122
	b. Nuclear Matter Saturation in the Presence of π and Δ	123
	c. Comparison of Brueckner-Bethe and Variational Results	123
	d. Method for Solving Three-Body Equations	124
	e. Isobar Degrees of Freedom and Three-Body Forces in Nuclear Matter and Light Nuclei	124
	f. Problems in the Use of Quark-Quark Potential Models for Nuclear Physics	125
	g. Baryon Magnetic Moments in the Quark Model	126
	h. Meson Clouds of Extended Sources	
	i. Correlated-Basis Perturbation Theory for the Ground-State Energy of Liquid ^3He	127
D.	INTERMEDIATE-ENERGY PHYSICS	128
	a. Phenomenological Hamiltonian for Pions, Nucleons and Δ Isobars	128
	b. DWIA Studies of Pion-Nucleus Inelastic Scattering	129
	c. Effective Interactions Derived from Relativistic Quantum Field Tbeories	129
E.	MICROSCOPIC CALCULATIONS OF HIGH-ENERGY COLLISIONS OF HEAVY IONS	130
	a. Classical-Equations-of-Motion Calculations of High-Energy Heavy-Ion Collisions	130
	b. Classical-Equations-of-Motion Calculations of Multiplicities for High-Energy Collisions of $^{20}Ne + ^{20}Ne$	130

		Page
	c. Improvements and Extensions of the CEOM Calculations	131
	d. Theory of High-Energy Heavy-Ion Collisions	131
F.	LIGHT ION DIRECT REACTIONS	133
	Coupled Channels Variational Method for Nuclear Rearrangement Reactions	133
G.	OTHER THEORETICAL PHYSICS	135
	Aharonov-Bohm Effect	135
VI.	THE SUPERCONDUCTING LINAC	137
	INTRODUCTION	137
A.	HEAVY-ION ENERGY BOOSTER	138
	1. MAIN FEATURES OF THE DESIGN	138
	2. STATUS OF THE BOOSTER	139
	3. NEAR-TERM PLANS	141
B.	INVESTIGATIONS OF SUPERCONDUCTING LINAC TECHNOLOGY	142
	1. RECENT ACCOMPLISHMENTS	142
	a. Accelerating Fields of Resonators	142
	b. Slow-Tuner Controller	144
	c. Fast Tuner	146
	d. Beam-Energy Measurement	146
	e. Superconducting Analyzing Magnet	147
	2. NEAR-TERM PLANS	148
C.	PROPOSAL FOR ATLAS	149
VII.	ACCELERATOR OPERATIONS	151
	INTRODUCTION	151
A.	OPERATION OF THE TANDEM-LINAC ACCELERATOR	152
	1. RECENT OPERATING EXPERIENCE FOR THE TANDEM	152
	2. OPERATION OF THE SUPERCONDUCTING LINAC	154
	3. UPGRADING THE TANDEM	156
	a. An International Study of Stripping Foils	156
	b. Development of the Terminal	157
	c. Ion Sources	157
	4. INSTALLATION AND IMPROVEMENT OF THE BOOSTER	159
	a. Linac Section A	159

	Page
b. Linac Section B	159
c. 300-Watt Refrigerator	159
d. Rebuncher/Debuncher	159
e. Energy-Measurement System	159
5. NEAR-TERM PLANS	160
a. Accelerator Operation	160
b. Booster Improvements	160
c. Tandem Improvements	160
d. Ion Sources	160
6. OUTSIDE USERS OF THE TANDEM-LINAC ACCELERATOR	161
7. OUTSIDE USERS OF THE TANDEM ALONE	162
B. OPERATION OF THE DYNAMITRON FACILITY	165
1. OPERATIONAL EXPERIENCE	165
2. UPGRADING OF THE DYNAMITRON	168
3. UNIVERSITY USE OF THE DYNAMITRON	168
VIII. GeV ELECTRON MICROTRON	171
INTRODUCTION	171
a. Microtron Model Magnet Studies	172
b. Plans for 1982	172
ATOMIC AND MOLECULAR PHYSICS RESEARCH	175
INTRODUCTION	175
IX. DISSOCIATION AND OTHER INTERACTIONS OF ENERGETIC MOLECULAR IONS IN SOLID AND GASEOUS TARGETS	177
INTRODUCTION	177
a. Molecular-Ion Structure Determinations	178
b. UV-Laser-Induced Photofragmentation	179
c. Electron-Capture Phenomena	181
d. Computer Simulations	181
e. Equipment Development	181
f. Stopping Power Measurements with Molecular Ions	182

		Page
X.	BEAM-FOIL RESEARCH AND COLLISION DYNAMICS OF HEAVY IONS	183
	INTRODUCTION	183
	a. Significance of Time-Reversal Symmetry for Time-Resolved Measurements of Hydrogenic and Other Atomic Observables	184
	b. Coherent Excitation of Hydrogen by a Thin Carbon Foil	184
	c. Molecular Effects on Lyman-α Emission in Beam-Foil Spectroscopy	184
	d. Molecular Effects in Beam-Foil Collision-Induced Alignment of He I	185
	e. Energy Dependence of Alignment in Foil-Collision-Excited n=3 States of He I	185
	f. Orientation and Alignment Parameters of Beam-Foil-Excited He I	186
	g. Quantum-Beat Studies of the ^{3}He Hyperfine Structure	186
	h. Lamb Shift and Fine Structure of n = 2 in Helium-like Chlorine, Sulfur, and Silicon	188
	i. Radiation from the Negative Lithium Ion	189
	j. Charge Changing Cross Sections of Xe^{n+} on Xe^{n+} (n = 1, 8)	189
	k. Position Sensitive Detector for UV Spectroscopy	190
XI.	PHOTOIONIZATION-PHOTOELECTRON RESEARCH	191
	INTRODUCTION	191
	a. Photoionization of Open-Shell Atoms	193
	b. Determination of Molecular Ion Structures by Photoelectron Spectroscopy	193
	c. Dissociation of Molecular Ions with UV Lasers	196
XII.	HIGH-RESOLUTION, LASER-RF SPECTROSCOPY WITH ATOMIC AND MOLECULAR BEAMS	199
	INTRODUCTION	199
	a. High-Precision Laser-rf Double-Resonance Spectroscopy of the $^2\Sigma$ Ground State of CaF	199
	b. Precise Determination of the v and N Dependence of the Spin-Rotation and Hyperfine Interactions in the CaF $X^2\Sigma_{1/2}$ Ground State	200
	c. Radio-Frequency Optical Double-Resonance Spectroscopy of SrF: The $X^2\Sigma$ State	200

		Page
	d. Hyperfine and Spin-Rotational Structure of CaBr $X^2\Sigma$ (v = 0) by Molecular-Beam Laser-rf Double Resonance	202
	e. Determination of Dipole and Quadrupole hfs in the Excited $B^2\Sigma$ State of $Ca^{79}Br$ and $Ca^{81}Br$	205
	f. Double Resonance, Fluorescence Spectroscopy and hfs in Pr I	205
XIII.	MÖSSBAUER EFFECT RESEARCH	207
	INTRODUCTION	207
	a. Advances in the Theory of Quantum Beats of Recoil-Free Gamma Radiation	207
	b. Improvements in the Techniques of Frequency Modulation	207
XIV.	THEORETICAL ATOMIC PHYSICS	209
	INTRODUCTION	209
	a. Radiation from the Negative Lithium Ion	210
	b. Autoionization Resonances in Atomic Tellurium	210
	c. Spin Polarization of Photoelectrons	211
	d. Beutler-Fano Resonances	211
	e. Spectroscopy of Few-Electron Ions	211
	APPLIED PHYSICS	213
INTRODUCTION		213
XV.	INTERACTION OF ENERGETIC PARTICLES WITH SOLIDS	215
	INTRODUCTION	215
	1. EXPERIMENTAL AND CALCULATED DEPTH DISTRIBUTIONS OF DAMAGE AND PROJECTED RANGES OF 20-keV ^4He IONS IN NICKEL	216
	2. SEARCH FOR MICROSTRUCTURAL INFLUENCES ON THE SPUTTERING OF ANNEALED ALUMINUM AND SINTERED ALUMINUM POWDER (SAP 895) UNDER D^+ AND $^4He^+$ BOMBARDMENT: YIELDS, ANGULAR DISTRIBUTIONS	222
	3. SURFACE EFFECTS INDUCED BY SIMULATED PLASMAS	228
	a. Two-Laminar and Three-Laminar Clad Materials for Fusion Applications	228

Page

b. Sputtering of TiB_2 Coatings under D^+ and $^4He^+$ Ion Bombardment: Total Yields 234

PUBLICATIONS FROM 1 APRIL 1980 THROUGH 31 MARCH 1981 239

STAFF MEMBERS OF THE PHYSICS DIVISION 263

NUCLEAR PHYSICS RESEARCH

INTRODUCTION

The Physics Division's program in nuclear physics covers a broad span of activities within that discipline. The object of this research is to understand the properties of atomic nuclei, their structure, the mechanisms of nuclear reactions, and manifestations of fundamental symmetries in nuclei. Work is carried out under a variety of subprograms: theory, heavy-ion physics, medium-energy physics and nuclear research. These categories do not represent a sharp separation between people—individual scientists often work in several different areas. This flexibility allows scientific problems to be addressed with a variety of techniques, and it avoids limiting individual scientists' activities to a particular subdiscipline.

The Physics Division operates a superconducting linac booster injected by a tandem accelerator, and a 4-MV Dynamitron. The linac is used almost entirely for nuclear research by Argonne staff and university users. Less than 25% of the Dynamitron is used for nuclear research. A small program in photonuclear research is carried out at the Chemistry Division's electron linac, and occasionally elsewhere. The medium-energy program is centered at the Los Alamos Meson Physics Facility.

Highlights

In medium-energy physics the analysis of inclusive pion inelastic scattering experiments from the LAS spectrometer has progressed and a new experiment to study pion absorption on ^{3}He and ^{4}He was carried out. The results indicate a very low cross section for pion absorption on an ($S = 0$, $T = 1$) nuclear pair. A design study was undertaken for the most cost effective option for a GeV electron accelerator and the microtron was chosen as optimal.

In heavy-ion physics the ATLAS project was in the President's Budget for funding beginning in FY 1982. This will bring the superconducting linac booster into a full-fledged accelerator providing heavy-ion beams up to 25 MeV/amu over much of the periodic table. Meanwhile the linac booster prototype is operating with increasing reliability and is used in a variety of experiments. Studies of resonance-like structures in $^{24}Mg + ^{16}O$, of fusion cross sections, developing a new technique of x-ray measurements, and of high-spin states on the edge of detectability constitute some of the scientific highlights. Much of the effort has gone into developing, constructing and testing apparatus associated with the linac facility and with these to explore the parameter space opened up by the linac.

In charged-particle research several experiments are underway in a program to study fundamental features of the weak interaction in nuclei, and the technique of accelerator detection has been extended to ^{26}Al, possibly ^{7}Be, and, with the linac, ^{59}Ni.

I. MEDIUM-ENERGY PHYSICS

INTRODUCTION

Medium-energy physics is primarily directed toward an understanding of the fundamental interactions which occur in nuclear matter. Since the pion is the basic quantum of the nuclear force, a clear picture of its propagation in nuclei contributes to our understanding of the underlying nature of nuclear forces. Pion interactions with both few-nucleon systems and complex nuclei provide a means for probing fundamental processes in increasingly complex environments. A comprehensive and precise experimental description of pion interactions with nuclei is a major objective of the ANL effort in medium-energy physics. Pion studies are carried out as part of a broad ranging nuclear program, which we expect to provide new insights into nuclear structure and nuclear processes mediated by pions. Studies of electron scattering at medium energies provide a complementary perspective into nuclear properties. At the present time most of the experimental activity is concentrated on measurements using the various pion beams of the Los Alamos Meson Physics Facility, although an experiment involving electron scattering is now planned at the MIT/Bates accelerator.
Recent trends in the ANL medium-energy program reflect an increasing interest in medium-energy physics research with electron beams. The subject has been widely discussed and there is an articulated national need for a high-energy, high-duty-factor electron accelerator to pursue electromagnetic studies of the nucleus. An ANL study group has explored the possibility of building such a facility at Argonne. They have concluded that a double-sided microtron is the most promising and cost effective option for achieving continuous beam operation of a 2-GeV high-intensity electron accelerator. One of the major technical questions is whether microtron sector magnets of the requisite stability and precision are attainable in a 1—2-GeV accelerator. To resolve this question we are carrying out a prototype study of the basic sector magnet for a 2-GeV double-sided microtron.

Accomplishments of the medium-energy program of the past year include the successful completion and utilization of a new facility at LAMPF, the Large Acceptance Spectrometer (LAS) and approval of a proposal for measurement of tensor polarization of the deuteron in e-d scattering.

A major area of study continues to be the competition between various reaction mechanisms involved in pion propagation through nuclear matter. These studies primarily focus upon "inclusive" spectra of particles that result from pion absorption or inelastic scattering. This program is greatly facilitated by the large solid angle and dynamic range of LAS which is necessary for coincidence experiments. These studies have shown that true absorption is a very energy-dependent fraction of the total reaction cross section on ^{4}He.

The high-resolution studies of elastic and inelastic pion scattering using the EPICS system are primarily directed toward understanding the relationship between pion-nuclear interactions and nuclear structure.

Elastic scattering provides information on the average pion-nucleus information and density distributions, while inelastic scattering may be considered in terms of the microscopic aspects of nuclear structure and pion-nuclear interactions. High-resolution spectroscopy at high-excitation energies appears to be a particularly sensitive tool for investigating nuclear structure in the continuum.

A prerequisite for understanding pion interactions in complex nuclei is a knowledge of the behavior of few-nucleon systems and their interaction with pions. Measurements of deuteron polarization, from both pion and electron scattering, provide a unique method for testing various models that attempt to describe the fundamental interactions. During the past year, the pioneering measurements of deuteron tensor polarization in π-d scattering were extended to provide the first measurements of the polarization angular distribution.

A. STUDY OF PION REACTION MECHANISMS

Our understanding of pion propagation in complex nuclei is still very incomplete even though such knowledge is crucial to a description of nuclei. The details of the competition between inelastic scattering and pion absorption are of importance, as are the processes involved in the absorption mechanisms. It has now been determined that more than two nucleons are generally involved in pion absorption so that the quasi-deuteron model can account for only half the absorption cross section on ^{4}He. A comparison of pion- and photon-induced reactions on ^{12}C suggests that the critical distance for pion absorption is comparable to the dimensions of ^{12}C, much longer than usually anticipated. Through the use of inclusive pion scattering from ^{4}He, the energy dependence of the partition of reaction cross section between absorption and quasi-free scattering has been achieved. Studies on heavier nuclei reveal that, in addition to quasi-free scattering, higher order processes and Pauli blocking are significant. Further tests of reaction models and the coupling between reaction mechanisms are required.

a. Pion Absorption Mechanism on Nuclei

H. E. Jackson, R. D. McKeown, M. Paul,* R. P. Redwine,† S. J. Sanders, J. P. Schiffer, R. E. Segel,‡ J. R. Specht, and E. J. Stephenson§

The analysis of inclusive proton spectra has been completed from LAMPF experiment 350: 100, 160, and 220 MeV π^+ and π^- on nuclear targets (^{4}He, ^{6}Li, ^{9}Be, ^{12}C, ^{27}Al, Ni, ^{181}Ta), measured over the angular range $30° \leq \theta \leq 150°$. The results on ^{4}He show that the clean two-nucleon pion absorption mechanism ($\pi + 2N \rightarrow 2N$) can account for only about half the absorption cross section. On heavier targets the shift of the spectra in proton energy with scattering angle has been analyzed in terms of the average number of nucleons that participate in absorbing the pion's momentum and total energy. The effective number of interacting nucleons for both π^+ and π^- incident, was found to be $\sim$3 for ^{12}C and increasing to $\sim$5.5 for ^{181}Ta. These effective numbers of nucleons are also consistent with the ratio of proton yields from π^+ and π^- induced reactions. The latter analysis was published[1] and the more complete data submitted to Physical Review C for publication.

---

*Hebrew University of Jerusalem, Jerusalem, Israel.

†Massachusetts Institute of Technology, Cambridge, Massachusetts.

‡Northwestern University, Evanston, Illinois.

§Indiana University, Bloomington, Indiana.

[1] R. D. McKeown et al., Phys. Rev. Lett. 44, 1033 (1980).

b. Comparison of Pion and Photon Induced Reactions on ^{12}C

R. D. McKeown, J. P. Schiffer, H. E. Jackson, M. Paul,* S. J. Sanders, J. R. Specht, E. J. Stephenson,† R. P. Redwine,‡ R. E. Segel,§ J. Arends,‖ J. Eyink,‖ H. Hartmann,‖ A. Hegerath,‖ B. Mecking,‖ G. Noldeke,‖ and H. Rost‖

The proton spectra from pions incident on ^{12}C, obtained from LAMPF experiment 350 were found to be very similar in shape to photon-induced proton spectra, with the energy of the photon equal to the total pion energy. A comparison of proton- and photon-induced proton spectra is presented in Fig. I-1. The photon-induced spectra were measured at the University of Bonn's electron synchrotron facility. The dependence of the shapes of the proton spectra on angle is also very similar for the two reactions. It seems that the protons observed arise from a common reaction mechanism (Δ production) for the two projectiles. The absolute cross sections for producing protons with pions or with photons are in the ratio of 55 ± 10, while the ratio of the total inelastic pion yield to the total photo-pion yield is 70 ± 20. Since pions form a Δ near the surface of the nucleus while photons produce Δ's uniformly throughout the nuclear volume, the near equality of the two ratios suggests that the critical distance for pion absorption is comparable to or greater than the dimensions of ^{12}C. A photon experiment on a heavier nucleus would be very interesting. These conclusions were reported in a communication to Physical Review Letters.[1]

c. Inclusive Inelastic Pion Measurements

R. D. McKeown, S. J. Sanders, J. P. Schiffer, H. E. Jackson, M. Paul,* J. R. Specht, E. J. Stephenson,† R. P. Redwine,‡ and R. E. Segel§

As a part of experiment 350, total pion yields were obtained, without pion energy measurement, for incident pion energies of 100, 160, 220 MeV, and a range of targets. The contribution of elastic scattering is negligible for angles $\theta \geq 90°$. The measured inelastic yields show an A dependence of

*Hebrew University of Jerusalem, Jerusalem, Israel.

†Indiana University, Bloomington, Indiana.

‡Massachusetts Institute of Technology, Cambridge, Massachusetts.

§Northwestern University, Evanston, Illinois.

‖University of Bonn, Bonn, West Germany.

[1] R. D. McKeown et al., Phys. Rev. Lett. 45, 2015 (1980).

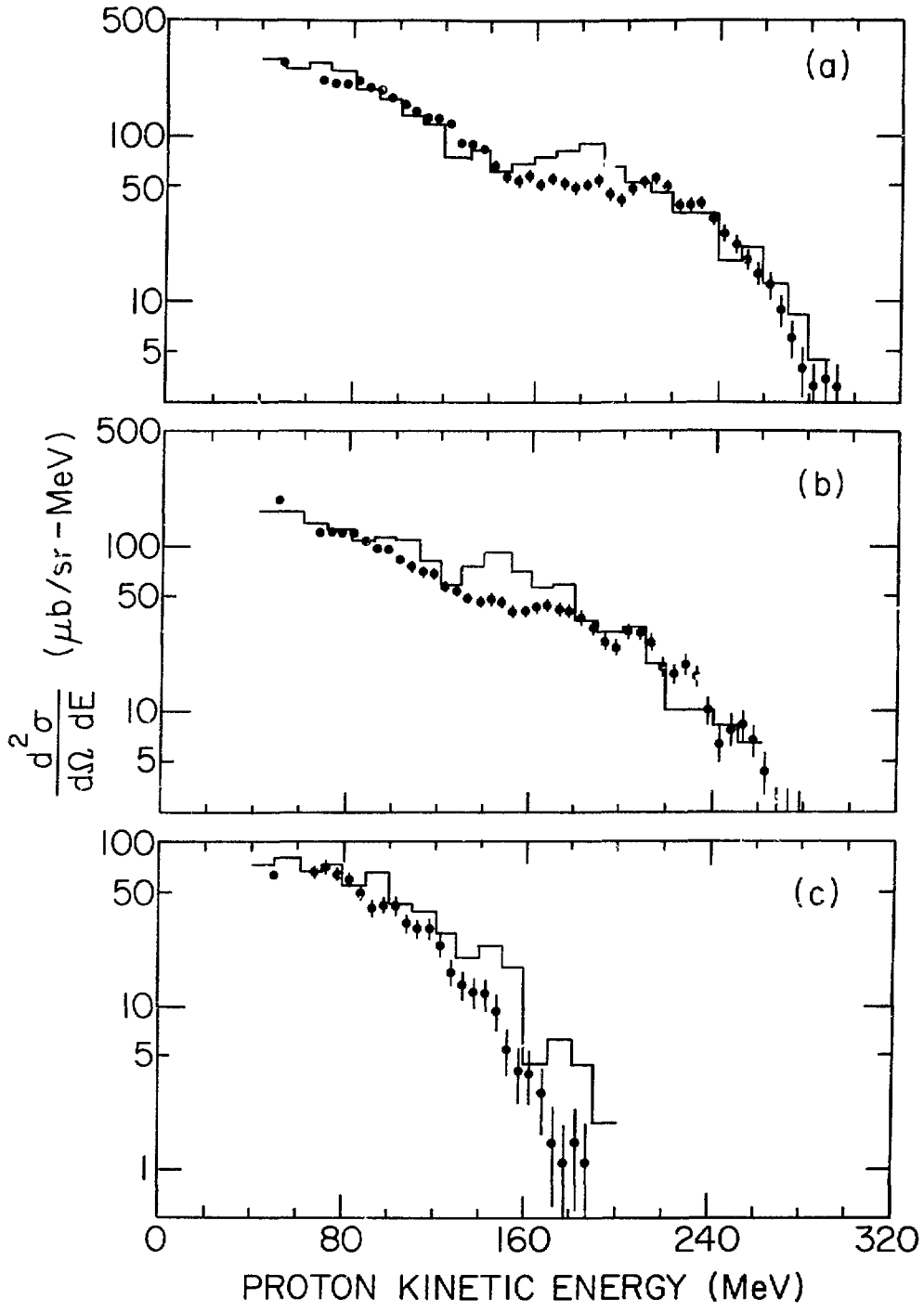

Fig. I-1. The proton-energy spectra from 220-MeV incident π^+ and π^- on ^{12}C have been averaged and plotted as solid points. The proton spectra from $^{12}C(\gamma,p)$ at E_γ = 343 MeV have been multiplied by 55 and plotted as histograms. The three plots correspond to three different laboratory angles: (a) $\theta(\pi,p) = 45°$, $\theta(\gamma,p) = 49°$; (b) $\theta(\pi,p) = 60°$, $\theta(\gamma,p) = 73°$; (c) $\theta(\pi,p) = 120°$, $\theta(\gamma,p) = 125°$.

$A^{0.47\pm0.03}$, not including ^{4}He whose inelastic yield is below this smooth dependence. The Coulomb corrected π^+/π^- ratios do not exhibit a significant deviation from unity, even for ^{181}Ta with a large neutron excess; the exception is ^{9}Be, where this ratio dips by ∿25%—apparently as a consequence of the loosely-bound valence neutron. The results have been submitted for publication in Physical Review C.

d. Study of the Pion Absorption Mechanism Through the A(π,p)X Reaction at T_π = 500 MeV

K. Stephenson, D. Ashery, R. J. Holt, H. E. Jackson, J. P. Schiffer, J. R. Specht, R. D. McKeown,* J. Ungar,* R. E. Segel,† and P. Zupranski†

We have measured inclusive proton spectra with 500-MeV π^+ on targets of ^{3}He, ^{4}He, ^{12}C, Al, Ni, and Ta at six scattering angles. These spectra are similar to data taken earlier in the Δ-resonance region in the sense that the relative angular distributions are consistent with a pion absorption mechanism which gives a multinucleon final state. If one assumes that the pion is not scattered before it is absorbed, then the data suggest the rescattering of the protons as they emerge from the nucleus is much larger than had been previously thought. Further analysis of the data is in progress and may help clarify this question.

e. The Isospin Dependence of Pion Absorption on a Pair of Nucleons

D. Ashery, R. J. Holt, H. E. Jackson, J. P. Schiffer, J. R. Specht, K. E. Stephenson, R. D. McKeown,* J. Ungar,* R. E. Segel,† and P. Zupranski†

The reactions ^{4,3}He(π^+,2p) and ^{4,3}He(π^-,pn) were studied at bombarding energy of 165 MeV. Outgoing protons were detected with a large acceptance spectrometer and the coincident protons or neutrons with plastic scintillators. The direct absorption on a nucleon pair was determined, for the two reactions, using kinematical restrictions. The cross section for absorption on a T=1 $^1S_0$ proton pair was found to be about 10^{-2} of the cross section for absorption on a T=0 $^3S_1$ proton-neutron pair. This ratio is much smaller than the value expected from isospin considerations alone. The dynamical suppression is attributed, at least in part, to the fact that $L_{\Delta N} = 0$ is forbidden in the intermediate state for absorption on the T=1 pair.

*California Institute of Technology, Pasadena, California.
†Northwestern University, Evanston, Illinois.

f. Inclusive π^+ Scattering from ^{4}He

S. M. Levenson,* D. F. Geesaman, E. P. Colton,† R. J. Holt, H. E. Jackson, J. P. Schiffer, J. R. Specht, K. E. Stephenson, B. Zeidman, R. E. Segel,‡ P. A. M. Gram,§ and C. A. Goulding||

Inclusive pion spectra from pion scattering from ^{4}He at T_π = 100, 160, and 220 MeV have been measured with the LAS spectrometer at LAMPF. The back angle spectra show a broad peak consistent with quasifree scattering. However, the energy integrated angular distributions for inelastic scattering do not follow the free nucleon angular distributions, but vary much more slowly with angle. In Fig. I-2 the ratios of the inelastic cross section (σ_{IN}) including charge exchange, and of the reaction cross section ($\sigma_R \equiv \sigma_{IN} + \sigma_{ABS}$) to the total cross section (σ_{TOT}) are shown as a function of energy for ^{4}He and ^{12}C.[1,2] While σ_R/σ_{TOT} is quite constant for both targets, the energy dependence of σ_{IN}/σ_{TOT} appears to be rather different for ^{4}He and ^{12}C. This implies that absorption is a much larger fraction of the total cross section for $\pi^+ + {}^4$He at 100 MeV.

g. Survey of Inclusive Pion Scattering Near the Δ_{33} Resonance

E. P. Colton,† D. F. Geesaman, R. J. Holt, H. E. Jackson, S. Levenson,* J. P. Schiffer, J. R. Specht, K. E. Stephenson, B. Zeidman, R. E. Segel,‡ P. Gram,§ and C. Goulding||

A comprehensive series of measurements of inclusive pion scattering from ^{12}C, ^{58}Ni, and ^{208}Pb with the LAS spectrometer have been completed. Pion energy spectra were measured at 7 angles from 30° to 146° at π^+ incident energies of 100, 160, and 220 MeV. Data were also obtained on an H_2O target at 100 MeV, on ^{12}C at 300 MeV, and on π^- scattering from ^{12}C and ^{208}Pb at 160 MeV.

As illustrated in Fig. I-3, the pion-energy spectra are dominated by a large peak at an energy near that corresponding to pions scattering from

*Thesis student, University of Chicago, Chicago, Illinois.

†Accelerator Research Facilities Division, ANL.

‡Northwestern University, Evanston, Illinois.

§Los Alamos National Laboratory, Los Alamos, New Mexico.

||Florida A & M University, Tallahassee, Florida.

[1] F. Binon et al., Phys. Rev. Lett. 35, 143 (1979).

[2] I. Navon et al., Phys. Rev. C 22, 717 (1980).

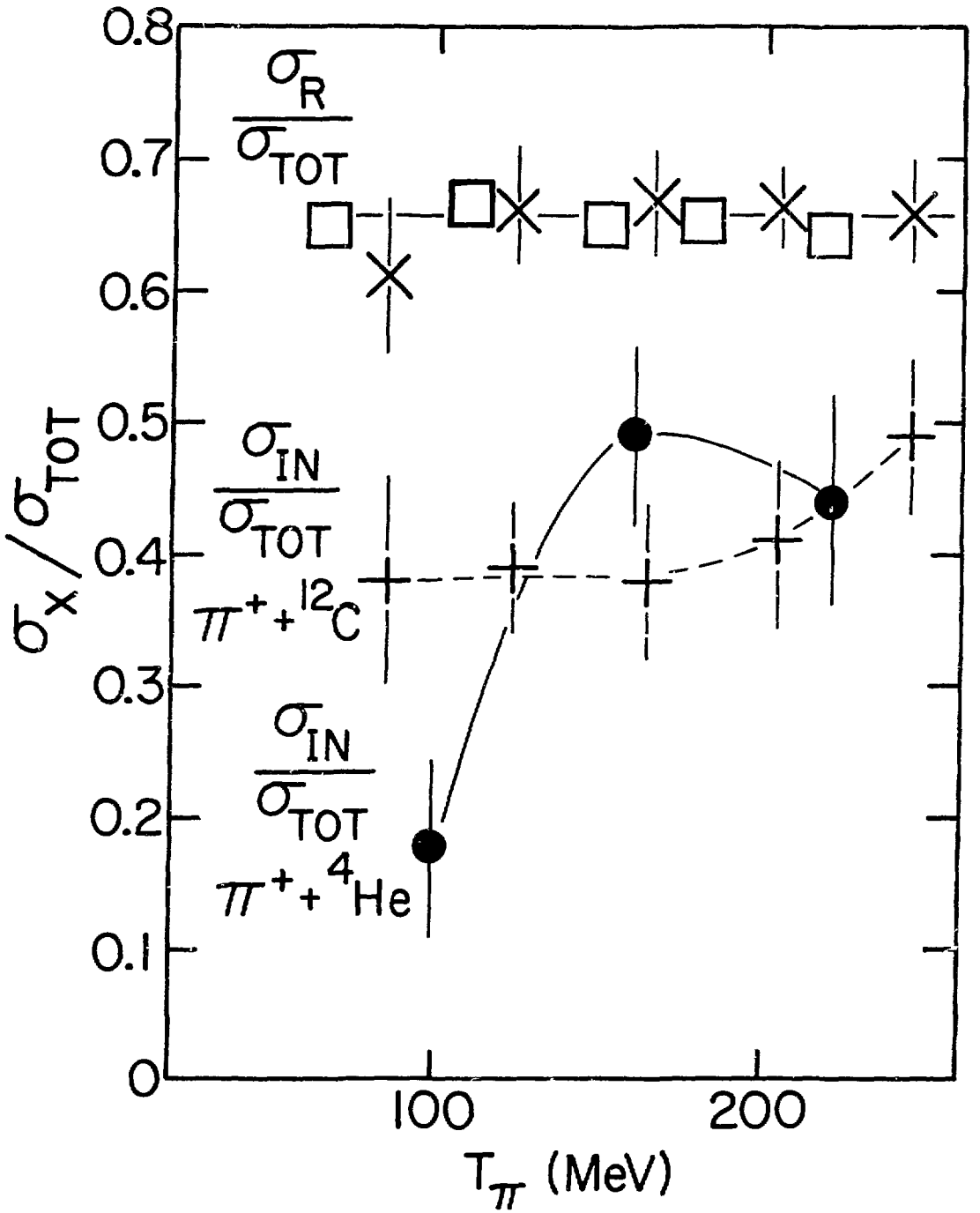

Fig. I-2. Ratio of σ_R and σ_{IN} to σ_{TOT} for ^{4}He (squares and circles, respectively) and ^{12}C (x's and pluses, respectively).

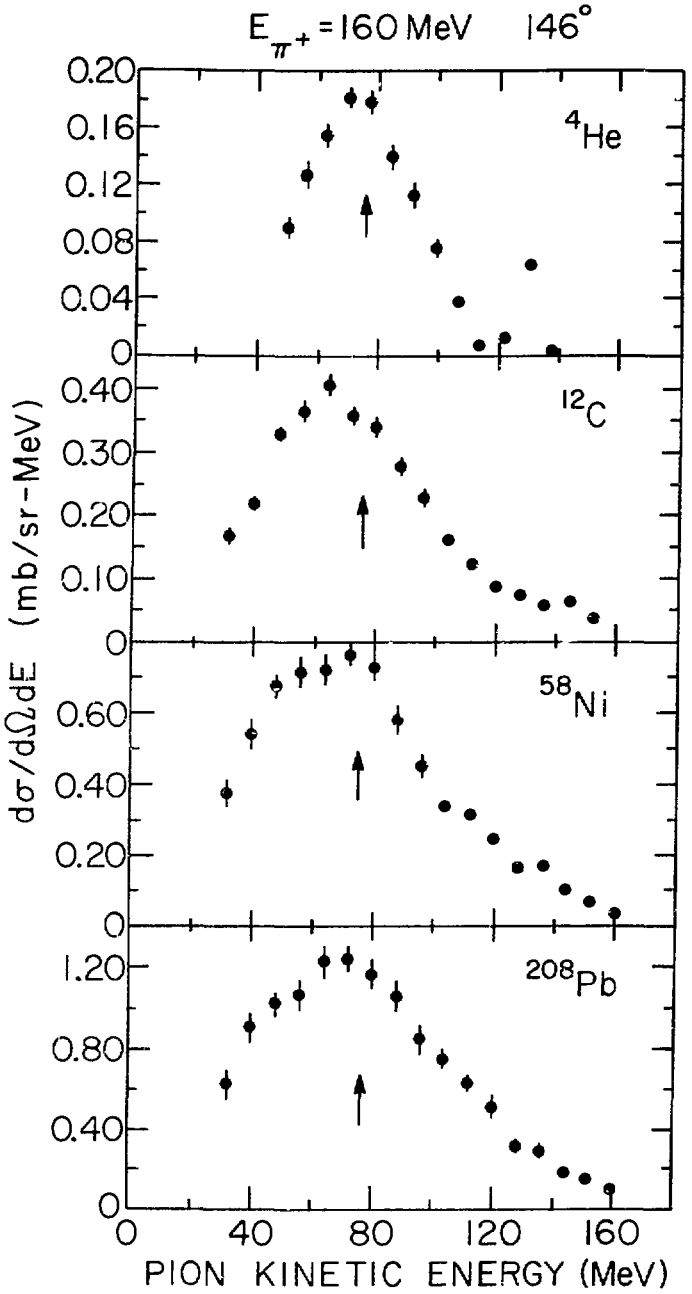

Fig. I-3. Energy spectra of 160-MeV π^+ scattered by ^{4}He, ^{12}C, ^{58}Ni, and ^{208}Pb to θ_{lab} = 146°. The arrows denote the pion energy of the elastic scattering of a 160-MeV pion from a nucleon at 146°.

a free nucleon. This indicates the importance of the quasifree reaction mechanism even in the presence of strong pion absorption. Indeed, the spectra look rather similar for each target and the angular distributions follow the free π-nucleon angular distribution at back angles. At forward angles, however, the significant yield of low-energy pions cannot arise from the quasifree mechanism and yield in the quasifree peak is lower than that expected from a free-nucleon-like angular distribution. These observations signal the importance of higher-order processes and Pauli blocking effects in the reaction mechanism.

Total inelastic scattering cross sections have been obtained for each target by integrating the energy and angular distributions. Inelastic scattering accounts for between 30% and 60% of the total reaction cross sections for these nuclei.

h. Large Acceptance Spectrometer (LAS)

E. P. Colton,* D. F. Geesaman, R. J. Holt, H. E. Jackson, S. Levenson,† J. P. Schiffer, J. R. Specht, K. E. Stephenson, B. Zeidman, R. E. Segel,‡ P. Gram,§ and C. Goulding‖

There has been a continuing effort to improve the operation of the Large Acceptance Spectrometer which was constructed at LAMPF in 1980 by Argonne in collaboration with other groups. This spectrometer is optimized for large solid-angle (∿25 msr) and momentum (±15%) acceptance with moderate resolution. A detailed analysis of the acceptance data obtained in LAMPF experiment 390, confirms that the spectrometer performs as expected, though further work is still required to improve the accuracy to which absolute cross sections can be determined.

Additional beam-optics calculations indicate that, with somewhat reduced solid-angle acceptance, the spectrometer can be used up to momenta of 1300 MeV/c by reducing the bend angle of the central ray to 30°. This also has the benefit of increasing the momentum acceptance to ±25%. The

*Accelerator Research Facilities Division, ANL.

†Thesis student, University of Chicago, Chicago, Illinois.

‡Northwestern University, Evanston, Illinois.

§Los Alamos National Laboratory, Los Alamos, New Mexico.

‖Florida A & M University, Tallahassee, Florida.

spectrometer is currently being reassembled with this bend angle for a (π,p) measurement (LAMPF experiment 562) to be run in March 1981.

Our experience in operating the spectrometer revealed that the original multiwire proportional chambers were not reliable. New wire chambers with higher mechanical integrity have been constructed. Four sets of wire planes will be read out using the PCOS II system while the four larger planes will be read out using segmented delay lines. These last chambers have been constructed using technology developed for the EPICS spectrometer.

All of these improvements will increase the utility of LAS for a broad range of medium-energy measurements. To date, 6 experiments have been completed or approved by the program advisory committee to run on the spectrometer, and several additional proposals are under consideration.

i. Fermi-Gas Model for π-Nucleus Inclusive Scattering

R. J. Holt and T.-S. H. Lee

Inclusive pion scattering data are becoming available from recent experiments at LAMPF and SIN. A central feature of the data is a peak which exhibits a quasifree π-N scattering behavior in both scattering angle and energy. As a first step toward understanding the data, we have applied the Fermi-gas model to π-nucleus scattering. In this model both a degenerate, zero-temperature and a finite-temperature Fermi gas can be employed. The results at large angles for the Fermi-gas model give a shape similar to the observed spectra for a wide range of nuclei.

B. HIGH-RESOLUTION STUDIES AND NUCLEAR STRUCTURE

High-resolution studies pion elastic and inelastic scattering primarily emphasize the relation between pion-nuclear interactions and nuclear structure. The measurements have now progressed from studies of macroscopic properties, such as optical-model parameters, deformation parameters, and rms radii of nuclei, to tests of microscopic descriptions of nuclear wavefunctions, identification of new states, and investigations of configurations that are not feasible with other probes. The particular usefulness of pion scattering in finding new states is demonstrated by the clear observation of the yrast 5^- state in ^{14}N (14.7 MeV) that had not been previously seen.

a. Scattering of Pions by Complex Nuclei

D. F. Geesaman, C. Olmer, B. Zeidman, G. S. Blanpied,* G. R. Burleson,* M. Devereux,* R. L. Boudrie,† C. L. Morris,† H. A. Thiessen,† R. E. Segel,‡ and L. W. Swenson§

Elastic and inelastic scattering of both π^+ and π^- by ^9Be, Si, ^{58}Ni, and ^{208}Pb has been studied at E_π = 291 MeV. The experiment was performed with the EPICS system at LAMPF with an overall system resolution of ∿600 keV. The angular distributions are generally smooth, showing much less structure than those previously measured at E_π = 162 MeV.

The elastic scattering data were described using optical potentials of the Kisslinger form, with parameters fit to the experiment data. Corresponding DWIA calculations for inelastic scattering to states in: ^9Be, 2.4 and 6.8 MeV, ^{28}Si, 1.8, 4.6, and 6.9 MeV, ^{58}Ni, 1.5 and 4.5 MeV, and ^{208}Pb, 2.6 MeV, are in reasonable agreement with the data. The deformation parameters required for the even-even targets agree with those obtained from a similar analysis of the 162-MeV data. However, a different deformation parameter is required for π^- excitation of the ^9Be $7/2^-$, 6.8-MeV state. This is interpreted as evidence for the increased importance of single-particle versus collective components of the nuclear wave functions as the pion energy changes from the 3,3 resonance energy to ∿100 MeV above the resonance energy. This series of high-resolution studies was completed with the submission of a paper for publication to Phys. Rev.

---

*New Mexico State University, Las Cruces, New Mexico.

†Los Alamos National Laboratory, Los Alamos, New Mexico.

‡Northwestern University, Evanston, Illinois.

§Oregon State University, Corvallis, Oregon.

b. Determination of Neutron Radii from Pion Scattering

B. Zeidman and D. F. Geesaman

The strong isospin dependence in pion-nucleon interactions near resonance implies a capability for differentiation of proton and neutron contributions in pion-nucleus scattering. With the use of a modified optical model, analyses of recent high-quality data from ANL and other groups indicate that rms-radius differences between neutron and proton density distributions can be deduced. Preliminary values for the differences in rms radii are 0.18 ± 0.05 fm between neutrons in ^{40}Ca and ^{48}Ca, 0.14 ± 0.05 fm between protons and neutrons in ^{48}Ca, and 0.1 ± 0.05 fm between protons and neutrons in ^{208}Pb. The most recent values obtained from proton scattering are consistent with the results from our pion analyses, in marked contrast to earlier proton scattering results which reported much larger neutron-proton rms-radius differences.

c. Excitation of High-Spin Particle-Hole States in ^{28}Si

D. F. Geesaman, B. Zeidman, C. Olmer,* S. Greene,† R. L. Boudrie,‡ R. E. Segel,§ and L. W. Swenson‖

Inelastic pion scattering has proved to be an excellent tool for studying high-spin, particle-hole, spin-flip excitations in nuclei. In our earlier work at 162 MeV on pion inelastic scattering to T=0 and T=1 6^- states in ^{28}Si (11.58 MeV and 14.34 MeV, respectively), we observed that the ratio $R = \sigma(T = 0)/\sigma(T = 1)$ was ~1.5 rather than the value of 4 expected from the pion-nucleon interaction. To test whether this discrepancy is due to the structure of the particular states, or a lack of understanding of the reaction mechanism, we repeated the experiment at E_π = 116 MeV. Spectra were accumulated at 65, 80, and 100° with a π^+ beam and 90° with a π^- beam. At this energy the 6^- states are much less prominent compared to other states in the spectra than at 162 MeV, and only an upper limit could be set on the yield of the 6^- T=1 state. In preliminary analysis, a lower limit

*Indiana University, Bloomington, Indiana.
†New Mexico State University, Las Cruces, New Mexico.
‡Los Alamos National Laboratory, Los Alamos, New Mexico.
§Northwestern University, Evanston, Illinois.
‖Oregon State University, Corvallis, Oregon.

was obtained for R which is slightly larger than the result at 162 MeV. Further analysis is under way along with calculations to attempt to explain the difference between spectra at the same momentum transfer for the two different energies.

d. Inelastic Pion Scattering from ^{10}B and ^{11}B

B. Zeidman, D. F. Geesaman, C. Olmer, G. C. Morrison,* G. R. Burleson,† S. Greene,† C. L. Morris,‡ R. L. Boudrie,‡ R. E. Segel,§ L. W. Swenson,‖ G. S. Blanpied,¶ B. R. Ritchie,¶ and C. Harvey**

In a continuation of our high-resolution studies of pion scattering on the EPICS spectrometer, we have measured π^+ and π^- elastic and inelastic scattering from ^{10}B and ^{11}B at E_π = 162 MeV. The boron targets of 110 mg/cm^2 areal density were prepared by sintering boron powder. Angular distributions were measured from 20 to 90° in 5° steps for π^+ and from 20° to 80° in 10° steps for π^-. The elastic angular distributions show rather shallow minima, suggesting significant quadrupole contributions to the elastic scattering at this energy. While π^+ and π^- cross sections to excited states were very similar with the ^{10}B target, as is seen in Fig. I-4, significantly different π^+ and π^- cross sections were observed for each of several ^{11}B states. In particular, the ratio $\sigma(\pi^-)/\sigma(\pi^+)$ is ∿9 for the 14.04-MeV, $11/2^+$ state as would be expected for a pure neutron excitation. As expected for a pure isovector transition to the 12.9-MeV T=3/2 state, the ratio $\sigma(\pi^-)/\sigma(\pi^+)$ is 1.

e. Inelastic Pion Scattering from ^{14}N

D. F. Geesaman, C. Olmer, B. Zeidman, G. C. Morrison,* G. Blanpied,† G. R. Burleson,† R. L. Boudrie,‡ R. E. Segel,§ R. E. Anderson,‡ and L. W. Swenson‖

Elastic and inelastic scattering of 162-MeV pions from ^{14}N was studied with the EPICS spectrometer at LAMPF. CH_2N_2 and CH_2 targets were

*University of Birmingham, Birmingham, England.
†New Mexico State University, Las Cruces, New Mexico.
‡Los Alamos National Laboratory, Los Alamos, New Mexico.
§Northwestern University, Evanston, Illinois.
‖Oregon State University, Corvallis, Oregon.
¶University of South Carolina, Columbia, South Carolina.
**University of Texas, Austin, Texas.

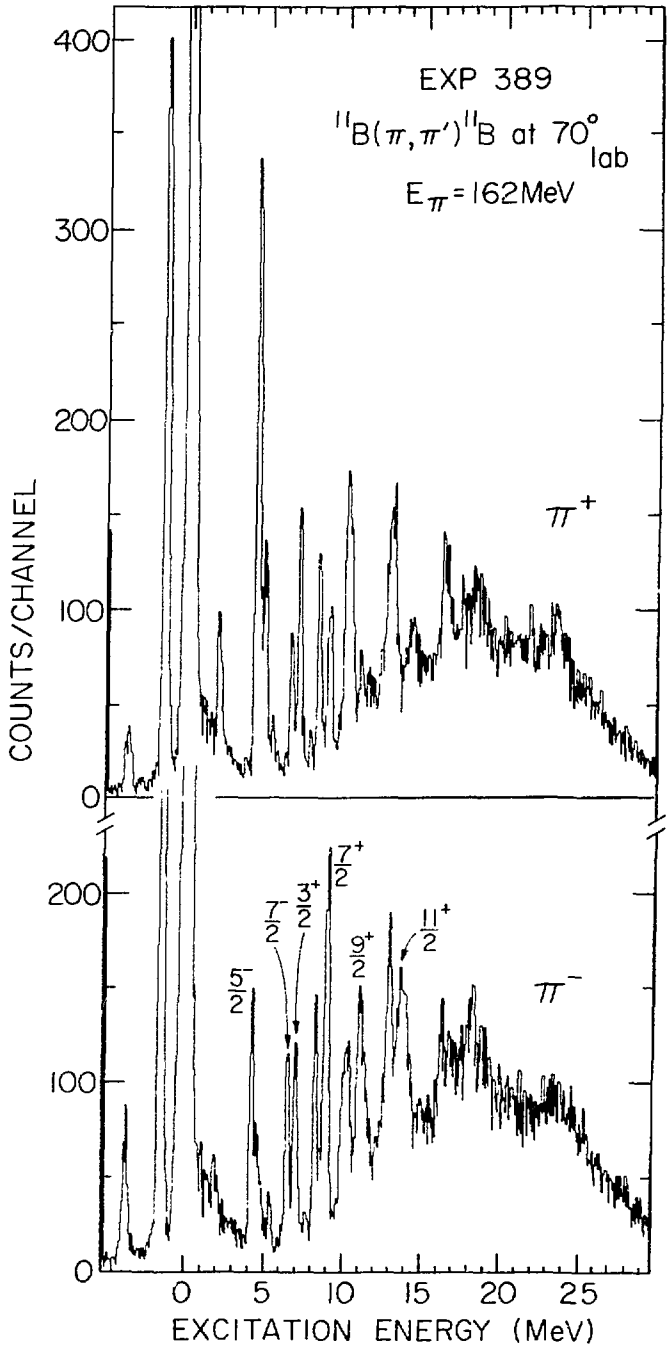

Fig. I-4. Spectra for $^{11}B(\pi,\pi')$ at 70°. The spins and parities of several levels are indicated.

employed at each angle, and the nitrogen spectra were constructed by subtraction. Many ^{14}N levels between 3 and 24 MeV were observed, but only an upper limit could be set on the cross section for the 0^+ T=1 state at 2.31-MeV excitation. Optical-model and microscopic DWIA analyses are in progress. The angular distributions for the majority of the states require L=3 transitions; however, at least one state seems to be populated by a higher multipole. This 14.7-MeV state may be the 5^- state which is predicted by shell-model calculations to be strongly excited in pion-inelastic scattering. Two states show consistent evidence of differing cross sections in π^+ and π^- scattering which may be indicative of strong isospin mixing.

f. Excitation of High-Spin Particle-Hole States in ^{54}Fe and ^{58}Ni

B. Zeidman, D. F. Geesaman, R. D. Lawson, C. Olmer,* R. L. Boudrie,† C. L. Morris,† H. A. Thiessen,† R. A. Lindgren,‡ G. R. Burleson,§ S. Green,§ W. B. Cottinghame,§ R. E. Segel,|| and L. W. Swenson¶

A high-resolution study of the inelastic scattering of π^+ and π^- by ^{54}Fe and ^{58}Ni was proposed. The principal objective is to locate and identify 8^- states that arise from promoting a $1f_{7/2}$ nucleon to the $1g_{9/2}$ orbital. The EPICS system will be used in the initial measurements at 170 MeV.

Since high-spin states resulting from the excitation of stretched, particle-hole configurations are selectively populated at large momentum transfer, angular distributions consisting of relatively few, widely spaced data points of good statistical accuracy suffice for positive identification of the 8^- states. Since ^{54}Fe and ^{58}Ni have neutron excess, both isoscalar and isovector interactions contribute to excitation of T=1 states, but only the isovector interaction is involved in excitation of T=2 states. There should therefore be differences between π^+ and π^- excitation of T=1 states, while the same cross sections are expected for T=2 states. Shell-model

*Indiana University, Bloomington, Indiana.

†Los Alamos National Laboratory, Los Alamos, New Mexico.

‡University of Massachusetts, Amherst, Massachusetts.

§New Mexico State University, Las Cruces, New Mexico.

||Northwestern University, Evanston, Illinois.

¶Oregon State University, Corvallis, Oregon.

calculations suggest that pion scattering will populate states that are not observable in either proton or electron scattering.

The proposal was accepted and the experiment is expected to be scheduled in 1982.

g. Discrete States from Pion Double-Charge-Exchange on Heavy Nuclei

B. Zeidman, D. F. Geesaman, R. J. Holt, E. P. Colton,* J. R. Specht, and K. E. Stephenson

The LAS spectrometer on the P^3 channel will be used in a survey of pion double-charge exchange (DCE) reactions to discrete states on a wide variety of targets. Based upon theoretical arguments, it is hoped that the DCE cross section will increase for $A > 60$ and make it possible to use this reaction as a spectroscopic tool. Targets of ^{58}Ni, ^{90}Zr, ^{120}Sn, and ^{208}Pb will be investigated to establish limits or measure cross sections for transitions to discrete states in the final nuclei. In order to enhance the differential cross sections relative to backgrounds, the (π^+,π^-) reactions will be studied near 0° scattering with ∿150-MeV pions. A 12-in. diameter, circular pole magnet has been constructed and will be placed at the pivot of LAS to deflect the primary pion beam away from the spectrometer. The experiment will be performed during the summer of 1981.

h. Study of the $^4He(\pi^-,\pi^+)$ Reaction at Small Angles

R. D. McKeown, D. F. Geesaman, R. J. Holt, H. E. Jackson, Jr., J. P. Schiffer, J. R. Specht, K. E. Stephenson, and B. Zeidman

A proposal to search for structure in the ^4n system via the $^4He(\pi^-,\pi^+)^4n$ reaction in the energy range $150 \leq T_\pi \leq 300$ MeV was submitted and approved. The Argonne Large Acceptance Spectrometer (LAS) will be used to analyze the emergent positive pions at small scattering angles, where cross sections for 0^+ states should be maximized. The binding energy of the ^4n system will be determined if structure is present in the measured spectra. With the π^- flux available at the P^3 channel, a sensitivity of better than 20 nb/sr should be attained. The experiment is expected to be scheduled for running time in late 1981.

---

*Accelerator Research Facilities Division, ANL.

C. TWO-NUCLEON PHYSICS WITH PIONS AND ELECTRONS

Studies of the deuteron provide the most stringent tests of our knowledge of reaction mechanisms as well as the basic nucleon-nucleon interaction. Pion elastic scattering from the deuteron is the simplest process for understanding the pion-nucleus reaction mechanism. Electron scattering from the deuteron provides constraints on the nucleon-nucleon interaction as well as the meson exchange currents. The development of a novel polarimeter has made it practical to study the polarization of the deuteron in both π-d and e-d elastic scattering. Thus far, this polarimeter has been used to measure the angular distribution of tensor polarization in π-d scattering. The results indicate a serious discrepancy with the theoretical calculations.

a. Deuteron Polarimeter Development

R. J. Holt, J. R. Specht, E. J. Stephenson, K. E. Stephenson, J. S. Frank,* M. J. Leitch,* J. D. Moses,* and R. M. Laszewski†

Thus far, two polarimeters have been completed and tested. The first is a relatively simple device which was used to test the feasibility of measuring tensor polarization t_{20} in π-d elastic scattering. The success of that feasibility study led to the development of a more sophisticated polarimeter which has made angular distribution studies of π-d scattering practical. In addition, the new polarimeter will be used for the measurement of tensor polarization in e-d scattering at the MIT/Bates Linear Accelerator Laboratory. The major features of the new polarimeter include: (i) high efficiency and T_{20} analyzing power, (ii) analyzing powers for the other polarization moments (it_{11}, t_{21}, t_{22}), and (iii) acceptance of a large deuteron beam emittance and a broad useful deuteron energy range. The polarimeter was calibrated with the polarized deuteron beam at the Berkeley 88-in. cyclotron.

b. Measurement of the Angular Distribution of Tensor Polarization in π-d Elastic Scattering

R. J. Holt, J. R. Specht, K. Stephenson, B. Zeidman, J. S. Frank,* M. J. Leitch,* J. D. Moses,* E. J. Stephenson,‡ and R. M. Laszewski†

The deuteron, being the simplest nucleus, provides a good "laboratory" for testing ideas of the π-nucleus reaction mechanism since the π-d

*Los Alamos National Laboratory, Los Alamos, New Mexico.

†University of Illinois, Urbana, Illinois.

‡Indiana University, Bloomington, Indiana.

system can be solved in an exact manner rather than the optical potential approach. True pion absorption which comprises a significant fraction of pion-induced reaction cross sections for all nuclei has been particularly difficult to incorporate into the theoretical calculations. The absorption process is believed to occur predominately on two nucleons. Thus, the deuteron is the simplest system for the study of pion-absorption effects. Recently, theoretical calculations[1] indicate that the effect of absorption on the elastic channel should show up most strongly in the polarization observables. The results of those calculations are shown in Fig. I-5. The main differences among the calculations are the way in which absorption is treated.

We have applied the newly-developed polarimeter to the study of the angular distribution of tensor polarization t_{20} in π-d scattering at T_π = 142 MeV. In particular, t_{20} was measured for deuterons which recoiled at laboratory angles of 17.5°, 28.9°, and 40.9°. Note that during the feasibility experiment last year, t_{20} was measured[2] for θ_d = 0°. The results are shown also in Fig. I-5. Clearly, the results are in disagreement with the calculations. One possible explanation for the disagreement is that the theories have not included the effects of a $^1D_2$ dibaryon resonance. A simple calculation based on the method of Kubodera et al.[3] suggests that the calculations would be in better agreement with the data if a $^1D_2$ dibaryon resonance were taken into account.

---

[1] A. S. Rinat et al., Nucl. Phys. A329, 285 (1979); C. Fayard et al., Phys. Rev. Lett. 45, 524 (1980); M. Betz and T.-S. H. Lee, Phys. Rev. C 23, 375 (1981).

[2] R. J. Holt et al., Phys. Rev. Lett. 43, 1229 (1979).

[3] K. Kubodera et al., J. Phys. G: Nucl. Phys. 6, 171 (1980).

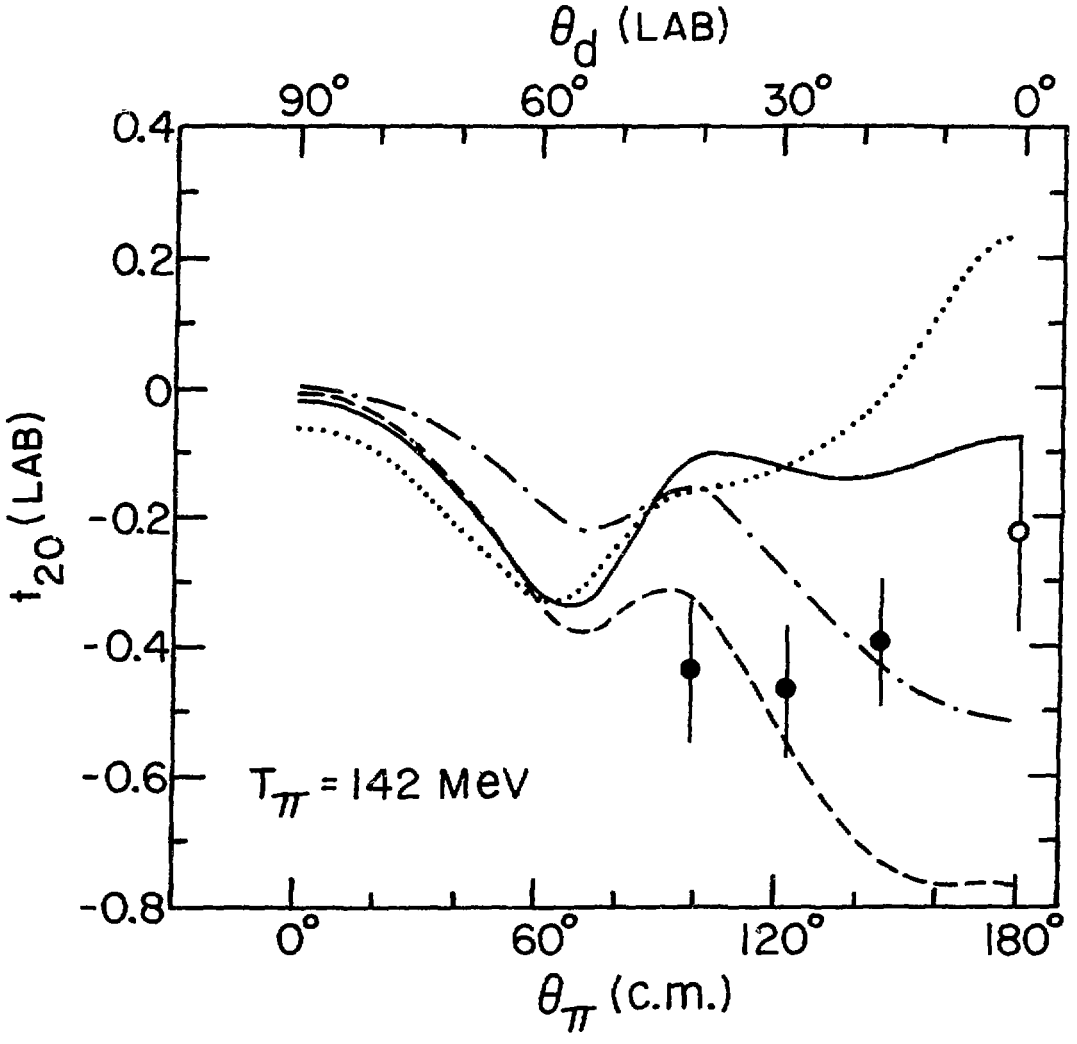

Fig. I-5. The curves represent the theoretical calculations of Ref. 1. The dashed curve represents a calculation with no absorption. The solid points are the present measurements, while the open circle is from Ref. 2.

c. Tensor Polarization in Electron-Deuteron Elastic Scattering

R. J. Holt, J. R. Specht, K. E. Stephenson, B. Zeidman, W. Haeberli,* W. Bertozzi,† R. P. Redwine,† M. Schulze,† W. Turchinetz,† R. Galoskie,‡ D. W. Saylor,‡ E. J. Stephenson,§ R. L. Burman,‖ J. S. Frank,‖ M. J. Leitch,‖ J. D. Moses,‖ and R. M. Laszewski¶

It is well known that only three form factors (charge, quadrupole, and magnetic) are necessary to describe e-d elastic scattering. Unfortunately, cross-section measurements alone do not allow one to unravel these three form factors. Thus far, only the magnetic form factor has been isolated. However, the charge and quadrupole form factors are sensitive to the short-range and tensor part, respectively, of the nucleon-nucleon interaction. The tensor polarization t_{20} is dominated by the interference term between the charge and quadrupole form factors.

Thus, we have proposed to measure t_{20} in e-d scattering at the MIT/Bates accelerator. The first phase of this measurement spans the momentum transfer range $q^2 \leq 9$ fm^{-2}. The second phase depends on the availability of the electron beam recirculator at Bates and will cover the momentum transfer range: $9 \leq q^2 \leq 14$ fm^{-2}. At present it is expected that the first phase of this experiment will be performed during this year.

*University of Wisconsin, Madison, Wisconsin.

†Massachusetts Institute of Technology, Cambridge, Massachusetts.

‡Worcester Polytechnic Institute, Worcester, Massachusetts.

§Indiana University, Bloomington, Indiana.

‖Los Alamos National Laboratory, Los Alamos, New Mexico.

¶University of Illinois, Urbana, Illinois.

II. HEAVY-ION RESEARCH AT THE TANDEM AND SUPERCONDUCTING LINAC ACCELERATOR

INTRODUCTION

The heavy-ion research program in the Argonne Physics Division is principally concerned with the many facets of the relationships between heavy-ion induced reactions and nuclear structure. Major interests are the structure of nuclei at high excitation, far from stability or in states of high-spin near the yrast line. The dynamics of heavy-ion reactions and the influence of nuclear structure upon them must be elucidated in order to extract the necessary information. These studies often require measurements with high precision over a wide dynamic range of energies and ion species as are now available from the tandem and linac booster. Continuing improvements in accelerator capabilities will allow investigations with high precision in regions not previously accessible.

The observation of resonance-like structure in quasi-elastic reactions on s-d shell nuclei has generated considerable interest in the underlying nature of such behavior. The exciting possibility is that these resonances signal the existence of states of unusual stability and structure at extremely high energies in the composite system. Emphasis has been placed on the $^{24}Mg+^{16}O$ system. In the past year measurements have been made at higher energies at both extreme forward and backward angles.

At bombarding energies not too far above the Coulomb barrier, fusion of heavy ions to form a compound system accounts for a major fraction of the total reaction cross section. Detailed study of fusion cross sections has revealed the presence of resonance-like structures in some fusion cross sections and a dependence of the maximum cross section for fusion upon the nuclear structure of the colliding nuclei. The dependence upon target-projectile combinations in the entrance channel and measurements of atomic x rays in the final channels have also been investigated.

At high spins, the rotational energy of nuclei becomes comparable to shell and Coulomb energies, thus opening up a new perspective in nuclear structure physics. Argonne work has concentrated upon nuclei where high-spin isomers are prevalent. The studies have focused upon the high-spin properties of the yrast states, levels which lie above them, and the general relationships between these states with few-particle configurations and the continuum. This program, which utilizes the gamma-ray facility, requires the high precision and wide variety of ion species available from the tandem-linac booster system.

Studies of reaction mechanisms are intertwined with nuclear-structure effects. Several studies of the energy dependence of reactions induced by heavy ions have been performed to map out the distribution of reaction strength as a function of energy and to investigate the reaction mechanism in reactions leading to discrete final states. Heavy-ion induced fission is

quite sensitive to the structure of both the initial and final nuclear pairs in addition to the structure of intermediate states. Studies of heavier systems at higher energies have become feasible with the advent of new ion species and higher energies.

Development of the target area for the superconducting linac booster continues to be the major instrumentation effort. The beam line and large scattering chamber became operational during the past year. The third beam line for the spectrograph is underway, while plans for the target room addition have been completed. Installation of the split-pole spectrograph and development of a large ionization chamber are in progress. The gamma-ray facility is operational.

A. RESONANT STRUCTURE IN HEAVY-ION REACTIONS

At Argonne, extensive studies exploring the strong resonance-like structures in s-d shell nuclei have been performed. Emphasis has been placed upon alpha-transfer reactions for which excitation functions at extreme forward and backward angles were measured. Angular distributions were also obtained. The ease with which the beam energy can be varied on the linac has proved to be a distinct asset. Resonant behavior has been observed in $^{16}O + {}^{24}Mg$ reactions at energies up to $E_{c.m.} \approx 53$ MeV. The persistence of resonant behavior over such a wide energy range up to such a high excitation energy in the composite system was not anticipated.

a. Resonance Strength to States at High Excitation Energy in ^{28}Si Populated Via the $^{24}Mg(^{16}O,^{12}C)^{28}Si^*$ Reaction

S. J. Sanders, D. F. Geesaman, W. Henning, D. G. Kovar, C. Olmer, M. Paul, and J. P. Schiffer

Excitation functions have been measured for $^{24}Mg(^{16}O,^{12}C)^{28}Si$ reaction populating states in ^{28}Si with $6.4 \leq E_x \leq 10$ MeV over the energy range $24 \leq E_{c.m.} \leq 36$ MeV. At each incident beam energy, cross sections were measured at three angles over the range $17° \leq \theta_{c.m.} \leq 21°$. More complete angular distributions ($10° \leq \theta_{c.m.} \leq 50°$) were measured at $E_{c.m.}$ = 30.5 and 32.6 MeV. Resonance-like structures are observed in the excitation functions[1] (see Fig. II-1) and strongly correlate with those seen previously at forward angles for the $^{24}Mg(^{16}O,^{12}C)^{28}Si$ (g.s.) transition.[2] This strongly supports the identification of the resonant character of the structures observed. Using different background assumptions, between 5% and 40% of the total width of the 30.8-MeV resonance can be attributed to $^{12}C + {}^{28}Si^*$ ($E_x < 10$ MeV) decays.

[1] S. J. Sanders, C. Olmer, D. F. Geesaman, W. Henning, D. G. Kovar, M. Paul, and J. P. Schiffer, Phys. Rev. C 22, 1914 (1980).

[2] M. Paul, S. J. Sanders, J. Cseh, D. F. Geesaman, W. Henning, D. G. Kovar, C. Olmer, and J. P. Schiffer, Phys. Rev. Lett. 40, 1310 (1978).

b. Resonant Behavior in the 0° Excitation Function of $^{24}Mg(^{16}O,^{12}C)^{28}Si$ at Linac Energies

S. J. Sanders, H. Ernst, W. Henning, C. M. Jachcinski, D. G. Kovar, and J. P. Schiffer

The strong resonant structures observed at the Argonne tandem in the 0° excitation function of the $^{24}Mg(^{16}O,^{12}C)^{28}Si$ reaction have prompted us to

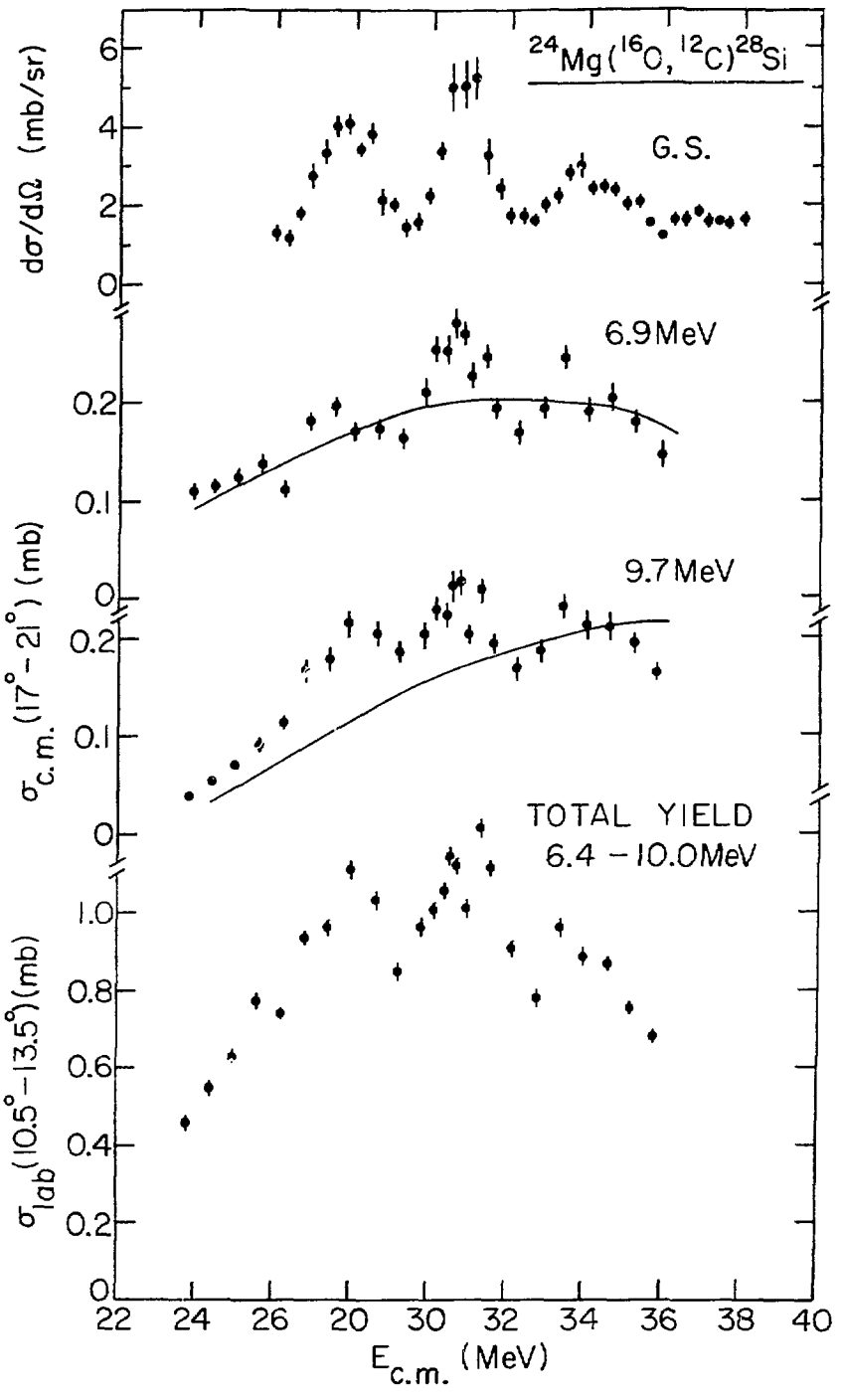

Fig. II-1. Excitation functions for states in ^{28}Si populated with the $^{24}Mg(^{16}O,^{12}C)^{28}Si$ reaction. The ground state excitation function is from Ref. 2. The curves are the results of DWBA calculations.

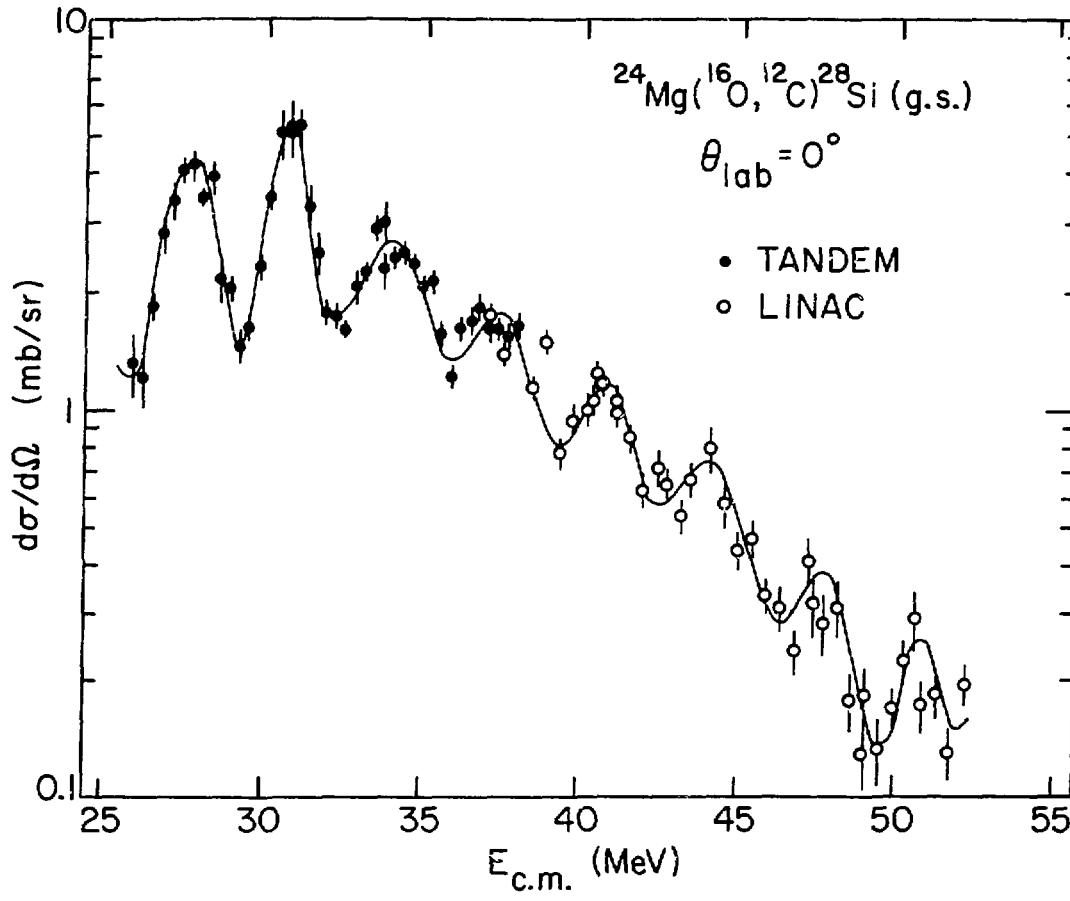

Fig. II-2. 0° excitation function for the $^{24}Mg(^{16}O,^{12}C)^{28}Si$ reaction, leading to the ground state in ^{28}Si.

extend these measurements to higher energy using the superconducting linac. With a ΔE-E surface barrier telescope and selected absorber foils, we were able to extend the range of measurements to $E_{c.m.}$ = 52.5 MeV. Surprisingly enough, the strong structures persist with nearly constant energy spacings as shown in Fig. II-2. An analysis in terms of a nonresonant background and coherent resonance amplitudes is presently under way. These tantalizing structures will be further investigated to determine spin, width, and other important parameters.

c. Measurement of Back-Angle Cross Sections in ^{16}O Induced Alpha Transfer on ^{24}Mg

S. J. Sanders,* H. Ernst, W. Henning, and J. Barrette†

Our extension of measurements at the Argonne superconducting linac of the zero-degree excitation function for the $^{24}Mg(^{16}O,^{12}C)^{28}Si$ (g.s.) reaction to $E_{c.m.}$ = 52.5 MeV (∿ three times the barrier height), showed that the resonance-like structures persist to even the highest energies. It was therefore compelling to also extend the 180° excitation functions for both the ground-state and 1.78-MeV first excited 2^+ state in ^{28}Si to cover the same energy range. Because of the low cross sections, the measurements were performed at the Brookhaven National Laboratory tandem using the large solid angle QDDD magnetic spectrometer. The results are shown in Fig. II-3. We find that the resonance features also persist in the 180° excitation function, with strong correlation between the 0^+ and 2^+ channels, but none are clearly evident between the forward- and backward-angle excitation functions for the ground-state channel (compare with Fig. II-2). We plan to compare these results to model calculations and measure detailed angular distributions at selected energies.

*Yale University, New Haven, Connecticut.

†Brookhaven National Laboratory, Upton, Long Island, New York.

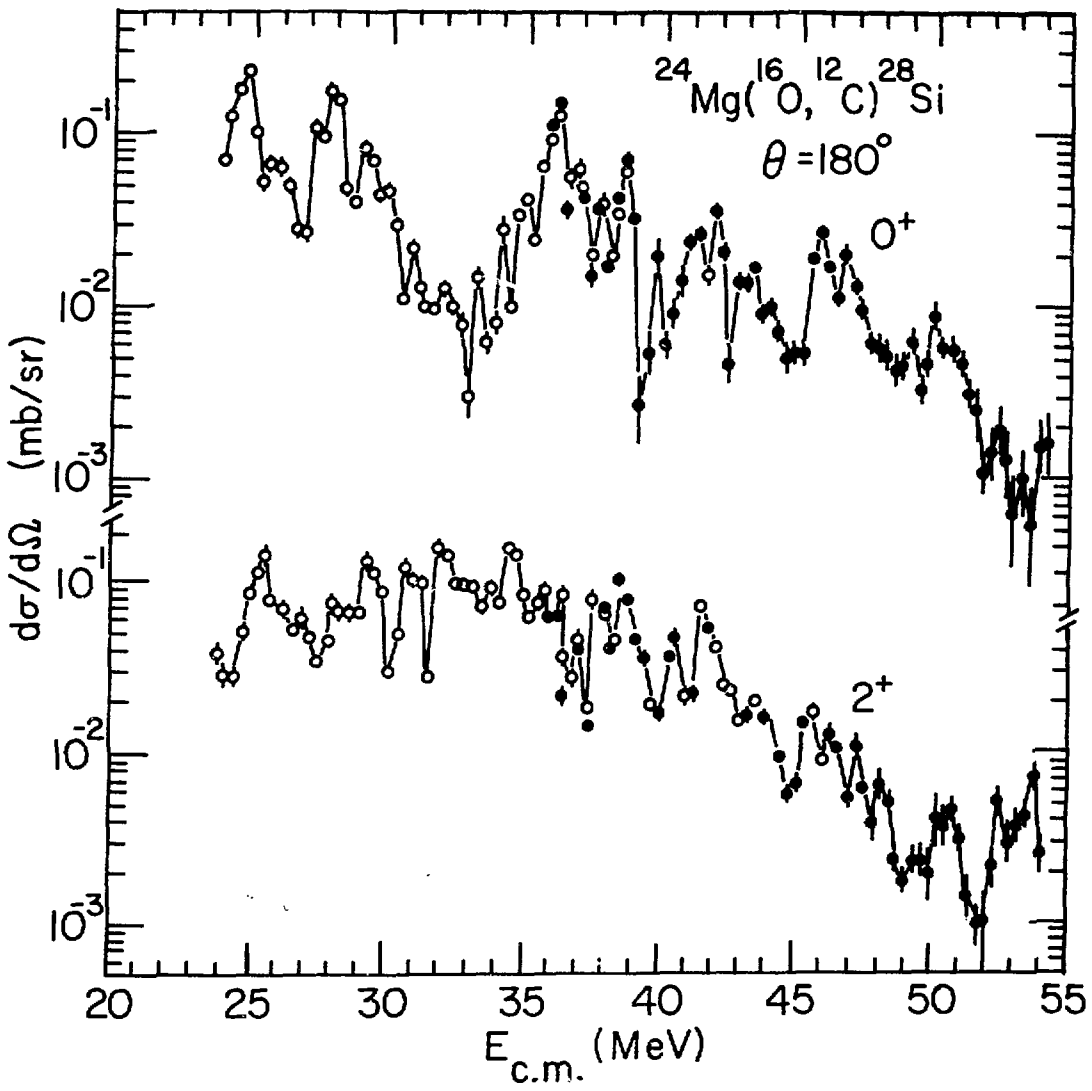

Fig. II-3. 180° excitation functions for the $^{24}Mg(^{16}O,^{12}C)^{28}Si$ reaction, leading to the ground state and the 1.78-MeV first excited 2^+ state in ^{28}Si.

B. FUSION CROSS SECTIONS

Detailed studies of the low energy fusion behavior of a large number of target-projectile combinations have been made at the tandem over the past several years. These studies are now being extended to higher energies and to heavier systems using the tandem-linac system. The effects of the structure of the target or projectile have been in both the systematics of maximum fusion cross sections and in differences between systems that differ by only one or two nucleons. The partition of reaction cross section into various evaporation residues provides information concerning the fused system. Studies involving heavier systems require new or improved techniques such as x-ray measurements or the use of an electrostatic deflector.

a. Fusion of $^{16}O + ^{24,26}Mg$ at Linac Energies

D. G. Kovar, C. Jachcinski, C. N. Davids, D. F. Geesaman, W. Henning, and S. J. Sanders

Previous measurements of the $^{16}O+^{24,26}Mg$ reactions have established the fusion cross-section behavior over the energy range $30 \leq E_{lab}(^{16}O) \leq 80$ MeV.[1] It was found that the fusion cross sections "saturate" ($\sigma_{fus}^{max} \approx 1100$ mb) at $E_{lab} \approx 60$ MeV with the cross sections for $^{16}O + ^{26}Mg$ approximately 100 mb larger than those for $^{16}O + ^{24}Mg$. In the present study, the interest was to extend the fusion measurements to the higher energies obtainable with the superconducting linac booster, and to establish whether differences between the two systems persist and whether the behaviors are consistent with the predictions of various models proposed. Angular distributions for elastic scattering and the evaporation-residue yields were measured at $E_{lab}(^{16}O)$ equal to 60, 100, and 138 MeV using a gas-ionization counter–silicon surface-barrier-detector ΔE-E telescope. Single-angle measurements were also obtained at several intermediate energies and the equivalent angle-integrated cross sections derived by interpolating between the complete angular distributions. The fusion cross sections for both systems were found to remain approximately constant up to an energy of $E_{lab} = 100$ MeV and to decrease at higher energies. The $^{16}O+^{26}Mg$ cross sections (shown in Fig. II-4) remain $\sim$100 mb larger than the $^{16}O+^{24}Mg$ cross sections from $E_{lab} = 60$ to 138 MeV.

---

[1] S. L. Tabor et al., Phys. Rev. C 17, 2136 (1978).

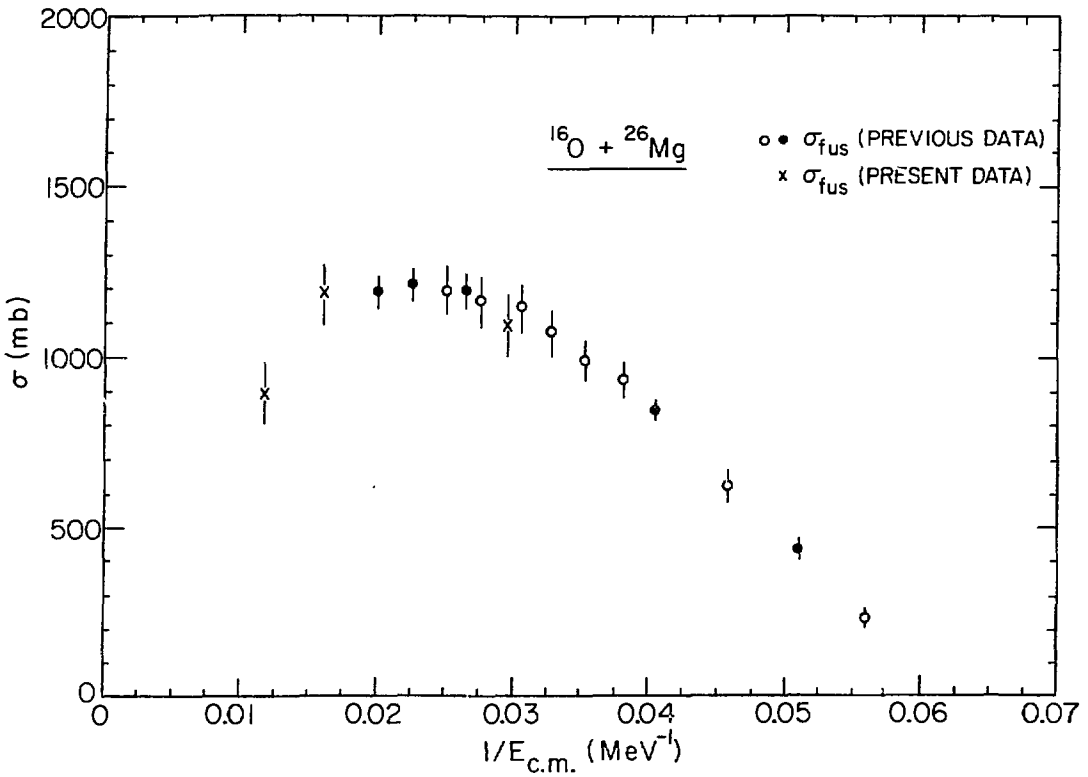

Fig. II-4. Fusion cross sections for the $^{16}O+^{26}Mg$ reaction. Full angular distribution measurements are indicated by the solid symbols, and single angle measurements are indicated by the open symbols.

b. Distribution of Evaporation Residue Strength in the Fusion of $^{18}O + ^{24}Mg$ and $^{16}O + ^{26}Mg$

R. A. Racca,* F. W. Prosser, Jr.,* K. Daneshvar,† C. N. Davids, and D. G. Kovar

Gamma yields were measured over the energy range 25 MeV $\leq E_{lab} \leq$ 70 MeV for $^{16}O + ^{26}Mg$ and 27 MeV $\leq E_{lab} \leq$ 65 MeV for $^{18}O + ^{24}Mg$. Earlier measurements[1] of the above systems have been made using particle detection methods. A comparison of that data with the results obtained for the $^{15}N+^{27}Al$ system[2] clearly showed an entrance channel effect in the barrier

*University of Kansas, Lawrence, Kansas.

†Thesis student, University of Chicago, Chicago, Illinois.

[1] S. L. Tabor et al., Phys. Rev. C 17, 2136 (1978).

[2] F. W. Prosser, Jr., et al., Phys. Rev. C 21, 1819 (1980).

dominated energy region. The purpose of this study is to measure the relative strengths of the various decay modes in each system. The results indicate that the fusion yield for the $^{16}O+^{26}Mg$ system is dominated by those residues with mass numbers 40 and 37, whereas for the $^{18}O+^{24}Mg$ system, the decay is dominated by fusion residues with mass numbers 39 and 36.

The experimental fusion yields have been compared with the predictions of a statistical evaporation model, CASCADE. For most of the residues, the calculation does a reasonable job in predicting the magnitudes and excitation functions. For the $^{16}O+^{26}Mg$ system, the dominant components are predicted correctly to be masses 40 and 37, but the calculated magnitudes are too small. In addition the calculated mass 36 yield is too large. For the $^{18}O+^{24}Mg$ system, the dominant components are predicted correctly to be masses 39 and 36, with the magnitude of the A=39 yield in agreement with experiment. The calculated yield of mass 36 is too large.

c. Search for Structure in the Fusion Excitation Function of $^{16}O + ^{24}Mg$

F. W. Prosser, Jr.,* R. A. Racca,* K. Daneshvar,† C. N. Davids, and D. G. Kovar

Gamma yields were measured over the energy range 40 MeV $\leq E_{lab} \leq$ 51 MeV in 350 keV intervals. Yields of the individual fusion residues produced in the reaction were obtained from observation of the various characteristic gamma rays. Previous measurements[1] of lighter α-particle systems show definite structure in the fusion excitation function. It has been shown[2] that the decays involving one or more α particles are largely responsible for this structure. Excitation functions for residues resulting from both alpha and nucleon boiloff have been obtained. Statistics are better than 5% for most of the residues seen. Possible structure at the limit of the statistics has been observed for some channels, but has not been verified. Further analysis of the data is in progress.

---

*University of Kansas, Lawrence, Kansas.

†Thesis student, University of Chicago, Chicago, Illinois.

[1] D. G. Kovar et al., Phys. Rev. C 20, 1305 (1979).

[2] J. J. Kolata et al., Phys. Lett. 65B, 333 (1976).

d. The Fusion of $^{24}Mg + ^{24}Mg$

C. M. Jachcinski, R. R. Betts,* C. N. Davids, D. F. Geesaman, D. G. Kovar, C. Olmer, M. Paul, S. J. Sanders, and J. L. Yntema

Oscillatory structures have been observed in the excitation functions of total fusion cross sections for $^{12}C + ^{12}C$, $^{16}O + ^{12}C$, and $^{16}O + ^{16}O$ (Ref. 1) and at a much weaker level, for $^{28}Si + ^{28}Si$.[2] We have studied the fusion of $^{24}Mg + ^{24}Mg$ to search for structure in the excitation function for this system. The evaporation residues resulting from fusion were detected in a ΔE-E gas-ionization-chamber— silicon surface-barrier-detector system. Evaporation residue and elastic-scattering angular distributions were measured at E_{lab} = 50 and 64 MeV, and single-angle measurements (θ_{lab} = 5.0°) were performed from E_{lab} = 50 to 64 MeV in 1-MeV steps. The general energy dependence of the cross section at these energies is in good agreement with the systematics of fusion reactions, although the possibility of weak oscillatory structures in the excitation function is not excluded.

To increase the sensitivity in the search for structure, we measured excitation functions in 250-keV ($\Delta E_{c.m.}$) steps from 27.4 ≤ $E_{c.m.}$ ≤ 39.9 MeV for the gamma rays emitted from the evaporation residues. These excitation functions show little evidence of correlated structure and an upper limit of 5% of the total fusion cross section can be set for a rapidly varying component of the fusion process.

The charged-particle measurements were extended to $E_{c.m.}$ = 66.2 MeV on the tandem-linac-booster accelerator system. The fusion cross section continues to rise with energy at the highest energies studied (see Fig. II-5) in contrast to many other systems where a maximum value of the fusion cross section has been reached at similar energies above the Coulomb barrier. In this respect the data are very similar to those obtained on the $^{28}Si + ^{28}Si$ system. In both cases the value of the total ion-ion potential at the critical radius is rather different from the value extracted for nearby systems.

---

*Chemistry Division, ANL.

[1] D. G. Kovar et al., Phys. Rev. C 20, 1305 (1979).

[2] S. B. DiCenzo et al., Phys. Rev. C 23, 2561 (1981).

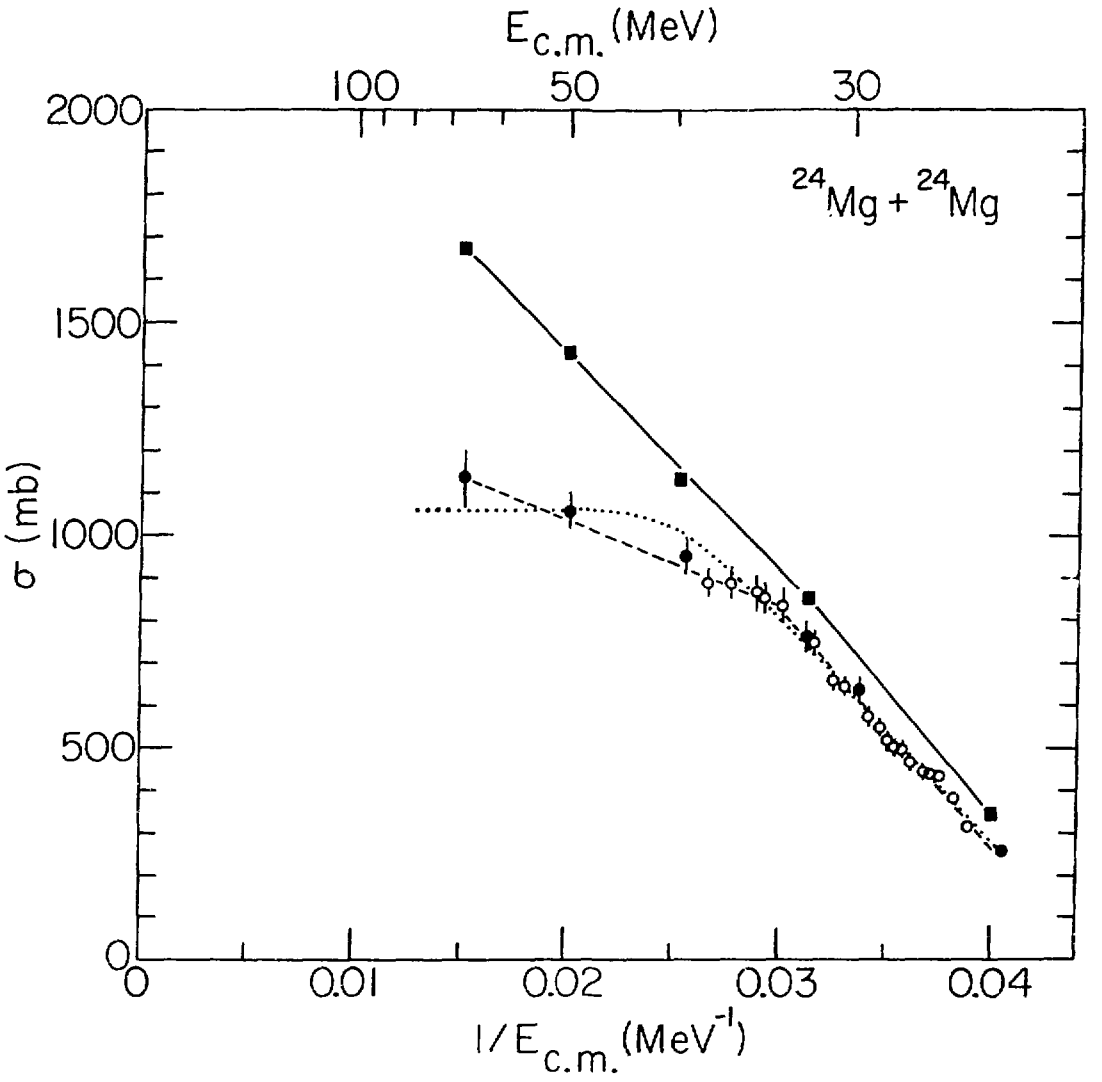

Fig. II-5. Total fusion cross sections for the $^{24}Mg+^{24}Mg$ system plotted as a function of $1/E_{c.m.}$. Full angular distributions are denoted by solid circles, and the single measurements are denoted by open circles. The solid curve is drawn to represent the total reaction cross section as determined by optical-model calculations of the elastic scattering (solid boxes). The dashed curve represents separate fits to the low-energy ($E_{c.m.}$ < 32 MeV) and high-energy ($E_{c.m.}$ > 34 MeV) fusion cross sections with the parameters R_B = 8.9 fm, V_B = 22.3 MeV, R_C = 6.8 fm, V_C = 14.2 MeV. The dotted curve represents a fit to the entire data set with R_B = 8.8 fm, V_B = 22.3 MeV, R_C = 5.8 fm, $\hbar\omega$ = 8.4 MeV, and V_C fixed to 0 MeV.

e. Measurement of Compound Nucleus K x-Ray Production Cross Sections for $^{37}Cl + ^{124}Sn$ and $^{32}S + ^{116,120,124}Sn$

H. Ernst, C. N. Davids, W. S. Freeman, W. Henning, and T. Humanic

We have recently extended our x-ray measurements to heavier compound nuclei, formed in the reactions $^{37}Cl + ^{124}Sn$ and $^{32}S + ^{116,120,124}Sn$. From evaporation residue-x-ray and x-ray– x-ray coincidence measurements, we derive a preliminary x-ray multiplicity of $\langle m_x \rangle \sim 1$, which is larger by two orders of magnitude than that found in the previously studied lighter system $^{28}Si + ^{48}Ti$, indicating highly-converted low-energy γ transitions. The large x-ray yields allow a very efficient determination of the branching ratios between n, p, α, and 2α evaporation channels, since the necessary Z resolution is easily obtained from the x-ray spectra as displayed in Fig. II-6(a). For the reactions $^{32}S + ^{116,120,124}Sn$, we have measured K x-ray excitation functions for the various evaporation channels between 130-MeV and 202-MeV incident ^{32}S energy. Some results are shown in Fig. II-6(b). These data are presently being compared with evaporation model calculations in order to understand the decay of the compound nucleus at very high angular momentum but comparatively low excitation energy, where shell corrections to the rotating liquid-drop model might be significant.

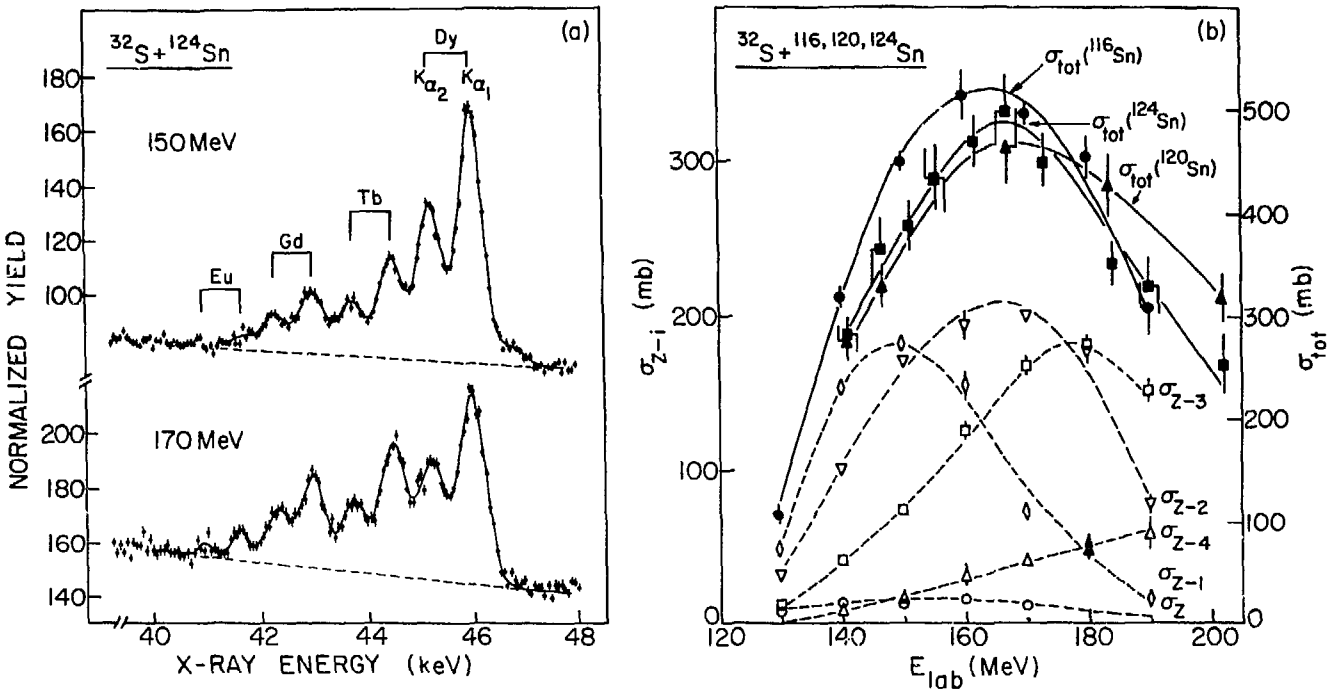

Fig. II-6. (a) x-ray spectra of evaporation residues from the reaction $^{32}S + ^{124}Sn$ at 150-MeV and 170-MeV incident energy. The $K_{\alpha 1}$ and $K_{\alpha 2}$ components for the various elements are indicated. The weaker K_β components which appear at higher energies are not shown. (b) Total x-ray production cross sections σ_{tot} (full symbols) versus E_{lab} for the reaction $^{32}S + ^{116,120,124}Sn$ leading to the $^{148,152,156}Dy$ compound nuclei. The open symbols show the partial cross sections from neutron (σ_Z) to 2α evaporation (σ_{Z-4}) for $^{32}S + ^{116}Sn$.

C. HIGH ANGULAR MOMENTUM STATES IN NUCLEI

This program investigates the structure at high spin of yrast states, the states just above the yrast line and the highly-excited continuum states. One aim has been to observe the variation of yrast structure as the neutron number increases from the closed shell N = 82 to N = 88, where prolate deformation begins to set in. To this end there has been a systematic investigation of a series of Dy isotopes with A = 148 to A = 154. Another objective has been to probe the evolution of the collective excitations built on aligned few-nucleon yrast states. Information on these collective excitations, which are excited with respect to the yrast line, has been obtained by investigating the yrast population pattern, the discrete gamma rays which directly feed the yrast states and the continuum gamma rays which connect highly excited levels. A third aspect of the program examines the validity of treating Z = 64 as a closed core. The experimental effort here is directed towards extracting the $(\pi h_{11/2})^n$ spectra as n increases from 3 to 6.

The experiments have utilized ^{32}S, ^{34}S, and ^{64}Ni beams from the superconducting linac and the recently completed gamma-ray facility which includes a sum spectrometer consisting of two 13-in. × 6-in. NaI crystals. There has been a close collaboration with Prof. P. J. Daly's group from Purdue University in this research program.

a. High-Spin Yrast Levels of $^{148,149,150,151,152}Dy$

T. L. Khoo, I. Ahmad,* J. Borggreen, P. Chowdhury, C. N. Davids, S. R. Faber, W. Kutschera, R. K. Smither, B. Haas,† H. R. Andrews,† O. Häusser,† P. Taras,† and D. Ward†

We have systematically studied the high spin levels of Dy isotopes as a function of neutron number outside the N=82 closed shell. The investigation of $^{148,149,151,152}Dy$ is finished and the results included in an extensive paper[1]; the study of ^{150}Dy is near completion. The yrast levels have been observed up to maximum spins of 22, (~47/2), 29, 71/2 and 40 as the neutron number increases from 82 to 86.

In each case it is observed that, for sufficiently large angular momentum input, there is almost 100% population of the yrast states up to or close to the maximum spin possible using only valence nucleons outside a Z=64, N=82 core. For larger spins the yrast population gradually decreases. The cause for this is not clear at present, but it may be related to an

*Chemistry Division, ANL.

†Chalk River Nuclear Laboratories, Chalk River, Ontario, Canada.

[1] B. Haas et al., Nucl. Phys. A362, 254 (1981).

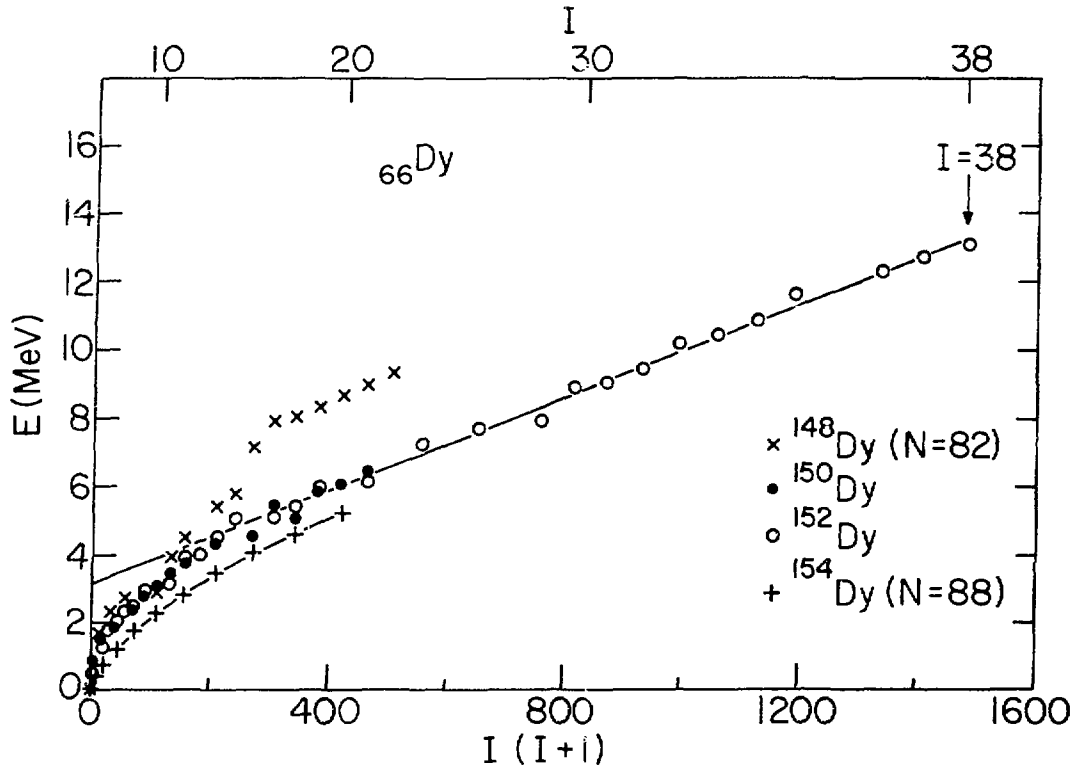

Fig. II-7. Plot of E vs I(I + 1) for the yrast states of several even Dy isotopes.

increased susceptibility to deformation when the core is broken and/or to an increase in the level density near the yrast line.

In ^{148}Dy the yrast line rises steeply above I = 10, the maximum valence spin, reflecting the energy cost associated with breaking the core (see Fig. II-7). The onset of core excitation in the more neutron rich Dy isotopes does not result in as prominent an increase in the slope of the yrast line. A possible explanation is that the gap above Z = 64 and N = 82 diminishes with the addition of neutrons—a consequence of the valence particles polarizing the core. The increased deformability of the broken core may also play a role.

While the yrast states of the Dy isotopes with $N \leq 86$ have predominantly single-particle configuration, those with $N \geq 90$ have prolate collective structures. We shall extend our studies to the N = 87 and N = 88 systems in order to observe the transition in yrast character and to study the competition between the prolate collective and oblate single particle modes.

b. Yrast Levels in ^{154}Dy

A. Pakkanen,* I. Ahmad,† J. Borggreen, P. Chowdhury, P. J. Daly,* Z. Grabowski, H. Helppi,* T. L. Khoo, Y. H. Park,* R. K. Smither, and J. Wilson*

The level structure of ^{152}Dy has been intensively studied in recent years, and the yrast states in this N=86 nucleus are now known up to a spin of 40. The yrast levels in ^{152}Dy are dominated by single-particle structures up to the maximum spin observed. On the other hand, the N=90 nucleus ^{156}Dy shows well-developed rotational bands typical of a prolate rotor. In the intermediate N=88 nucleus, ^{154}Dy, the yrast levels are firmly known only up to 16^+; our aim in the present study is to locate higher-lying states in this transitional nucleus, and to determine their character.

We performed in-beam γ-ray measurements using the ^{124}Sn(^{34}S,4n)^{154}Dy reaction, induced by 145—165-MeV ^{34}S beams from the linac. Extensive coincidence data were recorded using an array of three Ge(Li) detectors and a large NaI(Tl) sum spectrometer. Detection of γ rays belonging to the desired reaction channel was enhanced by setting suitable energy windows on the sum spectrum. The results obtained established the even-spin yrast states of ^{154}Dy up to a (32^+) level at 10 185 keV, and an odd-spin level sequence up to I = (29) at 9254 keV. No isomers with $T_{1/2} > 2$ ns were observed.

Plots of excitation energy vs I(I + 1) for the yrast states of ^{152}Dy and ^{154}Dy show that the effective moment of inertia for ^{152}Dy ($2\mathcal{J}/\hbar^2 = 147$ MeV^{-1}) is considerably larger than that of a rigid sphere ($2\mathcal{J}/\hbar^2 = 120$ MeV^{-1}), whereas the result for ^{154}Dy ($2\mathcal{J}/\hbar^2 = 124$ MeV^{-1}) is close to the rigid-sphere value. The large effective moment of inertia in ^{152}Dy is partly due to the occurrence of oblate aligned-particle configurations at the yrast line, but these do not appear to be present in ^{154}Dy below I = 28. Above this spin, however, our preliminary results indicate that the monotonic increase of yrast transition energies—symptomatic of collective behavior—gives way to irregular γ energies. This may be a reflection of the onset of single-particle states at the yrast line. If so, this could imply a transition from prolate rotation-aligned collective

*Purdue University, West Lafayette, Indiana.

†Chemistry Division, ANL.

structures to oblate few-particle configurations similar to those of ^{152}Dy. Further experiments, including lifetime measurements, will be necessary to confirm these speculations. After completing the analysis of our present data, we plan to perform lifetime measurements using a plunger which is currently being designed.

c. Search for a Very High Spin Isomer in ^{152}Er

P. Chowdhury, I. Ahmad,* Y. H. Chung,† P. J. Daly,† S. R. Faber,† Z. W. Grabowski, H. Helppi,† T. L. Khoo, A. Pakkanen,† R. K. Smither, and J. Wilson†

In the $^{152}_{68}Er_{84}$ nucleus, the existence of a very high-spin ($\sim$36 $\hbar$) isomer, with $t_{1/2} \sim 4$ ns at an excitation energy $\gtrsim$12.2 MeV, has been suggested,[1] in addition to an observed 32-ns isomer at 9 MeV. The recent availability of energetic ^{64}Ni beams from the Argonne Superconducting Linac allowed a preliminary investigation of this isomer. The residual nuclei, formed by the bombardment of a thin self-supporting ^{92}Zr target ($\sim$1 mg cm^{-2}) by a 293-MeV ^{64}Ni beam, were allowed to recoil into vacuum for a distance of 16 cm before being stopped by a catcher foil (80 mg cm^{-2} Pb). The recoil distance translates to a flight time of $\sim$13 ns for a 0.04 c recoil velocity attained with the Ni beam. The two halves of a sum spectrometer (two 6-in. × 13-in. NaI crystals) were used as separate total energy detectors in coincidence with a Ge(Li) detector. The target was placed 2 in. inside the first crystal, while the catcher foil was inside the second. This configuration allowed the first NaI to both detect the prompt γ radiation and effectively shield the second NaI and Ge(Li) from the prompt radiation. The second NaI thus detected the sum energy of delayed events only. Data were taken in a 8-parameter event-mode basis, which included the time between the Ge(Li) and both NaI crystals. By setting gates on the total energy, an almost unique selection of the 4n evaporation channel, leading to a residual ^{152}Er nucleus, can be achieved. In addition, appropriate time gates can lead to the enhancement of either prompt, singly delayed, or doubly delayed γ rays in the decay of the ^{152}Er nucleus. Preliminary analysis reveals that the

*Chemistry Division, ANL.

†Purdue University, West Lafayette, Indiana.

[1] J. Borggreen et al., Z. Phys. A294, 113 (1980).

sum spectrum observed in the second NaI in coincidence with the bottom yrast transitions in the ^{152}Er nucleus exhibits two peaks consistent with the existence of two isomers at 9 and ≥12.2 MeV, although the possibility of the higher-energy component being due to leakage of prompt radiation from the target has yet to be fully investigated. The results of this experiment advocate a more detailed investigation of this high-spin isomer.

d. Study of Continuum γ-Ray Spectra of ^{151,152}Dy

J. Borggreen, P. Chowdhury, T. L. Khoo, I. Ahmad,* R. K. Smither, S. R. Faber,† P. J. Daly,† C. L. Dors,† and J. Wilson†

We have utilized 148, 160, and 172-MeV ^{34}S beams from the Argonne linac to populate states in ^{151,152}Dy in an attempt to determine the relationship between the population of high-spin yrast states and the continuum of γ rays feeding these discrete states. We have observed continuum γ rays in a 10-in. × 12-in. NaI detector (with a 3-in. diameter central collimator) which were coincident with events in a sum spectrometer. By selecting high-sum energy slices, high angular momentum states are enhanced. The contribution of discrete lines is subtracted and the resultant spectra corrected for detector response (unfolded) to yield the true continuum spectra. By assuming the presence of only stretched transitions, we have used the 0° and 90° spectra to decompose the continuum spectra into a stretched dipole and a stretched quadrupole component. The stretched dipole component is located around 0.5 MeV, while the stretched E2 part shows two discernible components, centered around 0.6 and 1.3 MeV (see Fig. II-8). With increasing sum energy, and corresponding increase in angular momentum input, the following features are observed: (i) all components increase in multiplicity; (ii) the higher energy E2 component grows with respect to the lower energy one; and (iii) the centroid of the higher energy E2 component increases rapidly initially and then only gradually at the highest sum energies. The third feature is clearly observed by taking differences between successive slices [see Fig. II-8(b)] to reveal the transitions occurring in successive ℓ windows. These results, together with the feeding pattern of the yrast line, imply that the deexcitation of high-ℓ events

*Chemistry Division, ANL.

†Purdue University, West Lafayette, Indiana.

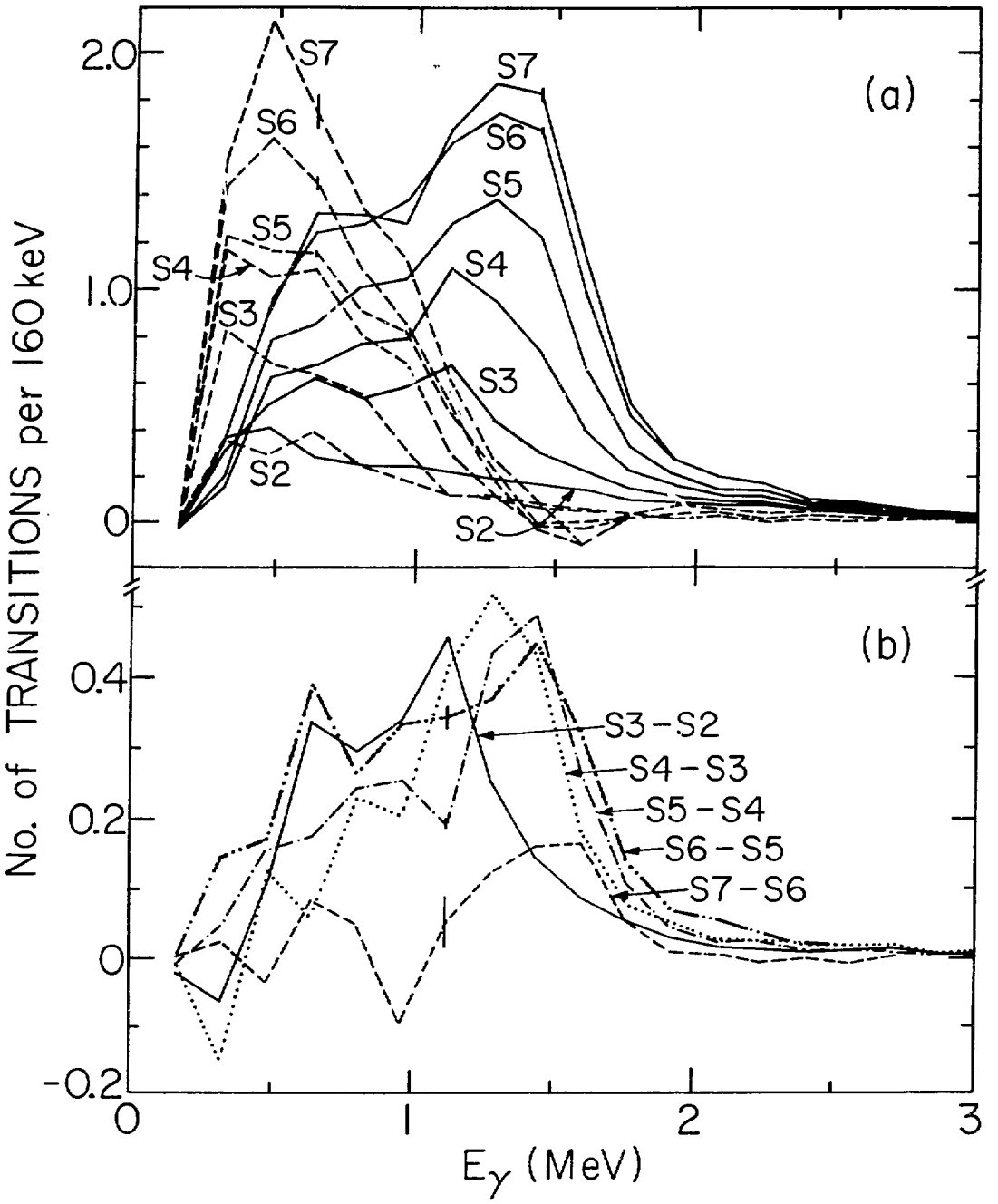

Fig. II-8. (a) Stretched quadrupole (solid lines) and stretched dipole (dashed lines) components of the unfolded spectrum of continuum γ rays coincident with sum energy slices 2 to 7, where each slice is $\sim$6 MeV wide. Contributions from discrete and statistical γ rays have been subtracted. (b) Differences between spectra associated with successive slices of Fig. II-8(a) for the stretched quadrupole component. Typical error bars are shown for each spectrum.

($\ell \gtrsim 30$) is not feeding the yrast line directly but is diverted by continuum cascades with significant E2 character, and only reaches the yrast line in the spin interval between 30 and 40. These results suggest the presence of collective structure above the yrast line, which, up to spin 38, is dominated by few-particle configurations.[1] (The nature of the yrast line beyond this spin has still not been determined.)

The occurrence of the dipole bump and its increasing multiplicity with increasing energy are not understood at present. If it has M1 character, it may be consistent with the emission from a rotating triaxial nucleus.

To determine whether the dipole component has magnetic or electric character, we plan to observe the conversion electron yield as a function of angular momentum by measuring the K x-ray yield as a function of sum energy. To provide unambiguous confirmation of collective structures above the yrast line, we intend to measure the lifetimes associated with the continuum transitions, either directly or by means of the feeding times of the highest spin yrast states. The latter measurement will employ a plunger, now being designed, which fits inside the sum spectrometer.

[1] P. Chowdhury et al., to be published in Phys. Rev. Lett.

e. Systematics of Continuum States in Dy and Er Nuclei

Z. W. Grabowski, S. R. Faber,* I. Ahmad,† P. Chowdhury, P. J. Daly,* H. Helppi,* T. L. Khoo, Y. H. Park,* A. Pakkanen,* R. K. Smither, and J. Wilson*

Our studies of the discrete yrast states of $^{148-154}$Dy isotopes have shown that while the yrast lines of $^{148-152}$Dy are predominantly of single-particle character, that of ^{154}Dy is mainly rotational. On the other hand, we have data indicating that the continuum states above the yrast line of ^{152}Dy have collective properties.[1]

The continuum γ spectrum in ^{152}Dy exhibits a stretched-dipole component centered around 0.6 MeV and a stretched-E2 component located around 1.3 MeV, while in the rotational Er nuclei it consists mainly of an E2 bump. The higher-energy edge of the E2 bump in rotational nuclei shifts up in

* Purdue University, West Lafayette, Indiana.

† Chemistry Division, ANL.

[1] P. Chowdhury et al., to be published in Phys. Rev. Letters.

energy with increasing angular momentum—as expected for a rotor—whereas that for ^{152}Dy shifts at a slower rate. It is thus of interest to study the evolution in the character of continuum spectra as the nature of the yrast states changes from single particle to collective with increasing neutron number. Consequently, we have used beams of ^{32}S, ^{34}S, and ^{64}Ni from the linac to produce $^{148-154}$Dy, ^{152,154,158}Er and have observed their continuum γ spectra in large NaI detectors operated in coincidence with a sum spectrometer. The data analysis is now in progress.

f. Lifetimes of Continuum States

S. R. Faber,* P. Chowdhury, I. Ahmad,† P. J. Daly,* Z. Grabowski, H. Helppi,* T. L. Khoo, A. Pakkanen,* Y. H. Park,* R. K. Smither, and J. Wilson*

Our studies suggest the occurrence of collective structures above the yrast line of ^{152}Dy, even though the yrast states are predominantly of few-particle structure up to the highest spin (40) observed. This inference stems partly from the occurrence of an E2 component centered at 1.3 MeV in the continuum γ spectrum of ^{152}Dy. Measurements of lifetimes of the continuum states should provide unambiguous confirmation of collectivity. To this end we plan two types of experiments: measurements of (a) the lifetimes associated with the continuum γ's, using a technique introduced by the group at Berkeley, and (b) the feeding times of discrete yrast states as a function of input angular momentum.

We have performed measurements to obtain the lifetimes associated with the continuum E2 bump. In order to obtain a large recoil velocity ($\sim$0.04 c), we have used a 273-MeV ^{64}Ni beam, recently available from the linac, and the ^{94}Zr (^{64}Ni,4n) reaction to form ^{154}Er, which has properties similar to ^{152}Dy.

The target, located inside the sum-energy spectrometer, was viewed by two large NaI detectors at 0° and 90°. The continuum bump and the 4n evaporation channel of interest were enhanced by setting a high sum-energy window. The 0° spectra obtained with the evaporation residue recoiling into a Pb stopper (stopping time $\sim$3 ps) and into vacuum were compared. In the latter case, the continuum-γ spectrum is expected to be completely

*Purdue University, West Lafayette, Indiana.

†Chemistry Division, ANL.

Doppler shifted in energy, while in the former, portions of the spectrum could be shifted to varying degrees, depending on the lifetimes of the states and the cascade history. The lower edge of the E2 bump revealed a larger relative Doppler shift than the higher edge. Analysis of the data is currently in progress.

g. The $(\pi h_{11/2})^3$ Spectrum in the Three Valence Proton Nucleus $^{149}_{67}Ho_{82}$

J. Wilson,* S. R. Faber,* P. J. Daly,* I. Ahmad,† J. Borggreen, P. Chowdhury, T. L. Khoo, R. D. Lawson, R. K. Smither, and J. Blomqvist‡

Recent investigations have shown that ^{146}Gd, with Z = 64, N = 82, is a particularly stable nucleus, and that high-spin excitations in adjacent few-valence-particle nuclei can be well described in terms of shell-model configurations. In the two-proton nucleus ^{148}Dy a complete $(\pi h_{11/2})^2$ spectrum has been identified, thereby furnishing the nucleon-nucleon-interaction matrix elements for $h_{11/2}$ protons. With this information, the level spectra of $(\pi h_{11/2})^n$ configurations in the N=82 nuclei with Z > 66 can be calculated.

We have performed the first study of yrast states in the three proton N=82 nucleus ^{149}Ho using 155—180-MeV ^{32}S beams on enriched ^{121}Sb and ^{122}Te targets. These targets were located at the center of a sum spectrometer consisting of two 33 cm × 15 cm NaI crystals with ports at 90° to the beam direction for two 15% Ge(Li) detectors. With this arrangement, five parameter $E_{\gamma 1}$, $E_{\gamma 2}$, E_{sum}, $t_{\gamma\gamma}$, and $t_{\gamma sum}$ data were accumulated. In the analysis, attention was focused on γ rays delayed with respect to the sum signal and particularly on a group of eight γ rays which were observed to be doubly delayed; specifically, they deexcite the lower of two isomers with half-lives exceeding 50 ns in the residual nucleus. These eight lines are assigned to ^{149}Ho because they showed the same excitation function behavior as a strong 1091-keV decay line of ^{149}Ho, their intensities accounted for virtually the entire population of the ^{149}Ho $11/2^-$ "ground state" in all the bombardments, and the coincident-sum energy was that expected from the $^{122}Te(^{32}S,p4n)^{149}Ho$ reaction channel.

---

*Purdue University, West Lafayette, Indiana.

†Chemistry Division, ANL.

‡Research Institute of Physics, Stockholm, Sweden.

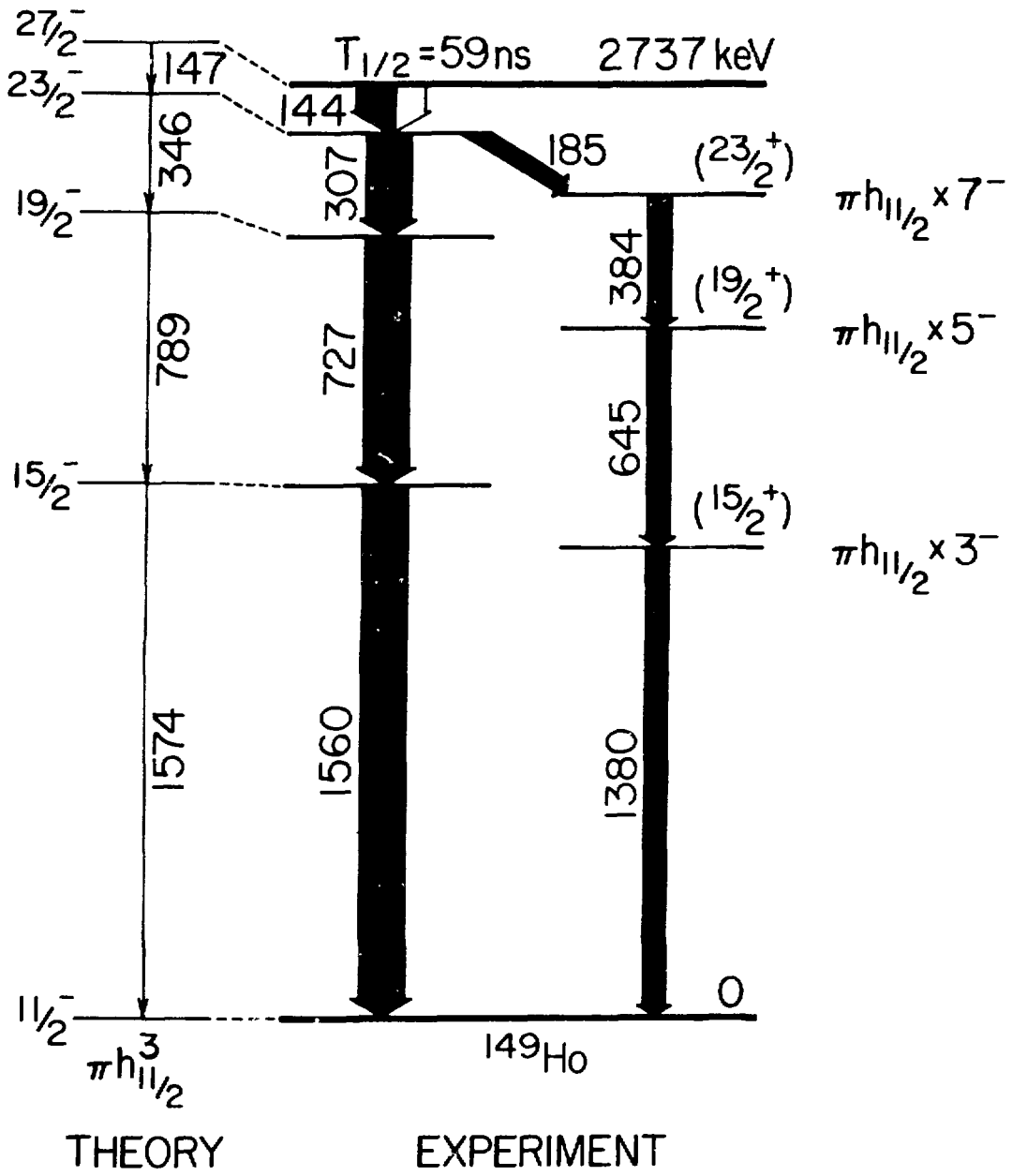

Fig. II-9. The ^{149}Ho level scheme and the calculated $\pi h^{3}_{11/2}$ spectrum.

The results, which have been published,[1] show that the $(\pi h_{11/2})^3$ spectrum is in very good agreement with that calculated using empirical matrix elements from ^{148}Dy (see Fig. II-9). The lifetime of a $27/2^-$ isomer in ^{149}Ho is also in excellent agreement with the predicted value. In addition to the $(h_{11/2})^3$ negative-parity states, positive-parity states, arising from their coupling to the 3^-, 5^-, and 7^- states in ^{148}Dy, are also observed. Again the agreement between experiment and theory is good. These results lend support to the contention that ^{146}Gd acts as a closed-shell nucleus.

[1] J. Wilson et al., Z. Phys. A296, 185 (1980).

h. Yrast Spectroscopy of the N=83 Nucleus ^{150}Ho

J. Wilson,* S. R. Faber,* P. J. Daly,* I. Ahmad,† J. Borggreen, P. Chowdhury, T. L. Khoo, R. D. Lawson, and R. K. Smither

In addition to the ^{149}Ho results described in the preceding contribution, the γ-ray studies with the ^{32}S + ^{121}Sb and ^{32}S + ^{122}Te reactions also yielded the first information about high-spin excitations in the N=83 nucleus ^{150}Ho. Isotopic identification of the ^{150}Ho γ rays was based on (1) excitation function and γγ coincidence results, (2) intensity balance with known radioactivity γ rays accompanying the β decay of the ^{150}Ho $(\pi h_{11/2}\nu f_{7/2})\ 9^+$ "ground state," and (3) the observed coincident-sum spectra. A few of these γ rays have been observed by other workers in survey studies of isomerism in the A=150 region. The present work[1] has identified three isomers in ^{150}Ho with half-lives of 17 ± 4 ns, 86 ± 12 ns, and >500 ns. The γγ coincidence and timing measurements have established the level scheme up to a 86 ns isomer at 2625 keV. Although transition multipolarities have not been determined, knowledge of the excitation modes in adjacent Tb, Dy, and Ho nuclei allow us to assign spin-parity values with some confidence. There is good agreement between the observed yrast sequence of $(\pi h_{11/2})^3\nu f_{7/2}$ levels and that calculated in the shell model (see Fig. II-10) using empirical nucleon-nucleon interactions for $h_{11/2}$ protons from the ^{148}Dy

* Purdue University, West Lafayette, Indiana.

† Chemistry Division, ANL.

[1] J. Wilson et al., to be published in Phys. Lett.

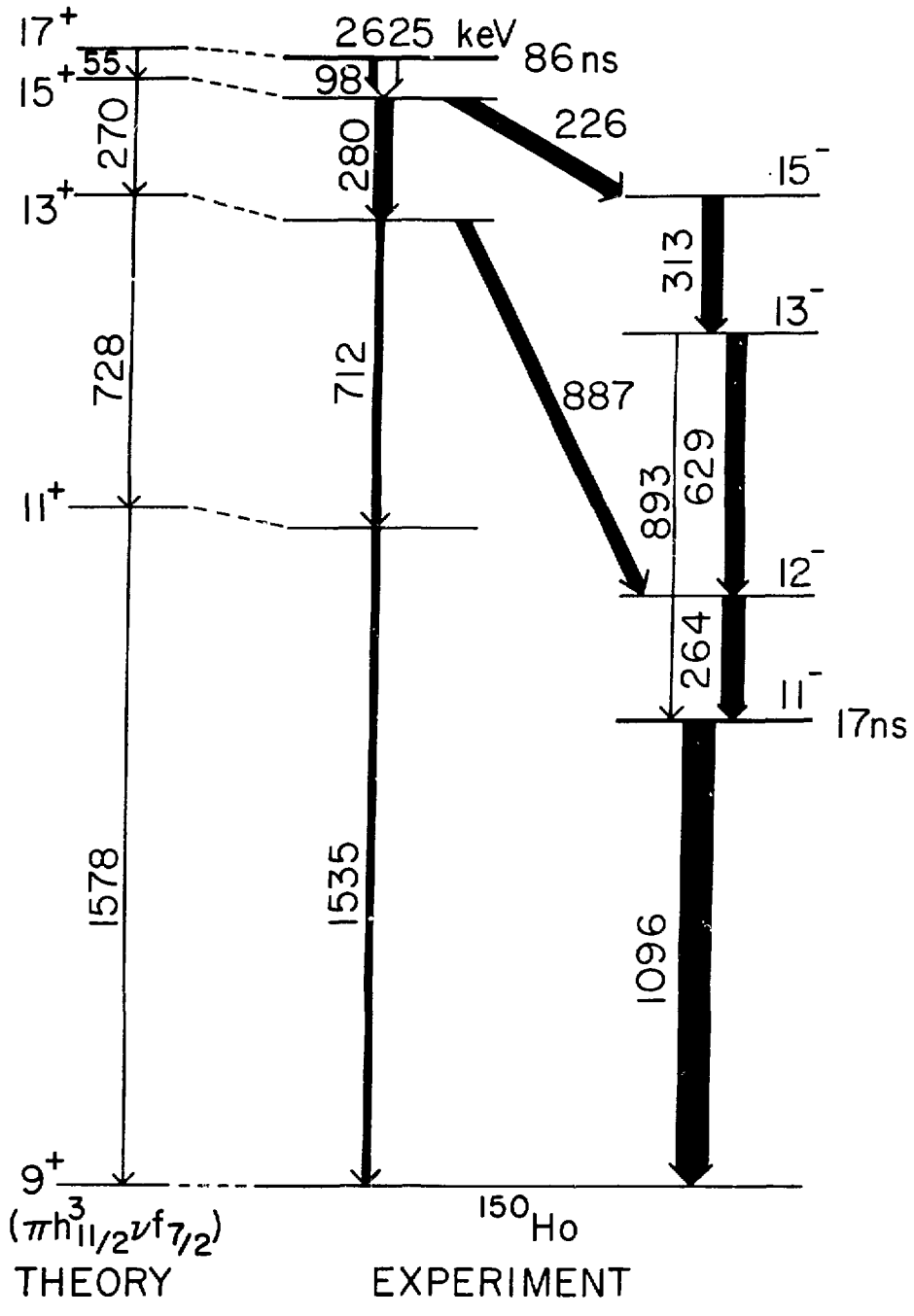

Fig. II-10. The ^{150}Ho level scheme and the calculated $(\pi h_{11/2})^3 \nu f_{7/2}$ yrast level spectrum.

spectrum and $\pi h_{11/2}\nu f_{7/2}$ interactions determined using the Schiffer-True central potential.

The transition probability obtained from the measured half-life of the 17^+ isomeric state

$$B(E2,\ 17^+ \rightarrow 15^+) = 176 \pm 24\ e^2fm^4$$

is about twice as large as the value determined for the $27/2^- \rightarrow 23/2^-$ $(\pi h_{11/2})^3$ transition in ^{149}Ho, clearly demonstrating that the $f_{7/2}$ neutron is not limited to a spectator role in the ^{150}Ho $17^+ \rightarrow 15^+$ transition. Using empirical proton and neutron effective changes deduced from ^{148}Dy and ^{150}Dy, respectively, the shell-model calculation yields a reduced transition probability in agreement with experiment.

The negative-parity states are also rather interesting; all have close structural relationships to known states of the adjacent nuclei ^{149}Dy, ^{149}Ho, and of the odd-odd isotone ^{148}Tb. The last-named nucleus features an M2/E3 isomeric 11^- state at 1006 keV, interpreted as the lowest member of a $\pi h_{11/2}\nu f_{7/2} \times 3^-$ multiplet, and a 12^- state at 1290 keV of dominant $\pi h_{11/2}\nu i_{13/2}$ character. The 11^- isomer and 12^- state in ^{150}Ho are obvious counterparts of those ^{148}Tb states.

Investigation of the ^{150}Ho yrast states lying between the 86-ns isomer and the much higher-lying ∿500-ns isomer is continuing.

D. REACTION MECHANISMS AND DISTRIBUTIONS OF REACTION STRENGTHS

In the past year studies of reaction mechanism and distributions of reaction strengths have been extended to higher energies and heavier target nuclei as a consequence of increased accelerator capability. Not only single-nucleon transfer, but all quasi-elastic channels (elastic scattering plus transfer) have now been studied at an energy far above the Coulomb barrier in the $^{16}O + ^{48}Ca$ system. Other studies include energy dependence of inclusive alpha-particle yields from ^{16}O induced reactions and reaction channel distributions for $^{32}S + ^{40,48}Ca$ systems. Fusion-fission reactions induced by Ni beams allow the formation of compound systems of high angular momentum and relatively low excitation energy, thereby enhancing the probability of observing pre-equilibrium effects.

a. Single-Nucleon Transfer Reactions Induced on ^{48}Ca by ^{12}C Beams at $E_{lab}(^{12}C) = 45$ MeV

J. Petersen,* R. Ascuitto,* D. G. Kovar, W. Henning, S. J. Sanders, and M. Paul

The analysis of discrete transitions in the $^{48}Ca(^{12}C,^{11}B)^{49}Sc$ and $^{48}Ca(^{12}C,^{13}C)^{47}Ca$ transfer reactions at $E_{lab}(^{12}C) = 45$ MeV, leading to low-lying states, has been completed. The purpose of this study was to investigate the reaction mechanism in heavy-ion induced single-nucleon transfer reactions. Studies have shown that transfer reactions in this mass and energy range cannot, in general, be well described by conventional DWBA calculations. Recently, an effective Q-value model has been proposed which was able to reproduce the angular distribution behaviors observed in single-nucleon transfers induced by ^{16}O on ^{48}Ca. The $^{12}C + ^{48}Ca$ system in the present study differs from $^{16}O + ^{48}Ca$ in that the ^{12}C projectile can be strongly excited to its first excited 2^+ state at 4.43 MeV. Calculations that neglect the inelastic excitation show that although the fits to the data are better using the effective Q-value model, the predictions still do not describe the detailed behavior. However, when the optical potential from a coupled-channels treatment of elastic plus 2^+ inelastic is used, the effective Q-value model gives an accurate description of the data.

---

*Yale University, New Haven, Connecticut.

b. Energy Dependence of Inelastic Scattering and Transfer Reactions of ^{16}O on ^{48}Ca

T. J. Humanic, H. Ernst, D. F. Geesaman, W. Henning, J. P. Schiffer, and B. Zeidman

In a previous experiment at the Argonne FN tandem accelerator, elastic, inelastic, and transfer-reaction channels in the reaction ^{16}O on ^{48}Ca were studied at E_{lab} = 56 MeV.[1] These data have proven extremely useful in tests of reaction-model calculations. With the availability of higher energy ^{16}O beams from the Argonne superconducting linac, it has now become possible to explore the energy dependence of the $^{16}O + ^{48}Ca$ system far above the Coulomb barrier. The only other system involving closed-shell nuclei, for which data exist over a large energy range, is $^{16}O + ^{208}Pb$. Large discrepancies are found between model predictions and data.[2]

Figure II-11 shows results for the $^{16}O + ^{48}Ca$ reaction measured at E_{lab} = 158.2 MeV. Experimental angular distribution and DWBA calculations are shown for some transfer channels. The DWBA curves were calculated with the use of optical-model parameters from a fit to the 158.2-MeV elastic scattering angular distribution, and using the same spectroscopic factor as at 56-MeV incident energy. Overall the data are rather well reproduced (except for the neutron transfer to the $^{17}O^*$ first excited state), and do not show the large discrepancies observed in the energy dependence of the $^{16}O + ^{208}Pb$ reaction.

---

[1] D. G. Kovar et al., Phys. Rev. C 17, 83 (1978).

[2] S. C. Pieper et al., Phys. Rev. C 18, 180 (1978).

c. Excitation Functions of Heavy-Ion Induced Fusion-Fission with ^{58}Ni Beams

W. Henning, H. Ernst, D. F. Geesaman, T. Humanic, F. Prosser,* R. Racca,* and B. Zeidman

We have extended our studies of heavy-ion-induced fusion-fission reactions to heavier systems by making use of the ^{58}Ni beams that have recently become available at the linac with energies that allow us to surmount the Coulomb barrier, even for heavy target nuclei. Excitation functions have been measured in the energy range 235 MeV $\leq E_{lab} \leq$ 319 MeV

---

*University of Kansas, Lawrence, Kansas.

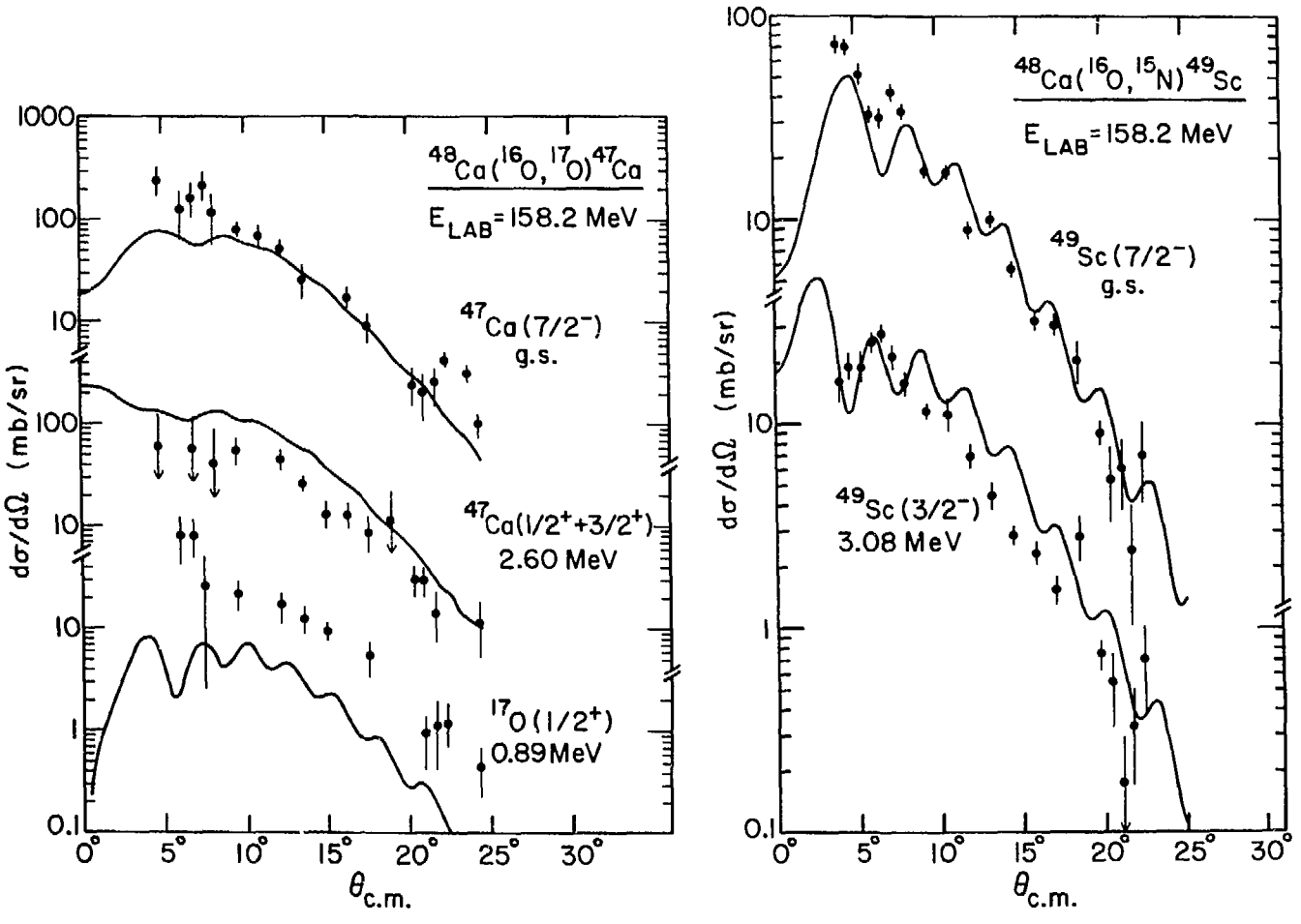

Fig. II-11. Single-nucleon transfer angular distributions for the $^{16}O+^{48}Ca$ reaction at 158.2-MeV incident energy.

for ^{58}Ni ions incident on targets of ^{118,124}Sn, ^{144,154}Sm, and ^{170}Yb. With the heavier ^{58}Ni projectiles, compound nuclei are formed at high angular momentum with lower excitation energy than is possible with lighter projectiles. This is expected to enhance the chance of survival against fission for exotic nuclei, one of the problems of central interest in these studies. The results are presently being analyzed. We plan to compare the excitation functions to predictions of the liquid-drop model and investigate to what extent shell effects are important. We further plan to extend these fission measurements to heavier targets (^{208}Pb, ^{238}U) and also complement them with direct fusion evaporation-residue measurements using an electrostatic deflector.

d. Fragmentation of ^{18}O Projectiles at 141 MeV

S. L. Tabor,* L. C. Dennis,* K. W. Kemper,* J. D. Fox,* K. Abdo,* G. Neuschaefer,* D. G. Kovar, and H. Ernst

The energy spectra and angular distributions between θ_{lab} = 7.5° and 40° of outgoing Li, Be, B, C, and N ions have been measured following the bombardment of ^{12}C, ^{27}Al, and ^{46}Ti targets with 141-MeV ^{18}O. The Z identification was provided by a ΔE-E telescope. All spectra exhibit broad continuum peaks centered at approximately the beam velocity. The shapes and angular distributions of these continuum structures are rather well described by a Serber-type fragmentation model,[1] which assumes that the unobserved fragment is transferred to the target.

The energy spectra of the fragments with $3 \leq Z < 8$ and their angular distributions are plotted in Figs. II-12 and II-13 for the reaction ^{18}O + ^{27}Al. The results are similar for the other targets, indicating that the observed fragments play only a spectator role in the reaction. A comparison[2] with earlier results obtained at Florida State University using a 72-MeV ^{18}O beam, shows that the fragmentation yield grows dramatically with increasing beam energy.

---

*Florida State University, Tallahassee, Florida.

[1] R. Serber, Phys. Rev. 72, 1008 (1947).

[2] S. L. Tabor, L C. Dennis, K. W. Kemper, J. D. Fox, K. Abdo, G. Neuschaefer, D. G. Kovar, and H. Ernst, to be published.

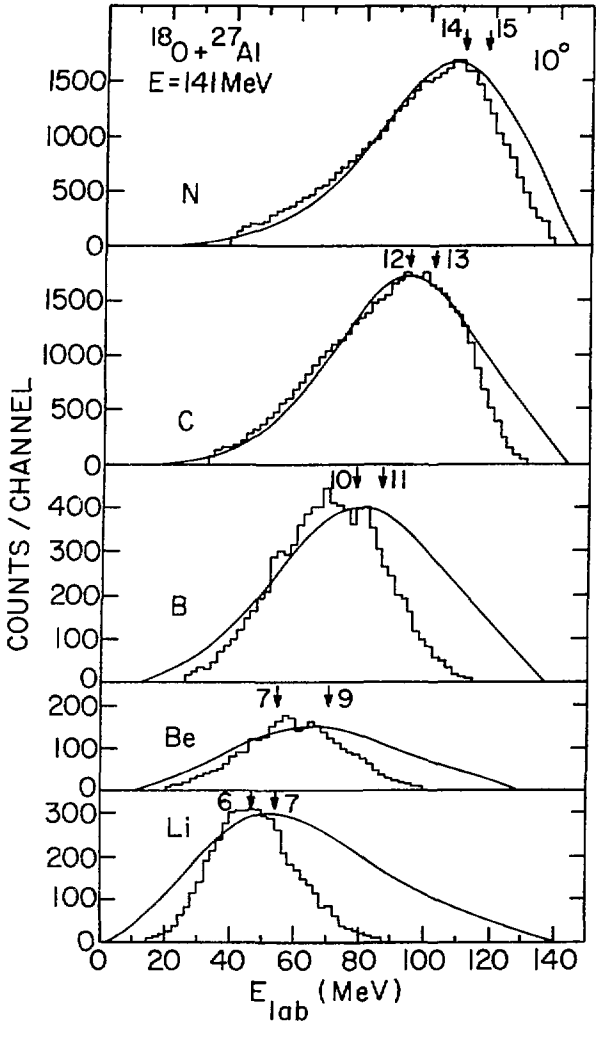

Fig. II-12. Energy spectra of fragmentation products from the $^{18}O+^{27}Al$ reaction at E_{lab} = 141 MeV and θ_{lab} = 10°. The solid lines are Serber-type model calculations. The arrows indicate the energy for a particle traveling at beam velocity.

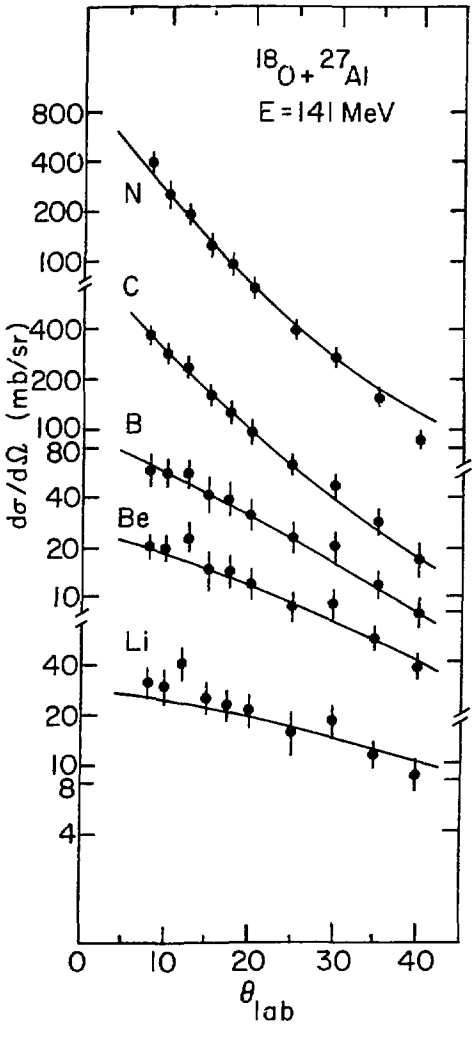

Fig. II-13. Angular distributions of fragmentation products from the $^{18}O+^{27}Al$ reaction at E_{lab} = 141 MeV. The solid lines are Serber-type model calculations.

e. Mechanism of Heavy-Ion Reactions at 7.5 to 20 MeV/amu: Singles and Coincidence Measurements of Light and Projectile-like Ejectiles

G. Bohlen,* M. Bürgel,* C. Egalhaff,* H. Fuchs,* A. Gamp,* H. Homeyer,* D. Kovar, and H. Gluge*

Inclusive cross sections for α particles and projectile-like fragments have been measured for the $^{20}Ne + ^{197}Au$ system at four bombarding energies between 150 and 400 MeV, and coincidence measurements at E_{lab} = 291 MeV using beams from the VICKSI accelerator. The most interesting observations in the singles measurements[1] regard to the widths of the momentum distributions for quasi-elastic fragments which are found to change slowly as function of bombarding energy and to be significantly smaller than those observed at very high energies (e.g., 2 GeV/amu). These observations contradict previously reported results[2] suggesting a rapid change in reaction mechanism near 20 MeV/amu, in particular the existence of a rapid onset of fragmentation or decay from a non-equilibrium high temperature subsystem. In the coincidence measurements the angular and energy correlations between α particles and projectile-like heavy ions indicate that the majority of α particles are sequentially emitted from projectile-like nuclei produced in the interaction.[3] In particular, excited levels or groups of levels in the emitting fragments (e.g., ^{20}Ne and ^{19}F) could be identified and shown to be correlated with levels strongly excited in light-ion inelastic scattering or transfer reactions. No evidence was found for significant contributions from direct elastic or inelastic breakup.

*Hahn Meitner Institut für Kernphysik, Berlin, West Germany.

[1] C. Egelhaaf et al., Phys. Rev. Lett. 46, 813 (1981).

[2] C. K. Gelbke, Proceedings of Deep-Inelastic and Fusion Reactions with Heavy Ions, edited by W. von Oertzen, Lecture Notes in Physics, Vol. 117 (Springer-Verlag, New York, 1980), p. 210; C. K. Gelbke et al., Phys. Lett. 70B, 415 (1977).

[3] H. Homeyer et al., Fall 1981 Nuclear Physics APS Meeting, Asilomar, 28-30 October 1981.

f. A Possible New Technique for the Measurement of Quadrupole Moments of Short-lived Excited States

H. Ernst, W. Henning, T. Humanic, T. L. Khoo, Steven C. Pieper, and J. P. Schiffer

A fast heavy ion subjected to a slowing-down force in a solid certainly experiences a strong electric field. Such a field must have a gradient which will be dominated by the dynamic spacial polarization of those inner electrons of the moving ion that are on the verge of being stripped off. Such a transient electric field gradient interacts with the quadrupole moment of the moving ion and causes a perturbation in the angular correlation of the decay γ rays emitted by the nucleus.

In an attempt to detect such a perturbation, two experiments were performed. In one case, 85-MeV ^{32}S ions from the tandem were inelastically scattered from 1.1 mg/cm^2 and 5 mg/cm^2 natural nickel targets; the thicker target was sufficiently thick to stop all recoil ions. The decay γ rays of the Coulomb-excited 2^+ states in either projectile or target nuclei were detected by three NaI detectors and a Ge(Li) detector in coincidence with the scattered ^{32}S ions measured in a Si surface-barrier detector. The geometry was optimized using Coulomb amplitudes calculated with the computer program Ptolemy. Targets of different thicknesses were chosen to observe changes in the perturbation of the angular correlation due to different interaction times. The stopping times of the moving ions were of the order of 1 picosecond, which is longer than the lifetimes of the first 2^+ states of $^{58,60}Ni$ and ^{32}S.

Because within error bars, no clear effect was observed in this first attempt, we performed a second experiment with higher sensitivity, making use of a 125-MeV ^{56}Fe beam from the superconducting linac and employing the kinematically reversed reaction on ^{24}Mg targets of 0.20 mg/cm^2 and 0.65 mg/cm^2 thickness. An experimental setup similar to that of the previous experiment was used. Figure II-14 shows the result of the optimization for the detector geometry. In this second measurement none of the targets is thick enough to stop either the recoiling or the scattered nuclei. The ^{56}Fe ions lose 6 MeV and 19 MeV in the thin and thick targets, respectively. The ^{24}Mg ions lose 3 MeV in the thin and 10 MeV in the thick target. The time the ions spend traveling through the target is a fraction of a picosecond, smaller than the several-picosecond lifetimes of their 2^+

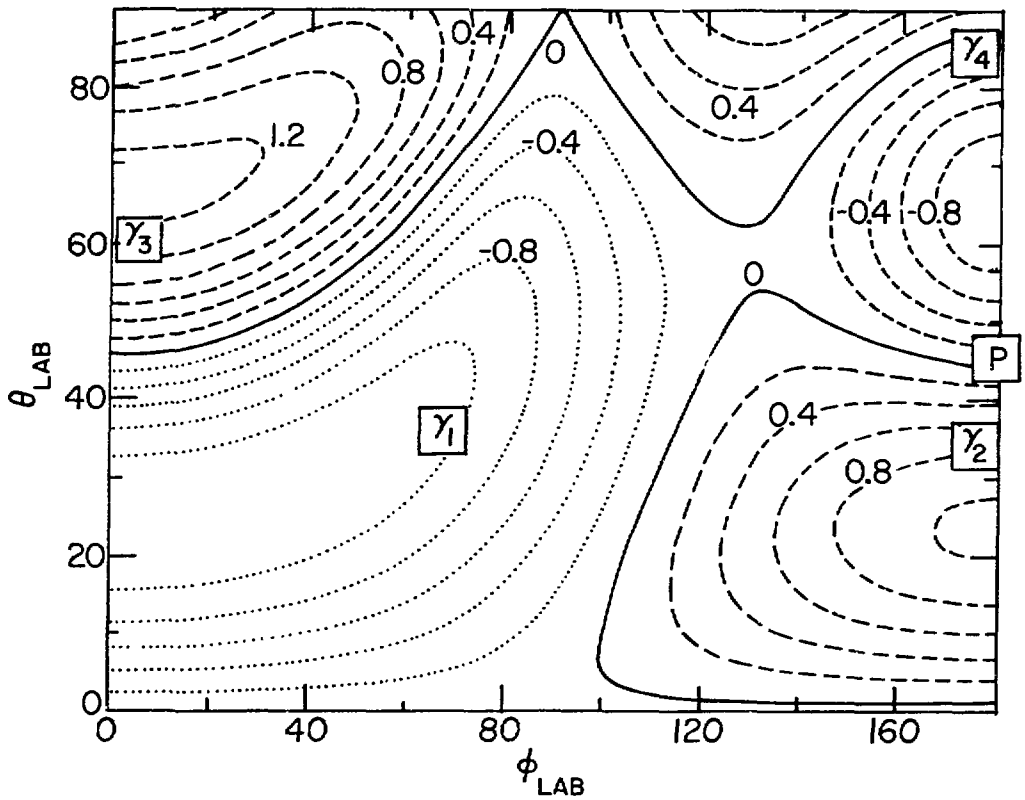

Fig. II-14. Contours of $[dP(\theta,\phi)/d(\omega\tau)]/\sqrt{P(\theta,\phi)}$ in the θ-ϕ plane for 120-MeV ^{56}Fe ions incident on Mg nuclei. P is the emission probability (normalized to unity on the sphere) of a γ ray emitted from Mg^* in coincidence with a recoiled Mg ion detected in the silicon detector; $\omega\tau$ is the quadrupole precession. The peaks of the contour plot indicate maximum sensitivity to such precession. The positions of the γ detectors, γ_1 to γ_4, and the particle detector, P, are indicated in the figure. As can be seen, γ_1 to γ_4 do not coincide exactly with the calculated maxima; the actual angles chosen are a compromise between the peak locations in this plot and in a similar one for Fe^*, since the decay γ rays of Fe^* and Mg^* were observed simultaneously. The finite solid angles ($\sim$35° diameter) of the detectors are taken into account by appropriate averaging. Note that the contours show the expected up-down symmetry as well as symmetry under inversion through the target.

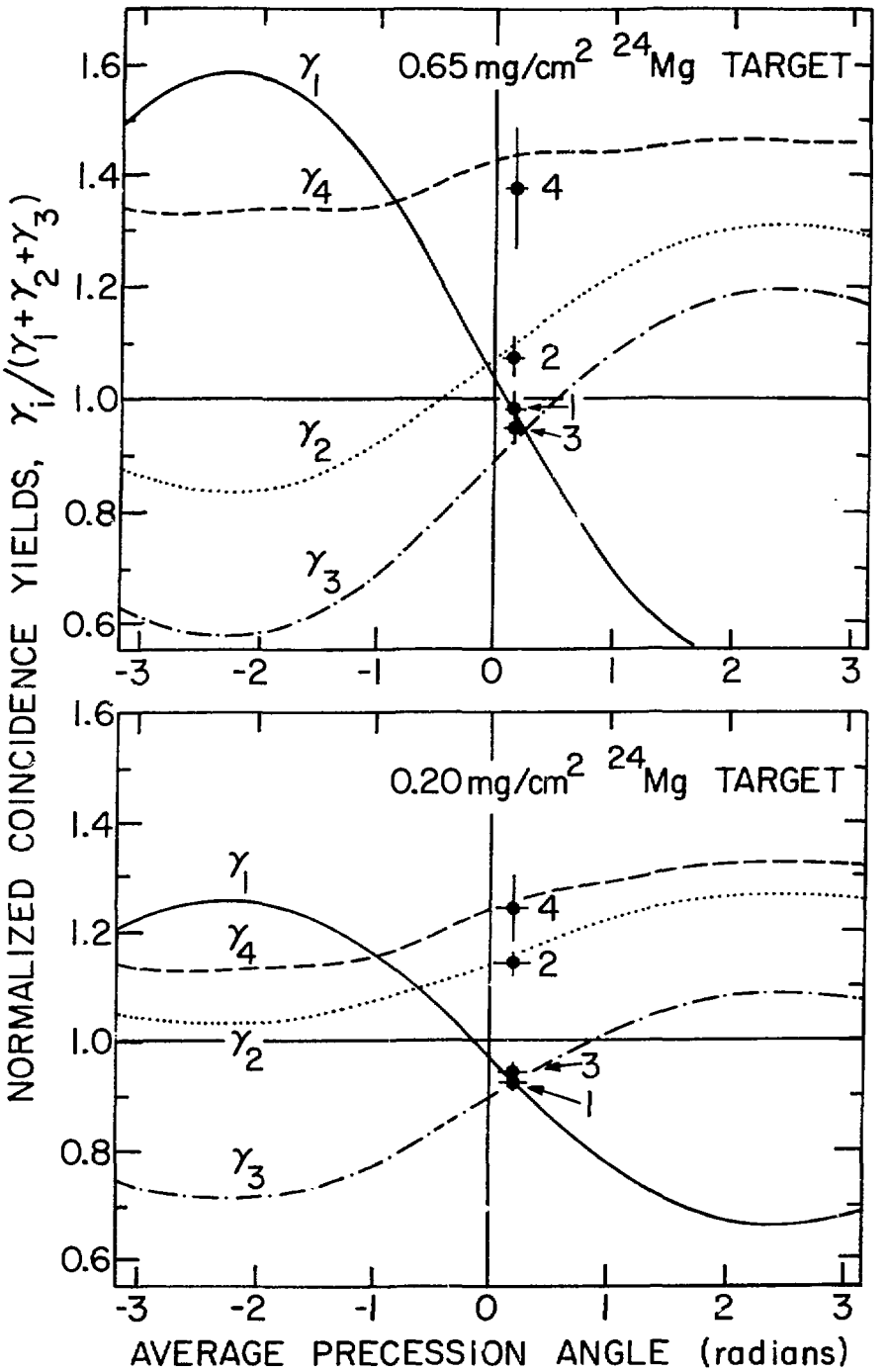

Fig. II-15. Comparison of the normalized particle-gamma coincidence yields with the calculations for the de-excitation of the first 2^+ state of ^{24}Mg for two different target thicknesses. The reaction was 120-MeV ^{56}Fe on ^{24}Mg.

excited states. Therefore the ions are still excited when recoiling into vacuum, and vacuum deorientation effects[1,2] have to be taken into account. This difficulty could have been avoided by having the ions recoiling in a gas-filled scattering chamber rather than into vacuum.

The best fit for the precession $\omega\tau$ (in radians) for excited Fe and Mg for the thick and the thin target gives:

$\omega\tau(Fe^*, \text{thick}) = 0.05 \pm 0.10, \quad \omega\tau(Fe^*, \text{thin}) = -0.16 \pm 0.08$

$\omega\tau(Mg^*, \text{thick}) = 0.18 \pm 0.08, \quad \omega\tau(Mg^*, \text{thin}) = 0.20 \pm 0.13.$

Here τ denotes the interaction time and ω the interaction frequency which is proportional to the product of the electric field gradient and the quadrupole moment of the excited nucleus. The vacuum deorientation parameter was also adjusted in these fits. The results for Mg^* are shown in Fig. II-15. Again, no unambiguous effects are found, in particular no significant change of $\omega\tau$ is seen between the thick and the thin targets. As an upper limit, one can estimate from our results that the transient electric field gradient is less than 10^{21} V/cm^2.

In future experiments one might improve the experimental setup and use more favorable projectile-target combinations at higher energies. If a transient electric field gradient effect can indeed be established, it could provide a rather useful technique for the measurement of quadrupole moments for states with lifetimes down to the ps region.

---

[1] P. M. S. Lesser, D. Cline, P. Goode, and R. N. Horoshko, Nucl. Phys. A190, 597 (1972).

[2] G. Goldring, Proceedings of the Heavy Ion Summer Study, Oak Ridge, 12 June-1 July 1972, CONF-720669, p. 438.

E. EQUIPMENT DEVELOPMENT

A significant expansion of experimental capability resulted from the completion of the first stage of the large 65-in. scattering chamber. This facility permits coincidence studies with the high precision required in heavy-ion reactions. Implementation of the spectrograph and a new target area will further enhance experimental flexibility and capabilities. The complexity inherent in heavy-ion reactions requires more sophisticated detection systems with increased sensitivity and flexibility. A large position-sensitive gas detector is being constructed and improvements in the gamma-ray facility will help to fulfill the needs. Target fabrication continues as a high-priority facet of the experimental program in view of the expanding demands of experiments.

a. Installation of Beam Lines in the Linac Experimental Area

J. Worthington, J. J. Bicek, C. E. Bolduc, W. F. Evans, and D. G. Kovar

During 1980 the second beam line in the linac experimental area was completed. Beams from the superconducting booster can now be carried to three experimental stations: an 18-in. scattering chamber and a gamma-ray station on the 0-degree beam line and a multipurpose 65-in. scattering chamber on the 19-degree beam line. Designs for these and the planned spectrograph beam line now incorporate resonant-phase pickups for accurate time-of-flight measurements of the beam energy. The spectrograph beam line is presently being installed and is expected to be operational by fall 1981. Construction of the target-room addition to house the off-line laser laboratory has started and first design objectives for the beam line serving this new target room addition have been established. Completion of this task is expected by the end of 1981.

b. 65-in. Scattering Chamber in New Target Area

J. N. Worthington, W. Henning, and J. J. Bicek

The first stage of the 65-in. scattering chamber has been completed and used in various experiments with beams from the superconducting linac. Four gear rings provide independent angular motions with an accuracy of $\lesssim$1/100 degree. This precision has proven extremely useful in measurements of absolute fusion cross sections in light systems at high incident energies, where accurate angular motion at very forward angles is necessary for a reliable normalization via Rutherford scattering. The detector and target motions are microprocessor controlled and can be operated from either the

target or the data room. The vacuum is essentially hydrocarbon free and results in carbon buildup of less than 1 $\mu g/cm^2$ during 2 days bombardment of a ^{48}Ca target with 50—100 nA of 158-MeV ^{16}O ions. No carbon buildup was observed on a Sn target bombarded with 30 nA of ^{58}Ni beam for nearly 24 hours. The off-center target position at the entrance of the scattering chamber was successfully used in x-ray coincidence measurements. We plan future additions to the chamber to allow for large-area gas detectors, and for radial and out-of-plane detector motion.

c. The Split-Pole Magnetic Spectrograph in the Linac Experimental Area

W. Kutschera, D. G. Kovar, C. E. Bolduc, W. F. Evans, and J. N. Worthington

The work on the setup of the Enge split-pole magnetic spectrograph originally used at the ANL cyclotron continued. This spectrograph is a twin of the one still in use in the tandem experimental area. While the linac spectrograph will be equipped with more modern technology, such as a cryogenic pumping system, it will remain compatible in most respects with the tandem spectrograph in terms of auxiliary equipment and detector systems. In particular, the ionization chamber focal plane detector successfully used for many years in heavy-ion experiments with tandem beams will be used as the basic heavy-ion detector for the linac spectrograph.

The spectrograph was put on its final position on the pad and optically aligned. An all-cryogenic pumping system consisting of a liquid-nitrogen cooled roughing stand and three 1000 ℓ/sec cryopumps operated with compressed helium gas was installed. First vacuum tests indicate that a pressure in the low 10^{-6} Torr range can be reached. Installation of the spectrograph beam line has been completed and a test beam of 247-MeV ^{32}S was focused into the spectrograph scattering chamber.

It is expected that the spectrograph will be operational in the fall of 1981 in its initial form. Future work will include an upgrading of the scattering chamber and an extension of the detector box. The latter will allow installation of a deeper gas detector, required for the higher energy beams from the linac.

d. A Position-Sensitive, Large Ionization-Chamber Heavy-Ion Gas Detector

H. Ernst and W. Henning

A large position-sensitive gas detector for heavy ions, with an entrance window of 150 mm × 16 mm and an active volume of 300 mm length and 60 mm height was designed. The position of the incident particles is measured with a single-wire proportional counter located off to the side near the entrance window. To allow high count rates, the charge-division method was applied. The total-energy signal is taken from the cathode using a double grid; energy-loss signals are taken from the anode which is divided into three strips.

There was little constraint on the detector design, so a clean geometry was chosen with small electrode capacitances, low gas pressures ($\lesssim$300 Torr), and a thin entrance window ($\lesssim$2.5 μm) without support grid. This minimizes effects which reduce energy and position resolution. The preamplifiers are kept outside the scattering chamber, which slightly deteriorates the energy resolution due to additional electronic noise. An energy resolution of 1.1% and a position resolution of 0.6 mm was obtained with heavy ions. In addition, the position information in vertical direction can be derived from the drift time of the electrons with a resolution of $\sim$2 mm. Figure II-16 illustrates the position resolution obtained.

e. Measurement of Fusion Cross Sections in Heavy Systems with an Electrostatic Deflector

H. Ernst and W. Henning

Over the past years considerable effort has been devoted at Argonne to the study of complete-fusion cross sections in lighter heavy-ion systems. With the higher-energy and heavier beams becoming available from the superconducting linac, we are now extending these measurements to considerably heavier compound systems. In order to solve the experimental problem of more forward-peaked angular distributions of the evaporation residues with increased energy and compound nucleus mass, we have developed an electrostatic deflection system that allows us to measure their yields at 0°. Deflector plates of 20 cm length separated by 2 cm and biased between 25—30 kV, together with a carefully designed collimator system, cleanly

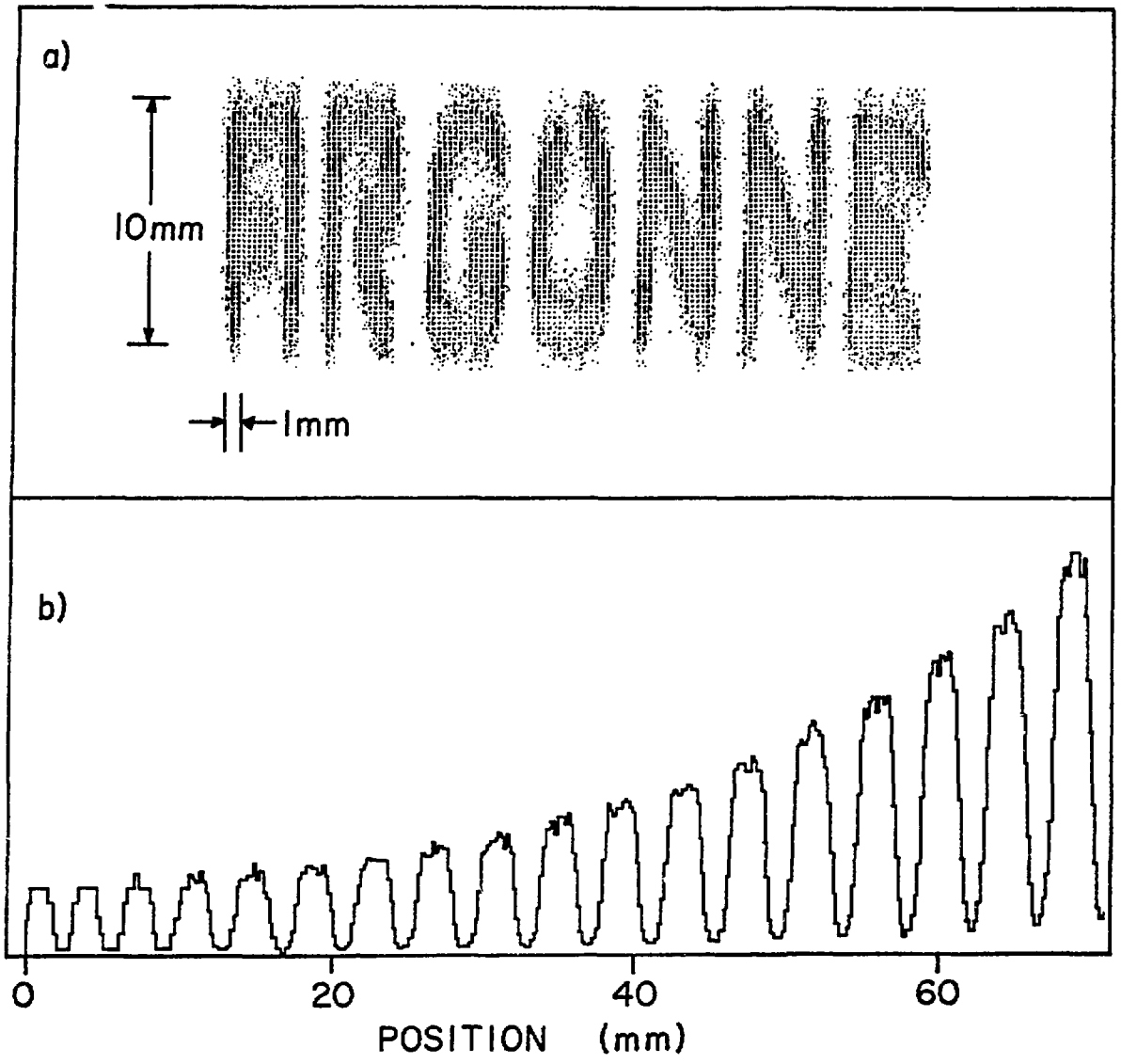

Fig. II-16. (a) Two-dimensional position spectrum recorded with an α source shining through a properly shaped paper mask placed in front of the window. (b) Position spectrum of 270-MeV ^{58}Ni ions elastically scattered from a ^{124}Sn target in the angular range between 30° and 10°. A slit mask with 2.4 mm wide openings was placed in front of the detector window.

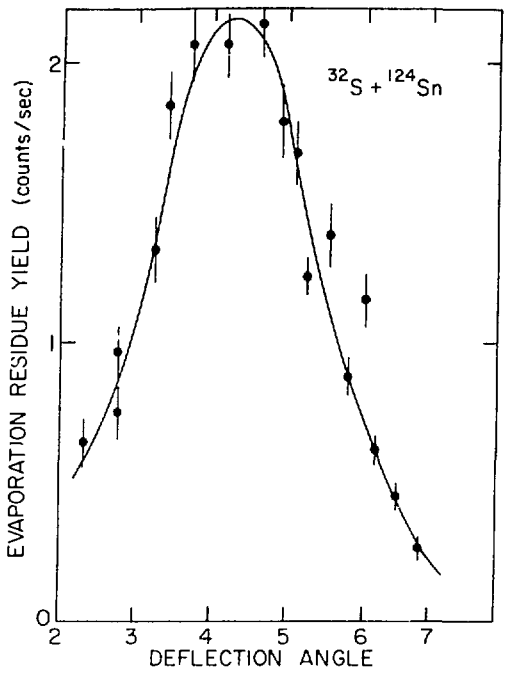

Fig. II-17. Profile of evaporation residues for the reaction $^{32}S + ^{124}Sn$ at 170 MeV measured as a function of the deflection angle from the beam axis at a constant deflection voltage of 25 kV. The ^{32}S beam current was 12 nA, the target thickness 150 μg/cm^2. The maximum yield corresponds to the evaporation residue yield emitted at 0°.

separate evaporation residues from elastic particles for the $^{32}S+^{116,120,124}Sn$ reactions measured at energies between 153 MeV and 220 MeV. In Fig. II-17 the evaporation residue yield is shown as a function of the deflection angle. We plan to use this system to study fusion reactions induced by beams of $^{32,34}S$, $^{40,48}Ca$, $^{58—64}Ni$, and $^{80,82}Se$.

f. γ-Ray Facility

S. R. Faber,* T. L. Khoo, A. Huston, and J. Worthington

The basic γ-ray facility on the 0° linac beam line has been in operation for about a year. Supports for large NaI detectors have recently been added. A digital angle readout for the Ge(Li) detector tables has been installed. We have constructed a stabilization system for the NaI detectors used in continuum γ-ray studies and for the sum spectrometer. This system employs optic fibers to fan out light from an LED to individual photomultipliers. The LED output is monitored by a PIN diode with a very stable response and is stabilized by a feedback circuit. In addition, we are presently designing a plunger system for lifetime measurements using

*Purdue University, West Lafayette, Indiana.

the recoil distance method. This plunger will be small enough to fit inside the sum spectrometer and can be controlled remotely.

g. Nuclear Target Making and Development

G. E. Thomas

The Physics Division has a facility which produces very thin targets for experiments at the tandem and Dynamitron accelerators, for experiments of other members of the Division, any other division at the Laboratory needing this service and occasionally for other laboratories and universities.

This year at the facility we produced targets varying in thickness from a monolayer to several mg/cm^2. The different elements, isotopes or compounds evaporated, rolled, anodized or oxidized included Al, AgCl, Al_2O_3, $^{nat,10,11}B$, ^{209}Bi, $BaCl_2$, Be, C, $^{nat,40,48}Ca$, ^{116}Cd, CaF_2, Fe, Formvar, FeS, ^{76}Ge, $^{nat,6,7}LiF$, $^{24,26}Mg$, melamine, NaCl, $^{nat,58,60,64}Ni$, Nb, $^{15}NH_4NO_3$, $^{nat,208}Pb$, ^{121}Sb, $^{nat,28,30}Si$, $^{nat,144,150,152,154}Sm$, $^{nat,116,118,120,124}Sn$, $^{nat,124,128,130}Te$, Ti, TiO_2, ^{48}Ti, Ta, ^{182}W, ^{92}Zr, and ^{170}Yb. Ti, Nb, and B standards consisting of 5, 25, and 50 monolayers deposited on 50 $\mu g/cm^2$ Al were also produced.

New techniques were developed to produce multilayered targets used for heavy-ion experiments. These are quite different targets from those used in the past and often time consuming to produce. A technique was developed by B. Zeidman and F. Karasek* to produce large area boron targets for medium-energy experiments.

The target fabrication program to produce better targets with higher purity is continuing. A split tube furnace is now in use and we are routinely reducing our separated isotopes to metallic form. Others in the Division are also using this facility.

Plans for the future include the completion of our third evaporation system, making our target-making laboratory more useful for other programs, fabrication of our multitarget evaporation system and new systems to improve the quality of our targets.

---

*Materials Science Division, ANL.

III. CHARGED-PARTICLE RESEARCH

INTRODUCTION

This activity involves a broad range of studies centered at the Dynamitron, Tandem, and Tandem-Linac accelerators in the Physics Division. These include studies of properties of isotopes of interest to explosive nucleosynthesis, laser spectroscopy of radioactive ions, accelerator mass spectrometry, fundamental aspects of weak interactions as evidenced in nuclear-decay processes, and parity violation in specific nuclear levels induced by neutral weak currents.

The charged-particle research program in the Physics Division is carried out by a number of researchers in the Division. A very substantial interaction with researchers in the university community is also involved. The charged-particle research uses the Dynamitron (25% of available time) and the Tandem system (15% of available time).

A. CHARGED-PARTICLE RESEARCH AT THE DYNAMITRON

This research activity centered around three programs during the past year. One of the programs is a study of fundamental aspects of the weak interaction via precision experiments using low-energy nuclear physics techniques. The main effort in this area over the past year is an attempt to determine the $\Delta T=1$ parity mixing between the 2^-, T=0 5.11-MeV and 2^+, T=1 5.16-MeV levels in ^{10}B. This mixing should be due to the weak neutral interaction between the nucleons. To the present no experiment has been sufficiently sensitive to demonstrate the effect of the weak neutral interaction between hadrons. Another ongoing activity in the weak interaction program is the development of an apparatus to allow precision measurements of beta spectra. The goal of this endeavor is to evidence weak magnetism in an unambiguous manner and to investigate the corrections (Coulomb, radiation) applied to measured spectra. The latter is to be accomplished by measurement of a superallowed $0^+ \rightarrow 0^+$ decay which must have an allowed shape. The measurements in the series of highly exothermic reactions between light nuclei resulting in all charged particles in the final state have been completed. These cross sections were of interest to technologists considering advanced fusion systems. At present, light ion reactions are selected for their interest to astrophysics—our coupling to the Physics and Astronomy Departments and the Enrico Fermi Institute of the University of Chicago is invaluable in this regard. Research is continuing in establishing a satisfactory technique to determine the $^4He(^3He,\gamma)^7Be$ absolute cross section. There is a controversy over the size of this cross section and the difference in present results (25%) leads to a difference in the measured solar neutrino flux using a ^{37}Cl detector of a factor of 2. The smallest program at the Dynamitron involves its occasional use to search for exotic charged particles such as quarks or stable heavy hadrons.

1. WEAK INTERACTIONS

a. Parity Violation in the 5.1-MeV J=2 Doublet of ^{10}B

C. A. Gagliardi,* S. J. Freedman,† G. T. Garvey, R. McKeown, R. G. H. Robertson, and T. J. Bowles‡

Since the discovery of the neutral weak current, there has been a great deal of effort to define its nature. To date, the leptonic and semileptonic results are well described by the SU(2) × U(1) gauge theory of Weinberg-Salam with a mixing angle $\sin^2\theta_w \sim 0.23$. Studies of the purely hadronic neutral current have been more ambiguous.

*Graduate Student, Princeton University, Princeton, New Jersey.

†Stanford University, Stanford, California.

‡Los Alamos National Laboratory, Los Alamos, New Mexico.

The only method available at present to study the hadronic neutral weak current is to measure parity-violating effects. It is natural to describe nucleon-nucleon parity-violating amplitudes in an isospin representation. When CP invariance is included, only the $\Delta T=1$ component can have a one-pion exchange contribution.

The $\Delta T=0$ and 2 currents arise from the exchange of multiple pions and heavier mesons, causing the associated parity violating interactions to have shorter range. This makes calculations of $\Delta T=0$ and 2 effects dependent on models of short-range correlations. In addition to the fact that the $\Delta T=1$ case is free of this particular theoretical uncertainty, the Cabibbo (charged) current contribution for $\Delta T = 1$ is suppressed by a factor of $\sin^2\theta_c$ relative to the neutral current. It would appear a good strategy to observe the neutral weak current by studying cases of pure $\Delta T=1$ parity violation.

Despite intensive efforts, previous experiments to measure pure $\Delta T=1$ parity violation have only set an upper limit on the size of the effect. We have undertaken a study of $\Delta T=1$ parity violation in ^{10}B to measure the mixing between the 2^+ T=1 state at 5.16 MeV and the 2^- T=0 state at 5.11 MeV. The 2^+ state is produced and decays via the $^6\vec{Li}(\alpha,\gamma)^{10}B$ reaction. A 1.2-MeV α beam from the Argonne Dynamitron is employed. The total cross section is given by

$$\sigma = \sigma_0(1 + \tfrac{1}{2} P_{zz} + HB\, p_z), \qquad (1)$$

where z is taken along the α-beam direction. B, the quantity of interest, is the parity mixing in the J=2 doublet and is calculated to be $B \sim 4 \times 10^{-6}$. H is an enhancement of the measured effect due to the different alpha widths of the two states and is $\sim$100.

The construction of a polarized ^6Li beam for the experiment is complete. The experimental apparatus is shown in Fig. III-1. The intense ^6Li atomic beam is produced by an oven with a large bore orifice. The oven holds 700 g of ^6Li and is capable of running $\sim$1 week at 850°C without refilling. The beam is collimated and then polarized using a pair of large gap (1.2 cm diam.), high field ($\sim$12.5 kG) sextupole magnets. The atomic polarization is converted to nuclear polarization using a weak field rf-transition unit. Atomic beam fluxes of $\geq 2 \times 10^{16}$ atoms/cm^2-sec and polarizations of $\sim$0.6 have been obtained.

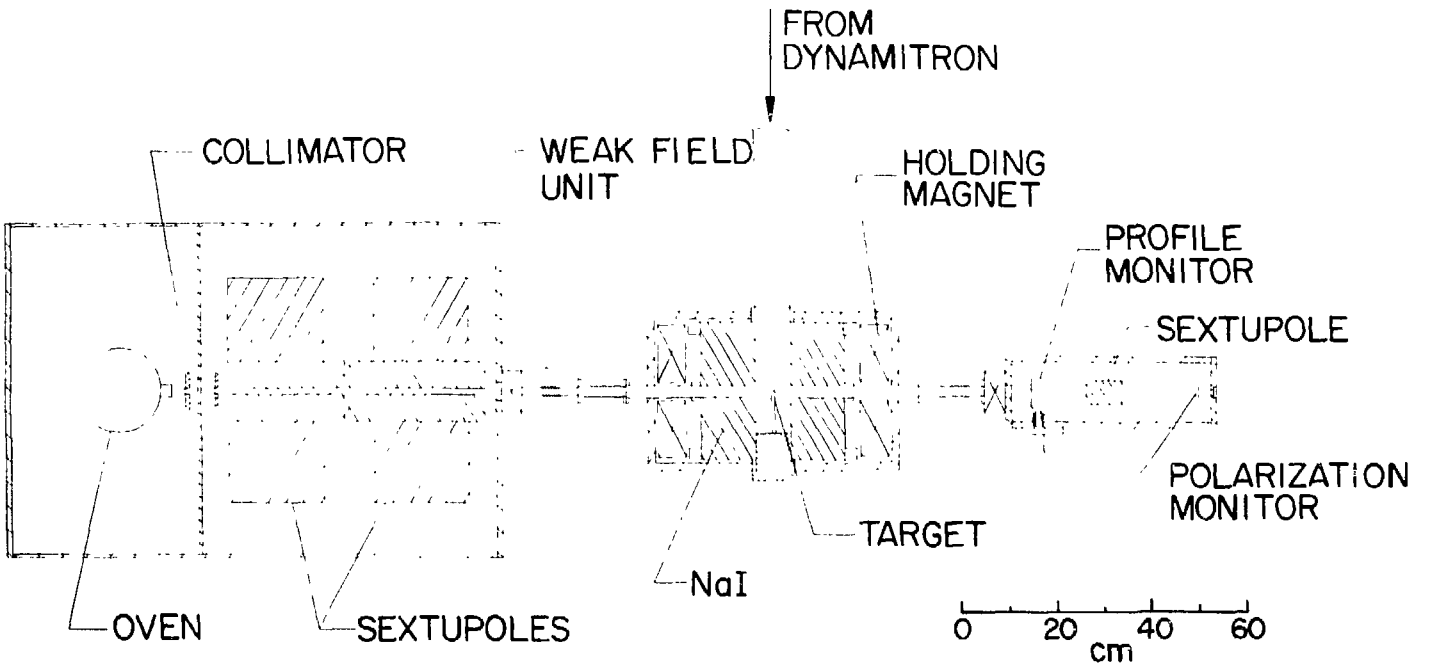

Fig. III-1. Layout of the atomic beam apparatus.

The $^{6}\vec{Li}$ impinges on a hot (~1100°C) oxidized tungsten surface in a 1.2 kG holding field. The sitting time is such as to provide the order of a monolayer target to a 50—100 μA beam with negligible depolarization. Subsequent γ decays are observed using a cylindrical NaI detector with a solid angle of 70% of 4π. The detector and holding field assembly have been constructed and tested. The detector resolution was found to be 8.7% FWHM for the ^{60}Co sum peak at 2.505 MeV. The detector gain is independent of the 1.2 kG holding field polarity at the 0.1% level.

Target development and characterization has been proceeding, using the $^{6}\vec{Li}(d,\alpha)^{4}$He reaction. In these the NaI detector holding magnet assembly is replaced by a separate chamber and magnet, with a 400 gauss holding field parallel or antiparallel to the atomic beam direction. This allows measurement of the target polarization by observing the parity allowed analyzing power of the reaction in Si detectors placed symmetrically at ±120°. Initial measurement using a gas cooled, beam heated target were unsuccessful because sufficient decoupling between beam current and target temperature could not be achieved. We are presently using a target which permits ohmic heating. Preliminary results of target thickness measurements versus target temperature have been obtained. They are shown in Fig. III-2.

b. Beta Spectrum Measurements

A. R. Davis* and G. T. Garvey

The measurement of beta spectra sufficiently accurate and reliable to see "weak magnetism" has proven most difficult to achieve. Although a great deal of attention was focused on this subject in the mid-1960's, it is not without present controversy. Only recently has the spectrum of the supposedly trivial $0^{+}\rightarrow 0^{+}$ decay been measured to a minimum accuracy (0.4%/MeV) required to see "induced current" effects. Many recent efforts have failed to convincingly extract a "weak magnetism" term because of experimental uncertainties. In addition, accurate measurements of $0^{+}\rightarrow 0^{+}$ beta shape factors will allow an examination of the procedures used for radiative corrections and a better limit to be set on the Fierz interference term which arises from possible scalar coupling.

*Thesis student, University of Chicago, Chicago, Illinois.

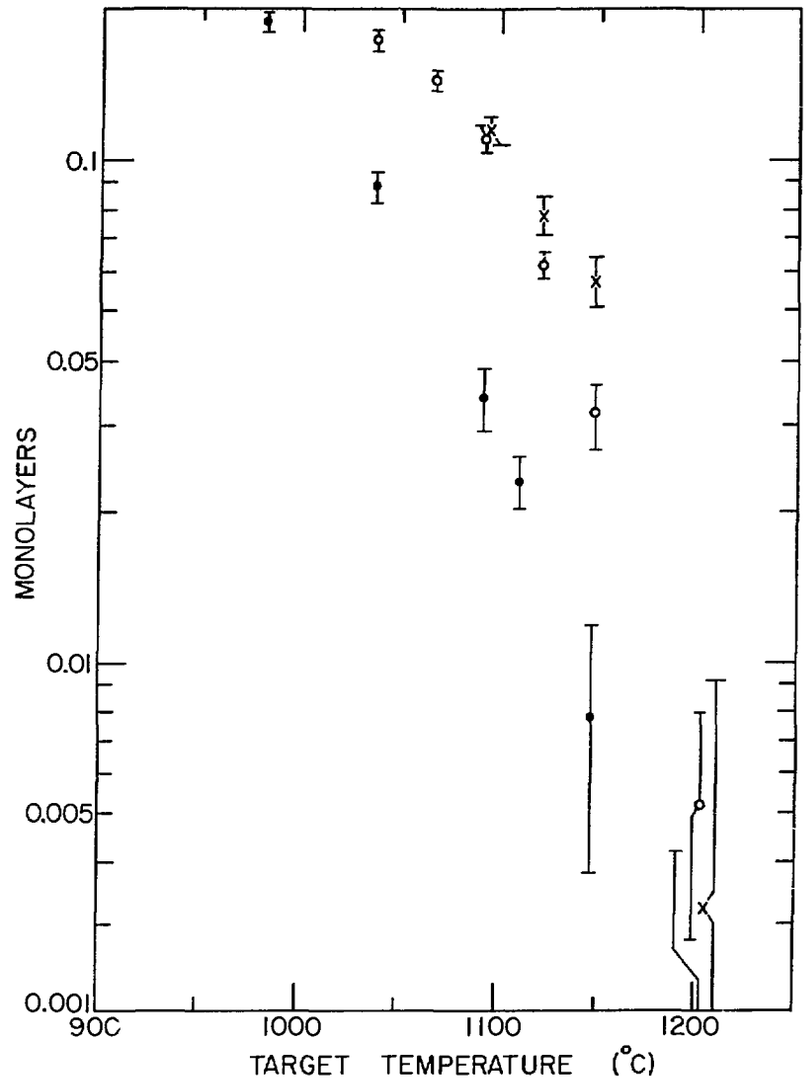

Fig. III-2. Average ^{6}Li target thickness measured with 3 different atomic beam intensities. The closed circles are for a lithium flux of ∿1.2 monolayers/sec, the open circles for ∿2.5 monolayers/sec, and the x's for ∿3.8 monolayers/sec.

Modern techniques using active slits, a flat field magnet, and position sensitive proportional counters will allow the measurement of beta spectra to the order of ~0.1%/MeV precision. To that end we have designed a system based on a 180° flat field magnet. Employing active slits to define the entrance to the magnet and a 2-dimensional detection system of resistive wires with electron drift time, a set of orbits can be measured that should be free of extraneous effects apart from source scattering. As thin targets (200 $\mu g\ cm^{-2}$) can be used while obtaining a minimum of 2×10^6 detected decays per day, we should be in a good position to take systematic data and extrapolate to zero source thickness. The $\beta^{\pm}$ energy spectrum will be calibrated by comparison to low energy (1—10 keV) positive and negative ion beams. The magnet is on hand and the detection system is under development. The entire system should be complete by this winter with data being taken over the next year.

c. Search for Parity Violation in ^{6}Li

R. G. H. Robertson, P. Dyer,* R. C. Melin,* A. B. McDonald,† W. G. Davies,† G. C. Ball,† E. D. Earle,† and T. J. Bowles‡

Data-taking on this experiment is now complete. A very successful run at Chalk River during which all components in the experiment performed reliably gave 25 000 $^2H(\alpha,\gamma)^6Li$ capture events. Analysis of the data is still in progress, but in a preliminary examination of it, an upper limit of 2×10^{-6} eV on the parity-violating alpha width of the 0^+ T=1 state was obtained at the 90% confidence level. This value is almost 3 orders of magnitude below the previous best limit. The theoretical estimate for the width is still in a very crude form, being a one-body calculation in which core excitation, heavy meson exchange, and many other potentially significant efforts have been neglected. On the basis of this estimate the neutral current enhancement must be less than 80. Work is continuing in an attempt to improve both the theoretical and the experimental analyses.

---

*Michigan State University, East Lansing, Michigan.

†Atomic Energy of Canada Limited, Chalk River Nuclear Laboratories, Chalk River, Ontario, Canada.

‡Los Alamos National Laboratory, Los Alamos, New Mexico.

d. Test of the Isobaric Multiplet Mass Equation from β-Delayed Proton Decay of ^{24}Si

A. G. Ledebuhr,* L. H. Harwood,* R. G. H. Robertson,* and T. J. Bowles

The highly proton-rich nucleus ^{24}Si has been produced via the ^{24}Mg(^{3}He,3n) reaction. The half-life of ^{24}Si was found to be 103(42) ms, and the energy of the protons de-exciting the T=2 state in the daughter, ^{24}Al, has been measured as 3912.7(37) keV. From detailed consideration of masses in the A=24 isobaric quintet (recently completed), it is concluded that this quintet constitutes a test of the isobaric multiplet mass equation as precise as the mass 9 quartet. In this case there is no need to introduce higher order terms to fit the mass differences. This work has been published in Phys. Rev. C.

*Michigan State University, East Lansing, Michigan.

2. REACTIONS USING LIGHT NUCLEI

a. Nuclear Reactions of Light Ions with ^{6}Li at Low Energies

A. J. Elwyn, R. E. Holland, C. N. Davids, J. E. Monahan, F. P. Mooring, and W. Ray, Jr.

Data analysis has been completed in the study of the ^{6}Li(^{3}He,p) reaction and a paper has recently appeared in the Physical Review.[1] Differential and total cross sections at incident energies between 0.5 and 2.0 MeV are presented, not only for the ground and first excited states in ^{8}Be, but for the 16.63- and 16.92-MeV states and the underlying charged-particle continua as well. With this completed work, the ongoing research program to measure absolute cross sections for reactions of light ions with ^{6}Li at energies below a few MeV has been substantially concluded.[2] The reactions studied include most of the processes (other than elastic scattering) that occur with significant probability at low energies between ^{6}Li and p, d, and ^{3}He ions. Angular distributions, total reaction cross sections, and

[1] A. J. Elwyn, R. E. Holland, C. N. Davids, J. E. Monahan, F. P. Mooring, and W. Ray, Jr., Phys. Rev. C 22, 1406 (1980).

[2] See, R. E. Holland, A. J. Elwyn, C. N. Davids, L. Meyer-Schützmeister, J. E. Monahan, F. P. Mooring, and W. Ray, Jr., IEEE Trans. Nucl. Sci. NS-28, 1344 (1981), and other references included therein.

thermonuclear reaction-rate parameters were obtained for both two- and three-body final states. The systematic nature of the data are relevant to the spectroscopy of light nuclear systems, reaction mechanism studies, and have proved to be of importance to the investigation of advanced fusion-fuel cycles. In connection with the latter topic, Fig. III-3 shows a comparison of the thermonuclear reaction-rate parameters for the sum of the various outgoing proton channels in the $^{6}Li(^{6}He,p)$ reaction [along with those for the primary $^{6}Li(p,^{3}He)$ reaction channel] compared to previous tabulated results.[3]

[3] J. Rand McNally, Jr., K. E. Rothe, and R. D. Sharp, Oak Ridge National Laboratory Report No. ORNL/TM-6914 (1979).

b. The $^{7}Li(d,p)^{8}Li$ and $^{7}Be(p,\gamma)^{8}B$ Reactions

A. J. Elwyn, C. N. Davids, R. E. Holland, and W. Ray, Jr.

Because of 25% discrepancies in the recent previous measurements,[1] an experiment to remeasure the total cross section in the $^{7}Li(d,p)^{8}Li$ reaction at incident energies of 0.7—0.8 MeV is under way. This cross section is used as normalization in the determination of the rate of the reaction $^{7}Be(p,\gamma)^{8}Be$, which, as a link in the proton-proton chain of nuclear reactions that take place in the sun, is of prime importance to the theoretical calculation of the number of solar neutrinos expected in current ^{37}Cl neutrino-capture experiments. While previous studies of the $^{7}Li(d,p)$ reaction observed either the delayed α particles following the ^{8}Li beta decay or the beta decay itself, we are using charged-particle time-of-flight techniques in conjunction with Si surface-barrier detectors to allow observation of the protons in the presence of a large deuteron background. It is expected that from accurate measurements of target thickness and integrated charge, total cross sections can be determined from measured yields to a precision of 10%. Furthermore, because of its importance to the solar neutrino problem, we are planning in the near future a remeasurement of the $^{7}Be(p,\gamma)^{8}B$ reaction cross section itself (at 250 keV $\leq E_p \leq$ 1 MeV),

[1] A. E. Schilling, N. F. Mangelson, K. K. Nielson, D. R. Dixon, M. W. Hill, G. L. Jensen, and V. C. Rogers, Nucl. Phys. A263, 389 (1976); C. R. McClenahan and R. E. Segel, Phys. Rev. C 11, 370 (1975); D. W. Mingay, S. Afr. Tydskr. Fis. 2, 107 (1979).

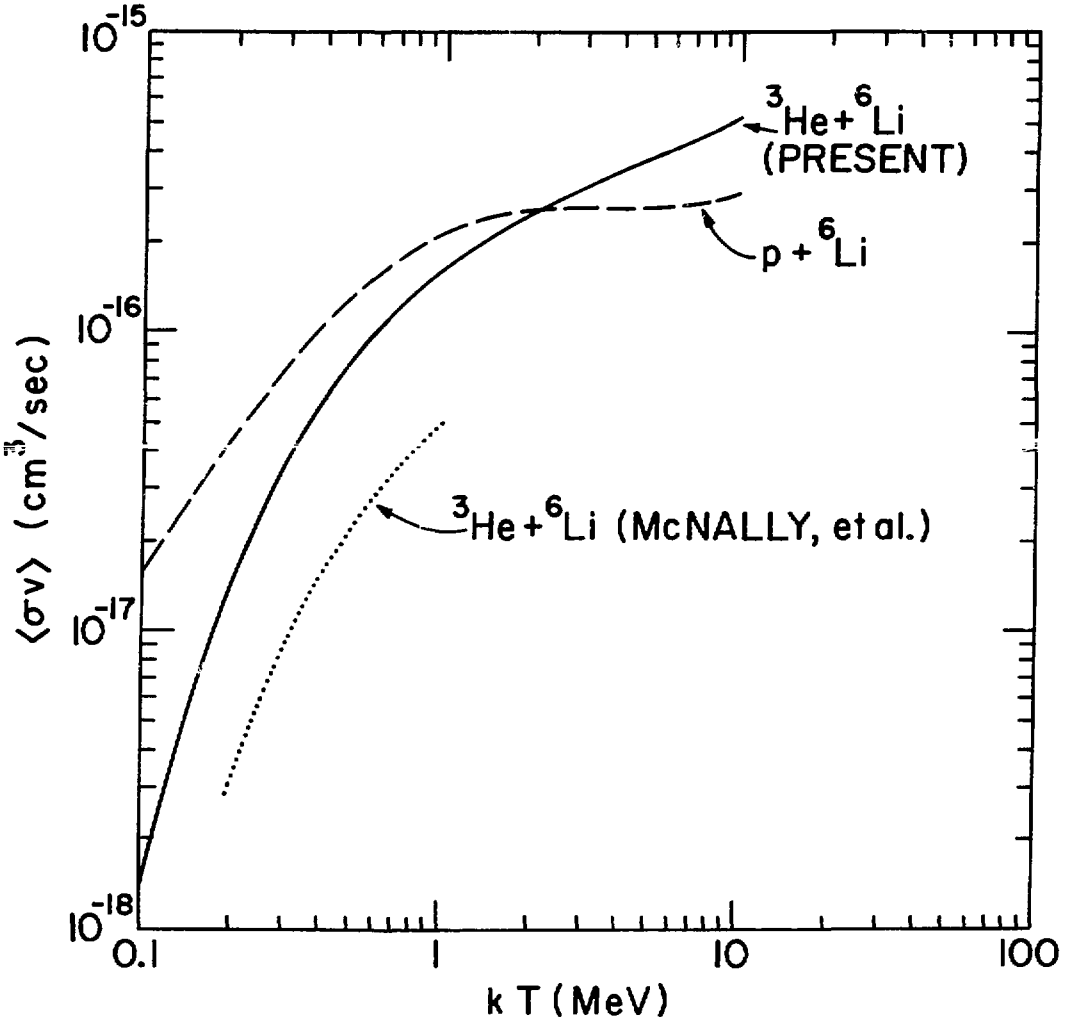

Fig. III-3. Comparison of thermonuclear reaction-rate parameters $\langle\sigma v\rangle$ for the sum of the various outgoing proton channels compared to previous tabulated results. Also shown are the results from measured $^6Li(p,^3He)$ reaction cross sections.

probably through the observation of the delayed alphas following the ^{8}B beta decay. The most recent previous study of this reaction at low energies appears as an unpublished report at an APS meeting in 1969.

c. $^{3}He(\alpha,\gamma)^{7}Be$

B. Filippone* and C. N. Davids

An extended He gas target with foil windows is being tested for use in measurements of the $^{3}He(\alpha,\gamma)^{7}Be$ reaction. This reaction is part of the chain of nuclear reactions responsible for energy generation in the sun. Knowledge of the rate of this reaction is important to calculations of the solar neutrino flux.

The measurement of the cross section is to be done in a novel way by stopping the recoiling ^{7}Be nuclei and counting the activity ($t_{1/2}$ = 53 days) away from the beam in a low background counting area. Using the $^{6}Li(d,n)^{7}Be$ reaction, large amounts of ^{7}Be were implanted in thick Au and Ta foils. These were subsequently bombarded with ^{3}He and ^{4}He to determine the retention efficiency for ^{7}Be. In cases where little or no blistering or flaking occurred, this efficiency was essentially 100%. Preliminary experiments with thin Ni foils also indicate a high ^{7}Be retention efficiency.

A Pb shielded Ge(Li) detector has been used to count the 478-keV γ ray which follows the decay of ^{7}Be. Current background measurements imply a 10% uncertainty in the cross section, with as few as 10^{6} ^{7}Be nuclei.

d. Calculations of the Solar Neutrino Flux

B. Filippone* and D. N. Schramm†

In connection with the $^{3}He(\alpha,\gamma)^{7}Be$ experiment mentioned above, new calculations of the flux of neutrinos from nuclear reactions in the solar interior have been performed within a standard solar model. Reconciling experimental observations and theoretical predictions of the detection rate of solar neutrinos has been a long-standing problem in astrophysics. Remeasurements and recalculations of several of the input parameters of the model along with preliminary indications of neutrino oscillations motivate

*Thesis student, University of Chicago, Chicago, Illinois.

†University of Chicago, Chicago, Illinois.

new calculations of solar neutrino production with emphasis on the effects of uncertainties in the input physics.

We have considered uncertainties in nuclear physics (the rates of the thermonuclear reactions in the solar core) as well as uncertainties in the composition and radiative transparency of the solar material. The calculations have been performed for both a ^{37}Cl and a ^{71}Ga detector. The results imply nearly a 50% uncertainty in the ^{37}Cl rate while the ^{71}Ga uncertainty is of order 10%. This is chiefly due to the higher sensitivity of ^{71}Ga to the more abundant low-energy neutrinos from the $H(p,e^{+}\nu_{e})^{2}H$ reaction. These neutrinos are nearly independent of conditions in the solar interior, other than the total solar energy output.

Work is continuing on the effects on the neutrino flux of various nonstandard models where the solar composition is mixed either by convection or diffusion.

e. Search for Superheavy Hydrogen

H. Ernst, W. Henning, W. Kutschera, and J. P. Schiffer

Considerations on the big-bang model of the early universe in conjunction with grand unified theories lead to the suggestion for the possible existence of very massive stable particles.[1] Estimates place concentration limits in terrestrial materials well within the reach of modern accelerator mass spectrometry.

We have started a search for anomalously heavy isotopes of hydrogen with the 4-MV Dynamitron, analyzing the accelerated ions close to zero degrees by the following technique: To eliminate the known isotopes of hydrogen a small magnetic field was introduced, sufficient to deflect the light isotopes onto a beam stop, but leaving very heavy isotopes essentially undeflected. A strong neutral beam component was eliminated by deflecting the charged particle with a electrostatic field into a ΔE-E telescope for nuclear charge identification. The two elements in the telescope were separated sufficiently to allow time-of-flight measurements to be carried out, in order to search for heavy particles. In addition a nickel foil was placed in front of the detector of sufficient thickness to stop any normal

[1] P. H. Frampton and S. L. Glashow, Phys. Rev. Lett. 44, 1481 (1980).

ions (with $Z \geq 2$) but thin enough to readily transmit hydrogen-like particles of any mass.

From preliminary tests we anticipate no problems in observing a heavy hydrogen isotope which is 10^{-15} of the primary hydrogenic beam, and with minor improvements we might be able to reach 10^{-17}.

The prior isotopic enrichment of the hydrogenic material is a key argument in the limits quoted in earlier experiments.[2] Hydrogen, strongly enriched in deuterium (from heavy water) was used, with the assumption that this would also have led to the enrichment of very heavy hydrogen-like species. Such enrichment, however, may be subject to some question. Most heavy water enrichment plants start with fresh water, and it is well known that deuterium is depleted by up to 25% in fresh water as compared to sea water. Is it possible that a very heavy hydrogen isotope, perhaps a hundred times the proton mass, will be depleted in fresh water by many orders of magnitude? We hope to be able to look at hydrogen beams bursting with ocean water, and are considering the possibility of examining water from salt beds on the ground that very heavy hydrogen atoms in ancient oceans may have concentrated in the water of crystallization rather than evaporate.

---

[2] T. Alvager and R. Naumann, Phys. Lett. B24, 647 (1967); R. A. Muller, L. W. Alvarez, W. R. Holley, and E. J. Stephenson, Science 196, 521 (1977); P. F. Smith and J. R. J. Bennett, Nucl. Phys. B149, 525 (1979).

3. NEAR FUTURE RESEARCH AT THE DYNAMITRON

Many of the experiments in this program are at frontiers of experimental technique and thus it is difficult to set definite schedules for completion because of unforeseen problems. The obstacles associated with ^{6}Li backgrounds in preparing a 0.1 monolayer target for the $^{6}\vec{\text{Li}}(d,\alpha)\alpha$ polarization measurement caused a six-month delay in the ^{10}B parity violation measurement. The ^{6}Li polarization as a function of surface coverage and sitting time will be completed in the spring of 1981, and a set of runs to measure the parity violation should be completed approximately six months after an appropriate target is constructed. The apparatus needed for the beta spectrum measurement will be completed by the end of 1981 and the measurements continue over the following year. The feasibility and costs of a reliable

absolute cross-section measurement of $^{3}He(^{4}He,\gamma)^{7}Be$ will soon be evaluated with a decision to proceed or not.

Programmatic research studying exothermic charged-particle reactions for future fusion devices is essentially complete and will cease unless there is an explicit request from the D.O.E. for such research. Future research will be directed at radiation capture processes in nuclei. These studies involve the capture of particles in reactions such as $^{16}O(\alpha,\gamma)^{20}Ne$ which is of interest in astrophysics as well as fixing absolute α-particle spectroscopic factors between these respective ground states. Another activity will investigate the giant (E2, J=0) resonance region in the upper reaches of the 2s-1d shell.

B. CHARGED-PARTICLE RESEARCH AT THE TANDEM ACCELERATOR

The two new research areas initiated in 1980, laser spectroscopy of radioactive atoms and accelerator mass spectrometry, have been actively pursued in 1981. For the laser program (in collaboration with researchers from the University of Minnesota and Iowa State University), a cryogenic helium-jet recoil transfer system has been designed and constructed. Assembly and checkout of the various components has begun. In accelerator mass spectrometry, two experiments with significant results in geophysical and astrophysical applications were completed. First experiments utilizing the unique features of the tandem-linac system have been performed. The study of nuclei far from stability using β- and γ-ray spectroscopy is proceeding. This program has concentrated on measuring the precise mass of nuclei which are important links in establishing the Q values for neutron deficient nuclei with $A \leq 50$. The program on $T=\frac{1}{2}$ mirror pairs in $f_{7/2}$-shell nuclei has continued with the spectroscopy of ^{47}Cr, an extremely difficult nucleus to study with any nuclear reactions. Systematics on Coulomb-energy shifts will be the interesting outcome of these experiments.

1. $f_{7/2}$ NUCLEI

The Gamma Decay of States in ^{47}Cr

G. Hardie,* A. J. Elwyn, L. Meyer-Schützmeister, and S. A. Gronemeyer†

As a continuation of our study of $T=\frac{1}{2}$ mirror pairs in $f_{7/2}$-shell nuclei,[1] ^{47}Cr, mirror of the much-studied nucleus ^{47}V, is being investigated. Experiments using the reactions ^{40}Ca(^{12}C,αn)^{47}Cr and ^{46}Ti(^{3}He,2n)^{47}Cr have been performed.

Gamma rays of 75.2 and 99.3 keV have been postulated as arising from the decay of the first two excited states in ^{47}Cr. Because of the low energies of these gammas, our initial gamma-gamma experiments used a Ge(Li) detector sensitive to high-energy (>100-keV) gamma rays and an intrinsic Ge detector sensitive to low-energy gammas. A later experiment with the ^{40}Ca(^{12}C,αn)^{47}Cr reaction used two large-volume Ge(Li) detectors.

The cross section for production of ^{47}Cr is very low for both reaction . A further complication with the (^{3}He,2n) reaction is the

---

*Western Michigan University, Kalamazoo, Michigan.

†Thesis student, Washington University, St. Louis, Missouri. Now at Fermilab, Batavia, Illinois.

[1] See, for example, S. A. Gronemeyer, L. Meyer-Schützmeister, A. J. Elwyn, and G. Hardie, Phys. Rev. C 21, 1290 (1980).

appearance of a 99.4-keV gamma from ^{44}Sc. Since ^{44}Sc is very strongly produced, the spectrum coincident with a gamma ray of about 99.3 keV is dominated by lines from ^{44}Sc. In addition, the decay of most low-lying states in ^{47}Cr is expected to proceed via several branches, thus aggravating problems associated with low cross sections. It should further be noted that isomeric states are not expected; thus the advantage of delayed-coincidence measurements are not available to us.

In spite of these difficulties, some progress has been made. The excitation energy of the first $\frac{3}{2}^+$ state has been established to be 471.2 keV (by observing the $\frac{3}{2}^+ \rightarrow \frac{5}{2}^-$ transition). An 1158.3-keV gamma coincident with both the 75.2- and 99.3-keV gammas permitted us to place the $\frac{11}{2}^-$ state at 1333.5 keV. We may also have located the $\frac{15}{2}^-$ state. In ^{47}V the $\frac{15}{2}^- \rightarrow \frac{11}{2}^-$ transition gives a 1320.1-keV gamma ray and a gamma of about this energy appears in the coincidence spectra of the 75.2- and 99.3-keV gammas. Because of the weakness of this gamma in these coincident spectra, the possibility that it arises from the $\frac{15}{2}^- \rightarrow \frac{11}{2}^-$ transition in ^{47}V, rather than ^{47}Cr, must be considered. However, a preliminary analysis indicates a slight (about 1 keV) energy difference between the weak line and the 1320.1-keV gamma from ^{47}V. If further work confirms this difference, the energy of the $\frac{15}{2}^-$ state in ^{47}Cr can be given.

Upon completion of the data analysis, the Coulomb displacement energies will be extracted. These displacements will then be compared with those in other $T=\frac{1}{2}$ pairs in the $f_{7/2}$ shell to enhance our knowledge of their systematics.

2. STUDY OF RADIOACTIVE NUCLEI

a. Decay of ^{72m}Br

C. N. Davids, B. Filippone,* and D. F. Geesaman

The 10.9 s isomer previously found in ^{72}Br is still under investigation. Earlier conversion-electron measurements on the 101-keV γ ray indicated an E2 multipolarity. More recent measurements point to its being a mixed M2-E3 transition. This would help to explain the long half-life

*Thesis student, University of Chicago, Chicago, Illinois.

for the decay, which also proceeds by β^+ emission. Further conversion electron studies are planned, with the aim of producing a thin source of ^{72}Br.

b. Mass and Low-Lying Levels of ^{106}In

J. Äystö,* B. Filippone,† C. Davids, and R. Pardo

Studies of the systematics of the masses of neutron-deficient nuclei with $Z \geq 50$ deduced from Q_{EC} values rely on the masses of a number of nuclides close to stability. One such nucleus is ^{106}In. It is known to have two β^+-unstable states, but neither has been conclusively identified as being the ground state. We have therefore begun to study the mass and low-lying states of doubly-odd ^{106}In, via the reaction ^{106}Cd(p,nγ)^{106}In. The measured mass excess of the low-spin isomer is -80 572 ± 15 keV.

In-beam γ-excitation functions and γ-γ coincidence experiments have been performed to locate levels ≤1.5 MeV in excitation. The (p,n) reaction at low energy preferentially populates the low-spin states of ^{106}In, such that many of the γ rays seen by other workers in the decay of ^{106}Sn should be found in the in-beam spectra. While all of these γ rays were observed, γ-ray threshold data disagree with some of the previous level placements.

In addition, several other γ rays, some apparently decaying to the known 6.3 min high-spin state of ^{106}In, were observed. In particular, the coincidence experiment revealed a 123.1 ± 0.1-keV γ ray which was unresolved in the singles experiment from the 122.5-keV line associated with the low-spin states. This new γ ray appears to define a separate family of states. A completed beam-off excitation function measurement (to determine a relative threshold for the β^+ decays of the high- and low-spin states of ^{106}In) currently under analysis as well as a planned remeasurement of the in-beam thresholds (with smaller energy steps and higher statistics) should aid in fitting these new γ rays into a level scheme for ^{106}In.

c. Helium-Jet Recoil Transfer System

C. N. Davids, B. Filippone,† and D. F. Geesaman

The helium-jet system has received further developmental effort in the past year. Reproducible transport of radioactivities with efficiencies around 50% have been achieved, using water vapor as an additive. A small

*University of Jyvaskyla, Finland.

†Thesis student, University of Chicago, Chicago, Illinois.

amount of air bled into the system enhances the transport by a significant amount. Care was taken to devise a means of accurately measuring the efficiency. The activities produced from bombarding ^{58}Ni by 35-MeV ^{11}B ions were used in the tests.

It is intended to adapt the room-temperature helium jet for use with the superconducting linac, in order to make yield measurements for the on-line laser spectroscopy experiments.

d. On-Line Laser Spectroscopy at the Argonne Superconducting Linac

C. N. Davids, G. W. Greenlees,* M. A. Finn,* D. A. Lewis,† and R. M. Evans†

This project, a collaboration between Argonne National Laboratory, Iowa State University, and the University of Minnesota, will use on-line laser spectroscopy to study the optical hyperfine structure of radioactive atoms. The objective is to extract information on spins, moments, and the variation of charge radii for ground states and isomers. The species under investigation will be produced by heavy-ion beams from the Argonne superconducting linac. The radioactive atoms recoil from the production target, become thermalized in a helium atmosphere, and then are transported by a liquid-nitrogen-cooled helium jet to the laser interaction region. Resonance fluorescence spectroscopy will be employed to observe the optical transitions. Essentially Doppler-free linewidths will be obtained by collimating the atoms into an atomic beam as they emerge from the helium jet. Two cooled photomultiplier tubes will detect the fluorescent light.

Figure III-4 shows an outline drawing of the target chamber, including the cryogenic helium jet and the laser interaction volume. The target cylinder, sealed by 8 mg/cm^2 Ta entrance and exit windows, has space for 5 or more foil targets. It is coupled to the 0.8 mm I.D., 50 cm long helium jet capillary tube by a funnel-shaped section. Both the capillary and target chamber are mounted on a large copper heat sink which is kept at 78°K by a continuous flow of liquid nitrogen.

The capillary discharges into a volume pumped by a 120 ℓ/s Roots blower, and is positioned over a skimmer with a 0.63 mm dia. hole. Below

*University of Minnesota, Minneapolis, Minnesota.

†Iowa State University, Ames, Iowa.

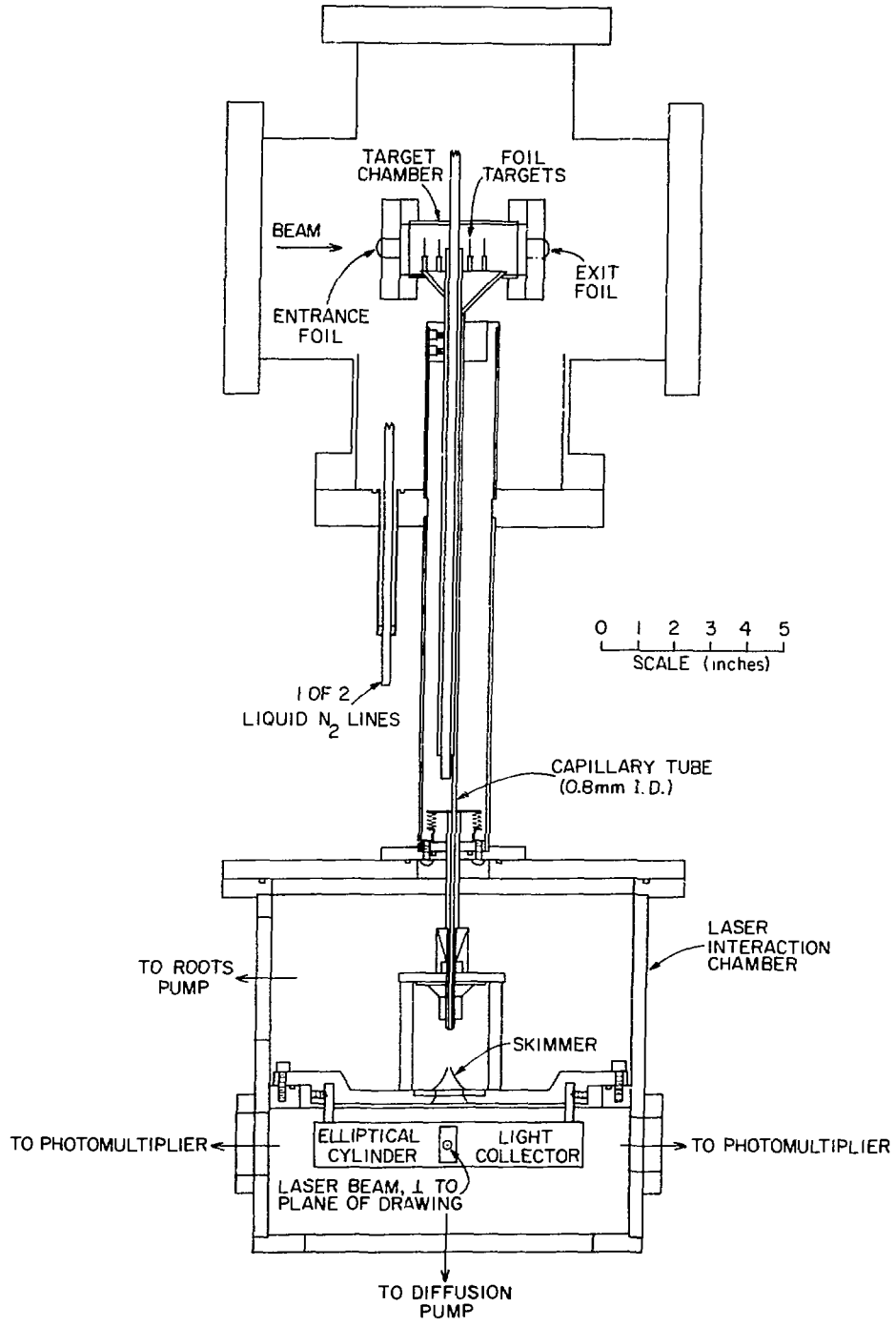

Fig. III-4. Outline drawing of target chamber cryogenic helium jet and laser interaction region.

the skimmer, the atomic beam is intersected at 90° by laser light at the common line focus of a double elliptical cylinder. Since the interaction region is 2 cm long, several hundred photons will be scattered on resonance by a single atom possessing an appropriate allowed transition. Pressure in this region is kept at $<3 \times 10^{-4}$ torr by a 6-in. diffusion pump directly below the cylinder.

To study the transport of radioactivities through the system, provision has been made for the insertion of catcher foils directly under the capillary exit and under the skimmer. In the first measurement, a beam of 59-MeV ^{12}C ions was used to bombard a natural Ni foil of thickness 1.1 mg/cm^2. Based on cross sections calculated with the program "Alice,"[1] the efficiency of the helium jet transport was estimated to be $\gtrsim$35%. Skimmer transmission was determined to be $2.6 \pm 0.2 \times 10^{-3}$ under the present conditions. It is hoped that this figure will be improved in future tests.

Figure III-5 shows a block diagram of the laser system. These components are located in a shielded room immediately adjacent to the linac beam line. The laser beam will be conducted through a hole in the wall to the interaction chamber, a distance of about 3 meters. Currently we have a CW ring dye laser, Spectra-Physics Model 380A, which is pumped by a 5 watt Ar^+ laser. The laser frequency is controlled using an offset locking technique,[2] based on a 6328 Å stabilized He-Ne laser. Light from the dye laser has a frequency width of less than 5 MHz, and the centroid can be controlled to an accuracy of several hundred kHz by the stabilization system. A separate atomic beam chamber for stable isotopes provides a convenient frequency reference. To set the laser frequency approximately within $\sim$0.5 GHz, a digital wavemeter based on a Michelson interferometer[3] has been constructed.

Initial experiments are planned for atomic transitions in which the photon burst technique[4] can be used. In this method, bursts of photons originating from multiple excitation of the same atom in the laser beam are recorded in separate multiplicity spectra as a function of laser wavelength.

---

[1] M. Blann, University of Rochester, Nuclear Structure Laboratory, Report No. COO-3494-29 (unpublished).

[2] H. Gerhardt and A. Timmerman, Opt. Commun. 21, 343 (1977).

[3] F. V. Kowalski et al., J. Opt. Soc. Am. 66, 465 (1976).

[4] D. A. Lewis et al., Phys. Rev. A 19, 1580 (1979).

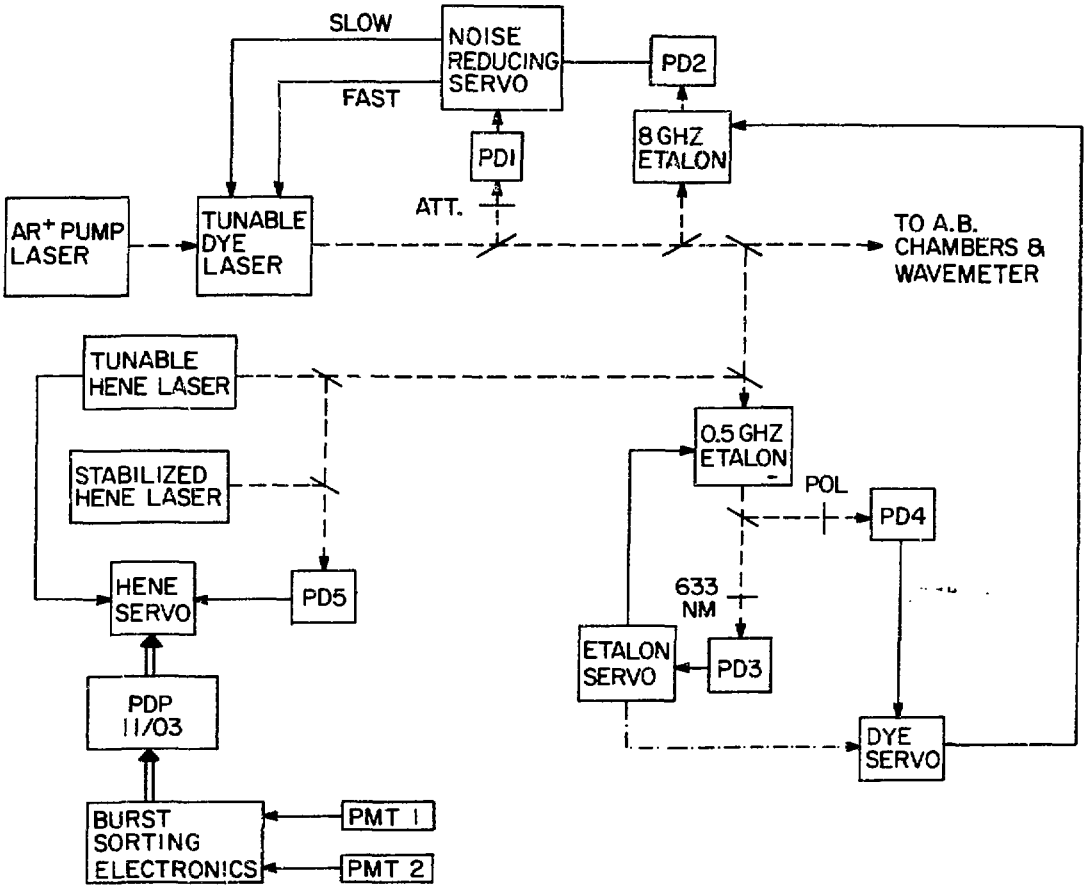

Fig. III-5. Block diagram of laser system.

The resulting suppression of random background noise leads to the ability to detect resonance-fluorescence peaks with as few as 10 atoms/s crossing the laser beam.

Barium will be the first element studied. It has an appropriate photon burst transition, and measurements of the isotope shift exist for many short-lived isotopes, thus providing a convenient testing ground for the techniques and apparatus.

3. ACCELERATOR MASS SPECTROMETRY

In experiments with Accelerator Mass Spectrometry (AMS), we use an entire accelerator system to measure minute concentrations of long-lived or stable isotopes in the range from 10^{-8} to 10^{-15}. Typically 1 to 100 milligrams of sample material are put into the ion source for such a measurement.

At Argonne we have three accelerator systems which can be used for AMS. One is the 9-MV FN tandem in conjunction with an Enge split-pole spectrograph. The second one is the combined tandem-superconducting linac system which at present boosts ions like Ni to over 300 MeV. This system is also equipped with a magnetic spectrograph of the same type as the tandem. Finally we have a 4-MV single-stage Dynamitron accelerator where ions can be analyzed with an all-electrostatic setup. While in the first half of the reported period two experiments at the tandem were completed, the second half was devoted to a number of exploratory experiments for detecting new (radio) isotopes using all three systems. The work on the Dynamitron is reported in Sec. III.A2e.

a. The Half-Life of ^{32}Si

W. Kutschera, W. Henning, M. Paul, R. K. Smither, E. J. Stephenson, J. L. Yntema, D. E. Alburger,* J. B. Cumming,* and G. Harbottle*

The result of our half-life measurement[1] was quite surprising since it yielded $T_{1/2}$ = 101 ± 18 yr, about a factor three shorter than previously accepted values. A similarly short value for the half-life, $T_{1/2}$ = 108 ± 18 yr, was found in an independent AMS measurement by the Rochester group.[2]

Figure III-6 summarizes past and present ^{32}Si half-life measurements. There is a clear trend towards shorter half-lives in recent years. The measurements labeled as "σ estimated" utilized the decay law $dN/dt = -\lambda N$, however, without measuring N explicitly. N was calculated from estimates on the respective production cross sections. In the accelerator measurements N was measured by the AMS technique. A serious discrepancy exists between the two geophysical measurements labeled "ice" and "sediment" and the accelerator measurements. Both geophysical results were obtained from the depth distribution of cosmic ray produced ^{32}Si in terrestrial reservoirs, ice from Greenland and sediment from the Gulf of California, respectively.

*Brookhaven National Laboratory, Upton, New York.

[1] W. Kutschera, W. Henning, M. Paul, R. K. Smither, E. J. Stephenson, J. L. Yntema, D. E. Alburger, J. B. Cumming, and G. Harbottle, Phys. Rev. Lett. 45, 592 (1980).

[2] D. Elmore, N. Anantaraman, H. W. Fulbright, H. E. Gove, H. S. Hans, K. Nishiizumi, M. T. Murell, and M. Honda, Phys. Rev. Lett. 45, 589 (1980).

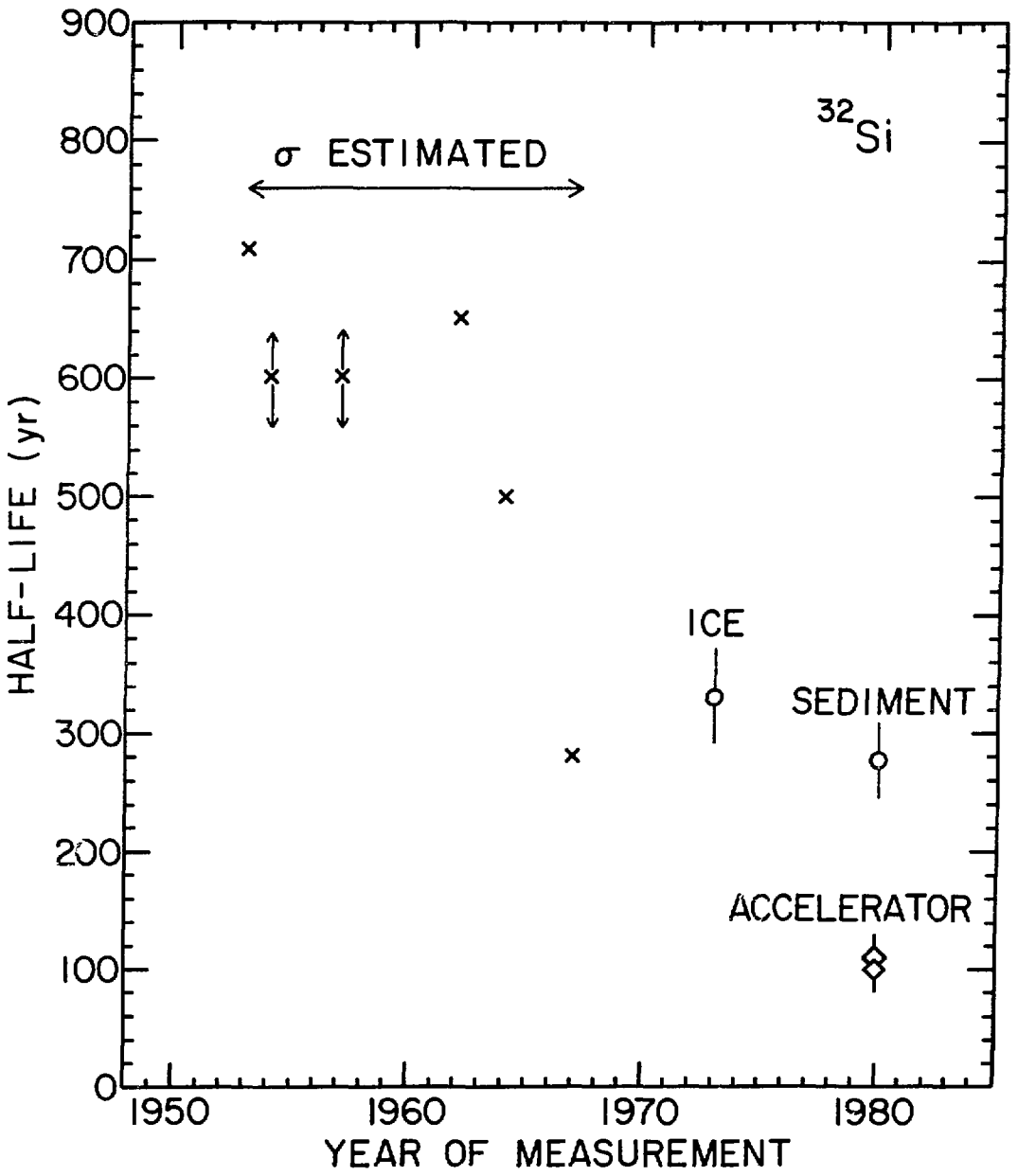

Fig. III-6. History of ^{32}Si half-life measurements.

A key assumption in these measurements is a constant influx of cosmogenic ^{32}Si into these reservoirs. If neither the geophysical nor the accelerator measurements are subject to unknown experimental errors, then the apparent discrepancy in half-life values indicates that the transport of ^{32}Si from the origin to the respective reservoirs is not understood. A somewhat less likely explanation would be variations in the cosmogenic ^{32}Si production caused by fluctuations in the cosmic-ray flux. It would be very desirable to have another measurement of the half-life by an independent method. With a sufficiently large amount of ^{32}Si it seems feasible to do a decay measurement following the decrease in activity over a period of a few years.

b. The Measurement of Nuclear Cross Sections

M. Paul,* W. Henning, W. Kutschera, E. J. Stephenson,† and J. L. Yntema

A simple way of measuring the total cross section of a nuclear reaction is to measure the radioactivity of the product nucleus. Usually, the total number of product nuclei is not very large and the method is therefore restricted to relatively short half-lives. If the product nuclei are analyzed by AMS, this limitation does not exist and the method can be extended.

At Argonne we have recently performed such an experiment to measure the cross section of the $^{26}Mg(p,n)^{26}Al$ ($T_{1/2} = 7.2 \times 10^5$ yr) reaction near threshold.[1] The results of these measurements are shown in Table III-I below. The third column in Table III-I gives the number of ^{26}Al ions detected. Since 10^{10}—10^{11} ^{26}Al nuclei were produced in the irradiation of the ^{26}Mg foils, the fraction of nuclei actually measured turned out to be only 10^{-9}. On the other hand, a comparison of column 3 and 7 shows that the number of ^{26}Al decays in the same time period is a factor of 10 smaller. For a decay counting experiment this number would be further reduced by the efficiency of detecting the decay radiation. The comparison shows that even for a very unfavorable condition of AMS detection, the ion counting technique can be more efficient. We are currently planning a similar measurement to study the $^{27}Al(n,2n)^{26}Al$ reaction cross section.

---

*Hebrew University of Jerusalem, Jerusalem, Israel.

†Indiana University, Bloomington, Indiana.

[1] M. Paul, W. Henning, W. Kutschera, E. J. Stephenson, and J. L. Yntema, Phys. Lett. 94B, 303 (1980).

TABLE III-I. Results of the $^{26}Mg(p,n)^{26}Al$ cross-section measurement.

Center-of-mass proton energy (MeV)	Running time (min)	$^{26}Al^{11+}$ ions (counts)	$^{27}Al^{8+}$ current (nA)	$^{26}Al/^{27}Al$ (10^{-11})	σ (mb)	^{26}Al decays
5.0	68	11	0.39	1.8 ± 0.6	7.4 ± 2.5	1
5.5	100	74	0.37	8.5 ± 1.3	37.3 ± 6.3	4
6.0	102	102	0.47	9.2 ± 1.3	28.2 ± 4.5	11
6.4	51	92	0.57	13.6 ± 2.0	42.6 ± 6.9	14
6.7	67	172	0.54	20.4 ± 2.6	65.2 ± 9.4	17
blank	33	0	0.32	< 0.4		

The cross sections covered in the present experiment lie in the millibarn range. It is conceivable to push this technique to the microbarn range or even lower with more favorable elements and/or improved ion sources and sample preparation techniques. In the present experiment the limiting factor was the extremely low output of Al^- (∿1 nA). It is well known that other elements like carbon, silicon or chlorine yield up to 10^4 times higher negative ion currents.

c. On the Detection of ^7Be

W. Kutschera, W. Henning, B. Myslek-Laurikainen, R. K. Smither, and J. L. Yntema

^7Be is a relatively short-lived radioisotope with a half-life of 53.3 d. It decays through electron capture with a 10% branch emitting a 478-keV γ ray. Therefore decay counting seems to be the obvious method for a ^7Be detection. However, if the total number of ^7Be atoms available for detection is below 10^5, the ion counting technique may become competitive. The measurement of such a low ^7Be yield is of interest to study the $^3He(\alpha,\gamma)^7Be$ reaction at extreme subcoulomb energies relevant for the ^7Be production in the interior of the sun.

We have started an investigation to detect ^7Be with the tandem accelerator system. ^7Be test samples were prepared via the $^9Be(\alpha,\alpha 2n)^7Be$ reaction bombarding thick Be metal discs with 42-MeV alpha particles from

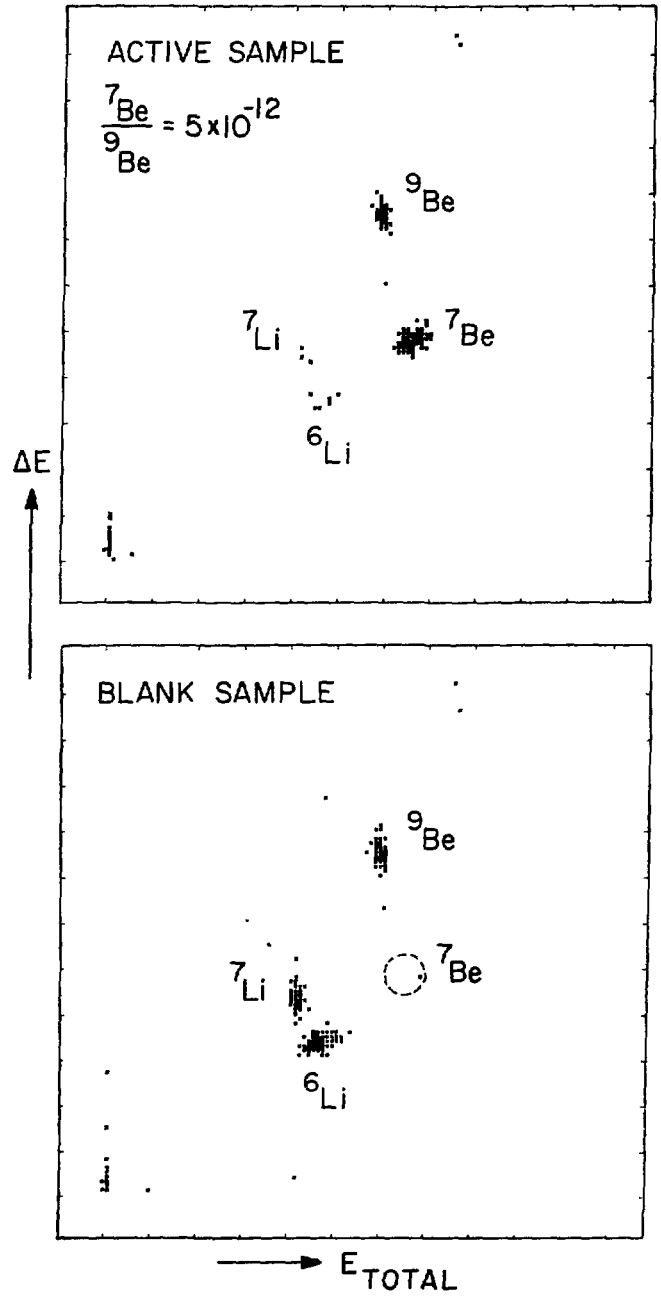

Fig. III-7. Two-dimensional density plots of the total energy E_{total} versus energy loss ΔE measured with the split-pole focal plane detector for two metallic Be samples. The upper spectrum was accumulated for 10 min, the lower one for 20 min.

the ANL cyclotron. Figure III-7 shows ion spectra from an irradiated and a blank sample measured in the focal plane detector of the Enge split-pole spectrograph. Running conditions were as follows: $^{9}BeH^{-}$ (from Be metal plus NH_3 spray) = 200 nA; 40 nA current in the spectrograph target chamber for 32.7-MeV $^{9}Be^{4+}$; $^{7}Be^{4+}$ counting rate = 0.33 sec^{-1}. From this one calculates a $^{7}Be/^{9}Be$ ratio of 5×10^{-12}. The blank sample gave only one ^{7}Be count in 20 min corresponding to a $^{7}Be/^{9}Be$ detection limit of 10^{-14}.

Although the sensitivity and cleanness of detection is very good, the overall efficiency is still too low to push the method into the desired range of below 10^{5} ^{7}Be atoms. From the sputter rate measured via the weight loss of the samples, a total detection efficiency of 1.7×10^{-5} was determined. By far the biggest loss is due to the low BeH^{-} yield. The BeH^{-}/Be(sputtered) ratio was measured to be 3×10^{-4}. Therefore, it appears that the low negative ion efficiency is the bottleneck for a high-efficiency detection of ^{7}Be. Improved ion source technology will hopefully change this situation in the near future.

d. Accelerator Mass Spectrometry of ^{59}Ni and Fe Isotopes at the Superconducting Linac

W. Henning, W. Kutschera, B. Myslek-Laurikainen, R. C. Pardo, R. K. Smither, and J. L. Yntema

We have obtained initial results in an attempt to use the Argonne tandem-linac system for accelerator mass spectrometry of medium-heavy nuclei. Nuclei of the radioisotope ^{59}Ni ($T_{1/2} = 7.5 \times 10^{5}$ yr) and of the stable isotope ^{58}Fe at low concentrations have been accelerated and clearly identified. The latter experiment is in preparation of a measurement of the half-life of ^{60}Fe($T_{1/2} \simeq 3 \times 10^{5}$ yr). For ^{59}Ni complete stripping to the maximum charge state $q_{max} = 28^{+}$ was employed to separate it from its ^{59}Co isobaric background ($q_{max} = 27^{+}$). For the study of ^{60}Fe, preliminary tests were performed with the stable radioisotope ^{58}Fe using a passive absorber foil for, essentially, a differential energy loss measurement.

The Argonne tandem-superconducting linac accelerator system presently provides beams of ≃5 MeV/nucleon in the mass region investigated here, approximately a factor of three higher in energy than the tandem alone. The advantage of higher energy from the linac comes at the expense of a higher isobaric ion-beam background, since the superconducting linac

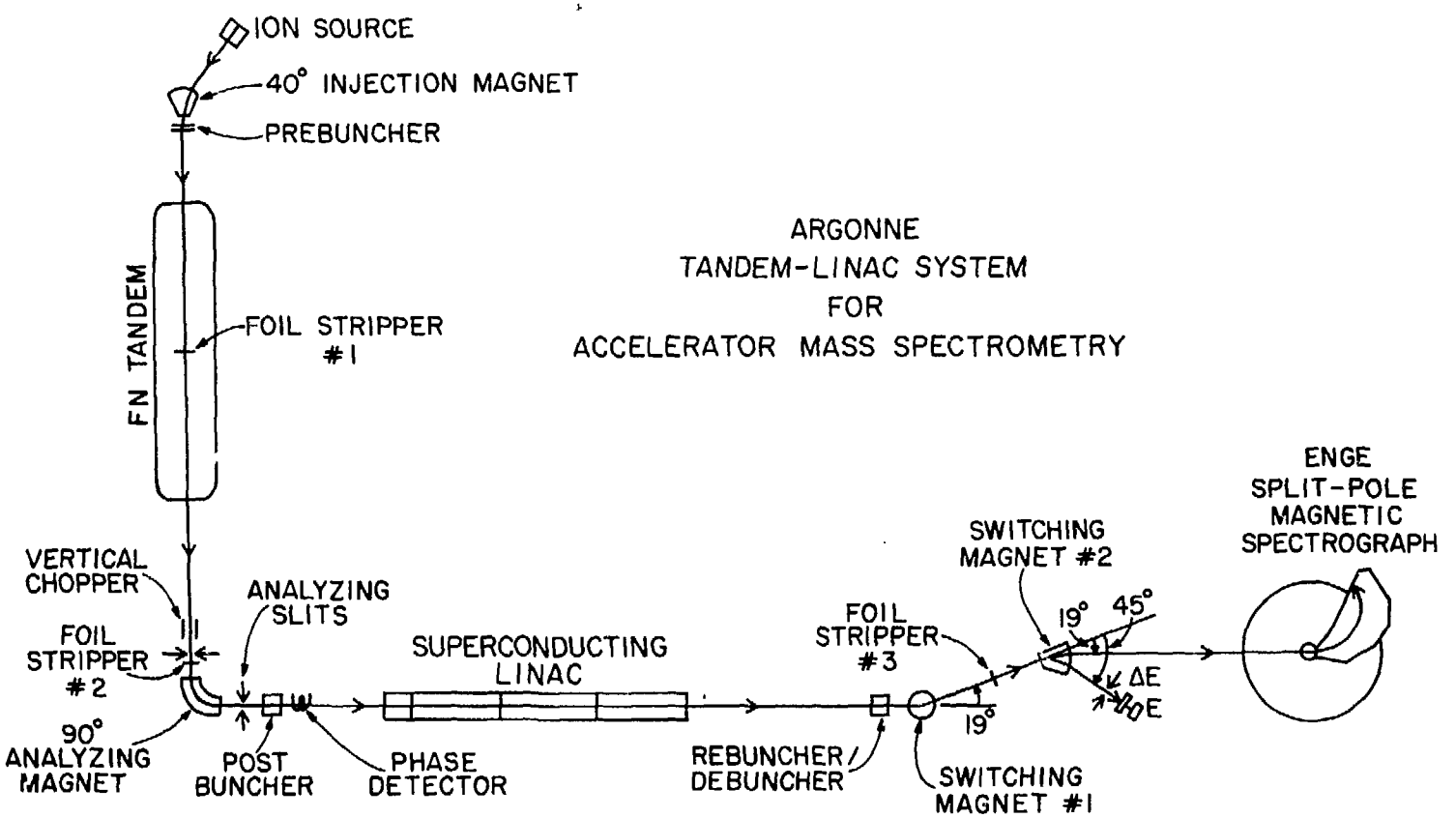

Fig. III-8. Schematic layout of the Argonne tandem-linac system, showing the essential components for accelerator mass spectrometry. The magnetic spectrograph was not yet used in the present measurements.

is an rf structure whose phase needs to be locked to the beam-pulse phase by actually sensing the arrival time of these pulses at the entrance of the linac (Fig. III-8). This requires a measurable beam of at least a few tens of picoamperes current. Therefore in order to accelerate radioisotopes of much lower intensity, we have developed the technique of an isobaric carrier beam, which then needs to be separated after acceleration. Although the carrier beam presents a difficult problem in separation, it can be used in three rather useful functions: (i) tuning of the accelerator system with the measurable beam, (ii) stabilizing the accelerator by slit-current (tandem) and phase-lock control (linac), and (iii) normalizing beam currents vs ion counts. Although the latter poses a number of problems, as for example the constancy of the relative negative ion output of different elements from the sputter source, it has the great virtue of allowing a continuous normalization without retuning the accelerator system.

To investigate the fully stripping technique, we have measured the charge-state distribution of some linac beams. Table III-II shows that for the lighter ions (^{35}Cl and ^{40}Ca) at ≈5 to 6 MeV/nucleon incident energy, an appreciable fraction (∿10%) is fully stripped. On the other hand, similar incident energies per nucleon for ^{59}Co and ^{58}Ni yield only a very small fraction of fully stripped ions (∿0.01—0.02%). This reflects the Z^2 dependence of the binding energy of the last electron which requires that the ion velocity increase proportionally to Z for equal stripping probability. It is conceivable that with the final linac configuration the stripping efficiency for the heavier ions of interest here can be increased by a factor of ≈100.

For the ^{59}Ni measurement, we prepared a 150 mg sputter pellet composed of approximately equal amounts of Co and Ni. It contained ^{59}Ni from neutron activation in a ^{59}Ni/Ni ratio of 1.3×10^{-7}. The tandem-linac system delivered a ^{59}Co-^{59}Ni beam of 328 MeV with about 2×10^9 ^{59}Co ions/sec. This beam was passed through stripper #3 (see Fig. III-8) and the second analyzing magnet (#2), set to select $^{59}Ni^{28+}$ ions at 45°. The particle energy spectrum measured under this condition with a Si ΔE-E telescope is shown in Fig. III-9. Although the ^{59}Ni counting rate was low (0.7 counts/min) due to the small stripping efficiency (see Table III-II), ^{59}Ni ions are clearly identified and separated from the ^{59}Co background.

TABLE III-II. Charge state distribution of various medium-heavy ion beams from the linac, after stripping in a 100 μg/cm^2 carbon foil.

Charge state	Charge state fraction (%)				
	^{35}Cl	^{40}Ca[a]	^{40}Ca	^{59}Co	^{58}Ni
	165 MeV	170 MeV	260 MeV	328 MeV	314 MeV
12	0.30				
13	1.3				
14	9.6				
15	37.8	6.4	0.40		
16	39.5	18.0	1.9		
17	11.5	36.8	14.1		
18		32.1	41.2		
19		6.3	33.7		
20		0.41	8.7	0.36	0.075
21				3.0	0.81
22				13.5	5.2
23				31.5	18.7
24				36.0	35.5
25				14.7	29.9
26				0.97	9.4
27				0.023	0.45
28					0.014

[a] 40 μg/cm^2 carbon foil.

Due to the multiple stripping involved in the present measurement, the sensitivity for detecting ^{59}Ni radioisotopes, ^{59}Ni/Ni $\approx 10^{-8}$, is rather low. Optimistically one might hope for two orders of magnitude improvement from an increased stripping fraction at higher incident energy, for another one to two orders of magnitude from an increased ion-source output, and of course for some increase in sensitivity from a longer measurement. Measurements in the range of ^{59}Ni/Ni $\approx 10^{-12}$ seem feasible in the future.

The ^{58}Fe tests were performed in preparation for a ^{60}Fe($T_{1/2} \approx 3 \times 10^5$ yr) lifetime measurement by accelerator mass spectrometry, similar to our recent measurement of the ^{32}Si half-life. Ni-Fe mixtures, of natural

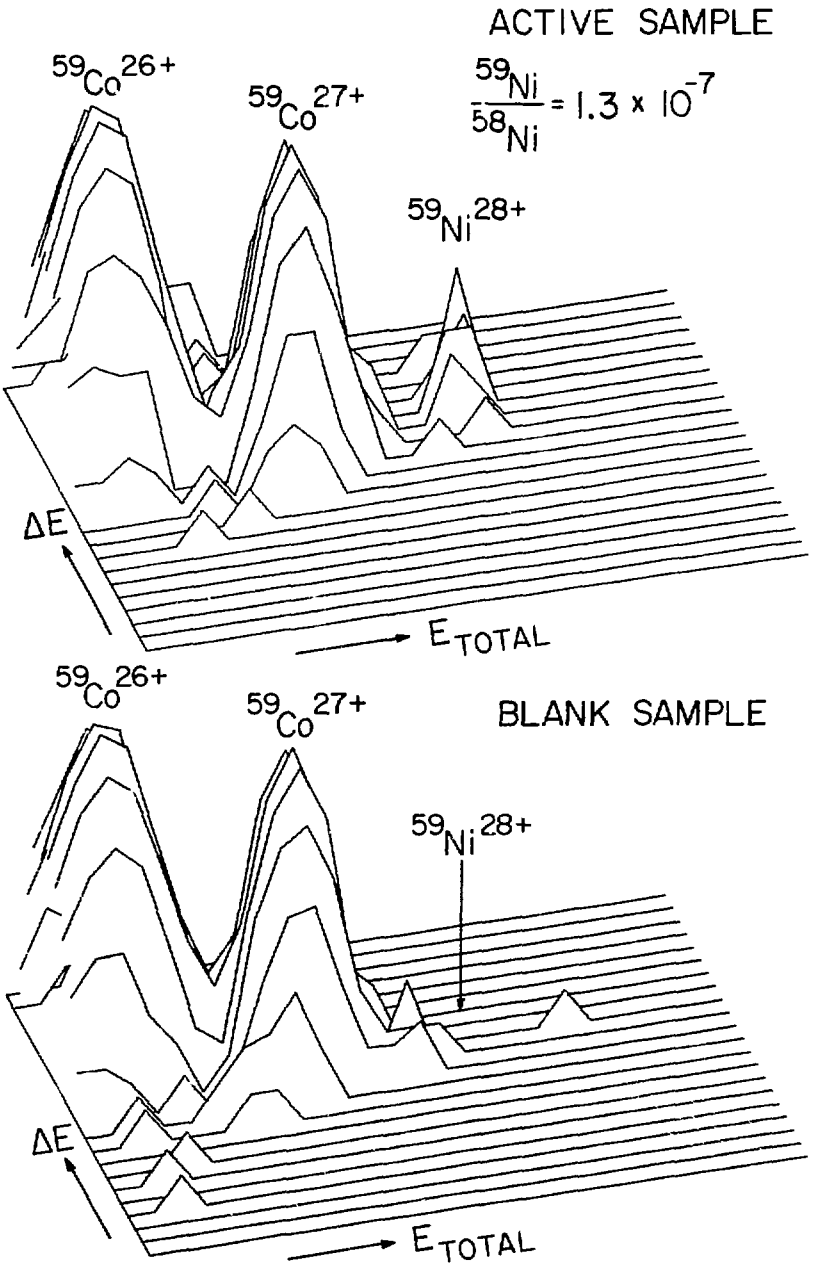

Fig. III-9. Isometric plot of total energy E_{total} versus differential energy loss ΔE for $^{59}Co(^{59}Ni)$ ions as measured with the Si ΔE-E telescope. The vertical scale is logarithmic, offset by 1 count such that a single count is showing.

abundance as well as depleted by a factor of 10^2 in ^{58}Fe (already only 0.3% natural abundance), were used as the sputter source materials. Only the terminal stripper was used in the accelerator system, resulting in an $^{58}Fe(^{58}Ni)$ beam of 169-MeV energy. The beam was again passed through the two analyzing magnets with a 1.7 mg/cm^2 aluminum foil placed approximately halfway between them. In this measurement the foil acted as a passive differential absorber resulting in a difference in energy loss for the ^{58}Fe and ^{58}Ni ions. The absorber foil thickness was chosen in such a way that the energy loss difference places the ^{58}Fe ions, with various charge states, halfway in magnetic rigidity between corresponding charge states of the ^{58}Ni ions. In this way the ^{58}Ni carrier beam background could be strongly suppressed by optimizing the second analyzing magnet setting for $^{58}Fe^{20+}$. The ΔE and E signals, and also the time of flight with respect to the pulsed beam structure of the linac, as recorded by the silicon detector telescope are shown in Fig. III-10 for a pure Ni, a pure ^{58}Fe, and a mixed Fe-Ni sample. The ^{58}Fe ions are unambiguously identified, with a sensitivity at present of $^{58}Fe/Fe \simeq 1 \times 10^{-7}$.

e. An Overview on Long-lived Radioisotopes

W. Kutschera and B. Myslek-Laurikainen

It is well established that with increasing half-life the counting of ions eventually becomes a more efficient detection method of radioisotopes than the counting of decays. However, where this transition occurs is difficult to define, since the detection limits of the two methods depend strongly on the specific radioisotope. In any case, we expect that this transition will be pushed towards shorter and shorter half-lives with improved detection efficiency of AMS. If we arbitrarily choose a half-life of one year for this limit, we are left with about 140 radioisotopes plotted in Fig. III-11. They cover a range of eighteen orders of magnitude. Out of these only nine have been used for AMS so far: ^{3}He, ^{10}Be, ^{14}C, ^{26}Al, ^{32}Si, ^{36}Cl, ^{41}Ca, ^{59}Ni, and ^{129}I. The large number not yet touched presents a great potential for this new technique.

The data plotted in Fig. III-11 were mainly obtained from the Table of Isotopes.[1] There are a few cases where more recent data sources

[1] Table of Isotopes, edited by C. M. Lederer and V. S. Shirley (Wiley, New York, 1978).

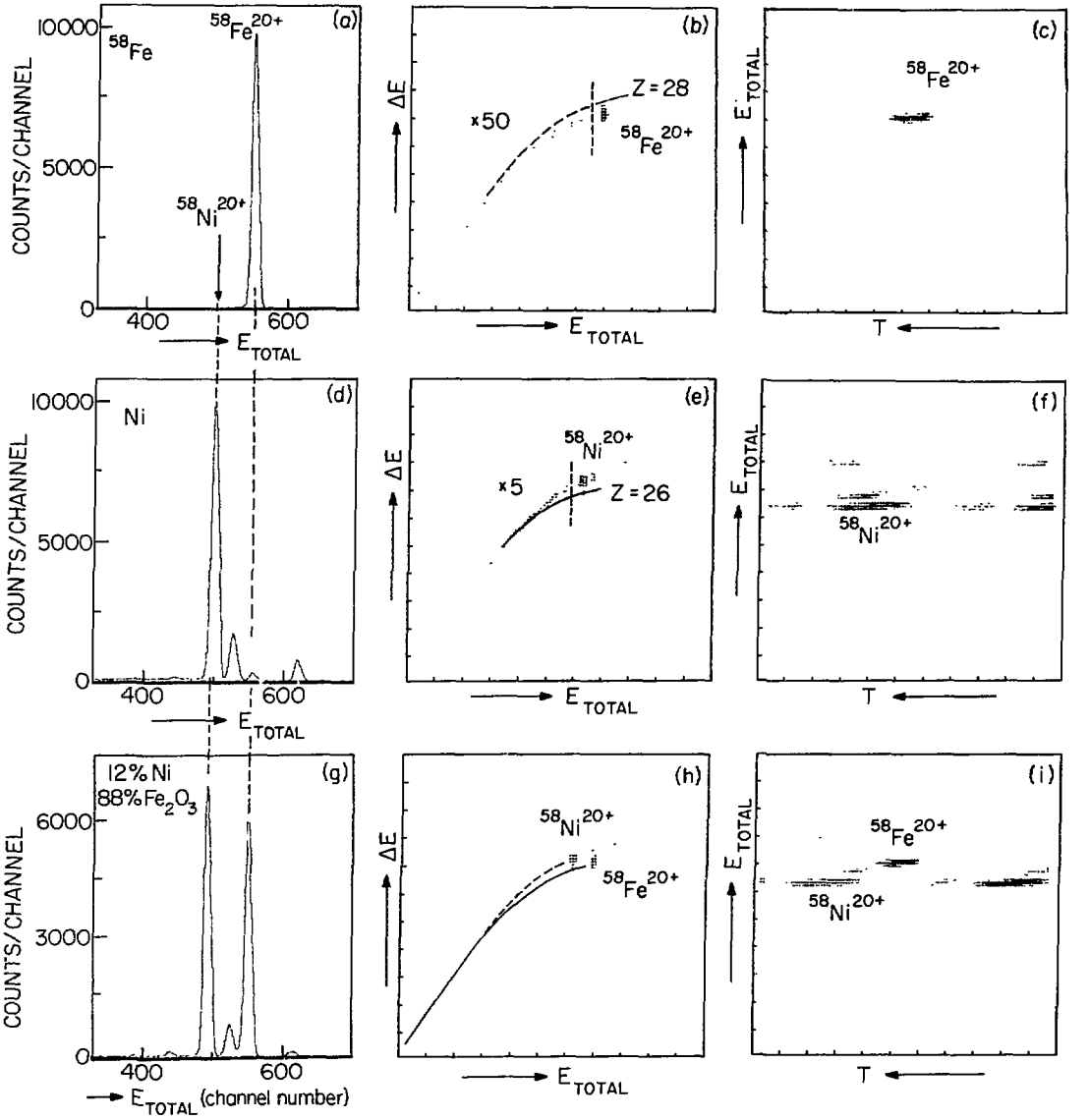

Fig. III-10. One- and two-dimensional spectra for ^{58}Fe and ^{58}Ni ions of the total energy, E_{total}, energy loss, ΔE and time-of-flight, T, measured in the Si ΔE-E telescope for three different ion source samples. The background peak in spectrum d, at the position of the $^{58}Fe^{20+}$ peak, arises mainly from slit-scattered ^{58}Ni ions of a different charge state, as obvious from the ΔE signal [not visible in (e)]. The time-of-flight spectra (c), (f), (i) cover a range of nearly twice the beam-pulse periods (20 nsec).

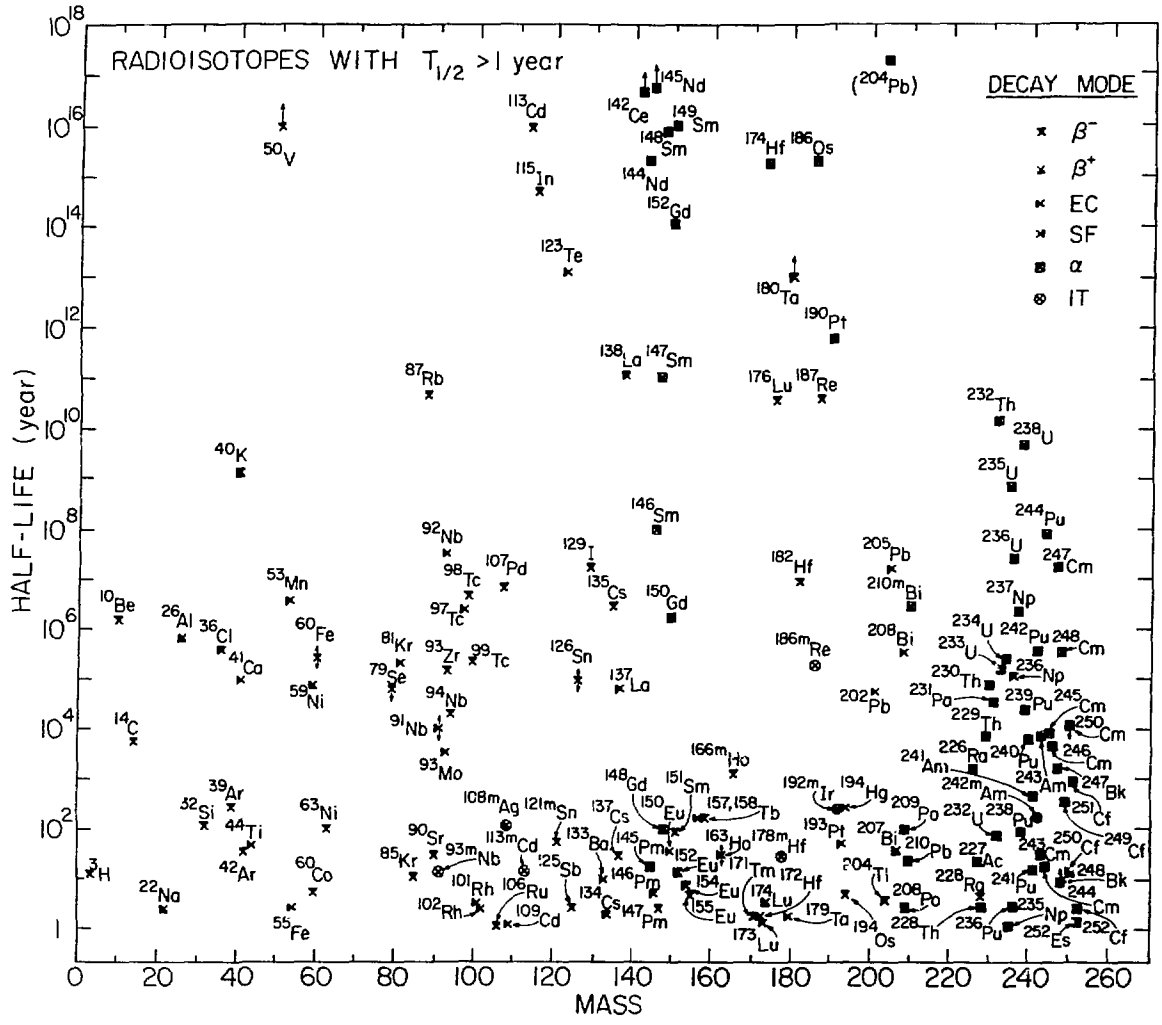

Fig. III-11. Long-lived radioisotopes. Data points are marked by symbols indicating single or multiple decay mode. Arrows mean that the half-life is only approximately known in the respective direction. Isotopes in brackets indicate that their assignment is questionable.

were used. Errors on half-life values have been omitted since they were in general too small to show up on the figure. It was noticed, however, that sometimes half-life values from different measurements scatter by far more than the quoted errors. There are a few radioisotopes whose half-life is very poorly known. Among them are ^{60}Fe, ^{79}Se, ^{91}Nb, and ^{126}Sn, all in a half-life range of around 10^5 years.

There appears to be a reduction of radioisotopes below the actinides with half-lives between 500 and 50 000 years. The special role of ^{14}C can clearly be seen. A similar gap shows up between 10^8 and 10^{10} years. Here ^{40}K plays a similar role as ^{14}C in the lower gap.

4. NEAR FUTURE RESEARCH AT THE TANDEM ACCELERATOR

With the steadily increasing availability of the tandem-linac system a gradual shift of the research effort from using the tandem alone to the combined accelerator system is expected. In 1982 the laser program will perform extensive experiments on neutron-deficient barium isotopes, to be produced via $Sn(^{12}C,xn)Ba$ reactions with linac beams. Accelerator mass spectrometry will continue to use the tandem alone for measuring long half-lives (e.g., ^{60}Fe) and cross sections of astrophysical interest [e.g., $^3He(\alpha,\gamma)^7Be$]. The tandem-linac system will be used to push this technique to heavier mass regions. In 1983 the laser program is likely to be extended to new mass regions, depending on the experience and current interest in this field. A steady effort to use the technique of accelerator mass spectrometry for the detection of very small numbers of atoms ($<10^5$) will continue through 1982—1983. The hope is to reach a sensitivity which is high enough to be applied to a solar neutrino detection experiment. Both the $f_{7/2}$ shell nuclei program and the study of radioactive atoms at the tandem will be continued with somewhat reduced effort in 1982 and 1983. In 1982 we hope to initiate a program that uses the large-volume high-resolution NaI photon detectors to measure the radiative capture of α particles.

IV. NEUTRON AND PHOTONUCLEAR PHYSICS

INTRODUCTION

The Argonne neutron-physics program has traditionally included measurements of the fundamental properties of the neutron. An experiment to measure the electric dipole moment of the neutron using stored ultracold neutrons has been undertaken. It is hoped that a sensitivity of around 1×10^{-25} e-cm will be attained by the end of 1981. This will provide a test of the Weinberg-Salam standard model in the gauge theory of weak interactions.

A major portion of the photonuclear program is devoted to studies using the Argonne threshold photoneutron facility. The photoneutron method allows one to study regions of excitation in nuclei which are inaccessible by other traditional neutron-induced reactions. The primary emphasis of photoneutron research at ANL are in the fields of giant resonances, basic reaction mechanisms in light nuclei and fundamental properties of the deuteron. Much of the effort during this year was devoted to the application of the new multidirectional electron-beam transport system to high-accuracy measurements of the angular distribution in deuteron photodisintegration. This work should provide the most stringent test available for the multipole composition of the photodisintegration process.

The second major effort is the study of the isospin splitting of the giant resonance in ^{60}Ni. This study is performed in collaboration with the photonuclear group at the University of Illinois. The purpose of the work is to determine the extent to which the giant resonance in vibrational nuclei is broadened by isospin splitting and by the collective motion of the nuclear surface. The photoneutron experiments are complementary with photon-scattering studies of the vibrational nuclei which were performed in collaboration with the group at the University of Illinois. Inelastic photon scattering from the vibrational nuclei should reveal information regarding the coupling of two collective modes in nuclei, namely, the giant-dipole oscillations and the surface vibrations. Elastic photon scattering, however, provides information on the amount of broadening of the giant dipole resonance and the relative strengths of isospin components of the resonance.

A. NEUTRON RESEARCH

Measurement of the Electric Dipole Moment of the Neutron

V. E. Krohn, G. R. Ringo, T. W. Dombeck, M. S. Freedman,* J. M. Carpenter,† and J. W. Lynn‡

The purpose of this project is to measure the electric dipole moment (EDM) of the neutron. Because this can be done by a measurement of frequency change, it can be done with great sensitivity and indeed is generally believed to be the most sensitive test available of time-reversal invariance. The present situation is that with about a factor of 10 improvement in sensitivity, a whole class of gauge theories—those which explain CP failure by introducing a new scalar field [e.g., S. Weinberg, Phys. Rev. Lett. 37, 657 (1976)]—can be given a definitive test.

Since the measurement of the neutron EDM is fundamentally a frequency measurement, its statistical uncertainty is inversely proportional to the duration of the measurement. It is therefore natural to try the measurement on ultracold neutrons (UCN). These neutrons of $v < 7$ m/s can be kept in a bottle for hundreds of seconds. We propose to do this using two unique features. First, we propose to use a pulsed neutron source and keep the inlet to the bottle open only when the pulsed source is on, thus allowing a buildup to an asymptotic density determined by the peak flux of the source instead of the average. This has the advantage that pulsed sources have peak fluxes that are much higher than the average fluxes of steady state sources of the same average power. Second, we propose to produce the UCN by Bragg reflection of considerably faster (400 m/s vs 7 m/s) neutrons from a moving mica crystal designed so that the reflected neutrons are almost stationary in the laboratory system. The advantage of this is that it avoids the problems of extracting the very delicate UCN from the hard to control environment in a high flux source.

The present state of the project is that both of these ideas have been tested and shown to be practical as have several other ideas for enhancing the production of UCN, such as the use of reflectors around the moving crystal and funnels to concentrate the UCN in real space at the

*Chemistry Division, ANL.

†Intense Pulsed Neutron Source Program Division, ANL.

‡University of Maryland, College Park, Maryland.

expense of their concentration in velocity space. It has been shown that we have the technique for obtaining satisfactory crystal packages from the limited supplies of fluoridated mica (fluor-phlogopite) available in the world. This is important because this material is the best available reflector of 400 m/s neutrons—considerably better than natural mica. The measured flux of UCN suggests that the pulsed neutron source now under construction at Argonne (IPNS-1) will give a UCN density in a bottle competitive with that available at the high-flux reactor at Grenoble where another EDM measurement is underway.

The next stage of the project is to show that we can build bottles appropriate for the EDM measurement having neutron retention lifetimes of at least 30 seconds (200 second bottles exist). Then we must build such a bottle in a combined magnetic and electric field and measure the effect of reversing the electric field on the precession rate.

B. PHOTONUCLEAR PHYSICS

a. Photodisintegration of the Deuteron

R. E. Holland, R. J. Holt, H. E. Jackson, R. D. McKeown, J. R. Specht, and K. E. Stephenson

The deuteron is the simplest nuclear system for the study of the meson exchange and virtual isobar effects. Theoretical predictions indicate that the angular distribution of photoneutrons near threshold should be sensitive to final state interactions and momentum dependent effects in the N-N potential. Furthermore, the measurements[1] at Mainz of the $D(\gamma,p)$ reaction at 0° are in disagreement with all theoretical predictions at moderate photon energies. Thus, it is essential to have accurate measurements of the angular distribution of photoneutrons from the $D(\gamma,n)$ reaction from threshold to 20 MeV.

[1] R. J. Hughes, A. Zieger, H. Wäffler, and B. Ziegler, Nucl. Phys. A267, 329 (1976).

(i) Angular Distributions

The relative angular distributions at 45°, 90°, and 135° have been measured from E_γ = 3.5 to 10 MeV for the $D(\gamma,n)H$ reaction. The results are shown in Fig. IV-1. The error limits shown are of the order of 2%. The data are compared with three calculations: those of (a) Hadjimichael[1] with only E1 and M1 multipoles, (b) Hadjimichael[2] with all multipoles up to M2, and (c) Partovi.[3] These data illustrate the necessity for including multipoles higher than M1 even below an excitation energy of 10 MeV. It appears from these results that the theory and experiment will be in disagreement above 10 MeV. Data taken at higher energies are currently under analysis. The collimators for the 155°-flight path have been installed and an initial trial run at 155° has been performed.

[1] E. Hadjimichael, Phys. Lett. 46B, 147 (1973).

[2] E. Hadjimichael, private communication (1980).

[3] F. Partovi, Ann. Phys. 27, 79 (1964).

(ii) The $D(\gamma,\vec{n})H$ Reaction

Theoretical studies indicate that this reaction is particularly sensitive to meson-exchange effects in the N-N potential. Previous measurements of this kind typically have been of relatively low statistical

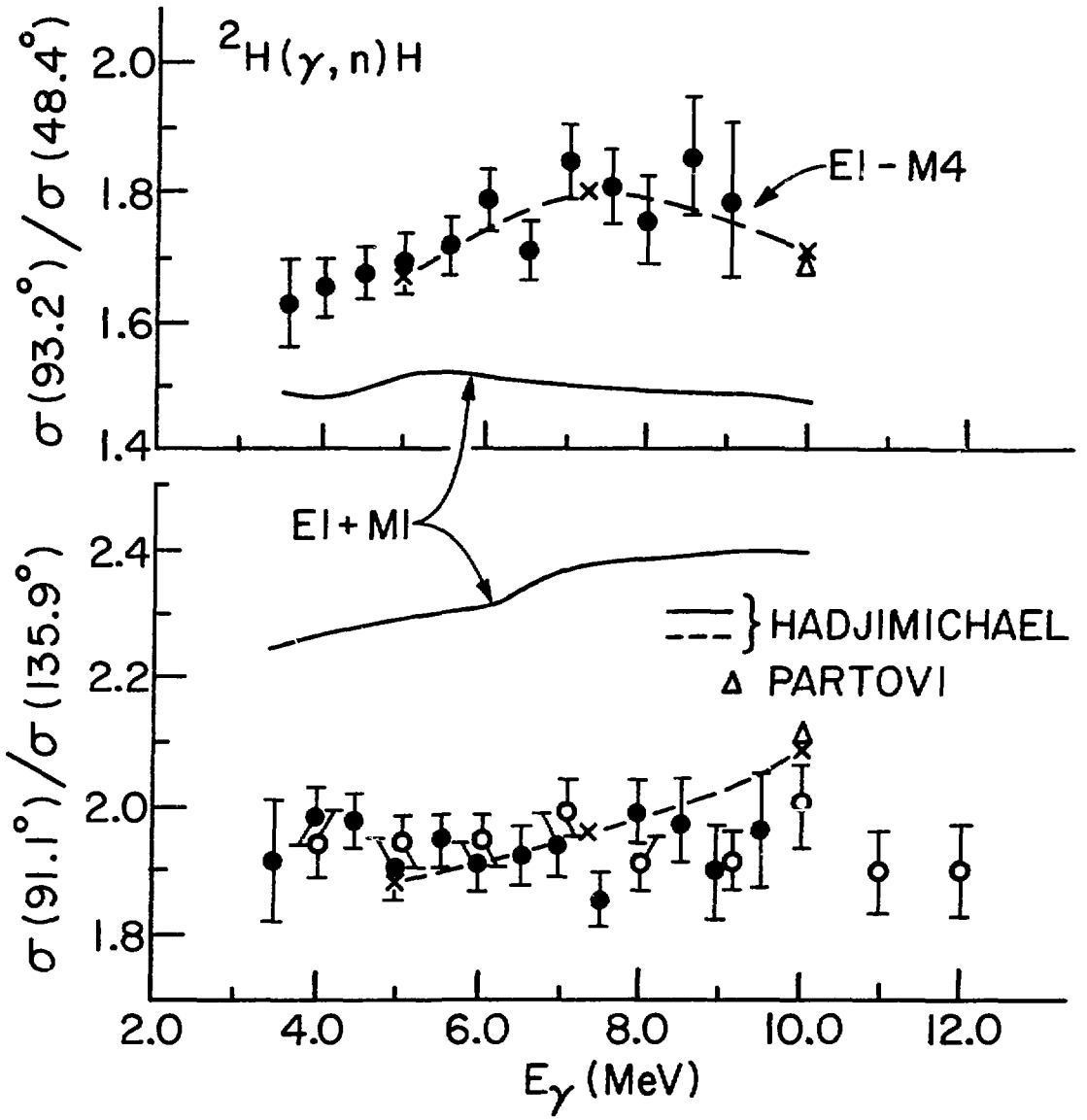

Fig. IV-1. The solid circles represent the results of the present measurements for the D(γ,n)H reaction. The solid curve is the result of a calculation in which only E1 and M1 multipoles are included; whereas, the dashed curve represents the calculation with multipoles through M4. The triangles indicate the calculations of Partovi.

accuracy, and thus, have not provided a conclusive test of the theoretical predictions. With the intense-pulsed bremsstrahlung source available at the ANL high-current electron linac and with the development of high-efficiency neutron polarimeters, we plan to measure the photoneutron polarization from this reaction with high accuracy. Design of the polarimeters is underway. These measurements are expected to proceed after the angular distributions have been studied.

b. Doorway Resonances in ^{29}Si

R. J. Holt, H. E. Jackson, J. R. Specht, and K. E. Stephenson

Since the discovery of doorway states in ^{29}Si, the theoretical advances in describing the $^{28}Si+n$ system have become more sophisticated. In the most recent theory the $^{28}Si(n,\gamma)^{29}Si$ reaction was described within the formalism of Boridy and Mahaux by constructing particle-vibration basis states. These theories indicate that there may be a substantial amount of radiative strength for doorway resonances above the present experimental observations.

The angular distributions at 90° and 135° were measured for the $^{29}Si(\gamma,n_0)^{28}Si$ reaction. This experiment made use of the pico-pulse and 25-m flight paths for high resolution, the multidirectional beam transport for high-accuracy angular distribution measurements and a specially-fabricated $^{29}SiO_2$ quartz sample. The cross sections are currently being interpreted in terms of an R-matrix theory.

c. Isospin Splitting of the Giant Dipole Resonance in ^{60}Ni

T. J. Bowles,* R. J. Holt, H. E. Jackson, R. D. McKeown, A. M. Nathan,† and J. R. Specht

The question of isospin splitting of the giant dipole resonance in non-self-conjugate nuclei has long been an issue in photonuclear physics. Although there are a number of theoretical calculations which predict the amount of splitting and the relative strength of the two components, the experimental work is very sketchy.

---

*Los Alamos National Laboratory, Los Alamos, New Mexico.

†University of Illinois, Urbana, Illinois.

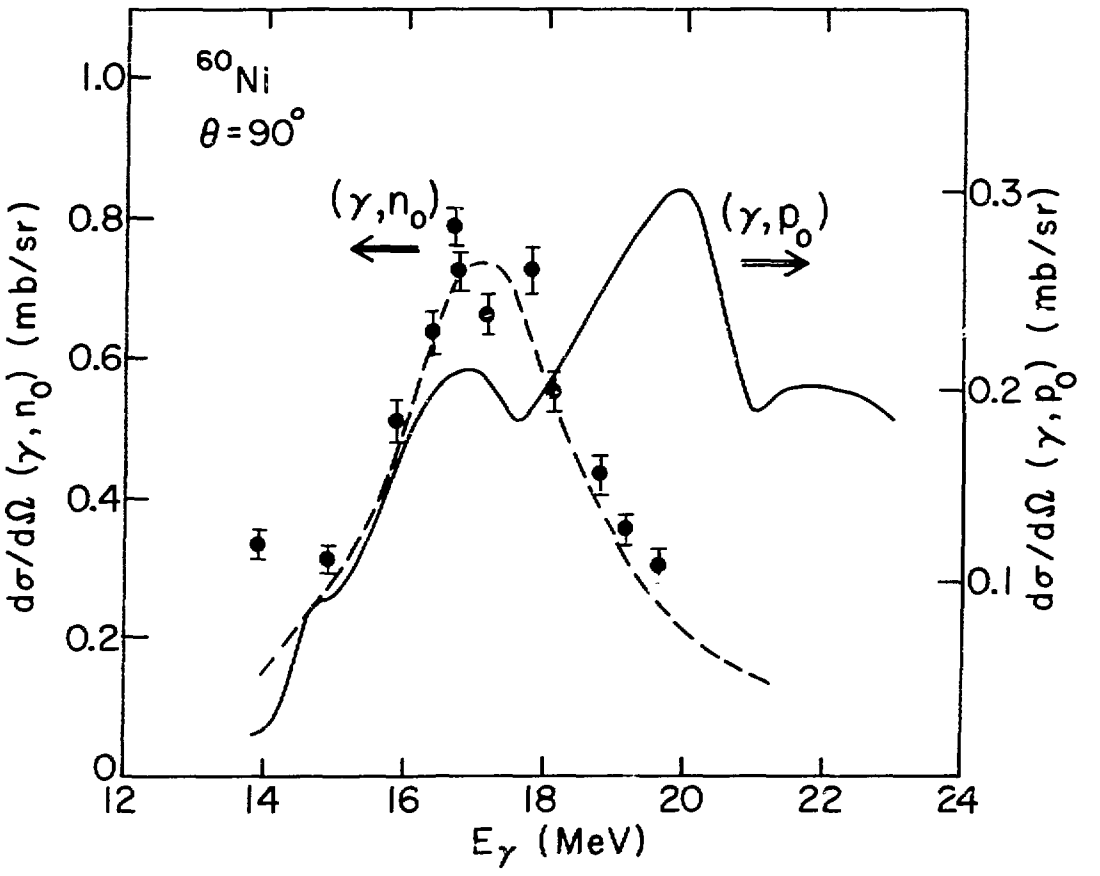

Fig. IV-2. The solid circles represent the cross section at 90° for the ^{60}Ni(γ,n$_0$)^{59}Ni measurements. The solid curve illustrates the results of a ^{59}Co(p,γ$_0$)^{60}Ni measurement. The dashed curve is due to a Lorentzian shape with a width determined from the (p,γ$_0$) data.

The photoneutron reaction is a selective probe for isospin splitting. For example, in a (γ,n$_0$) reaction only photoneutrons from the $T_<$ component are allowed by the isospin selection rules; whereas in (p,γ) reactions, both components can be excited.

The cross section at 90° for the ^{60}Ni(γ,n$_0$)^{59}Ni reaction was measured between 14 and 20 MeV. Since the first excited state in ^{59}Ni is only 340 keV above the ground state, it was necessary to take 12 separate runs and analyze only the top ∿200 keV of the spectra. This ensured that only ground-state photoneutrons were observed. The results of this work are shown in Fig. IV-2. The data are compared with (γ,p$_0$) results from

Diener et al.[1] (see the solid curve in Fig. IV-2). There are clear isospin dependent effects in the cross section. There are two distinct peaks in the (γ,p_0) data and only one in (γ,n_0). This is consistent with the isospin-splitting model of Goulard and Fallieros.[2] The relative strengths of the two components of the giant-dipole resonance are being deduced from the elastic photon scattering measurements for ^{60}Ni.

[1] E. M. Diener, J. F. Amann, P. Paul, and S. L. Blatt, Phys. Rev. C 3, 2303 (1971).

[2] B. Goulard and S. Fallieros, Can. J. Phys. 45, 3221 (1967); R. Ö. Akyüz, and S. Fallieros, Phys. Rev. Lett. 27, 1016 (1971).

d. Photon Scattering by the Giant-Dipole Resonance in Vibrational Nuclei

T. J. Bowles, R. J. Holt, H. E. Jackson, R. M. Laszewski,* R. D. McKeown, A. M. Nathan,* J. R. Specht, and R. Starr*

Quasi-monochromatic photons have been used to measure elastic and inelastic photon scattering cross sections in the giant dipole resonance (GDR) region of ^{52}Cr, Fe, ^{60}Ni, ^{92}Mo, and ^{96}Mo in an experiment in which the elastic and inelastic scattering are resolved. The elastic scattering cross sections show clear evidence for isospin splitting of the GDR. The inelastic scattering to low-lying vibrational levels, which is a measure of the coupling between the GDR and collective surface vibrations, is in qualitative agreement with the predictions of the dynamic collective model. However, when examined in detail, this model does not provide an adequate description of the scattering data.

* University of Illinois, Urbana, Illinois.

V. THEORETICAL PHYSICS

INTRODUCTION

The nuclear theory program deals with the properties of nuclei and with the reactions and interactions between nuclei and a variety of projectiles. Our main areas of concentration are the following.

A. Heavy-ion direct-reaction theory.

B. Nuclear shell theory and nuclear structure.

C. Nuclear matter and nuclear forces.

D. Intermediate-energy physics.

E. Microscopic calculations of high-energy collisions of heavy ions.

F. Light ion direct reactions.

G. Other theoretical physics.

Recent progress and plans for future work in these seven main areas of concentration are presented below.

A. HEAVY-ION DIRECT-REACTION THEORY

Heavy-ion scattering at energies just above the Coulomb barrier typically exhibits large cross sections to several low-lying states (inelastic scattering) and smaller cross sections to many states reached by few-nucleon transfer reactions. Attempts to predict these cross sections (both inelastic and transfer) with the distorted wave Born approximation (DWBA) have often been unsuccessful, suggesting the necessity of coupled-channels calculations. Such calculations including all of the transfer channels are clearly not yet possible. However the very fact that there are so many particle-transfer channels and the small cross section to each one suggests that the effects of these channels on the elastic and inelastic scattering wavefunctions should be accountable for by the imaginary part of the optical potential. The few strongly populated inelastic channels could have important explicit effects that are not naturally accounted for by a complex optical potential.

In the last few years we have developed techniques for heavy-ion coupled-channels calculations and have incorporated these methods into Ptolemy, a program for the computation of heavy-ion direct reactions. We are now in a position to analyze heavy-ion inelastic scattering at energies from below the Coulomb barrier to several times the Coulomb barrier. We hope that the coupled-channels calculations will be able to accurately reproduce the inelastic scattering data. If so, the coupled-channels Born approximation may be adequate for the transfer reactions.

Heavy-ion inelastic scattering should be a useful tool for extracting nuclear-structure information about low-lying collective states. In such scattering both Coulomb and nuclear excitation are important and the interference between these two processes can often be clearly seen. Second-order terms in the coupling potential can also have measurable effects and these terms can distinguish between different models (rotational, vibrational) for a given state.

A Program for Coupled-Channels Calculations of Heavy-Ion Inelastic Scattering

M. H. Macfarlane, S. C. Pieper, and M. J. Rhoades-Brown

The program Ptolemy has been extended to do coupled-channels calculations for heavy-ion inelastic scattering. The techniques described in our previous report are used. The program uses the collective model with rotational or vibrational matrix elements (other matrix elements may be directly given in the input). Mutual excitation of both nuclei can be computed. The program has been designed to make easy the specification of a variety of reactions (e.g., only one or both nuclei may be excited, there may be channels in which both nuclei are excited, channels may be coupled in first or second order, nuclear and Coulomb deformations need not be related). The most frequently

used loops have been constructed so that they run very efficiently on Argonne's IBM 370/195 (the solution of the coupled differential equations proceeds at a rate of about five million floating point operations per second).

B. NUCLEAR SHELL THEORY AND NUCLEAR STRUCTURE

Extensive calculations have been carried out to provide well-tested nuclear structure input for interpreting current experiments. This input is obtained from models which are in good agreement with energy level spectra and electromagnetic properties of the nuclei in question. Although the many-body nuclear shell model provides most of the input, some also comes from the interacting boson model. The work has been aimed at interpreting inelastic scattering of intermediate energy pions by nuclei, understanding high-multipolarity magnetic transitions seen in electron scattering and high-spin states seen in heavy-ion reactions.

a. Pion Excitation of States of Non-normal Parity by Inelastic Scattering

T.-S. H. Lee and D. Kurath

Many experiments are underway to study excitation of nuclear states by inelastic scattering of pions with energy near the (3,3) resonance. We have made extensive calculations for the nuclei ^{10}B, ^{11}B, ^{12}C, ^{13}C, ^{14}C, ^{14}N, and ^{15}N with the distorted wave impulse approximation (DWIA) formulated in momentum space, where the input is the nuclear transition density from shell model calculations. For excited states with parity opposite to that of the ground state we find that strong transitions in these nuclei are caused by the J(LS) operators 4(31), 3(30), 2(11), and 1(10), where J, L, and S are, respectively, the total, orbital, and spin angular momentum of the particle-hole operator. Each of these operators leads to a distinctive angular distribution in the DWIA calculation. We have developed approximate formulas to estimate the excitation cross section for particular states from the transition density matrix elements without carrying out the lengthy DWIA calculations.

The approximation formulas enable us to survey the many states in a large region of excitation for strong transitions and do DWIA calculations only for these. Since the same transition densities are relevant for excitation by inelastic electron scattering, we can then present calculated cross sections for a range of excitation in each nucleus, point out the differences which arise when the projectiles are e^-, π^+, or π^-. Our general results have been published[1] with application to ^{13}C, and comparison will be made with the other nuclei when experimental results are analyzed. Our most recent analysis of the excitation of ^{12}C near 19.25 MeV is shown in Fig. V-1.

[1] T.-S. H. Lee and D. Kurath, Phys. Rev. C 22, 1670 (1980).

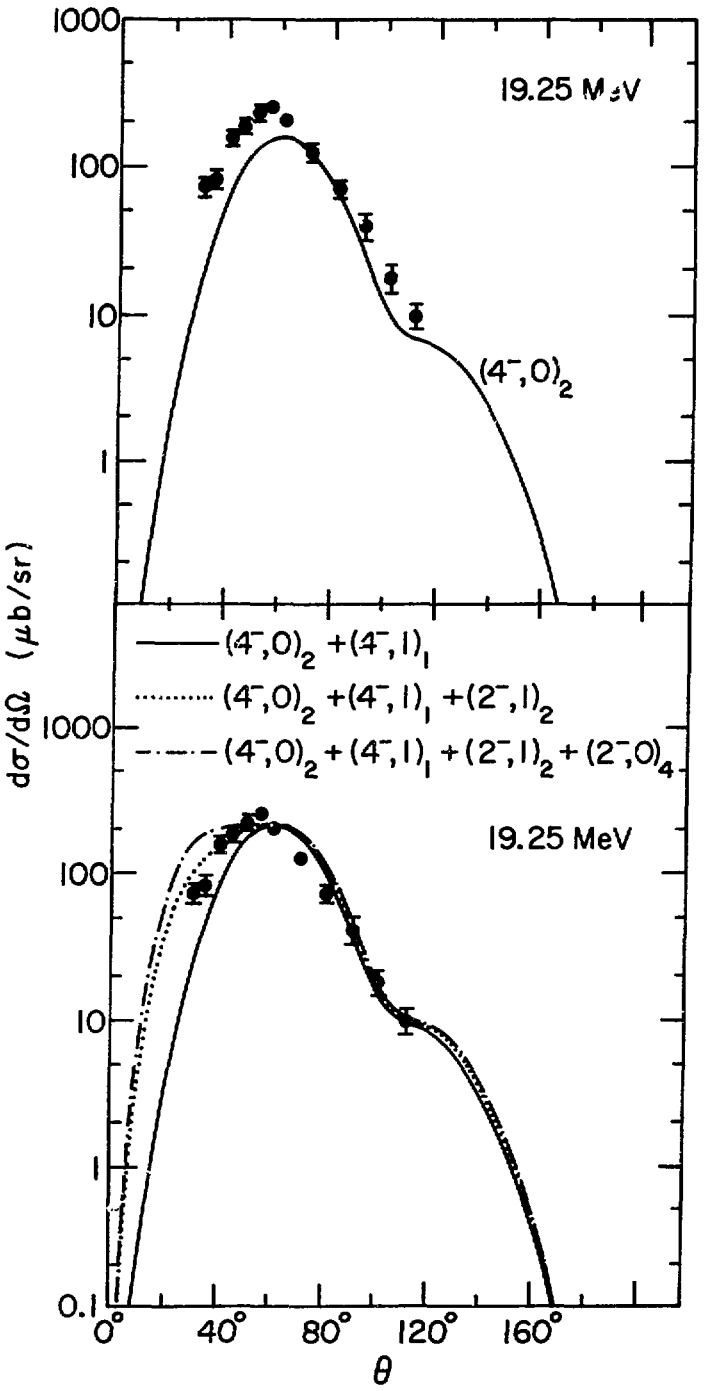

Fig. V-1. DWIA calculation of $^{12}C(\pi,\pi')^{12}C^*$ (19.25 MeV) is compared with the data.

b. Parity Mixing in ^{10}B

W. D. Teeters and D. Kurath

The mixing of the (JT) = (2^-0) and (2^+1) states near 5 MeV in ^{10}B offers a test of the weak interaction neutral current effects in nuclei. We have calculated[1] this matrix element in a complete 1 $\hbar\omega$ space, free of spurious center-of-mass excitation using the full two-body form of the parity-violating interaction. With the "best values" of the Weinberg-Salam model of weak interactions our value for the matrix element is 0.2 eV. We also find that a one-body approximation comes within 10% of this value which is several times smaller than the standard $\vec{\sigma}\cdot\vec{p}$ one-body approximation. The result is relevant for a current experimental measurement of the effect.

[1] D. Kurath and W. Teeters, Phys. Lett. 101B, 5 (1981).

c. Theory of the Nuclear Shell Model

R. D. Lawson

In November 1980 the above titled book was published by Oxford University Press in the series "Oxford Studies in Nuclear Physics." The book is 534 pages in length and deals with the use of the nuclear shell model in the interpretation of experimental data. This book is the outgrowth of lectures presented by the author at Argonne National Laboratory and at various universities—in particular State University of New York, Stony Brook; Rijkuniversiteit, Groningen; Technische Hochschule, Darmstadt; and the Vrije University, Amsterdam.

d. Nuclear Structure Studies of ^{149}Ho and ^{150}Ho

R. D. Lawson

It has been conjectured by the Julich Group that Z = 64, N = 82 acts as a doubly closed shell. If this is the case, the low-lying states of $^{148}_{66}Dy_{82}$ provide the $(\pi h_{11/2})^2_I$ matrix elements needed to carry out nuclear structure calculations for nuclei with N = 82 and 64 < Z ≤ 76. Calculations were carried out for the spectrum of the "three particle nucleus" ^{149}Ho. A $27/2^-$ isomer with 56 ns half-life was predicted at 2.856 MeV, together with the decay sequence $27/2^- \rightarrow 23/2^- \rightarrow 19/2^- \rightarrow 15/2^- \rightarrow 11/2^-$. The Argonne-Purdue

collaboration subsequently found an isomer with 59 ns half-life at 2.737 MeV which underwent the predicted decay sequence.[1]

Recently the three-proton, one-neutron nucleus ^{150}Ho has been produced and an 86 ns 17^+ isomer has been identified at 2.625 MeV undergoing a $17^+ \to 15^+ \to 13^+ \to 11^+ \to 9^+$ decay sequence. A shell model calculation which identifies these states as $[(\pi h_{11/2})^3 \times (\nu f_{7/2})]_I$ leads to the conclusion one should observe a 17^+ isomer at 2.631 MeV with $\tau_{1/2}$ = 101 ns undergoing the decay $17^+ \to 15^+ \to 13^+ \to 11^+ \to 9^+$ with decay energies in excellent agreement with experiment.[2]

[1] J. Wilson, S. R. Faber, P. J. Daly, I. Ahmad, J. Borggreen, P. Chowdhury, T. L. Khoo, R. D. Lawson, R. K. Smither, and J. Blomqvist, Z. Phys. A 296, 185 (1980).

[2] J. Wilson, Y. H. Chung, S. R. Faber, A. Pakkanen, P. J. Daly, I. Ahmad, P. Chowdhury, T. L. Khoo, R. D. Lawson, and R. K. Smither, Phys. Lett. 103B, 413 (1981).

e. Expected $(h_{11/2})^n$ States in the Nuclei $^{150}_{68}Er_{82}$, $^{151}_{69}Tm_{82}$, and $^{152}_{70}Yb_{82}$

R. D. Lawson

Since the Z=64, N=82 closed shell configuration accounts so well for the states of ^{149}Ho and ^{150}Ho, calculations have been carried out for the N=82, Z=68, 69, and 70 nuclei. The $(\pi h_{11/2})^2_I$ interaction energies deduced from the spectrum of $^{148}_{66}Dy_{82}$ can be shown to conserve seniority to a high degree and as a consequence one predicts very long-lived isomers in these nuclei. Experiments are now underway to test these predictions. This work has been accepted for publication in Z. für Physik.

f. 10^- States in ^{90}Zr

A. Amusa and R. D. Lawson

In ^{54}Fe the simple $(f_{7/2}, g_{9/2})$ model of the 8^- states leads to the prediction that the M8 electron scattering strength should be distributed over several levels and the theoretical results are in qualitative agreement with experiment.[1] On the other hand, recent electron scattering experiments on ^{90}Zr have found only one 10^- state. The simplest shell model

[1] R. A. Lindgren, J. B. Flanz, R. S. Hicks, B. Parker, G. A. Peterson, R. D. Lawson, W. Teeters, C. F. Williamson, S. Kowalski, and X. K. Maruyama, Phys. Rev. Lett. 46, 706 (1981).

configuration ($2p_{1/2}$, $1g_{9/2}$, $1h_{11/2}$) for these states would predict thirty possible 10^- levels. Our calculations predict that although most of the strength should be concentrated in the yrast 10^-, a second state with about one-quarter the intensity of the first should be seen about 700 keV higher in energy.

g. $^{18}O(t,p)^{20}O$ Reaction

A. Amusa and R. D. Lawson

Recently two particle transfer to the low-lying states of ^{20}O has been studied by the Pennsylvania group. They have analyzed their data on the basis of the ($1d_{5/2}$, $2s_{1/2}$, $1d_{3/2}$) shell model. However, it is well known that the ground state of ^{18}O contains a substantial four-particle, two-hole component and one can also show that the first excited 0^+ state in ^{20}O is mainly six-particle, two-hole. We are calculating spectroscopic factors for two-nucleon transfer including the four-particle, two-hole components in the ^{18}O ground state and the six-particle, two-hole components in the ^{20}O wave functions.

h. Study of Pion Double-Charge-Exchange (π^+, π^-) Reactions from Oxygen Isotopes

T.-S. H. Lee, Guang-Lie Li,* and Chu Hsia Li*

The mechanism of pion-nucleus double-charge-exchange (DCE) involves at least two nucleons. The DCE reaction is therefore expected to be useful in the study of two nucleon correlations in nuclei. In the impulse approximation, the DCE mechanism is made up of two elementary πN single-charge-exchange scatterings mediated by intermediate states ϕ_N of the nucleus with (Z+1) protons and (N-1) neutrons. Previous work has shown that by including a few low-lying intermediate states, ϕ_N, the calculated DCE cross sections severely disagree with the data. We have carried out DCE calculations for the oxygen isotopes by using the closure approximation to sum all intermediate states. It is shown that the coherent sum of contributions from all intermediate states are essential to shift the first minimum of the differential cross section away from that of the optical model, and hence yield a better description of the data. Our study also indicates that the

*State University of New York, Stony Brook, New York.

double scattering mechanism is probably not sufficient to describe the DCE processes. A paper describing this work has been published in Physics Letters 99B, 200 (1981).

i. Test of Interacting Boson Model by Pion Scattering

T.-S. H. Lee and F. Iachello*

An important assumption of the interacting-boson model of nuclear collective excitations is that the interaction between neutron bosons and proton bosons must be symmetric in the F-spin representation of the group SU(6) × SU(2). This assumption has a definite dynamical consequence in determining the relative strength between the neutron and proton excitations. Because of the fact that the $\pi^+p(\pi^-n)$ interaction is 9 times stronger than the $\pi^+n(\pi^-p)$ interaction, we have shown that this assumption can be sensitively tested by comparing the π^+ and π^- inelastic scattering. DWIA calculations for the isotope chains of Xe, Ba, and Ce have been published in the Proceedings of the Second IBM Conference held in June 1980.

*University of Groningen, Groningen, The Netherlands.

C. NUCLEAR MATTER AND NUCLEAR FORCES

In the microscopic theory of nuclei as systems of interacting nucleons, one aims to use two-body potentials that fit nucleon-nucleon scattering data and the deuteron properties to calculate the properties of nuclei. Basic properties are nuclear radii and total binding energies, i.e., saturation properties. Nuclear matter is a testing ground for saturation properties.

To treat nuclear matter, we need a method for obtaining accurate approximate solutions of the many-body Schrödinger equation. We have been developing the Brueckner-Bethe method, formulated in terms of the coupled-cluster equations, for this purpose. We have tested the accuracy by a variety of calculations with different two-body potentials. The results indicate that the calculated saturation point for nuclear matter is uncertain by about ± 0.1 fm^{-1} in Fermi momentum and ± 2 MeV in energy per particle. We are thus in a position to learn which, if any, two-body potentials that are fitted to scattering data and the deuteron can also account for nuclear saturation.

Ultimately nucleon-nucleon potentials must be reconciled with the theory of hadron structure. We are exploring some implications of quark models for nuclear forces.

A nuclear-matter saturation curve has been calculated for the Paris potential. This potential differs in several important ways from the Reid potential, which we treated earlier. The Paris and Reid results, when combined with Zabolitzky's calculations for light nuclei and with earlier less accurate nuclear matter calculations, suggest a most interesting and important conclusion: No two-body potential that is fitted to scattering data and deuteron properties can account for nuclear saturation. The Betz-Lee model which contains explicit pions as well as delta isobars implies effective three-body interactions and may thus avoid this discrepancy. Preliminary results are encouraging.

a. Nuclear Matter Calculations with the Paris Potential

B. D. Day

A detailed nuclear-matter calculation was made earlier for the Reid potential (augmented in partial waves with $j > 2$ by a potential consistent with empirical phase shifts). The more recent Paris potential gives an excellent fit to two-body data but differs from the Reid potential in several respects: (1) It has a weaker tensor force than Reid, the D-state probability in the deuteron being 5.8% and 6.5% for Paris and Reid, respectively. (2) The Paris potential has a strong momentum-dependent component of the form $p^2V(r) + V(r)p^2$, in contrast to Reid. (3) The short-range repulsion is much weaker for Paris than for Reid. A detailed calculation was made for

the Paris potential and saturation was found at E/A = -17.6 MeV, k_F = 1.60 fm^{-1}, quite close to the Reid result of (-17.2 MeV, 1.52 fm^{-1}) [the empirical saturation point is at (-15 ± 1 MeV, 1.36 ± 0.06 fm^{-1})]. Thus the two potentials, in spite of their differences. obey the trend observed in lowest-order calculations, i.e., enough binding can be obtained only at the cost of too high a density, and the correct density is obtained only at the cost of too little binding. It will be interesting to make similar calculations for the Bonn potential, which is qualitatively different from both Reid and Paris, and for the Bethe-Johnson potential, which in lowest order saturates at a lower density than Reid or Paris.

b. Nuclear Matter Saturation in the Presence of π and Δ

F. Coester, B. D. Day, and T.-S. H. Lee

We have calculated the binding energy and saturation density of nuclear matter for the Betz-Lee Hamiltonian (see Sec. V.D.a) in the reaction matrix approximation. In this approximation the quantitative consequences of the delta instability are negligible. The saturation point falls on the line formed by other lowest order calculations. The position of the saturation point on that line justifies the expectation that the three-body correlation effects will bring the calculated saturation point of the Betz-Lee model into the vicinity of the empirical value. This work was reported in an invited talk at the Second International Conference on Recent Progress in Many Body Theories at Oaxtepec, Mexico, January 1981. The proceedings have been published by Springer Verlag in "Lecture Notes in Physics," pp. 169-176.

c. Comparison of Brueckner-Bethe and Variational Results

B. D. Day

For central forces Fermi-hypernetted-chain (FHNC) variational calculations, if used carefully, can give reliable upper bounds to the true ground-state energy. The Brueckner-Bethe method can be tested by requiring that it give an energy no higher than the upper bound. For the central potential v_2, defined to have the radial shape of the central part of the Reid ^3S-^3D potential, the results of this test were found earlier to be satisfactory. For the central potential v_1, defined to have the radial shape

of the Reid ^1S potential, a reliable variational upper bound at $k_F = 1.8$ fm^{-1} is -141.4 MeV, some 21 MeV below the two-body Brueckner-Bethe result of -120.5 MeV. A recent calculation by Grangé and Lejeune of the three-body Brueckner-Bethe term gave only 7 MeV additional binding out of the required 21 MeV. Their method of calculation involved several untested approximations. We therefore repeated the calculation using our three-body method, which avoids those untested approximations. The three-body contribution was found to bring the Brueckner-Bethe result to within 1 MeV of the upper bound. Thus a situation that seemed cause for alarm has provided further evidence for the reliability of the Brueckner-Bethe method.

d. Method for Solving Three-Body Equations

B. D. Day

A paper has been accepted by Phys. Rev. C describing the methods developed to solve the three-body equations in nuclear matter. Enough detail is given so that the reader can reproduce both the formulas and numerical results. This should be helpful in identifying any possible conceptual or numerical errors.

A pedagogical introduction to the coupled-cluster formulation of the Brueckner-Bethe method was given at the Errico Fermi School in Varenna and will be published in the proceedings of the school.

e. Isobar Degrees of Freedom and Three-Body Forces in Nuclear Matter and Light Nuclei

R. B. Wiringa

Conventional nucleon-nucleon (NN) potential models that fit the two-body scattering data and deuteron properties do not explain the empirical saturation properties of nuclear matter or the binding energy and radii of finite nuclei. One possible solution suggested by many people is to include isobar degrees of freedom in the interaction model. In the past year, in work begun at the Los Alamos National Laboratory and continuing at Argonne, a variational method for calculating nuclear matter properties of interaction models that have NN-NΔ and NN-$\Delta\Delta$ transition potentials has been developed. The method includes cluster terms with $\geq$3 bodies, and thus should be sufficiently accurate for investigating the matter properties of such models. Studies of the available NΔ interaction models indicate:

(1) the higher the fraction of intermediate range attraction in the two-nucleon system that is provided by coupling to isobar states, the lower the binding energy and saturation density of nuclear matter, (2) NN↔NΔ and NN↔ΔΔ couplings provide roughly equal amounts of attraction and Δ-state percentage, and (3) there is considerable sensitivity to the diagonal part of the NΔ↔NΔ and ΔΔ↔ΔΔ interactions not apparent in the low-energy two-nucleon phase shift data. This work is now being prepared for publication.

Although much investigatory work on NΔ models has been done by numerous authors, no models have been published that give good quality phase shifts comparable to the Paris and Urbana NN models. Thus it is not yet possible to decide if isobar interaction models can cure the problem. A collaboration with R. Smith and T. Ainsworth of the State University of New York at Stony Brook has begun to build new models of good quality for which accurate nuclear matter calculations can be done. It is planned to systematically study a number of models to find the effect on matter of different components in the potentials.

One advantage of isobar interaction models is the automatic inclusion of a significant part of the two-pion-exchange-three-nucleon force (2PE3NF). An alternative approach to three-body forces is to use a conventional NN model and add phenomenological three-body potential terms to the Hamiltonian. This approach is being pursued with J. Carlson and V. Pandharipande of the University of Illinois at Urbana. A search for a Hamiltonian that will explain both nuclear matter properties and the binding energies and radii of three- and four-body nuclei is being conducted. The latter are being calculated in a variational Monte Carlo method developed in Urbana and now being run at Argonne. Preliminary results indicate a model three-nucleon potential motivated by 2PE3NF significantly improves the binding energies of the light nuclei and the saturation properties of nuclear matter.

f. Problems in the Use of Quark-Quark Potential Models for Nuclear Physics

Harry J. Lipkin

The confining color-exchange two-body potential successfully used in calculations of hadron structure is shown to be inapplicable to calculations of the hadron-hadron forces. The multiquark Hamiltonian with these forces has peculiar long-range effects which do not correspond to experimentally observed interactions. The confining two-body force becomes "anticonfining"

in the color octet and sextet states and gives a negative infinite energy when the pair are separated by an infinite distance. These sextet and octet couplings do not occur in normal color singlet mesons and baryons. However, when more than three particles are present, at least one pair must be partially in an anticonfining state. For states which are not overall color singlets or triplets, the eigenvalue spectrum of the Hamiltonian is shown to be unbounded from below. In the color-singlet sector, the Hamiltonian is positive definite if the potential does not increase too rapidly at large distances. The harmonic oscillator potential is the limiting case for which the potential is positive definite. A potential with a higher power of the distance always gives a Hamiltonian unbounded from below for a sufficiently large number of particles. Even for potentials which are positive definite there are unphysical long-range Van der Waals forces. Rigorous results are obtained for the value of the power law of the potential above which the Hamiltonian is unbounded from below for the general case of N colors and an arbitrary number of particles. A paper (together with O. W. Greenberg) is in press in Nuclear Physics A.

g. Baryon Magnetic Moments in the Quark Model

Harry J. Lipkin

Analysis of the experimental baryon magnetic moments shows a disagreement between experiment and the simple broken-SU(3) quark model predictions which indicates that the contributions of the nonstrange quarks to the strange baryon magnetic moments are quenched relative to their contributions to the nucleon moment. There is no analogous quenching for the strange quark contribution. The analysis is model independent and includes effects of configuration mixing and relativistic corrections. A paper is in press in Physical Review.

h. Meson Clouds of Extended Sources

F. Coester and J. Parmentola

If one wishes to reconcile the quark structure of nucleons with traditional nuclear theory, the most promising models are bag models with pion fields coupled to quarks on the surface of the bag. Depending on the size of the bag, the pion cloud is then a significant part of the physical

nucleon and its properties give rise to the nucleon-nucleon interaction. Variational approximations to the one-nucleon states can be obtained by known methods. Straightforward calculations will check the consistency of this picture. Such calculations are in progress.

i. Correlated-Basis Perturbation Theory for the Ground-State Energy of Liquid ^{3}He

J. W. Clark

The Fermi-hypernetted-chain (FHNC) method, when applied to variational wave functions of Jastrow-type, gives accurate upper bounds for the ground-state energy of liquid ^{3}He. For the Lennard-Jones interatomic potential, the upper bound at the experimental equilibrium density is -0.8 deg/atom, which is quite far above the experimental value -2.5 deg/atom. The variational calculation has been improved by using perturbation theory in a correlated basis, while treating the Jastrow wave function as an unperturbed ground state. The matrix elements needed for the second-order perturbation correction are evaluated using FHNC. The perturbation correction lowers the energy substantially, to about -1.8 deg/atom. This agrees well with the preliminary result of -2.2 deg/atom for the exact energy, obtained by Kalos using the Green's Function Monte Carlo method.

D. INTERMEDIATE-ENERGY PHYSICS

The pion-nucleus interaction is dominated by the formation of the Δ resonance. A desirable theoretical framework for the study of intermediate-energy physics is a straightforward extension of conventional nuclear theory to include pion and Δ degrees of freedom. The interactions should allow pion production and absorption without modifying the single-nucleon states. We have constructed such a model by fitting the πN and NN scattering data. The model proves to be successful in describing the scattering and absorption of pions by the deuteron. It has been extended to construct a many-body Hamiltonian suitable for the study of pion-nucleus interaction and nuclear matter.

Pion-nucleus inelastic scattering has been studied using distorted-wave impulse approximation (DWIA). The transition matrix elements of the effective π-nucleus potential are calculated from the off-energy shell π-nucleon scattering amplitudes and the nuclear wave functions. The diagonal matrix element of the effective potential is determined empirically by fitting to elastic scattering data. This DWIA model has proved quite successful in interpreting many inelastic scattering data.

a. Phenomenological Hamiltonian for Pions, Nucleons and Δ Isobars

M. Betz* and T.-S. H. Lee

We have constructed a Hamiltonian for a nuclear system consisting of pions, nucleons, and Δ isobars. The basic ingredients of the model are: (a) a $\pi N \rightleftarrows \Delta$ vertex interaction in the resonant (3,3) channel, (b) a direct two-body interaction in other πN channels, (c) a two-body interaction V_o for the $NN \rightleftarrows NN$ and $NN \rightleftarrows N\Delta$ transition. All two-body interactions in each partial wave are parameterized by a low-rank separable kernel. The parameters are determined by fitting the πN phase shifts up to 300 MeV and NN phase shifts up to 800 MeV. With all parameters so determined, we have calculated cross sections for πd elastic scattering and for the reaction $\pi d \rightarrow pp$. The results agree well with the available data in the energy region near the resonance.[1] We are working on improvements of the model. The conventional one-boson-exchange (OBE) mechanism has been used to parameterize the two-baryon interaction V_o. The computer program has been modified to carry out NN scattering calculations using a nonseparable V_o. As a first step we have combined the Bonn OBE model with our $\Delta \rightleftarrows \pi$ interaction and neglected interactions in the NNπ channel. The NN scattering phase shifts below

*TRIUMF, University of British Columbia, Vancouver, B.C., Canada.

[1] M. Betz and T.-S. H. Lee, Phys. Rev. C 23, 375 (1981).

300 MeV are not changed significantly when Δ is treated as an unstable particle. The NN inelasticity above 300 MeV is mainly due to the NΔ interaction in low partial waves. The program is being extended so that three-body effects in πNN channel can be included in the fit to the NN data up to 800 MeV.

b. DWIA Studies of Pion-Nucleus Inelastic Scattering

T.-S. H. Lee, J. Parmentola, and others

The DWIA model has been used to study the pion-nucleus inelastic scattering throughout the nuclear periodic table. The model proves to be adequate to investigate the structure of low-lying nuclear excited states (see Sec. V.B). We have extended the model to study the recent inclusive $A(\pi,\pi')$ data from the ANL group, which exhibits features of quasi-free scattering mechanism. By using the closure approximation to sum the undetected final nuclear states, the energy-integrated differential cross section is expressed in terms of one-body and two-body nuclear densities. Calculations have been carried out for the target nuclei ^{4}He, ^{12}C, and ^{58}Ni. It is found that the DWIA model can also account for the inclusive inelastic scattering data at large angles.

c. Effective Interactions Derived from Relativistic Quantum Field Theories

H. G. Kümmel

We have investigated the formal derivation of models of nuclear systems at intermediate energies from relativistic quantum-field theories in a Fock-space framework. The model spaces are subspaces of the Fock space. The model operators that map the full theory onto the model space preserve the relativistic invariance of the theory. Their construction does not necessarily depend on perturbation expansion. The Goldstone boson in a ϕ^4 theory has been treated as a nonperturbative example. This work was reported in an invited talk at the Second International Conference on Recent Progress in Many Body Theories at Oaxtepec, Mexico, January 1981. The proceedings have been published by Springer Verlag in "Lecture Notes in Physics," pp. 177-185.

E. MICROSCOPIC CALCULATIONS OF HIGH-ENERGY COLLISIONS OF HEAVY IONS

The study of heavy-ion collisions at energies greater than about 100 MeV/nucleon seems the only way of obtaining information about the properties of nuclear matter at high densities and temperatures and about possible new states of nuclear matter. Because of the relatively large mean free path and associated large nonequilibrium phenomena, an adequate description of such collisions must in general be a microscopic one. We initiated and are continuing (with A. D. MacKellar) classical equations-of-motion (CEOM) calculations of high-energy heavy-ion (HE-HI) collisions for laboratory energies from about 100 MeV to about 1 GeV/nucleon. The CEOM method is a completely microscopic but classical approach whose essence is the calculation of all nucleon trajectories using a two-body potential between all pairs of nucleons. The unique feature of this approach is that it includes finite-range interaction effects (in particular potential-energy effects) for realistic potentials and hence does not assume that nuclear matter is a dilute fluid as do the Boltzmann-equation/cascade calculations. Thus, for example, the CEOM approach includes effects corresponding to collisional relaxation, or even hydrodynamic type behavior, in a background average potential due to the long-range part of the nucleon-nucleon interaction. In fact our studies have suggested a description and an associated kinetic equation in which "collisions" due to the short-range repulsive part of the interaction take place in a background average potential due to the longer-range attractive part of the interaction.

a. Classical-Equations-of-Motion Calculations of High-Energy Heavy-Ion Collisions

A. R. Bodmer, C. N. Panos,* and A. D. MacKellar†

A paper with the above title has appeared in Phys. Rev. C 22, 1025-1054 (1980). This paper gives an account both of the procedures used in our CEOM calculations and of the quite comprehensive results obtained for $^{20}Ne + {}^{20}Ne$ and $^{40}Ca + {}^{40}Ca$.

b. Classical-Equations-of-Motion Calculations of Multiplicities for High-Energy Collisions of $^{20}Ne + {}^{20}Ne$

A. R. Bodmer and C. N. Panos*

A paper with the above title has been published.[1] In it we present and discuss results for the nucleon multiplicity for $^{20}Ne + {}^{20}Ne$ at a laboratory energy of 800 MeV/nucleon obtained with classical-equations-of-motion calculations. The nucleon-multiplicity distributions were obtained

*University of Ioannina, Ioannina, Greece.

†University of Kentucky, Lexington, Kentucky.

[1] A. R. Bodmer and C. N. Panos, Nucl. Phys. A356, 517 (1981).

as a function of impact parameter b. We found that the average multiplicity decreases quite rapidly with b, but that there is a quite wide spread of multiplicities for a given b as reflected by the large standard deviations of the multiplicity distributions for a given b. This indicates, at least for equal-mass, light nuclei, that measurement of the multiplicity distribution can only determine the impact parameter with rather poor resolution—to about half a nuclear radius for "central" collisions.

c. Improvements and Extensions of the CEOM Calculations

A. R. Bodmer, L. Arnellos,* and A. D. MacKellar†

We are developing and improving the CEOM calculations in order to extend their scope and flexibility. Thus we are developing momentum dependent potentials with more satisfactory binding and scattering properties. We intend to make more complete relativistic calculations [to $O(v^2/c^2)$], to study a larger range of projectile and target nuclei, to study two-nucleon correlations and other cross sections and to study questions, such as entropy production, suggested by calculations or by experimental results. Eventually we aim to include pion production in our CEOM calculations.

d. Theory of High-Energy Heavy-Ion Collisions

A. R. Bodmer

In the past we have made a comparative assessment and analysis of the different basic approaches to high-energy heavy-ion collisions (in particular: hydrodynamics, cascade/Boltzmann-equation calculations, CEOM calculations). This analysis has clarified the complementary nature of these approaches and their respective merits, and also that none of these approaches is clearly valid.

As a continuation and development of these studies we are currently attempting to obtain a better theoretical understanding of high-energy heavy-ion collisions by consideration of Wigner functions. In particular we are interested in finding a suitable kinetic equation description of the kind

*Thesis student, University of Illinois, Chicago Circle Campus, Chicago, Illinois.

†University of Kentucky, Lexington, Kentucky.

suggested by our CEOM calculations but which also includes Pauli effects and which would be applicable for lower energies, namely in the range of about 50—200 MeV/nucleon where there is currently no suitable microscopic description. The computational implementation of such a description could be by means of appropriately modified CEOM calculations.

F. LIGHT ION DIRECT REACTIONS

Coupled Channels Variational Method for Nuclear Rearrangement Reactions

M. Kawai

The method of coupled channels has been recognized as a powerful tool for theoretical analyses of multistep direct nuclear reactions. It is a standard method of analysis for inelastic scattering of particles accompanied by collective excitation of nuclei. For rearrangement processes, however, the use of the method has been very limited because of the computational difficulty involved. The main source of the difficulty is the difference between the internal and relative coordinates of rearranged channels. This difference gives rise to nonlocal coupling kernels between rearranged channels and a set of coupled integro-differential equations for the wave functions of relative motion in coordinate space. Computation of the kernels for all pairs of the coupled channels and then storing the values is a formidable task and is not feasible except for very limited cases. The method will not be useful in practice until this difficulty is overcome.

To cope with the situation, we have developed a variational method of the Kohn-Hulthen-Kato type by means of which one can calculate the S-matrix elements of rearrangement reactions. The method was tested for simple cases of (d,p) reactions and the associated (d,d) and (p,p) scattering processes and turned out to be extremely efficient and accurate.

The coupled-channels variational method is now being applied to some (d,p) reactions allowing for the possibility of breakup of the deuteron in the course of the process. The purpose of the calculation is partly to see the power of the method in the simple reaction process and partly to perform a critical survey of the previous work on the effect of breakup of the deuteron in (d,p) and (d,d) processes based on various approximations. The present method is capable of simulating those approximations as approximations to the full coupled-channels calculation. Through the comparison of these simulations with the full coupled-channels calculation and with each other, one can make a critical survey of the approximations in the previous works.

Calculations have been carried out on $^{16}O(d,p)^{17}O$ leading to the $\frac{1}{2}^+$ single-neutron state of ^{17}O, and the associated $^{16}O(d,d)^{16}O$ and $^{17}O(p,p)^{17}O$

scattering processes. The continuous spectrum of deuteron-breakup states has been discretized by diagonalizing the Hamiltonian of the n-p system in a basis set of 11 Gaussian functions. The energy eigenvalues of the discretized states range from the deuteron binding energy up to 360 MeV. Calculations with the full coupling of all the channels, including the proton channels, have been performed for the first time.

The method is extremely powerful in this problem of 12 coupled channels including a rearranged one. It has enabled us to carry out detailed studies of the effects of the deuteron-breakup states and the coupling of the proton channel and a quantitative review of various approximations in previous works. Among various results, it has been found that the effect of the deuteron-breakup states is large. It is larger, the lower the angular momentum and the energy, but is important even at 60 MeV. The coupling of the proton channel, however, becomes rapidly unimportant as energy increases. This justifies the previous calculations at high energy which all neglected this coupling. They are, however, certainly not justified at energies lower than 20 MeV.

G. OTHER THEORETICAL PHYSICS

Aharonov-Bohm Effect

M. Peshkin

(1) According to conventional quantum mechanics, the behavior of charged particles can be influenced by magnetic fields in regions from which the particle is rigorously excluded. This phenomenon, called Aharonov-Bohm effect, has been discussed widely in the context of scattering experiments, and it is often suggested that there is no Aharonov-Bohm effect; the observed phenomena depend upon the actions of local fields only. Such interpretations are difficult to refute clearly because of the complexities of the scattering problem. I have noted that the bound state problem is much simpler. To avoid the Aharonov-Bohm effect in theory requires abandoning a fundamental principle of quantum mechanics; either energy differences must be said not to be observable in principle, or angular momentum must be said not to be conserved. I also point out that the quantization of the fluxoid in superconducting rings and Josephson junctions provides a powerful experimental confirmation of Aharonov-Bohm effect in bound states. This work was published in Phys. Rev. A 23, 360 (1981).

(2) One may go further and ask whether the Aharonov-Bohm effect can be removed from quantum mechanics by altering the theory in some acceptable way. That possibility can never be disproved categorically, but I have analyzed the bound-state problem in a cylindrically symmetric geometry to show that such an alteration of the theory could not be a minor one; it would require a radical revision of our understanding of the conservation and quantization of angular momentum. The key point is that a charged particle is the source of an electric field. When the particle moves in the presence of an external magnetic field, the particle may be excluded from the magnetic field region but its electric field nevertheless penetrates the magnetic field region. The crossed electric and magnetic fields contain angular momentum equal to $e\Phi/2\pi c$, where Φ is the total magnetic flux, independently of the particle's position as long as it remains in the region from which the magnetic field is excluded. In any theory which quantizes the total angular momentum in integer units $n\hbar$, the kinetic angular momentum $r \times mv$ is quantized in the noninteger units $r \times mv = n\hbar - e\Phi/2\pi c$. However, it is the kinetic angular momentum which determines

observable quantities such as the energy, through the centrifugal barrier. Therefore the energy eigenvalues depend upon the confined magnetic field .r total angular momentum is quantized in the usual way, independently oi the detailed structure of the theory. I have also shown in similar ways that the conservation of angular momentum runs into serious troubles in the absence of Aharonov-Bohm effect. This work will be published in Physics Reports.

VI. THE SUPERCONDUCTING LINAC

R. Benaroya, L. M. Bollinger, R. C. Pardo, K. W. Shepard, J. Aron,* B. E. Clifft,* K. W. Johnson,* P. Markovich,* and J. M. Nixon*

INTRODUCTION

The Superconducting Linac Project has two main components, both of which are developmental in nature. One is the specific task of designing, building, and testing a small superconducting linac to serve as an energy booster for heavy ions from the FN tandem electrostatic accelerator. The second, more general part, consists of investigations of various aspects of superconducting rf technology. Although most of these investigations are now aimed at the immediate needs of the booster, many of them are of fairly general interest for accelerator technology.

Both parts of the Superconducting Linac Project are jointly supported and administered by the Chemistry and Physics Divisions.

---

*Chemistry Division, ANL.

A. HEAVY-ION ENERGY BOOSTER

The booster project, started in mid-1975, is concerned with the design, construction, installation, and testing of a small superconducting linear accelerator (linac) to serve as an energy booster for heavy-ion beams from the FN tandem accelerator. The principal objectives of the project are to develop a new accelerator technology and to build the prototype for a heavy-ion energy booster that can be used to upgrade the performance of any tandem accelerator. The overall design is highly modular in character in order to provide maximum flexibility for future modifications and/or improvements. Sixteen resonators of the planned 24-resonator system were in place in March 1981, and additional resonators will be completed and installed soon.

By the end of the present reporting period, the booster was being used routinely (but not continuously) to provide beams for nuclear-physics research. This operational experience is summarized in Sec. VII of this document.

1. MAIN FEATURES OF THE DESIGN[1]

A schematic representation of the booster as it is expected to be at completion is shown in Fig. VI-1. The heart of the system is the split-ring resonator, a three-gap structure made of superconducting niobium. Superconducting solenoids at frequent intervals confine the radial excursions of the beam. The basic accelerating section of the linac consists of a linear array of these resonators and solenoids within a cryostat that can be isolated from the others both with respect to vacuum and cryogenics.

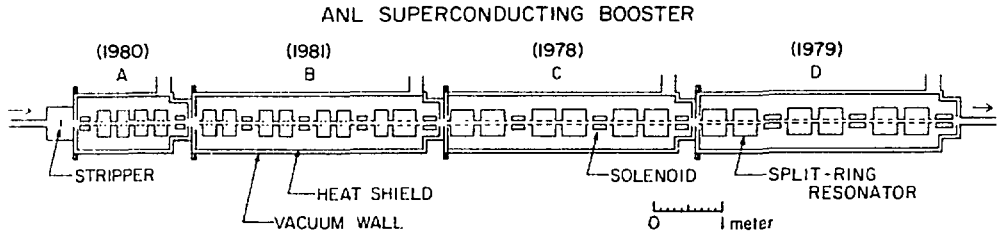

Fig. VI-1. Schematic representation of the planned heavy-ion booster. Sections A, C, and D are installed and in use in March 1981.

[1] For more detail, see the Proposal for ATLAS and its Addendum, obtainable from the Physics Division, Argonne National Laboratory (1978).

The booster makes use of resonators that have two lengths. One type is 35.6 cm long and is optimized for a projectile velocity $\beta \equiv v/c = 0.105$ (sections C and D). A second type is 20.3 cm long and is optimized for $\beta = 0.060$ (sections A and B). The resonators are cooled to a temperature of 4.7°K by forced-flow, two-phase helium from a refrigeration system.

The total rf power required for the booster is only 3.6 kW. This is to be compared with a need for about 2 MW of rf power for an equivalent room-temperature linac. The control of the linac as a whole is accomplished with the assistance of a dedicated small computer. This approach allows rapid tuneup of the accelerator.

For ions in the lower half of the periodic table, the final 4-section booster is expected to provide beam energies that are equivalent to those from a very large (~30-MV terminal) tandem. A sophisticated beam-bunching system allows the beam out of the linac to have the same good quality as the beam from the tandem. The beam energy can be varied easily by changing the phase and/or amplitude of the last resonator.

2. STATUS OF THE BOOSTER

The heavy-ion booster has been a working reality throughout the year ending in March 1981. Sections A, C, and D are now on line, and they are being used regularly to accelerate beams for the nuclear-research program.

Some major changes in the system during the past year are summarized below.

Low-β Resonators

Four low-β resonators have been completed, installed in section A, and put into service. They are routinely used at accelerating fields greater than 3.5 MV/m. One of the new units is shown in Fig. VI-2.

Helium Refrigerator

A CTI model-2800 helium refrigerator was installed in late 1980. With the two compressors now on hand, this unit provides 200 watts of additional cooling. The new refrigerator and the original smaller unit are operated in parallel with no significant control problems.

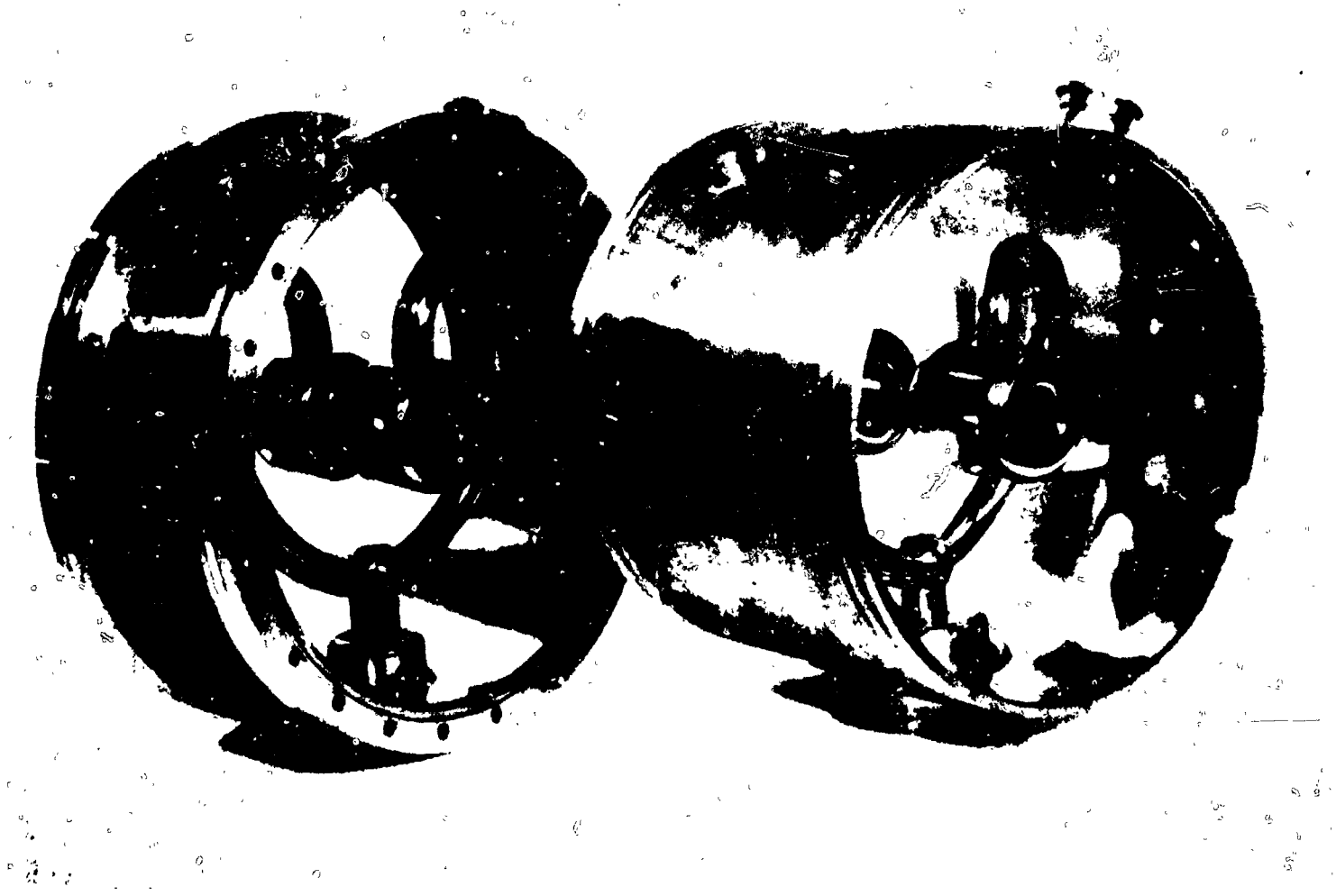

Fig. VI-2. The two types of resonators used in the heavy-ion booster. The smaller unit is the low-β structure.

By adding a third compressor, the capacity to the new refrigerator can be expanded to 300 watts, enough to be adequate for the needs of the planned ATLAS system.

Computer Control System

The computer-based control system for the linac has been refined substantially.

Beam Rebuncher

The rebuncher on the output beam line has been installed and put into service. It is now used frequently in the experimental program.

3. NEAR-TERM PLANS

The energy-measurement system described in Sec. VI.B will be installed and put into service. This time-of-flight system, which is expected to measure energies to an accuracy of a few parts in 10^4, will greatly improve the quality of the operation for many experiments.

Refinement of the linac-control system will continue in an effort to make the energy-changing routine even more convenient and reliable than it is now.

The fourth and final section of the booster (section B) will be installed. Since seven of the eight resonators in this section are low-β units, the availability of section D will substantially increase the beam energy for ions with $A > 40$.

B. INVESTIGATIONS OF SUPERCONDUCTING LINAC TECHNOLOGY

This program, carried out jointly by the Chemistry and Physics Divisions, is concerned with investigations of the general aspects of applications of superconducting technology to the acceleration of heavy ions. Most of the recent activities have been related to the development of an accelerating structure of the split-ring type made of niobium. Investigations of this type will continue, but the program is broadening steadily to include developmental work on other aspects of accelerator technology, including (1) the development of superconducting magnets for use in bending, controlling, and analyzing heavy-ion beams and (2) the advancement of time-of-flight technology.

The choice of all recent developmental work has been guided by the urgent developmental needs of the heavy-ion booster. Nevertheless, most of the investigations undertaken are of general interest to superconducting-linac technology.

1. RECENT ACCOMPLISHMENTS

a. Accelerating Fields of Resonators

K. W. Shepard

For some years now it has been our goal to have resonators operate on line with a maximum surface electric field E_{max}^{sur} of 20 MV/m when the rf-power dissipation is 4 watts, which corresponds to an accelerating field of 4.25 MV/m for the high-β unit. Although we are still some distance from this goal, the possibility of achieving even higher fields is suggested by two recent accomplishments: (1) off-line tests have demonstrated that the existing resonators can be conditioned to $E_{max}^{sur} > 20$ MV/m, and (2) computer studies indicate that resonator design can be improved significantly.

(i) Reduction in Electron Loading

Both the high-β and low-β resonators have for some time been able to operate with $E_{max}^{sur} \simeq 20$ MV/m during off-line tests, and it has seemed that even higher fields could be achieved if the electron loading could be reduced by more complete conditioning. This hoped-for improvement has recently been demonstrated by conditioning a low-β resonator by means of pulsed operation with a 1.5 kW rf amplifier, which applies about four times as much peak power as was formerly used. After such treatment, the low-β resonator operated at $E_a = 5.2$ MV/m with a power dissipation of 4 watts and was stable for CW operation at 6.0 MV/m; for this unit, $E_{max}^{sur} = 4.4\ E_a$.

This result clearly establishes a new performance standard for superconducting low-frequency accelerating structures.

Although the off-line performance of resonators now approaches or, in some cases, exceeds our long-term goal, the on-line performance does not. There are two aspects to this: (1) the difficulty of conditioning the units on-line and (2) the tendency of the on-line units to decondition. The difficulty in the initial conditioning is simply that, because the input probe in the on-line units is fixed, it is difficult to get enough rf power into the resonator during conditioning. This practical problem will undoubtedly be solved in time.

The phenomenon of deconditioning is poorly understood, but some observable behavior is as follows. Typically, the maximum useful field of a newly-conditioned resonator decays to stable operation at a value about 10% lower with a time constant of a few days. Parts of the deterioration in performance can be removed easily and rapidly ($\sim \frac{1}{2}$ hour) by conditioning, and the original performance can be obtained by more vigorous effort. Unfortunately, the useful field level for routine acceleration is the lower level to which the field decays in roughly two days.

Controlled tests have shown that the tendency to decondition is reduced by on-line heating of the resonators before cool down. Because of the presence of indium seals, the temperature must be limited to $\sim$100°C. Even so, two days of pumping at this modest temperature improves the resonator stability to an important degree. Presumably, this improvement results from the removal of gas from interior surfaces of the resonator. It is entirely possible that further improvement can be made simply by more thorough baking.

The maximum useful field level of a resonator typically remains stable for thousands of operating hours, but about half of our units have finally undergone a transition to significantly poorer performance. In most cases this change appears to be associated with some major accident such as a massive vacuum failure, but in several cases there is no obvious cause. Even the changes associated with vacuum accidents are hard to understand since our units have often been exposed to some air without ill effects. Based on experience to date, the original good performance can be restored by lightly electropolishing the surfaces, a procedure that requires several days of effort per resonator. Restorations of this kind are being carried out, unit by unit, when the linac operating schedule permits.

In summary, the performance of the ANL split-ring niobium structure is excellent relative to other superconducting structures for heavy ions, but important improvements can still be made.

(ii) Resonator Design

A reexamination of resonator design has been undertaken because a new class of resonators is needed for the proposed ATLAS linac. The technical challenge for ATLAS is to design a unit that is effective in all respects for the higher projectile velocities involved. Our solution is a split-ring resonator operating at 145 MHz, 3/2 times the frequency of the present resonators and 3 times the beam-pulse frequency. At this frequency, the resonator housing is the same as that of the present $\beta = 0.105$ resonator, and the new unit will have optimum acceleration for ions with $\beta \approx 0.16$. All aspects of the design have been optimized to minimize the surface field E_{max}^{sur} for a given accelerating field E_a and (under the assumption that E_{max}^{sur} sets the limit on E_a) it has been found that E_a can be increased about 20% beyond our earlier estimate. The stored energy of the new design is about the same as that of the $\beta = 0.105$ resonator.

The main features of the design for the $\beta = 0.16$ resonator are shown in Fig. VI-3. The developmental effort required to turn this computer design into a working unit is now in progress, with the objective of completing the task in early 1982. It is expected that the hardest part will be the fabrication in niobium of the complex shapes involved.

The calculated result for the ATLAS resonators indicates that the $\beta = 0.06$ and $\beta = 0.105$ resonators used in the booster can also be improved significantly by modifying their designs. This possibility is of no immediate interest for the booster, since most of its resonators exist, but it is important for future applications of superconducting-linac technology.

b. Slow-Tuner Controller

K. W. Shepard

The rf frequency of each resonator in the booster is continuously adjusted by means of a helium-filled bellows that deflects an end plate in response to frequency-error and phase-error signals. This system works well except that it involves the rapid and repeated operation of pressure-controlling

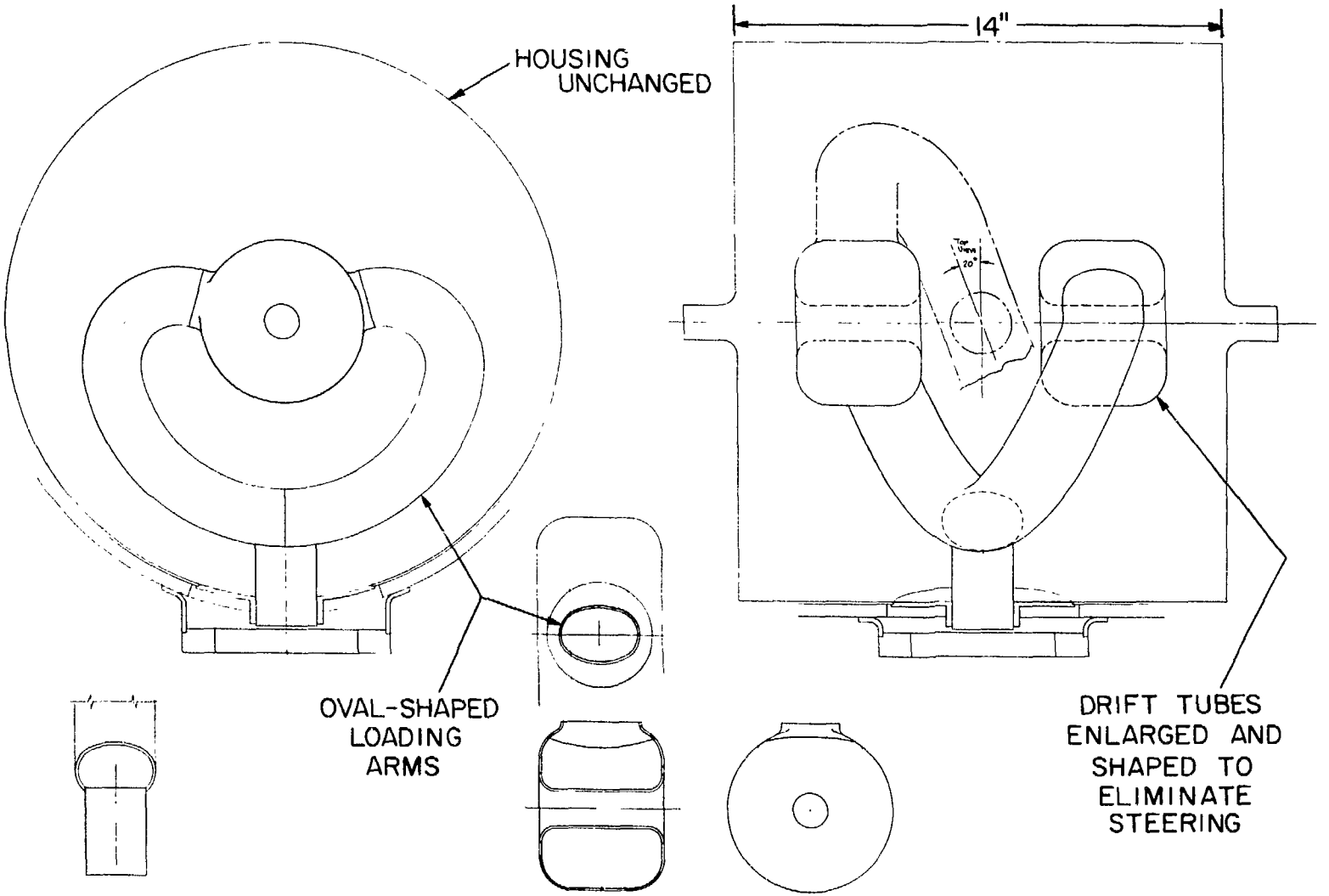

Fig. VI-3. Design for the β=0.16 resonator to be used in ATLAS.

valves which tend to fail. In order to increase operational reliability, effort has been devoted to the development of a new kind of pressure controller that involves heating helium gas at temperatures near 5 K. The use of such a low temperature has two major advantages: (1) the gas pressure can be varied over a wide range by heating and (2) the response time is easily made small because of the low heat capacity of the metal housing.

Tests on a prototype pressure controller are encouraging. If the developed device is as successful as is expected, it will eliminate at least 20% of operational failures of the booster.

c. Fast Tuner

K. W. Shepard

Work has started on the development of a new concept for a fast tuner for the superconducting resonators. This concept involves the use of a balanced pair of piezo-electric disks to form a voltage-controlled reactance (VCX). Although exploratory investigations gave promising results, we don't expect to continue the work now because of the need to focus on more urgent tasks.

d. Beam-Energy Measurement

R. C. Pardo and R. N. Lewis*

To date we have been largely dependent on surface-barrier detectors to measure beam energy, but a time-of-flight system that is expected to be much better is nearing completion. The basic idea of the new system is to measure ion velocity by passing the pulsed beam continuously through two bunch-arrival-time detectors placed about 10 m apart along the beam line. The primary technical challenge is to find a detector that is nondestructive and has an excellent time resolution even for weak beams.

Fortunately, a beam-excited resonator of the kind already in use in our bunching system has all of the required characteristics: it transmits all of the incident beam without significant change, it can measure the mean arrival time of a train of pulses with an accuracy of 10 to 20 ps, and it can detect 10 pA of beam current.

*Electronics Division, ANL.

An energy-measurement system consisting of a pair of helix resonators and their associated electronics has been built and partially tested. It is already clear that the system will work, but the circuits have had to be modified to suppress more effectively the meaningless information that the resonant detector receives when the linac is out of lock. The system is expected to measure beam energy continuously with an accuracy of about 2 parts in 10^4 for a typical beam.

If the energy-measurement system works as well as is expected, it should have wide-spread applications since it can measure the energies of pulsed heavy-ion beams more accurately, conveniently, and inexpensively than magnetic analyzers.

e. Superconducting Analyzing Magnet

R. P. Smith,* L. E. Genens,* L. M. Bollinger, and J. R. Erskine

The present 90° analyzing magnet of the tandem is inadequate in two respects: (1) its mass × energy product is only 52, which is too small to bend many heavy ions of interest and (2) the magnet is not isochronous and thus is a major source to pulse broadening. A project aimed at designing and building a beam analyzer that will eliminate both problems is in progress.

Because of the small space available, an analyzer with the required bending power (mass × energy ≈ 500) must be superconducting. The planned system will consist of two superconducting 45° bending magnets and two special room-temperature quadrupoles to provide the needed focusing. Since there is a beam waist between the bending magnets, the system is approximately isochronous.

Each superconducting magnet is a split solenoid with iron pole tips and an iron yoke. The central field is 6 Tesla, and the radius of the field is about 27 cm. A prototype of such a magnet has been designed and is being built by the Laboratory's Accelerator Research Facilities Division. As of January 1981, the coil has been wound, iron for the yoke and shield have been procured, and fabrication of the cryostat has started.

Although the prototype superconducting magnet now under construction is aimed at the specific need for a tandem-beam analyzer, the magnet is also regarded as a prototype for the large switching magnets that are needed for

*Accelerator Research Facilities Division, ANL.

beams from ATLAS. Our experience is also expected to be of interest to others with energetic heavy-ion beams.

2. NEAR-TERM PLANS

Much of the effort in 1982 will be devoted to the continuation of the tasks that are in progress during 1981.

The prototype of the ATLAS resonator will be completed and tested in early 1982 and, if necessary, any defects will be eliminated.

The energy-measurement system will be completed and put into service in 1981, but it is likely that routine use will reveal some imperfections; if so, these will be eliminated. Once the system is working well, we will undertake to use it to control the output-beam energy.

Investigations of electron loading in resonators will continue in 1982 along the same lines as described above. In particular, an effort will be made to identify the mechanism responsible for the sudden deterioration in performance of some resonators. Also, we will attempt to establish the easiest effective technique for restoring resonator performance.

C. PROPOSAL FOR ATLAS

The Argonne Tandem-Linac Accelerator System (ATLAS) is a proposed heavy-ion accelerator to be formed by enlarging the booster and by adding a large new target area, as shown in Fig. VI-4. The resulting system, consisting of the existing tandem and a 7-section linac, will have a performance that is approximately equivalent to that of a 50-MV tandem with two strippers.

ATLAS is aimed squarely at the needs of precision nuclear-structure physics, providing beam energies up to 25 MeV/A, easy energy variability, and beams of exceptionally good quality. The short-pulse character of the beam will be emphasized so as to maximize its usefulness for time-of-flight and other timing measurements. An unusual feature of the facility is the capability of providing beams simultaneously for two independent experiments without a loss of intensity to either.

ATLAS was initially in the President's Budget for funding in FY 1981 but was subsequently deferred. This delay is giving us time to perfect the plans and to make other preparations that will allow the project to start with maximum efficiency when the line-item construction funds are finally available. Particular effort is being devoted to the following preconstruction activities: (1) procurement of niobium, (2) fabrication of a prototype of the new resonator to be used in ATLAS, and (3) preparation of an advanced conceptual design for the building.

The ATLAS project is now in the President's Budget again and it seems likely that the project will be authorized in FY 1982, but the level of funding in the first year of the project is still quite uncertain.

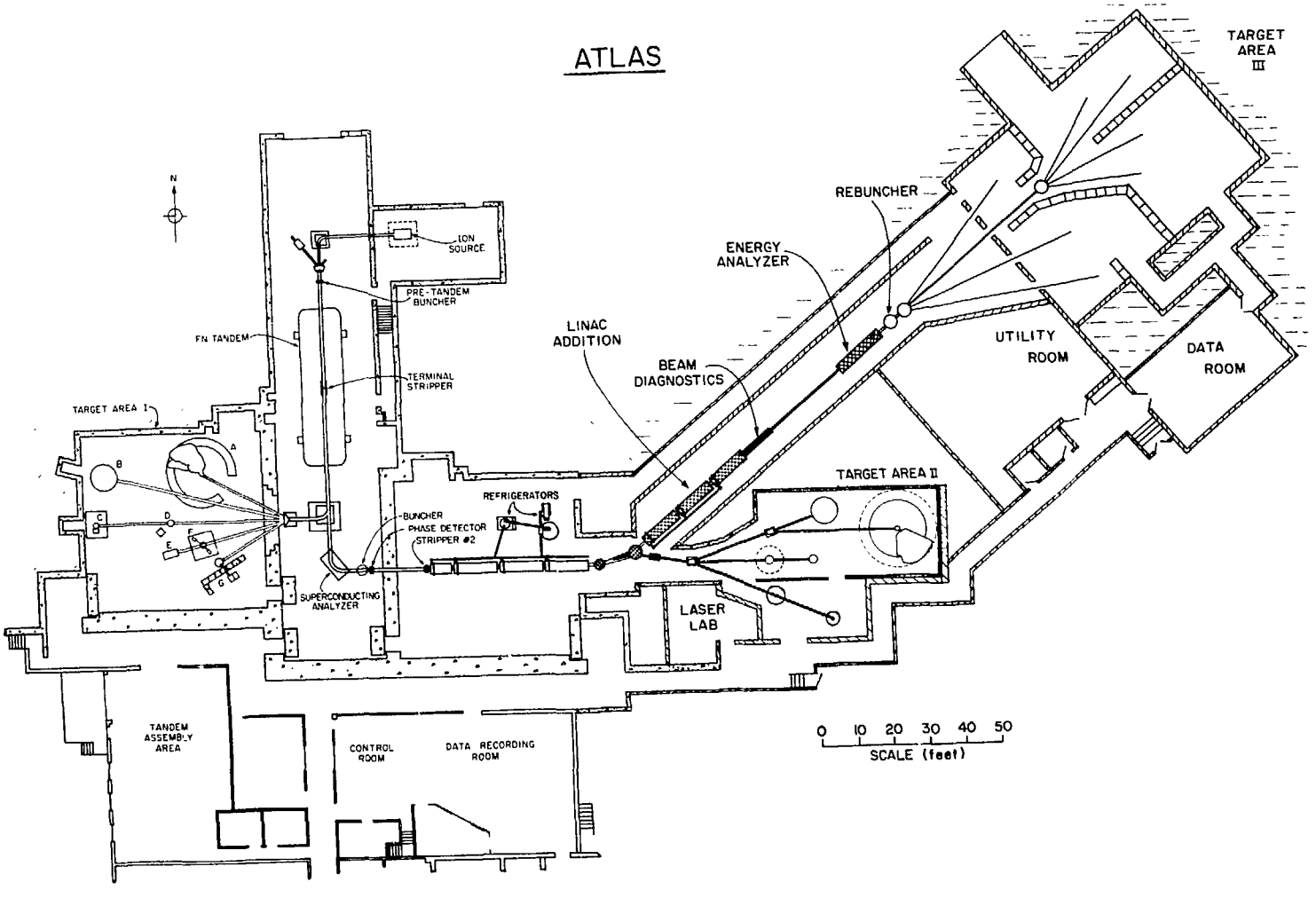

Fig. VI-4. Layout of the proposed ATLAS facility.

VII. ACCELERATOR OPERATIONS

INTRODUCTION

This section is concerned with the operation of both the tandem-linac system and the Dynamitron, two accelerators that are used for entirely different research. Developmental activities associated with the tandem and the Dynamitron are also treated here, but developmental activities associated with the superconducting linac are covered separately in Sec. VI, because this work is a program of technology development in its own right.

A. OPERATION OF THE TANDEM-LINAC ACCELERATOR

This activity consists of the operation of the tandem-linac accelerator system so as to provide beams of nuclear projectiles for research in several areas of nuclear physics and occasionally in other areas of science. The accelerator system consists of a 9-MV tandem electrostatic accelerator and several sections of a superconducting-linac energy booster. The linac is now (March 1981) about 2/3 completed. Its accelerating voltage already exceeds the 13.5 MV projected in the original design. The tandem-linac system is now equivalent in energy to a 19-MV (terminal) tandem with two strippers. Completion of the linac is expected late in 1981, at which time the layout of the whole facility will be as shown in Fig. VII-1.

Because of the modular design of the booster, it can be effectively used to accelerate ion beams before it is completed. During the past year, the booster was operated about half of the time and the tandem alone was used during the other half. By mid-1981, the booster mode will be the dominant mode of operation.

1. RECENT OPERATING EXPERIENCE FOR THE TANDEM

P. K. DenHartog, C. E. Heath, F. H. Munson, Jr., and J. L. Yntema

During 1980, the tandem operated for 5096 hours. Beams of protons, deuterons, ^{4}He, ^{7}Li, ^{11}B, ^{12}C, ^{13}C, ^{16}O, ^{18}O, ^{24}Mg, ^{27}Al, ^{28}Si, ^{31}P, ^{32}S, ^{34}S, ^{37}Cl, ^{40}Ca, ^{56}Fe, ^{59}Co, ^{58}Ni, ^{60}Ni, and ^{64}Ni were accelerated for the experimental program.

The operating schedule of the tandem is somewhat variable because of the variety of activities in progress. During 1980, when the tandem was used as a stand-alone machine, the operation was usually scheduled for only five days weekly in order to reduce costs. When the full tandem-linac system was used, however, operation was usually scheduled seven days weekly because of the great demand by users for running time.

The tandem normally operates at terminal voltages between 8.5 and 8.7 MV when it functions as the injector into the linac. In this range, the terminal voltage, particle transit time, and the beam position are exceedingly stable, as required. As a stand-alone machine, the tandem can operate at a higher terminal voltage (in excess of 9 MV) because the beam-stability requirements are usually less demanding.

After about 15 000 hours of operating time, the enclosed-corona voltage-distribution systems of both the column and the accelerator tube were reworked in 1980. This included replacement of all corona-needle

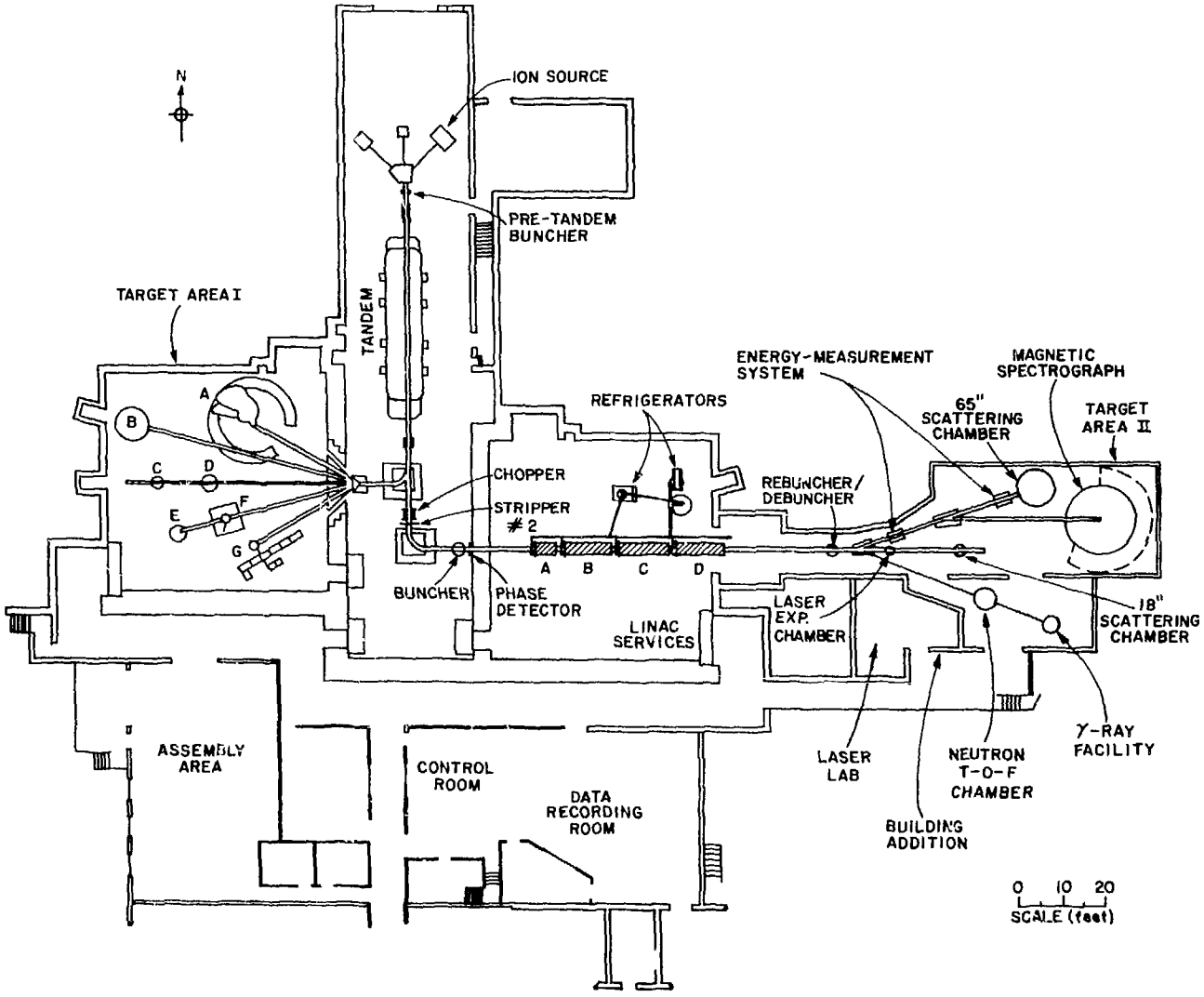

Fig. VII-1. Layout of the tandem-linac facility in the configuration expected to be operational in late 1981.

assemblies and the sandblasting of corona chambers, where required. Inspection of the components showed that the operating time of 15 000 hours was clearly too long for the corona system associated with the accelerator tube: the corona chambers showed considerable sulfur deposits and the needles were badly worn, even though the wear was uniform. It is likely that the desired continuous corona discharge had degraded to a state of intermittent sparking. To avoid this, the corona system associated with the tubes should probably be serviced every 10 000 to 12 000 hours. In contrast, the corona system associated with the column displayed much less deterioration and may well have a lifetime in excess of 15 000 hours.

There were no major modifications of the tandem as a whole during 1980. However, progress was made in a number of developments of immediate importance to the experimental program.

2. OPERATION OF THE SUPERCONDUCTING LINAC

R. Benaroya, L. M. Bollinger, R. C. Pardo, and K. W. Shepard

The booster was scheduled for operation about 40% of the total time during 1980. Almost all of this running time was devoted to the nuclear-physics research program, with less than 10% used for accelerator development. The time between running periods was used to make various major improvements in the booster.

The number of useful resonators on line has increased steadily with time, and by now the linac provides a very respectable energy increase. A matter of special satisfaction is the fact that, although only 2/3 of the planned resonators have been installed to date, the demonstrated accelerating voltage is already greater than the 13.5 MV that was projected when the booster was first proposed in 1974.

The accumulated operating experience is by now quite large—a total of at least 5000 hours of beam-acceleration time. This experience gives us realistic guidance on what to expect for future operating characteristics and has revealed the numerous practical problems that limit operational efficiency during routine use of the booster. The extensive operational experience has also shown that certain possible problems of a more fundamental kind do not exist to a significant extent: problems such as serious

radiation damage of the superconducting surfaces and the "thing you haven't thought of" that was formerly mentioned so frequently by those who were skeptical about the practicality of a superconducting linac.

By now, a wide variety of beams have been accelerated by the tandem-linac system. These include ^{12}C, ^{16}O, ^{18}O, ^{24}Mg, ^{28}Si, ^{32}S, ^{34}S, ^{37}Cl, ^{40}Ca, ^{56}Fe, ^{58}Ni, ^{59}Co, and ^{64}Ni. Both single stripping (terminal only) and double stripping are used, depending on the beam energy required.

The maximum beam energy available from the booster in March 1981 is equivalent to that from a 19-MV tandem with two strippers. By late 1981, when the booster has been completed, the tandem booster system is expected to be equivalent to a 25-MV tandem.

The range of projectiles that can be accelerated by the tandem-booster system is gradually being expanded. Until October 1980, the upper limit for useful beams (i.e., beams with energies above the Coulomb barrier) was about A = 40 because only high-β resonators were in use. The installation of four low-β resonators then extended the upper limit to about A = 66. When section B has been installed ($\sim$ May 1981), the mass limit will be extended very much higher, in so far as the booster is concerned, but then the ion mass will be limited by other factors such as the lifetime of stripper foils, the need for a lens in the tandem terminal, and the limited bending powers of several magnetic elements between the ion source and the linac.

One of the most valuable attributes of the booster is the exceptional ease with which the beam energy can be changed. Under many circumstances, once the resonators have been calibrated for a particular ion, the experimenter simply instructs the control computer what new energy is required, and it is rapidly done. This capability is proving to be unexpectedly valuable for measuring excitation functions with a level of detail that has rarely been undertaken heretofore. The optical elements of the output beam line must still be tuned manually, but computer control will be implemented in time.

One of the most important questions about the linac at the present stage of development is its operational reliability. One indication that it is quite good is the fact that the linac is run without operators in the area except during the normal 40-hour work week. Once a run has started, the experimenters monitor the operation of the machine and carry out routine operational functions such as changing the beam energy. The linac-development staff are on call to fix serious malfunctions. The tandem operators, of whom

at least one is always present, are now being trained to carry out some maintenance functions on the linac.

In quantitative terms, during a run the linac is operational on the average about 85% of the time that it is needed—that is, when the tandem and the experimenter's apparatus are also working. In practice, this means that some runs are almost trouble free and in others an important fraction of time is lost. In a run during December 1980, the system ran for four complete days without any trouble whatsoever. During a running period, the booster is rarely out of operation for longer than eight hours at a time, and no running period has ever had to be canceled.

3. UPGRADING THE TANDEM

P. J. Billquist, P. K. DenHartog, C. E. Heath, F. H. Munson, and J. L. Yntema

Most of the developmental effort on the tandem is aimed at improving its heavy-ion capability. During the past year, particular emphasis has been devoted to the refinement of our foil-stripping technique, which is especially important to us because of the difficulty of implementing gas stripping of heavy ions in the terminal of an FN-model tandem.

a. An International Study of Stripping Foils

P. K. DenHartog, W. Henning, R. C. Pardo, G. E. Thomas, J. L. Yntema, P. Maier-Komor,* and D. Tolfree†

An extensive set of measurements involving participants from several laboratories has been made on the performance of stripping foils in the tandem terminal, using ^{58}Ni as the test beam and a terminal voltage of 8.5 MeV. The survey included three kinds of foils: (1) those prepared by ethylene cracking at Daresbury-Harwell, Chalk River, Heidelberg, and Argonne, (2) normal carbon foils from Munich, Chalk River, and the Arizona Foil Co., and (3) normal carbon foils irradiated with a laser beam at the Technical University, Munich. Some foils were mounted as slackened foils. The foil thickness ranged from 2 $\mu g/cm^2$ to more than 15 $\mu g/cm^2$.

Two kinds of measurements were involved in the foil-performance tests: (1) a determination of ion-beam transmission as a function of time

*Technical University of Munich, West Germany.

†Nuclear Structure Facility, Daresbury, United Kingdom.

and (2) a measurement of energy straggling by means of the time-of-flight technique outlined in the 1979-1980 Annual Report. From the data obtained, the effective lifetime can be defined unambiguously for a given set of beam requirements.

For our needs, some of the foils thought to have long lifetimes were found to be useless because of poor beam transmission, presumably due to excessive foil thickness. The longest effective lifetime was obtained with an unslackened foil made at the Max Planck Institute, Heidelberg, for which the lifetime was several times longer than for the normal foils. With most of the foils, the effective lifetime was set by a gradual decrease in beam transmission, presumably caused by foil thickening, rather than by a sudden rupture.

Based on the results of the foil-performance survey, it is now clear that a major limitation in foil stripping is the foil-thickness problem, both because most foils are too thick initially and because many appear to thicken with use. We will continue to attack both aspects of the problem.

b. Development of the Terminal

P. K. DenHartog, C. E. Heath, and F. H. Munson

An improved control system for the foil changer in the terminal has been completed and successfully used for a number of months. This system, which uses fiber-optic control links and a microprocessor in the terminal, allows a much improved management of the stripper foils, thus resulting in more efficient use of foils and a substantial decrease in down time for reloading of the foil changer. In view of the great interest now in the acceleration of nickel and other heavy beams which degrade foils rapidly, this increased efficiency has proven to be quite important.

c. Ion Sources

P. J. Billquist and J. L. Yntema

The main operating source for the tandem-linac system is the inverted Cs sputtering source originally developed at Florida State University. In 1980, considerable effort was made to refine this source and to develop beams of particular ions needed by the experimental program.

The beam intensity obtainable from the inverted sputter source was increased by a factor of 2.5 by improving the internal optics. This increase in intensity is particularly valuable for beams which are inherently weak (e.g., CaH^-) or for beams from enriched isotopic material (e.g., ^{64}Ni).

Substantial improvements in Ca beams were made by hydrogenation of the Ca source material.

The influence of the shape of the sputter target was investigated. It was found that a flat surface is adequate for some ions, whereas for others the beam intensity can be increased substantially by using cones with an included angle of about 60°.

For ^{16}O, it was found that the energy distribution of the $^{16}O^-$ ions from the source can be substantially influenced by the cone material. The energy spread of ions produced by flowing oxygen gas over a single-crystal Si cone is substantially smaller than the energy spread of ions produced with a Ni cone. A possible explanation of the difference is that the energy spread depends on whether the effective target material is adsorbed or absorbed oxygen.

The sputtering results on a number of cones indicate that more than 60% of the negative-ion beam originates in a spot of about 1.5 mm diameter. This property allows small samples to be used as sputter targets in the inverted source. The use of compressed pellets has been extended to isotopically-enriched nickel samples.

Work on the ANIS (Aarhus) source has continued, and satisfactory operation has been achieved on the test stand. Also, a version of the Wisconsin high-intensity source SNICS has been built. In order to achieve a workable source system, a new extraction-acceleration system is under construction, and operation with both sources on the tandem is planned for late 1981-early 1982. It is expected that these sources will increase the beam intensities for Al, Ti, Fe, and Zr ions, and thus these sources will complement the capabilities of the inverted sputtering source.

The major parts of a new He-ion source have been purchased. Installation of the completed source, which is expected to provide 5 μA of the beam at an injection energy of about 70 keV, is scheduled for late 1981.

4. INSTALLATION AND IMPROVEMENT OF THE BOOSTER

J. Aron,* R. Benaroya, L. M. Bollinger, B. E. Clifft,* K. W. Johnson,* P. Markovich,* J. M. Nixon,* R. C. Pardo, and K. W. Shepard

Recent progress on the installation of the superconducting energy booster is briefly summarized here. A more complete discussion of the main developmental activities associated with the linac is given in Sec. VI.

a. Linac Section A

The installation of Section A with 4 low-β resonators was completed in 1980 and was put into service in early 1981. It functions as planned.

b. Linac Section B

Four resonators are now being installed in Section B, and this partly completed system will be put on line in May 1981. The remaining four resonators needed to complete the system will be installed in October 1981, and this installation will mark the completion of the booster.

c. 300-Watt Refrigerator

A CTI-2800 refrigerator was put into operation in late 1980. The 200 watts of refrigeration capacity provided by the two compressors now installed is more than enough to meet the needs of the booster. The capacity can be increased to 300 watts by adding a third compressor.

d. Rebuncher/Debuncher

A superconducting rebuncher/debuncher was installed on the linac-output beam line in late 1980. This system is functional, but some effort is still needed to reduce the vibration level of the device to the desired level.

e. Energy-Measurement System

An energy-measurement system which makes use of two rf resonators excited by the pulsed beam has been installed and will be put into service in late 1981. The system is expected to measure the output-beam energy of the booster with an accuracy of about $\Delta E/E \simeq 2 \times 10^{-4}$.

*Chemistry Division, ANL.

5. NEAR-TERM PLANS

a. Accelerator Operation

The final section of the booster will be on line by late 1981, thus reducing the need to interrupt the operation in order to install new equipment. In principle, it should be feasible to operate the full Tandem-Linac system for about 80% of the time, in so far as the hardware is concerned. However, the present level of operating personnel is not large enough to support such a full schedule. Rather, we expect to be able to operate the tandem-linac system about half of the total time available.

The tandem will continue to be operated as a stand-alone machine for a small fraction of the time. The capability of being able to use the tandem alone is advantageous, both as a way of supporting a broad range of research and for operational efficiency.

b. Booster Improvements

The final section of the booster will be installed on line in late 1981, but the work of making it work well will extend into 1982.

Numerous tasks will be undertaken with the objective of reducing costs and increasing the reliability of the booster. These tasks include: (a) upgrading the liquid-nitrogen distribution system, (b) upgrading the slow tuners of the resonators, (c) refining the beam-tuning system, and (d) refining the linac-control program.

c. Tandem Improvements

During 1982, the main task will continue to be to upgrade the terminal in all respects. This will involve continuing to try to improve foil stripping, completing the development of a good terminal-communication system, and starting work on the lens required to increase the transmission of very heavy ions.

d. Ion Sources

The upgraded test bed will be in operation by 1982, which will greatly facilitate the work on ion sources. The main emphasis in 1982 will

be to develop new beams of immediate interest to the experimental program. Most of these will be in the mass range $40 \leq A < 80$ and will include isotopes of Ca, Fe, Ni, and Se. Since some of the ions of interest involve low-abundance isotopes, considerable effort will be devoted to improving the efficiency of utilization of small samples.

6. OUTSIDE USERS OF THE TANDEM-LINAC ACCELERATOR

a. University of Kansas

F. W. Prosser, Jr., and R. A. Racca (D. G. Kovar, C. N. Davids, W. Henning, J. P. Schiffer, and D. F. Geesaman)

A number of experiments have been performed on the measurement of fusion cross sections in various light heavy-ion systems. Both charged-particle and γ-ray yields have been determined. On the tandem-linac, fusion-fission cross sections were determined for $^{58}Ni + {}^{118}Sn$. Earlier work was done on excited states in ^{28}Si from the $^{16}O(^{16}O,\alpha)^{28}Si \rightarrow {}^{24}Mg + \alpha$ reaction.

b. Purdue University

P. Daly, A. Pakkanen, H. Helppi, S. Faber, J. Wilson, C. L. Dors, and Y.-H. Chung (T. L. Khoo and R. K. Smither)

This group collaborates with the ANL tandem-linac γ spectroscopy group. They have performed studies of the feeding of yrast states in $A \sim 150$ nuclei, and the link between the highest-known yrast states and the continuum region.

c. University of Maryland

A. Mignerey, H. Breuer, V. Viola (also at Indiana University), (K. Wolf,* C. Davids, and R. Betts*)

Using 7.4- and 6.0-MeV/nucleon ^{37}Cl beams from the tandem-linac, the product mass and charge distributions from deep-inelastic collisions with ^{40}Ca and ^{209}Bi targets have been studied. Structure in the energy-loss spectra of individual products from symmetric heavy-ion systems was also observed.

---

*Chemistry Division, ANL.

d. Brooklyn College

J. Lebowitz (W. Henning and B. Back*)

Deformation effects on the fusion-fission cross section for the S + Sm system.

e. Florida State University

L. C. Dennis, S. L. Tabor, K. W. Kemper, J. D. Fox, and (D. G. Kovar)

This group studied the fragmentation of ^{18}O at 141 MeV by bombarding ^{12}C, ^{27}Al, and ^{46}Ti targets with the ^{18}O beam from the tandem-linac. Energy spectra and angular distributions were measured for the Li, Be, B, C, and N ions produced during bombardment.

f. Iowa State University, University of Minnesota

D. A. Lewis (ISU), G. W. Greenlees (UM), (C. Davids)

A new collaboration between the Physics Division, Iowa State University, and the University of Minnesota is about to begin at the tandem-linac. The experiments will be in the general category of on-line laser spectroscopy of radioactive atoms, and will focus on the determination of isomer and isotope shifts in the optical spectra of neutron-deficient heavy nuclides. In order to perform these experiments, a substantial investment is being made in the construction of a new laboratory and a cryogenic helium-jet transfer system.

7. OUTSIDE USERS OF THE TANDEM ALONE

Although the tandem is now used as an injector of the linac most of the time, it is still used somewhat as a stand-alone accelerator. The research of this kind carried out by outside users in 1980 is summarized below.

a. Western Michigan University (1975-1980)

G. Hardie, (L. Meyer-Schützmeister and A. Elwyn)

These experiments involve studies of $f_{7/2}$-shell nuclei. Early experiments emphasized determination of the energies, spins, branching ratios, multipolarities and lifetimes of high-spin states and the comparison of

*Chemistry Division, ANL.

these results with shell-model calculations based on an inert ^{40}Ca core and all active nucleons in the $1f_{7/2}$ shell. More recently the nuclei ^{43}Ti and ^{45}V have been investigated. As these nuclei are members of mirror pairs, Coulomb displacement energies could be extracted. Coulomb shifts have been found to vary systematically with mass number in the $1f_{7/2}$ shell. An attempt is being made to understand these shifts. Work on Coulomb-displacement energies is continuing with the study of ^{47}Cr, mirror of the much studied nucleus ^{47}V.

b. Northwestern University (1975-1980)

R. E. Segel, K. Raghunathan, L. L. Rutledge, and (L. Meyer-Schützmeister)

This program has involved the measurement of radiative capture in the giant resonance region. Reactions studied include $^{54}Fe(\alpha,\gamma)^{58}Ni$ and $^{86}Sr(\alpha,\gamma)^{90}Zr$. In each case both E1 and E2 capture radiation were observed, indicating that the isoscalar quadrupole giant resonance has a direct α-particle decay branch.

c. University of Pittsburgh (1980)

J. V. Maher and (L. Meyer-Schützmeister)

A study of the properties of the giant dipole resonance by radiative capture of alpha particles.

d. Max-Planck-Institute, Heidelberg (1980)

H. V. Klapdor and (W. Henning)

The $^{12}C(^{10}B,d)^{20}Ne$ reaction.

e. University of Birmingham (1980)

G. C. Morrison, (D. F. Geesaman, W. F. Henning, D. G. Kovar, and B. Zeidman)

Three-nucleon transfer reactions on ^{11}B.

f. Yale University (1980)

J. Petersen, (W. F. Henning, and D. G. Kovar)

Single-nucleon transfer reactions induced by ^{12}C on ^{48}Ca at 45 MeV.

g. Brookhaven National Laboratory (1980)

D. Alburger, (W. Henning, and W. Kutschera)

Half-life of ^{32}Si by accelerator mass spectroscopy.

h. University of Michigan (1978-1980)

A. L. Hanson, D. Vincent, W. Halsey, and (C. Davids)

The $H(^{19}F,\alpha\gamma)^{16}O$ reaction was used to study the depth profile of hydrogen implanted in Mo single crystals. The effect of damage by low-energy He implantation was also determined.

i. Beloit College (1978-1980)

J. C. Stoltzfus, (J. Erskine, and D. G. Kovar)

Development of a focal-plane charged-particle detector for the split-pole spectrograph.

B. OPERATION OF THE DYNAMITRON FACILITY

The Physics Division operates a high-current 4.5-MV Dynamitron accelerator which has unique capability as a source of ionized beams of most atoms and many molecules. Among the unusual facilities associated with the Dynamitron are (1) a beam line capable of providing "supercollimated" ion beams permitting angular measurements to accuracies of 0.005 degree, (2) a beam-foil measurement system capable of measuring lifetimes of a few picoseconds, (3) an experimental system dedicated to measuring absolute nuclear cross sections at low energy, (4) a precise angular-correlation system for weak-interaction studies, and (5) a simultaneous irradiation system by which heavy ions from the Dynamitron and helium ions from a 2-MV Van de Graaff accelerator are focused on the same target. An advanced PDP-11/45 computer system is used for on-line data analysis and for the control of experimental systems.

1. OPERATIONAL EXPERIENCE

A. J. Elwyn, R. L. Amrein, and A. E. Ruthenberg

Overall, the Dynamitron continued to perform well during the past year. The normal operating schedule was twenty-four hours a day, five days a week. Very little running was done on weekends during calendar year 1980.

During the year the accelerator was staffed a total of 5496 hours. Of this time 3996 hours (73%) were scheduled for experimental research during which a beam was provided to the experimenters 84% of the time. Machine preparation time used up 5% of the scheduled research time and machine malfunctions the remaining 11%. Scheduled accelerator improvements (including the upgrading program) and modifications used a total of 1500 hours or 27% of the total available time.

The great versatility of the Dynamitron continued to be exploited by the research staff. Ion currents on target varied from less than a nanoampere to about 25 microamperes with ion energies ranging from 0.4 to 3.7 MeV. A wide range of both atomic and molecular ions were delivered on target. They included $^{1}H^{+}$, $(^{1}H_{2})^{+}$, $^{2}H^{+}$, $(^{1}H_{3})^{+}$, $^{3}He^{+}$, $(^{2}H_{2})^{+}$, $^{4}He^{+}$, $^{4}He^{++}$, $(^{1}H^{2}H_{2})^{+}$, $(^{4}HeH)^{+}$, $(^{2}H_{3})^{+}$, $^{7}Li^{+}$, $^{12}C^{+}$, $^{14}N^{+}$, $^{16}O^{+}$, $(^{16}O^{1}H)^{+}$, $(^{16}O^{1}H_{2})^{+}$, $^{20}Ne^{+}$, $(^{12}C^{16}O)^{+}$, $(^{14}N_{2})^{+}$, $(^{12}C^{16}O^{1}H)^{+}$, $(^{16}O_{2})^{+}$, $^{40}Ar^{+}$, $^{84}Kr^{+}$, $^{132}Xe^{+}$.

During the year a total of 62 investigators used the Dynamitron in some phase of their experimental research. Of these, 28 were from the

Physics Division, 14 were from other Argonne research divisions, 13 were outside users (not temporary appointees) from other research facilities, 6 were members of the Resident Graduate Student Program, and 1 was an Argonne Faculty Research Participant. Of the scheduled time, 70% went to members of the Physics Division, 24% to other Argonne divisions, and 6% was exclusively assigned to outside users. However, outside users collaborated in experiments that used 20% of the total available time, and participants in the Resident Graduate Student Program worked on experiments that used 34% of the time.

Experimental activity at the facility proceeded normally from the start of the year until the end of August. During this period most maintenance work was of routine nature. One problem encountered was an apparent increase in the intensity of 120-kHz rf voltage picked up on the high-voltage terminal. This was manifested as an energy modulation of the ion beam, and indicated an energy resolution of more than a few keV, a value which was detrimental to the research efforts of at least two user groups. Some effort was expended in attempts to understand and correct the problem. Although not successful at the time, the situation has, subsequent to the upgrading program (see below), been vastly improved.

Starting in September 1980, the Dynamitron was shut down and the project (mentioned in last year's report) was initiated to provide a number of modifications which it is hoped will upgrade the maximum energy of the accelerator to the vicinity of 5 MV. The following major changes have now been completed: (1) An additional SF_6 storage vessel has been installed, connected in parallel with the present one. This will eventually allow the insulating gas pressure in the machine to be increased from 90 to 135 psig. (2) An SF_6 on-line gas purifier was bought and installed via connecting pipes to the pressure vessel. (3) New single-piece Plexiglas supporting frame members have been bought and installed to replace the old jointed members. (4) A new toroidal induction-coil frame was purchased and the coil assembly (which provides the rf power for high-voltage generation) has been completely rebuilt, using the original pie-shaped coils. (5) In addition, a variable air-core capacitor has been installed in the high-voltage terminal which along with a previously-installed capacitive balance plate between the top Dee and the pressure-tank wall allows the 120-kHz rf ripple on the terminal to approach very close to a null. Subsequent measurements (after the rebuilt

machine was closed up) of the beam-energy spread, by determination of thick-target γ-ray yields from nuclear reactions, have indicated that the energy modulation associated with the rf pickup is ≤600 eV so that at present the overall energy resolution is significantly less than 1 keV.

The above modifications took about two months to complete and check out. Since then, the machine has been operating with (mostly) only routine maintenance problems and relatively spark free at energies up to about 4 MeV. It has not yet been possible to test the maximum energy-holding capability of the rebuilt accelerator at an SF_6 pressure above 90 psig, so that it is too early to know if other improvements (e.g., replacement and modification of the accelerator tube and/or solid-state rectifiers) will be necessary in order to accelerate particles to 5 MeV. However, the machine has been operated without an accelerated beam to an energy of 4.7 MV. Further improvement in the electrical configuration associated with the added terminal capacitor (to prevent damage to various components due to sparking) appears to be important to subsequent high-voltage operation. The active consulting assistance of Dr. Alexander Langsdorf, now retired, has been invaluable to the progress that has so far been made, especially in connection with the improvement in reducing the rf ripple on the terminal.

During the past year the IMSAI 8080 microcomputer has been operated routinely for mass scans. Use of the computer to log the various accelerator parameters read off of the control panel of the machine (rather than have the operators write the numbers down manually) is expected to become routine very shortly. The fiber optics light-link system, designed by National Electrostatics Corp., has been installed, but testing of the system and the actual monitoring in conjunction with the computer of the accelerator parameters within the high-voltage terminal has not yet started.

Lithium ion beams with intensities up to about 4 microamperes are now routinely accelerated in the Dynamitron. Further ion-source development to provide beams of, e.g., lithium hydride ions (which are important to the structure studies of at least one of the atomic physics research groups), has still not proved successful. Other commitments made it impossible to spend much time on this development program during the past year. The use of the Penning ion source has allowed the successful acceleration of up to 1 microampere of $^4He^{++}$ ions through the machine. It is expected that this will stimulate the initiation of new experimental research programs.

2. UPGRADING OF THE DYNAMITRON

During the past year, the Dynamitron has run reasonably well and is heavily used by several research groups. The first part of a program to upgrade the energy of the Dynamitron to the vicinity of 5 MV was completed during 1980. The main effort during 1981 and 1982 will be to test the maximum energy-holding capability of the rebuilt machine, and if necessary, to replace or modify the existing accelerator tube and/or the solid-state rectifiers in order to achieve successful operation at or near 5 MV. In connection with Dynamitron operation at these energies, it is hoped that during 1982—1983 a completely new and more efficient gas-handling system can be designed and built. During 1981 the fiber optics light link, installed in the past year, will be tested and, in conjunction with the IMSAI 8080 microcomputer, employed for the monitoring of the various source parameters within the high-voltage terminal. Beams of Li ions were routinely accelerated during the past year. In 1981 and 1982, ion-source development will be continued, particularly to satisfy user needs for beams of Be, B and their hydrides (as well as Li hydride), and usable beams of doubly-charged He ions. In this connection, efforts to install terminal pumping will continue.

3. UNIVERSITY USE OF THE DYNAMITRON

F. P. Mooring, A. J. Elwyn, and R. L. Amrein

The Argonne Dynamitron continues to be a valuable research facility for scientists from outside institutions. It is not only the accelerator itself that attracts outside investigators but also the unique associated experimental equipment as well as the on-going research program being conducted at the Dynamitron.

Most visiting scientists chose to collaborate with local investigators on problems of common interest. A few, however, worked as an independent group. Some came for a one-time-only experiment, but most are participants in research programs that have spanned a period of several years.

During the year thirteen scientists came from eight outside institutions to use the Dynamitron. They came from five states and two foreign countries. They participated in experiments that used 20% of the time scheduled for research. A list of those institutions from which users of the Dynamitron came during 1980 is given below. The list includes the name of the institution, the title of the research done, and the names of the principal investigators. The names of local collaborators are enclosed in parentheses.

a. Los Alamos National Laboratory

Parity Violation in the 5.1-MeV, J=2 Doublet of ^{10}B

T. J. Bowles, S. J. Freedman,* R. G. H. Robertson,* (A. R. Davis, C. A. Gagliardi, G. T. Garvey, R. D. McKeown, and B. Myslek-Laurikainen)

b. University of Lyon

Structure Determination for the H_3^+ Molecular Ion

J.-C. Poizat, (P. J. Cooney, N. Cue, A. K. Edwards, D. S. Gemmell, K. Inglis, E. P. Kanter, I. Plesser, J. A. Rothstein, and B. J. Zabransky)

c. Marquette University

Radiation Damage of Covalent Crystal Structures

L. Cartz, R. Fournelle, A. Gowda, F. G. Karioris, K. Ramasami, and G. Sarkar

d. Michigan State University

Parity Violation in the 5.1-MeV, J=2 Doublet of ^{10}B

R. G. H. Robertson, T. J. Bowles,* S. J. Freedman,* (A. R. Davis, C. A. Gagliardi, G. T. Garvey, R. D. McKeown, and B. Myslek-Laurikainen)

e. Notre Dame University

Observation of the Optical Emission from the Negative ^7Li Ion

A. E. Livingston, (H. G. Berry, R. Brooks, J. Hardis, and W. J. Ray)

f. Purdue University

A Measure of the Response Function of a Large NaI Crystal for High-Energy Gamma Rays

S. R. Faber, (I. Ahmad, J. Borggreen, T. L. Khoo, R. K. Smither, and P. Chowdhury)

g. Stanford University

Parity Violation in the 5.1-MeV, J=2 Doublet of ^{10}B

S. J. Freedman, T. J. Bowles,* R. G. H. Robertson,* (A. R. Davis, C. A. Gagliardi, G. T. Garvey, R. D. McKeown, and B. Myslek-Laurikainen)

---

*From another outside institution.

h. Weizmann Institute

A Study of the Effect of Projectile Excitation on Coulomb Explosions

Z. Vager, (D. S. Gemmell, E. P. Kanter, I. Plesser, and B. J. Zabransky)

The Resident Graduate Student Program is open to students that have finished their course work and passed their prelims. They come to Argonne and perform their final thesis research here. Six members of this program worked at the Dynamitron during 1980. Altogether they participated in experiments that used 34% of the time allotted to research. Those who used the accelerator are listed below, together with their home university and their local thesis advisor.

a. A. R. Davis, University of Chicago
J. P. Schiffer, advisor

b. R. DeSerio, University of Chicago
H. G. Berry, advisor

c. B. Filippone, University of Chicago
C. N. Davids, advisor

d. C. A. Gagliardi, Princeton University
G. T. Garvey, advisor

e. T. J. Gay,* University of Chicago
H. G. Berry, advisor

f. J. Hardis, University of Chicago
H. G. Berry, advsior

---

*Received doctoral degree during the year.

VIII. GeV ELECTRON MICROTRON

INTRODUCTION

A strong consensus has developed recently in the nuclear physics community that research with electromagnetic probes in the 1—2-GeV range generated by a high current 100% duty factor electron accelerator represents an exciting new frontier. A national nuclear research facility consisting of a 2-GeV electron accelerator and ancillary experimental areas would provide the research capabilities needed to exploit this opportunity. In the long-range plan of the DOE/NSF Nuclear Science Advisory Committee, an accelerator of this type is planned for construction starting in 1985. It is envisioned as a multibeam electron accelerator furnishing intense beams of high-energy electrons simultaneously to high-resolution spectrometers and other experiments in nuclear sciences. Argonne intends to compete vigorously for the approval to construct such a facility at Argonne. Because of superior beam quality, lower capital and operating costs which characterize its performance, a double-sided 2-GeV electron microtron has been chosen by Argonne scientists as the accelerator system to be used to generate the electron beams.

The unique capabilities of the ANL facility will include the ability to deliver continuous beams, with excellent energy resolution and high intensity. On demand up to three extracted beams will be available with individually variable energies over the range 0.5—2.0 GeV. The beams will be delivered to three experimental areas which will provide experimental facilities for high-resolution electron scattering studies, medium resolution coincidence experiments, and measurements requiring monochromatic or bremsstrahlung photon beams. The 2-GeV microtron project has been organized at Argonne in order to carry out the research and development necessary to prepare a construction proposal for the facility. Current planning includes development of a detailed microtron design with complete cost and time schedule in 1982.

The main element of the microtron research and development project is an engineering and design study of the basic sector magnet used to generate the magnetic guide field for a 2-GeV double-sided continuous beam electron microtron. Because of the strong vertical defocusing forces present at orbit entry and exit from a magnet of typical design, it is necessary to configure and determine the fringe fields accurately and establish a system of additional focusing elements which will ensure orbit stability and high beam transmission. Design of an appropriate sector magnet has been completed. A prototype of the portion of the magnet corresponding to the fields traversed in the first six turns of beam operation in a 2-GeV accelerator, i.e., 50—300 MeV has been completed. Field measurements in progress will be used to test assumptions made in the preliminary design studies. Pending confirmation of orbit stability, a complete prototype will be constructed. Orbit calculations and beam breakup analysis based on the measured field configurations will also be carried out.

a. Microtron Model Magnet Studies

A high-precision magnetic-field mapping system to be used to study field profiles in prototype test magnets has been designed and constructed. Software development for the computer-control and data-acquisition system was completed early in 1981. The system consists of a Hall probe mounted on a computer-controlled manipulator and minicomputer data-acquisition system. Pole faces for a partial prototype magnet have been fabricated and assembled with a return yoke, and excited to design values. Measurements of the field profiles are in progress. The magnet measuring system is shown in Fig. VIII-1, together with one of the earliest partial prototype magnet configurations. At the same time, an analyst team has developed orbit analysis programs, RAYTRACE and TRANSPORT in interactive versions, and run them with theoretical models which are expected to approximate the kind of field configurations found in the test magnets. Further use awaits data on actual field profiles. Preliminary specifications have been established for a full prototype magnet and engineering design and procurement activities have begun. During the remainder of 1981 we expect to continue examination of the technical and scientific requirements for all aspects of a 2-GeV accelerator facility.

b. Plans for 1982

Prototype testing of the microtron sector magnet will be completed during this period. Field measurements will be made with a precision of ±0.1% and a spatial resolution of ±0.5 mm. The results will be used in a computer analysis to demonstrate orbit containment and develop a model of beam dynamics which will establish the current threshold for beam breakup in a c.w. microtron.

Early in 1982 a critical decision point is anticipated on the optimum design for a 2-GeV electron accelerator. Magnet studies at ANL will have been completed. Studies of possible rf accelerating structures at LANL will have reached a definitive stage and limits on electron-beam breakup thresholds will have been estimated in the 170-MeV microtron system under construction at the National Bureau of Standards. We plan to develop a microtron design with a cost and time schedule in 1982. This design will be incorporated into a proposal for a complete 2-GeV c.w. electron accelerator research facility to be built at Argonne.

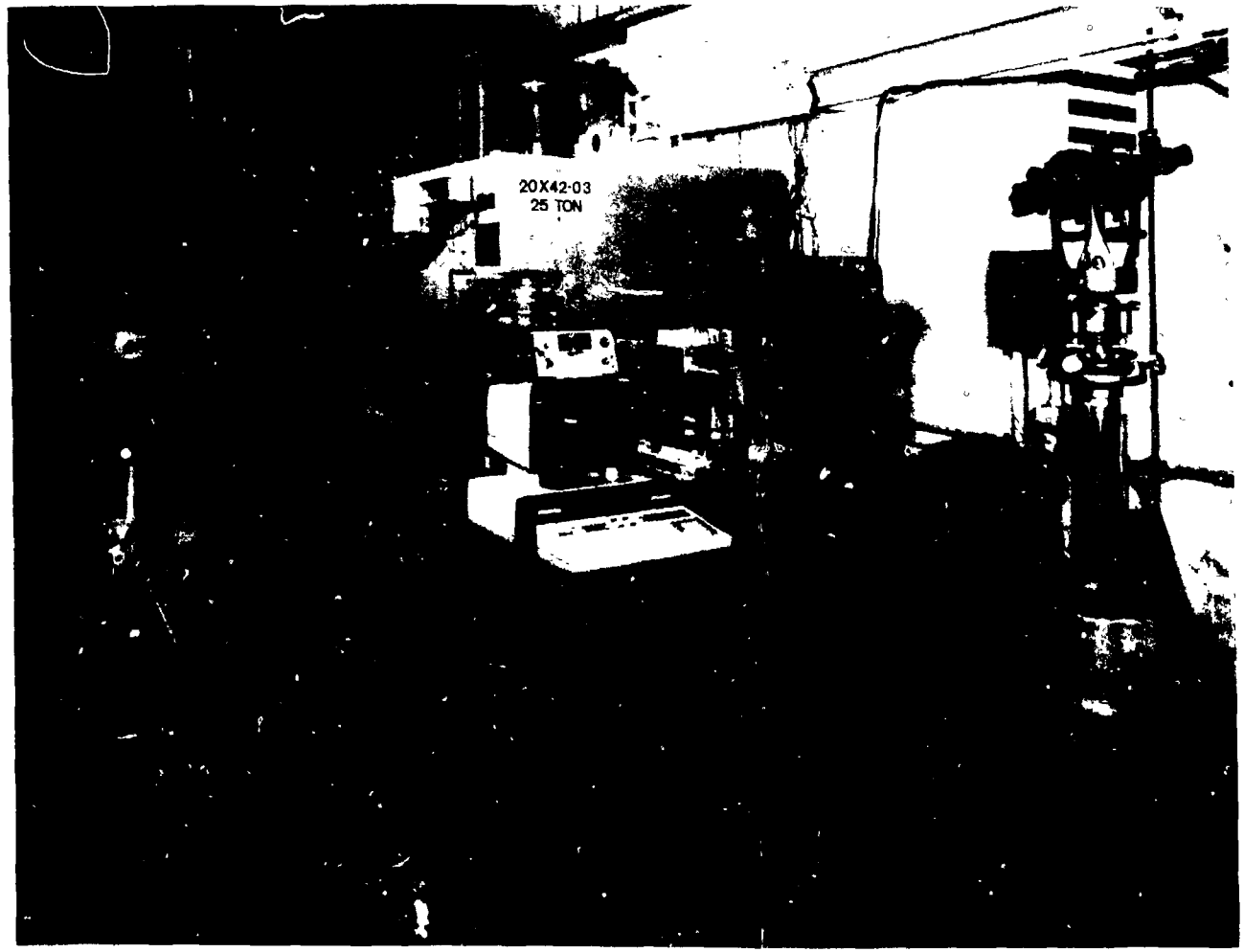

Fig. VIII-1. Microtron sector magnet measuring system.

ATOMIC AND MOLECULAR PHYSICS RESEARCH

INTRODUCTION

The Atomic Physics research in the Physics Division consists of six ongoing experimental programs as follows:

(1) Dissociation and Other Interactions of Energetic Molecular Ions in Solid and Gaseous Targets (D. S. Gemmell, E. P. Kanter)

(2) Beam-Foil Research and Collision Dynamics of Heavy Ions (H. G. Berry)

(3) Photoionization-Photoelectron Research (J. Berkowitz)

(4) High-Resolution, Laser-rf Spectroscopy with Atomic and Molecular Beams (W. J. Childs, L. S. Goodman)

(5) Mössbauer Effect Research (G. J. Perlow)

(6) Theoretical Atomic Physics (K. T. Cheng)

IX. DISSOCIATION AND OTHER INTERACTIONS OF ENERGETIC MOLECULAR IONS IN SOLID AND GASEOUS TARGETS

INTRODUCTION

Tightly collimated beams of molecular ions with energies variable in the range 0.5—4.0 MeV are directed onto thin (∿100 Å) foil or gaseous targets. The distributions in energy and angle are measured with high resolution (∿0.05° and ∿300 eV) for the resultant collisionally-induced dissociation fragments. The two major aims of the work are (a) a general study of the interactions of fast ions with matter, but with emphasis on those aspects unique to the use of molecular-ion projectiles and (b) a study of the structures of the incident molecular ions. These two different aspects of the work are mutually interdependent. In order to derive structure information about a given molecular ion, one needs to know details about the way the dissociation fragments collectively interact with the target in which the dissociation occurs. Similarly, a knowledge of the structure of the incident molecular clusters is important in understanding the physics of their interactions with the target. We have therefore begun our work with careful studies involving beams of the simplest and relatively well understood diatomic molecular ions (H_2^+, HeH^+, etc.). Even with these, several new and interesting phenomena have been encountered (e.g., the interactions between the molecular constituents and the polarization oscillations that they induce in a solid target, the marked differences in dissociations induced in gases as compared with those in foils, the anomalously high transmission of some molecular ions through foils, and striking electron capture phenomena when compared with atomic ions). As our understanding of these phenomena develops, we plan to go on to studies involving more complex projectile ions.

In 1980 we continued the work, begun last year, of developing techniques for determining the stereochemical structures of molecular projectiles by coincident detection of dissociation fragments. The preliminary data have shown us the most important problems which need to be addressed in order to obtain precise structural information. Most prominently, these problems include the need for a more detailed understanding of the physical processes involved in the interactions of these fast molecular ions with both solid and gaseous targets. In addition to that aspect, we also sought a better understanding of the influence of vibrational effects on our coincidence measurements. To that end, we concentrated our efforts on the H_3^+ ion and its deuterated forms. We also performed a study of the dependence of our Coulomb explosion results on the ion-source conditions.

The first successful UV laser-induced photodissociation of a fast molecular-ion beam was carried out. That measurement demonstrated our ability to perform some state selectivity of the molecular ions reaching the target chamber.

Improvements to the experimental apparatus included the development and use of new fast gas-filled avalanche detectors for the coincidence work. A new gas cell was constructed and installed to be used in modifying the vibrational-state populations of incident molecular beams.

Other highlights in 1980 included:

a. Molecular-Ion Structure Determinations

D. S. Gemmell, P. J. Cooney, N. Cue, I. Plesser, J.-C. Poizat, Z. Vager, and G. Carney*

(i) Coincidence Measurements

We have previously demonstrated that the structures of simple triatomic molecular-ion projectiles can be determined by recording spatial and temporal coincidences of two or more dissociation fragments from a given projectile. We presently have the ability to measure double or triple coincidences and to record simultaneously precise information on angles of emission, fragment-charge states, energies, and flight times from the target.

Coincidence results obtained so far (e.g., for H_2O^+) have yielded bond angles and bond lengths consistent with known equilibrium structures. A complication of those analyses, however, is the effect of the initial vibrational-state population of the incident molecular-ion beam. To further explore this point, we have concentrated our attention on the simplest triatomic ion, H_3^+ and its deuterated species.

The coincidence distributions are broad and asymmetric. The fact that the results for the deuterated species seem to show the differences predicted by calculations which include both bending and breathing vibrations indicates that these distributions are not dominated by multiple scattering effects. It is hoped that with improvements in our computer simulations of the dissociation process we can unfold these vibrational effects from the measured distributions.

(ii) Singles Measurements

Although we did perform a few measurements of singles spectra for purposes of structural determinations (e.g., a comparison of fragment spectra from HCO^+ and CO^+ beams), most such measurements were aimed at studying the

*Chemical Engineering Division, ANL.

effects of varying ion-source conditions on the vibrational-state populations of our molecular-ion beams. Our singles data give a direct measure of the Coulomb energies of the exploded molecular clusters in the beams. This in turn leads to a determination of the distribution of internuclear separations for the incident molecules. Such distributions are a good indication of the relative vibrational excitation of the incident molecular ions.

An extensive study was conducted for the foil-induced dissociations of the H_2^+, HeH^+, OH^+, and OH_2^+ molecular ions. Changes of ion-source feeder gas compositions and pressures were found to have no measurable influence on the vibrational state populations of the molecules reaching our target chamber. Further, with the exception of HeH^+ beams, vibrational-state populations were found to be independent of whether a duoplasmatron or rf ion source was used to produce the molecular-ion beams. For HeH^+, it was found that the beams produced in our rf source were vibrationally "hotter" than beams produced in the duoplasmatron source. Further influences of this difference of vibrational state populations were observed in studies of neutral fragments and transmitted molecules from HeH^+ beams produced in the two ion sources. It was an important confirmation of the model developed last year to explain the transmission phenomena that calculations using the "hot" vibrational state population observed with the rf-source produced HeH^+ beam correctly predict the threefold increase of transmitted-ion yield observed with that beam.

b. UV-Laser-Induced Photofragmentation

A. K. Edwards, R. Kutina, N. Cue, D. S. Gemmell, K. Inglis,* E. P. Kanter, and B. J. Zabransky

The photofragmentation of a 2-MeV H_2^+ beam was accomplished with an ArF laser (193-nm photons). The H^+ photofragments were energy analyzed in our electrostatic analyzer and the potential energy released in the projectile rest frame was determined (Fig. IX-1). The released energy corresponds to absorption from low-lying vibrational levels of the $1s\sigma_g$ ground state to the dissociative $2p\sigma_u$ state of H_2^+.

The short wavelengths of the excimer laser allowed the excitation of molecular transitions not obtainable previously. In addition to the spectroscopic data available from such measurements, these experiments demonstrated

*Graduate student, State University of New York, Albany, New York.

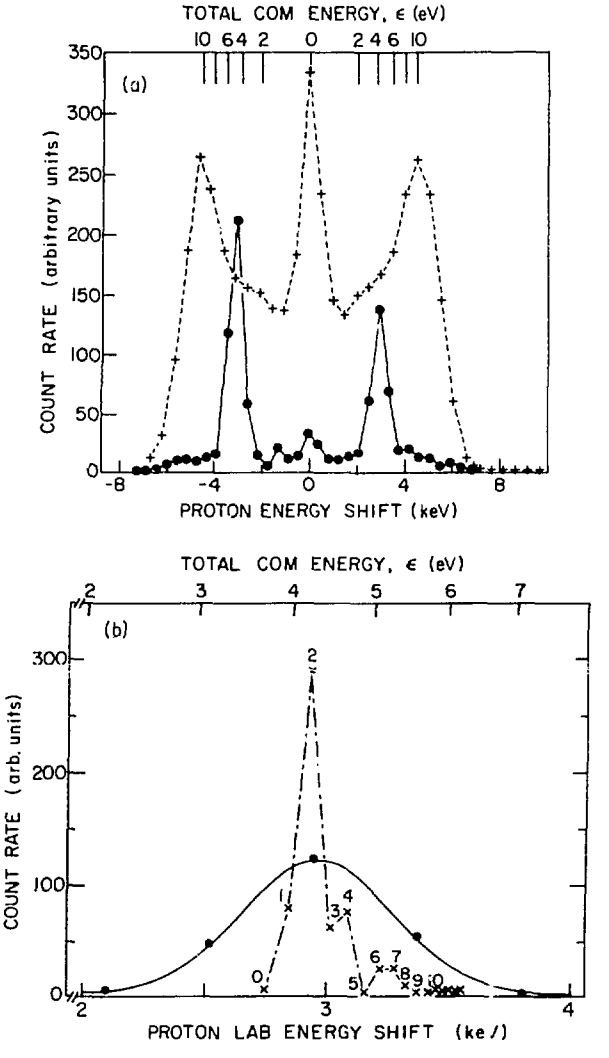

Fig. IX-1. (a) Comparison of zero-angle energy spectra for H^+ resulting from the dissociation of 2-MeV H_2^+. The solid curve is for laser-induced dissociation. The dashed curve is observed for gas-induced collisional dissociation. The upper abscissa shows the correspondence between proton energy in the lab and the total energy released in the dissociation in the center-of-mass (COM) frame of the incident molecule. (b) Zero-angle proton energy spectrum for the laser-induced dissociation of 2-MeV H_2^+. The chained curve is the result of a calculation. The numbers above the points denote the vibrational quantum numbers. The solid curve is the measured photofragmentation spectrum of (a) after subtracting the background of gas-induced dissociation. The background is 2.1×10^{-5} of the measured gas-induced dissociation spectrum.

an important state-selection mechanism that could be useful in our studies of stereochemical structures of molecular ions.

c. Electron-Capture Phenomena

D. S. Gemmell, P. J. Cooney, N. Cue, A. K. Edwards, E. P. Kanter, I. Plesser, Z. Vager, and B. J. Zabransky

Joint distributions in energy and angle for H^0 fragments from the foil-induced dissociation of HeH^+ and H_2^+ molecular ions have revealed new information about the electron-capture process. It is now apparent that these fragments must arise as a result of electron capture to dissociative molecular states. In an extensive series of measurements, we have mapped out the dependence on beam energy and target thickness of these neutral-fragment distributions. It is hoped that through detailed model calculations of the magnitude of the Coulomb explosions as well as the observed orientation dependence of the yields for these neutral fragments, a more complete picture of the electron-capture processes involved will emerge.

d. Computer Simulations

D. S. Gemmell, I. Plesser, K. T. Cheng, E. P. Kanter, and M. F. Steuer

It has become clear that it is important for several aspects of the work outlined above that improved methods of simulating our experiments on the computer are necessary for a proper interpretation of the experimental data. We have this year incorporated several new features into our computer simulations of the foil-induced dissociations of diatomic molecular ions. These include the ability to use widely differing models for the electron-polarization wake trailing the fragment ions in the solid, a Monte-Carlo style multiple scattering correction, and the inclusion of post-foil electron capture into dissociative states.

e. Equipment Development

D. S. Gemmell, I. Plesser, M. F. Steuer, and B. J. Zabransky

Several projects were carried out during 1980 to improve existing experimental apparatus and to develop new equipment:

(1) Two fast gas avalanche detectors were designed and constructed. These detectors give us the ability to achieve subnanosecond timing with

dissociation fragments of only a few tens of keV energy, such as those that are observed in the breakup of heavy polyatomic molecular ions.

(2) The conversion to cryogenic pumps in our scattering chamber and flight tube sections of the beam line has improved our vacuum by a factor of two. This has greatly reduced the problem of charge-changing collisions of heavy-ion fragments in the long flight path between the target and the electrostatic analyzer.

(3) A new target rack was constructed which allows the use of seven solid targets as well as a newly designed gas jet. This gas jet, and the increased vacuum pumping speed mentioned above, has allowed us to increase the gas-target density in the beam by more than a factor of four over our old design.

(4) We have constructed and installed a gas cell between the two bending magnets at a point just before the beam is finally inflected into our beam line.

(5) The first stage of the Dynamitron upgrade has now been completed.

f. Stopping Power Measurements with Molecular Ions

D. S. Gemmell, E. P. Kanter, M. F. Steuer, and B. J. Zabransky

In a further effort to study the atomic-collision phenomena affecting the motion of fast ions in solids, we have begun a series of precision measurements of the stopping powers for homonuclear diatomic molecules. Preliminary findings so far have shown that contrary to observations with light and fast molecular ions, 1—2-MeV N_2^+ ions suffer an energy loss per atom that is lower than that for equal velocity N^+ ions.

X. BEAM-FOIL RESEARCH AND COLLISION DYNAMICS OF HEAVY IONS

INTRODUCTION

Our present fast ion-beam atomic physics program consists of three major parts, two of which are investigations in atomic structure, and one of which involves collision physics. Part (1) involves work mainly at the Argonne Tandem accelerator (30—100-MeV ion energy), and Parts (2) and (3) involve the Argonne Dynamitron accelerator (0.5—4-MeV ion energy), and a low-energy test-bench facility (0.02—0.15-MeV ion energy).

(1) Atomic Structure of Highly Stripped Few-Electron Ions. This work provides tests of ab initio relativistic and quantum electrodynamic calculations (both by ourselves and others—see contribution of K. T. Cheng, Sec. XIV). We have recently completed a set of precision measurements of the $1s2s\ ^3S$—$1s2p\ ^3P$ transitions of helium-like Si, S, and Cl in collaboration with A. E. Livingston at the University of Notre Dame. These results provide the first tests of multielectron contributions to QED theory. We have developed a position-sensitive detector technique to multiplex the observed spectra, which provides enhanced data collection rates.

Further ab initio calculations of transition energies in ions of 2—10 electrons are continuing, particularly in order to improve our estimates of relativistic and QED contributions.

(2) Atomic Structure of Other Ions. We have begun a search for excited states of negative ions which are sufficiently metastable against auger electron emission that they decay radiatively. We verified the first such emission from a doubly excited state of the negative lithium ion, and further work is now continuing with other ions.

We completed our work on the decay times and wavelengths in the one-electron Kr VIII spectrum. Some preliminary level-identification work has continued on the homologous spectra in Ne and Ar and the yrast spectra of the alkaline earth ions of the same species.

(3) Foil Interaction with Fast Ions. Work has continued in the study of optical polarization, both linear and circular, of the light emitted from fast ions passing through thin tilted carbon foils. The observations on the energy and tilt angle dependence for singlet states in helium have been completed, and the triplet states are now under study.

We have studied the total yield and alignment of excited atomic states from observations of the light yield from molecular ion projectiles incident on thin foils. The molecular interactions within the solid and at the final surface of the foil can be studied in this way.

a. Significance of Time-Reversal Symmetry for Time-Resolved Measurements of Hydrogenic and Other Atomic Observables

Gerald Gabrielse*

Time-resolved measurements of atomic observables are analyzed using a Liouville space formulation and a Hermitian unit tensor base. Each observable is labeled by a time-reversal quantum number, allowing exploration for the first time of the close relationship between time-reversal symmetry and the time evolution of atomic observables. The experimental reconstruction of atomic observables (at t = 0) from subsequent time-resolved measurements of the anisotropy and polarization of emitted electric-dipole photons is discussed.[1]

This work constitutes part of G. Gabrielse's Ph.D. thesis.

*Thesis student, University of Chicago, Chicago, Illinois.

[1]G. Gabrielse, Phys. Rev. A 22, 138 (1980).

b. Coherent Excitation of Hydrogen by a Thin Carbon Foil

H. G. Berry, T. J. Gay,* and R. Brooks

Continuing our observations of coherence of opposite parity states (e.g., 2s-2p states) produced in thin foil excitation of hydrogen (thesis work of G. Gabrielse, 1979), we have observed its variation for molecular-ion (H_2^+ and H_3^+) impact. The coherence rapidly disappears when a neighboring proton is within a few atomic diameters at the exit foil surface. These results help to set a distance estimate on the foil-hydrogen interaction. A detailed analysis shows that the 2s-2p coherence is affected by the long-range Coulomb field of the receding protons. Repulsive molecular states are formed at small internuclear distances near the foil surface.

*Thesis student, University of Chicago, Chicago, Illinois.

c. Molecular Effects on Lyman-α Emission in Beam-Foil Spectroscopy

R. L. Brooks and H. G. Berry

We have studied the total yield of Lyman α (emission from the 2p state) from atomic hydrogen after dissociation of fast H_2^+ and H_3^+ ions in thin carbon foils. All the observations show the same two-exponential decay of $H^0(2p)$ as a function of internuclear separation at exit surface, suggesting

two independent population mechanisms in the reconstitution region. Further analysis is in progress.

d. Molecular Effects in Beam-Foil Collision-Induced Alignment of He I

T. J. Gay,* H. G. Berry, and R. DeSerio*

We have measured the alignment of beam-foil collision-excited states of He I by bombarding carbon foils of various areal densities (1.3—110 $\mu g/cm^2$) with beams of He^+ and HeH^+. We have also measured the total light yield of several transitions in He I, He II, and H as a function of foil thickness using beams of HeH^+ ions. He I alignment decreases in all cases for the thinnest foils when molecular projectiles are used. Total light intensities generally increase with thin foils (small proton-He emergent internuclear separation), but a few decrease or are independent of foil thickness. We are able to explain several features of the alignment and intensity data in terms of formation of quasi-molecular states at or near the foil surface. Alignment reduction results from incoherent Stark mixing of the He I states in the field of the close proton.[1]

This work constitutes part of T. J. Gay's Ph.D. thesis.

*Thesis student, University of Chicago, Chicago, Illinois.

[1]T. J. Gay et al., Phys. Rev. A 23, 1761 (1981).

e. Energy Dependence of Alignment in Foil-Collision-Excited n=3 States of He I

T. J. Gay,* H. G. Berry, R. DeSerio,* H. P. Garnir, R. M. Schectman,† N. Schaffel,† R. D. Hight,† and D. Burns‡

We have measured the beam-foil collision-induced alignment of the $3p\,^1P$, $3p\,^3P$, $3d\,^1D$, and $3d\,^3D$ states of He I for He^+ beam energies between 30 and 1300 keV. The alignment of all four states is found to vary with beam current density as well as energy. The number of secondary electrons emitted per incident ion has also been measured as a function of foil temperature and beam energy. The rate of change of alignment and secondary-electron emission as a function of energy are correlated. The energy dependence of

*Thesis student, University of Chicago, Chicago, Illinois.

†University of Toledo, Toledo, Ohio.

‡University of Nebraska, Lincoln, Nebraska.

alignment may be understood in terms of simple impact-excitation kinematics.[1]

This work constitutes part of T. J. Gay's Ph.D. thesis.

[1] T. J. Gay et al., Phys. Rev. A 23, 1745 (1981).

f. Orientation and Alignment Parameters of Beam-Foil-Excited He I

H. G. Berry, R. L. Brooks, T. J. Gay,* R. DeSerio,* R. M. Schectman,† and E. H. Pinnington‡

The alignment and orientation produced by the tilted-foil excitation of He have been studied for a wide range of foil tilt angles and outgoing-atom velocities.

In particular, two quantum states of different orbital angular momentum ($3p\,^1P$ and $4d\,^1D$) were investigated and the results were compared with a number of previously proposed models. The results suggest contributions due to electron pickup and secondary electron as well as bulk effects. Additional work needs to be done to completely elucidate the detailed nature of the interaction.

Initial work on the $3p\,^3P$ state (at Argonne and the University of Edmonton, Alberta) shows rather different values of the same parameters as measured for the $3p\,^1P$ state. The results are almost independent of beam energy between 100 and 1000 keV (Fig. X-1).

*Thesis student, University of Chicago, Chicago, Illinois.

†University of Toledo, Toledo, Ohio.

‡University of Alberta, Edmonton, Alberta, Canada.

g. Quantum-Beat Studies of the ^3He Hyperfine Structure

V. F. Streif, R. L. Brooks, and H. G. Berry

The technique of beam-foil spectroscopy was used to study the hyperfine structure of ^3He by the observation of zero-field quantum beats. Experimental results were obtained for the $2p\,^1P$—$nd\,^1D$ transitions for $n = 3$ to 8, and preliminary results for $2s\,^3S$—$3p\,^3P$ and $2p\,^3P$—$4d\,^3D$. Theoretical predictions were made of the $nd\,^1D$ and $nd\,^3D$ hyperfine structure for $n = 3$ to 10. To within the experimental precision of ±2—4 MHz, we find good agreement with theory.

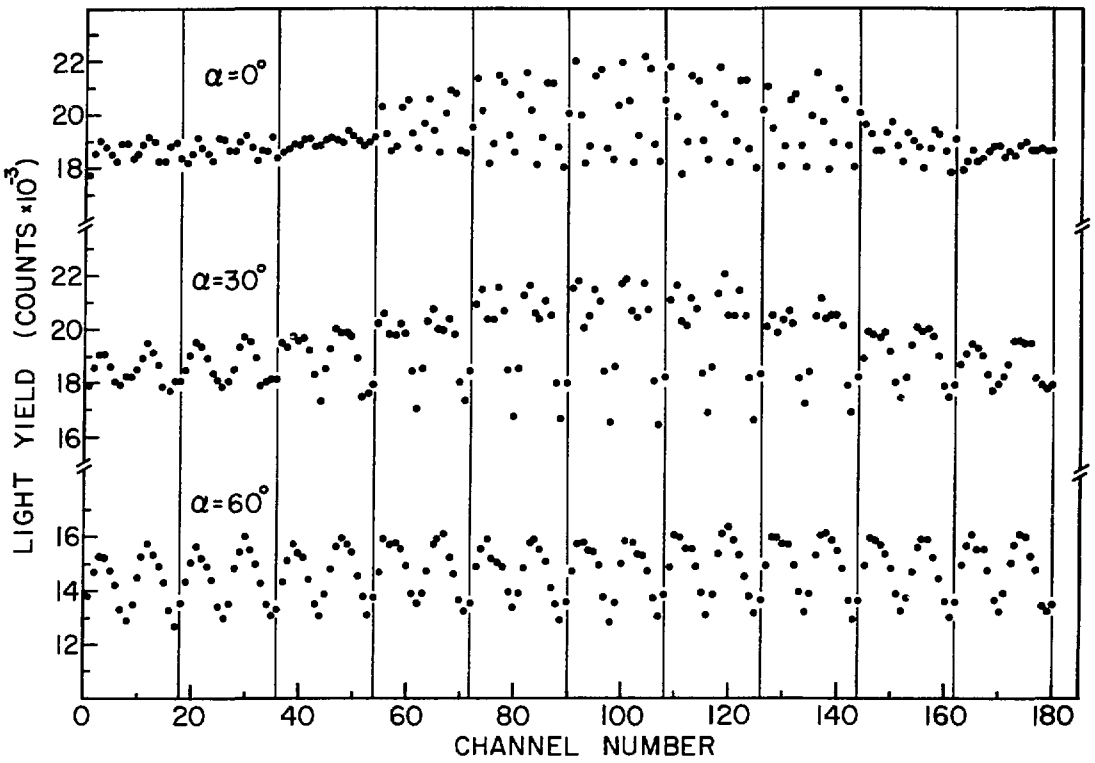

Fig. X-1. Polarization data observed for a set of foil tilt angles (α = 0°, 30°, 60°), each taken over one beat length of J = 1—2 of the 3889 Å, $2s^3S—3p^3P$, He I transition. The beam energy is 300 keV. The data consist of an 18 step rotation (20 degrees/step) of the phase plate at 10 equidistant positions along the beat.

h. Lamb Shift and Fine Structure of n = 2 in Helium-like Chlorine, Sulfur, and Silicon

R. DeSerio,* H. G. Berry, R. L. Brooks, A. E. Livingston,† and S. Hinterlong†

We have completed a set of precision wavelength measurements of the transitions $1s2s\ ^3S_1$—$1s2p\ ^3P_{0,2}$ of the helium-like ions of silicon, sulfur, and chlorine. We have calculated the wavelengths of these transitions for Z = 2—50 using a nonrelativistic 1/Z expansion, one-electron Dirac energies, plus relativistic corrections in first-order perturbation theory, plus one-electron QED or Lamb-shift corrections. By comparisons of

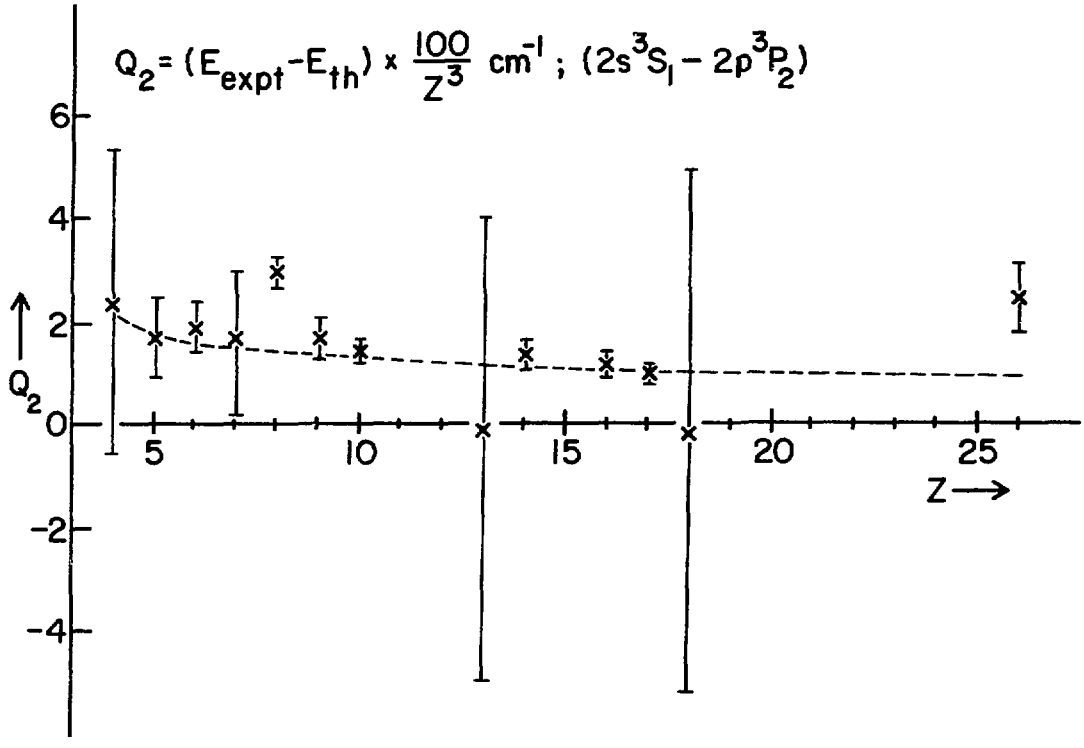

Fig. X-2. The difference between experiment and theory for the wavelength $1s2s\ ^3S_1$—$1s2p\ ^3P_2$. The Argonne measurements are those for Z = 14, 16, and 17. The dashed line is our calculation of 2-electron QED corrections.

*Thesis student, University of Chicago, Chicago, Illinois.

†University of Notre Dame, Notre Dame, Indiana.

measurements of Z = 4—26 and theory, we find a discrepancy which is approximately 0.015 Z^3 cm^{-1}. We have shown that this arises from a first-order screening correction to the one-electron Lamb shift and we have obtained an ab initio estimate of the correction (Fig. X-2).

This work constitutes part of R. DeSerio's Ph.D. thesis.

i. Radiation from the Negative Lithium Ion

R. L. Brooks, J. E. Hardis,* H. G. Berry, and L. J. Curtis†

Optical emission from negative ions formed by the beam-foil interaction had not been considered feasible prior to the recent theoretical assignment of the observed emission at 348.9 nm to the $1s2s2p^2\ ^5P—1a2p^3\ ^5S^0$ transition of Li^-. By alternately applying an electric field parallel and antiparallel to the beam, the intensity of the emitted light, as a function of distance from the foil, assumes a signature unique to the ionic charge. Using such a technique, we have confirmed that the radiation is emitted from the negative lithium ion. Supporting evidence is offered by the zero polarization measured with the foil tilted to 50°. In addition, we have established the cascade-free nature of the decay curve whose lifetime is 2.28 ± 0.05 ns. We have identified the transition in heavier isoelectronic ions.

*Thesis student, University of Chicago, Chicago, Illinois.
†University of Toledo, Toledo, Ohio.

j. Charge Changing Cross Sections of Xe^{n+} on Xe^{n+} (n = 1, 8)

H. G. Berry and M. Mazarakis*

A double accelerator system providing 20—100-keV singly-charged ions from each source was built, which incorporates magnetic-quadrupole focusing and magnetic-dipole momentum analysis to provide Xe^+ ion beams on target at ultrahigh vacuum of 10^{-9} torr. Beams were produced on target in November 1979. Successful measurements by Gilbody (Belfast) of the relevant Xe^{+1} cross sections prompted a reduction in effort on this experiment. The Physics Division (H. G. Berry) is now involved in only an advisory role. An alternative colliding beam experiment has been designed which uses

*Accelerator Research Facilities Division, ANL.

Xe^{1+} to Xe^{8+} beams of the 1.5-MV Dynamitron of the Argonne Heavy-Ion Fusion Facility. The original beam is split magnetically and the two separated beams are returned to a collision region at a variable crossing angle. The design has several improved signal-to-background advantages as well as allowing for high-charge-state cross-section measurements.

k. Position Sensitive Detector for UV Spectroscopy

R. DeSerio,* J. Hardis,* H. G. Berry, and R. L. Brooks

We have adapted a Galileo channelplate detector as a one-dimensional position sensitive detector at the exit focus of our UV spectrometer. Nonlinearities in the resistive anode provide a limit in the precision of the effective spectral dispersion curve obtained. Hence, we are investigating several techniques of digitized multianode arrays to reduce this problem. Work is in progress.

*Thesis student, University of Chicago, Chicago, Illinois.

XI. PHOTOIONIZATION-PHOTOELECTRON RESEARCH

INTRODUCTION

Our photoionization research program is aimed at understanding the basic processes of interaction of light with molecules, the electronic structures of molecules and molecular ions, and the reactions of molecular ions, both unimolecular and bimolecular. The processes and species we study are implicated in a wide range of chemical reactions, and are of special importance in outer planetary atmospheres and in interstellar clouds. Our work also provides fruitful tests for theories of electronic structure, which help in the evaluation of widely applicable models for multielectron systems. Most of this work is of a fundamental nature, but we also use the precise methods developed here to determine thermochemical quantities (heats of formation and ionization potentials) directly relevant in, e.g., reactions with ozone in the stratosphere and possible side reactions in a magnetohydrodynamic generator. Our experimental studies utilize five pieces of apparatus—two photoionization mass spectrometers and three photoelectron energy analyzers—each with special features.

(1) A three-meter normal-incidence vacuum-ultraviolet monochromator combined with a quadrupole mass spectrometer. This apparatus is capable of the highest resolution currently achieved in photoionization studies. It is also convenient for investigations of wavelength-dependent photoelectron spectra.

(2) A one-meter normal-incidence VUV monochromator mated with a magnetic-sector mass spectrometer. This apparatus has higher mass resolution, is less discriminatory in relative ion-yield measurements, and can be used to study metastable ions. Higher intensity for weak signals can also be achieved.

(3) Two cylindrical-mirror photoelectron-energy analyzers, which accept a large solid angle of photoelectrons, close to the "magic angle" of 54°44'. One has been extensively used for the determination of the photoelectron spectra of high-temperature species in molecular beams, and the other has on occasion been mated with the three-meter monochromator for studies of photoelectron spectra as a function of wavelength.

(4) A hemispherical electron-energy analyzer incorporated in a chamber which permits one to rotate the analyzer over a substantial fraction of 4π. This device is intended for angular-distribution measurements, and also enables us to study very-high-temperature species.

A new study, initiated during the past year, is the observation of dissociation fragments following the direct interaction of ultraviolet photons with molecular ions. For this purpose, an excimer laser has been utilized, together with the magnetic-sector mass spectrometer.

Two major technical changes and improvements have dominated our efforts this year. The first was the development of a multitask minicomputer. The purposes of this minicomputer are several-fold.

(1) To enable us to conduct at least two experiments simultaneously.

(2) To have the computer perform many of the tasks we have previously done manually.

(3) To monitor and record a wide range of experimental variables (several pressures, temperature, many potentials, light and ion intensities, wavelength), some of which were only occasionally observed previously.

(4) To optimize a complex set of experimental variables.

(5) To have an on-hand awareness of the progress of a long experiment. Previously such experimental data were deposited on magnetic tape and processed by the main ANL computer, with a turnaround time of approximately one day.

(6) Much of the data handling will also be performed by this computer.

(7) It should make possible an advanced stage of the laser photodissociation experiment described below.

The main computer interfacing is now completed, and its first test on the photoionization mass spectrometry experiment is about to be undertaken.

The second major innovation was the combining of an excimer laser with our existing magnetic sector mass spectrometer in order to directly study molecular-ion states and decomposition products. Much of our earlier work in vacuum ultraviolet photoelectron spectroscopy (PES) has resulted in a knowledge of the characteristics (energy, symmetry, etc.) of molecular ion states, and from photoionization mass spectrometry (PIMS), a knowledge of fragmentation products and their thresholds. By directly interacting laser beams with molecular ions, it is possible to obtain higher resolution, and hence finer detail (e.g., rotational analysis) of these states. Perhaps of greater interest to us is the possibility of studying molecular ions which have no molecular counterparts, and hence cannot be studied by PES and PIMS. Examples are Li_2Cl^+, H_3^+, HeH^+. Some experiments of this type have been performed elsewhere, but with much less energetic laser sources, typically ≤ 2 eV, which enable only the more weakly bound molecular ions to be studied. Our excimer laser can provide up to 6.45 eV, and hence can dissociate most molecular ions.

The disadvantage of this laser is that it is pulsed, with a duty fraction of 10^{-7}. Hence, intense ion beams must be generated, and coincidence counting techniques are required. During the past year we have solved both of these problems, and have observed the energy distribution of protons following dissociation of H_2^+ by 6.45-eV photons. Our present detection system is tedious, since it involves an exit slit and ion multiplier. To obtain a kinetic energy scan, we must laboriously repeat the photodissociation experiment for several settings of magnetic or electric fields, each corresponding to a particular kinetic energy of the proton. The next stage in the development of this experiment will be to replace the slit-multiplier combination with a multichannel plate and readout system, so that a range of kinetic energies can be simultaneously monitored. For the reading out and interpretation of the signals, the minicomputer will be essential.

Other technical progress included the completion of the photoionization mass-spectrometric studies of atomic iodine and atomic tellurium, and a preliminary photoelectron spectrum of atomic tellurium.

a. Photoionization of Open-Shell Atoms

J. Berkowitz, G. L. Goodman, and C. H. Batson

We have now completed the photoionization mass-spectrometric studies of atomic iodine and atomic tellurium. For the latter, we were able to find a better source (Cu_2Te) than the one we initially used (Ag_2Te), providing a larger atomic component in the vapor.

For iodine, most of the features in the autoionization resonance spectrum have been identified and assigned to several s- and d-like Rydberg series converging to the higher ionization limits $^3P_0$, $^3P_1$, $^1D_2$, and $^1S_0$ of the $5s^25p^4$ configuration.

For tellurium (see Fig. XI-1), we also observe autoionization resonance features assigned to s- and d-like Rydberg series converging to the higher ionization limits $^2D_{3/2}$, $^2D_{5/2}$, $^2P_{1/2}$, and $^2P_{3/2}$ of the $5s^25p^3$ configuration. In addition, a window resonance series and additional peaks have been assigned as converging to the $5s5p^4\ ^4P_{3/2}$ state of Te^+. In both elements, the d-like series exhibit anomalous resonance profiles similar to those in the heavier noble gases. At the present time, the theory (relativistic random phase approximation combined with quantum-defect theory) describing the resonance structure in the noble gases is in satisfactory accord with experiment, but is in its early stages for open-shell atoms such as iodine and tellurium. These experiments represent almost the only relevant data for the open shell halogens and chalcogens currently available to test the newer theories.

The paper describing our results has now appeared in Phys. Rev. A.

b. Determination of Molecular Ion Structures by Photoelectron Spectroscopy

G. L. Goodman and J. Berkowitz

A NATO Advanced Study Institute was conducted in October 1980 on the topic "Molecular Ions: Geometric and Electronic Structure." The Institute was organized and directed by J. Berkowitz and K.-O. Groeneveld (Frankfurt, West Germany).

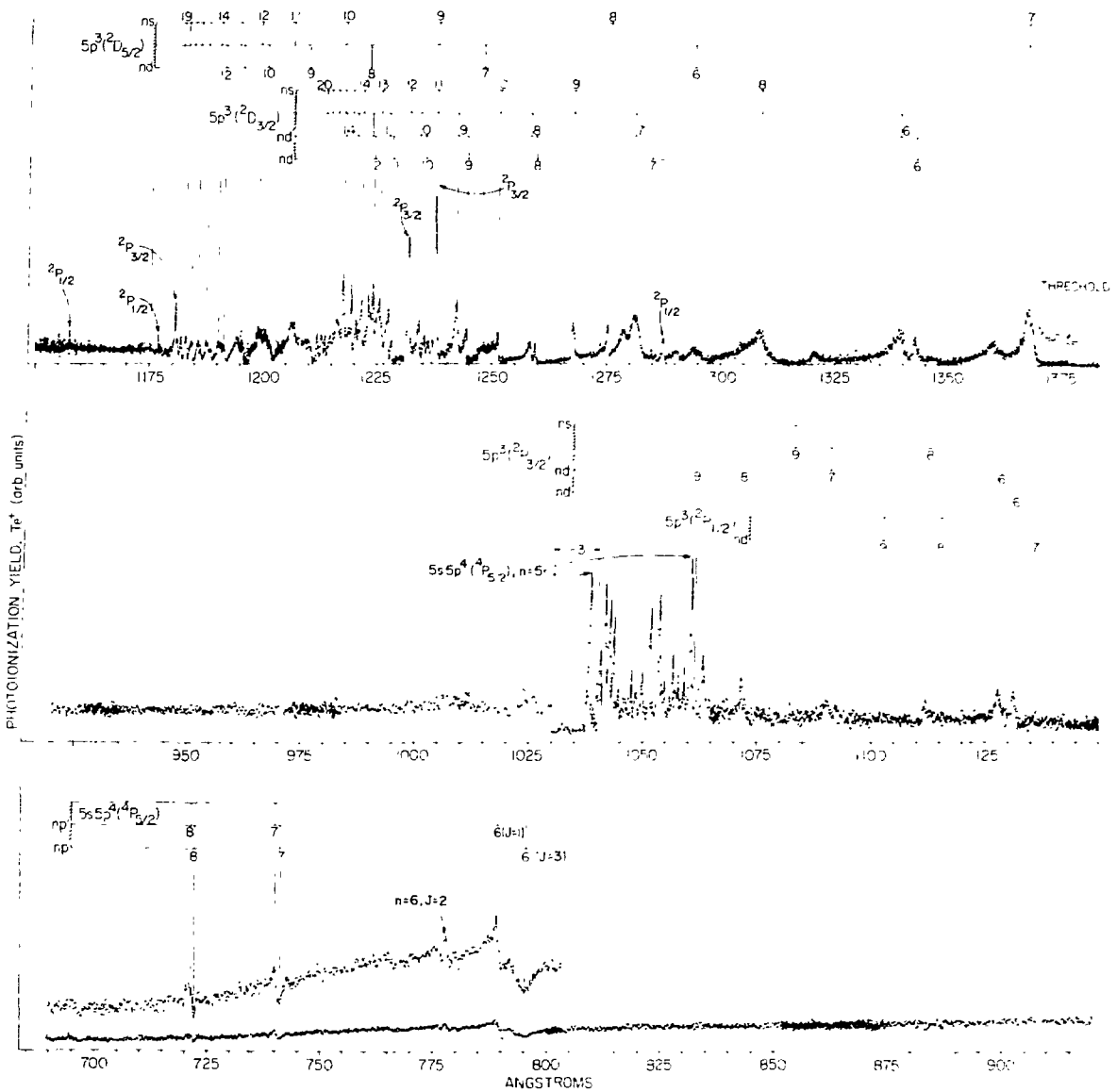

Fig. XI-1. Relative yield of Te^+ in the photoionization process $Te(^3P_2) + h\nu \rightarrow Te^+ + e$. Identified Rydberg series and their convergence limits are indicated. The running Rydberg indices are chosen to correspond to the convention adopted by Moore, i.e., $n \simeq n^* + 4$ (ns series) and $n \simeq n^* + 2.5$ (nd series). For the $5s5p^4np$ series, $n \simeq n^* + 3.5$, conforming to the calculations of Cheng and Kim.

One very important means of determining the structure of molecular ions is available to us through photoelectron spectroscopy. In particular, the geometric structures of molecular ions can be deduced from photoelectron spectra by making use of Franck-Condon analyses of the spectra if the geometric structure of the progenitor neutral molecule is known. We have reviewed recent work making use of harmonic and Morse approximations for diatomic molecules, and extended them to include conditions where a significant Boltzmann distribution of initial states exists. We find that it is still

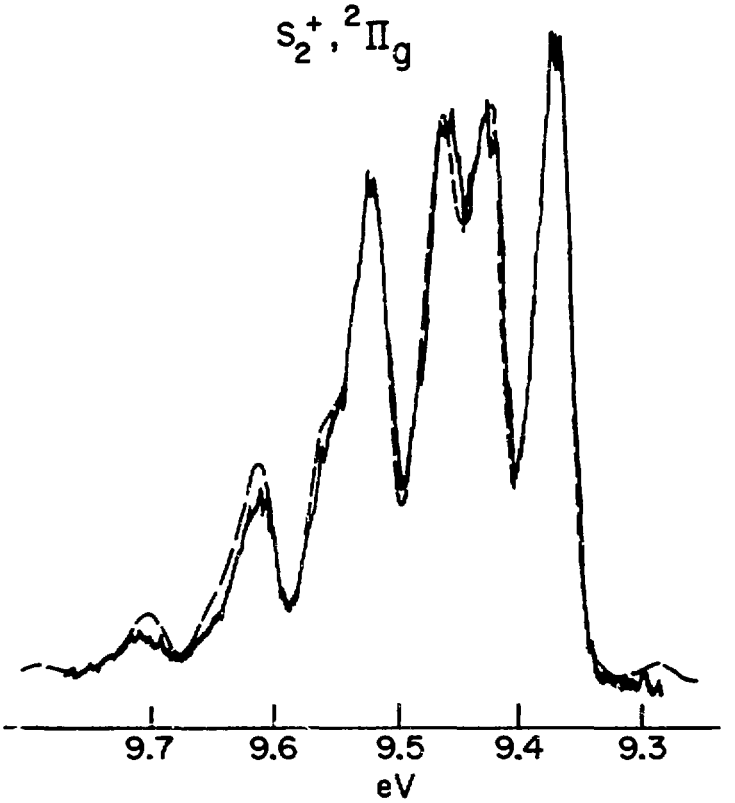

Fig. XI-2. To calculate $\underset{\sim}{L}^i$, one must know or assume $\underset{\sim}{G}^i$ and $\underset{\sim}{F}^i$. The corresponding $\underset{\sim}{G}^n$ and $\underset{\sim}{F}^n$ are usually known. $\underset{\sim}{F}^i$ is usually assumed to be diagonal, with some elements corresponding to observed frequency intervals in a progression in the ionic state, and others (not observed) chosen identical or similar to ground-state elements. $\underset{\sim}{G}^i$ can be taken to be identical to $\underset{\sim}{G}^n$ for an initial calculation, which results in $\underset{\sim}{L}^i$ and, hence, a new geometry. The new geometry defines a revised $\underset{\sim}{G}^i$.

possible to deduce geometric structures in such studies, even if the photoelectron spectrum is not vibrationally resolved. Several applications are given, and where possible, comparisons are made with optical data. The photoelectron spectrum of S_2 (Fig. XI-2) displays resolved or partially resolved vibrational and spin-orbit structure. The calculated spectrum is seen to provide a very good fit to the experimental curve. The parameters for best fit yield an internuclear distance, vibrational frequency and spin-orbit separation for S_2^+.

The application of Franck-Condon analysis to polyatomic molecules is more difficult. We summarize various approaches to the problem, including methods that rely solely on experimental data and others which simulate the experimental spectrum by using ab initio calculations. The methods are quantitatively compared in several instances. Finally, we summarize our current knowledge of polyatomic molecular ion structures as determined by Franck-Condon methods.

This work will be published in a book containing the invited lectures at the NATO Institute, sometime in 1981.

c. Dissociation of Molecular Ions with UV Lasers

R. Kutina and J. Berkowitz

Our knowledge of the energies, states and geometries of molecular ions is derived from a variety of sources, including PES, emission spectroscopy and some recent techniques involving lasers. One of the latter methods involves the interaction of a tunable laser beam with a beam of molecular ions. At photon energies coincident with the difference in energy between upper and lower state, photoabsorption will occur. Since the molecular ion beam is too tenuous, the attenuation of the laser light is too small to observe. If the upper state is predissociated, however, an ionic product of different mass will be produced and one can follow the photoabsorption process indirectly by monitoring the fragment. The high resolution of a tunable laser enables one to observe detailed features, such as rotational fine structure. However, currently available lasers that are intense and tunable are limited in photon energy to $\sim$2.5 eV, which limits this method to selected transitions in a few molecular ions.

We have been experimenting with an excimer laser with the goal of extending such studies to higher photon energy, and thereby extending significantly the general applicability of the method. Our excimer laser can generate several lines, with energies up to 6.45 eV. This higher energy is sufficient to photodissociate most molecular ions. There are a few tricks we can use to provide tunability. At the present time, we have been concerned with the feasibility of the method. Toward this end, we have generated a fairly intense molecular ion beam by electron impact in our magnetic sector mass spectrometer. It is intercepted by the laser beam in the field-free region between electrostatic acceleration and magnetic deflection. If dissociation occurs, the fragment ion should appear at a new mass given by $m^* = (m_f)^2/m_p$, where m_f, m_p are the nominal masses of fragment and parent ion. Any breadth to the m^* peak in excess of that in m_p is attributed to kinetic energy released in the dissociation. Since we observe primarily the longitudinal component of fragment velocity, we can anticipate two peaks, corresponding to forward and backward recoil of the fragment. The interval between these peaks is a measure of the most probable kinetic energy release. For polyatomic ions, there will be additional breadth due to partitioning of the excess energy among vibrational and rotational, as well as translational modes. Hence, it is important to measure the entire distribution.

At the present time, we have succeeded in measuring H^+ from the dissociation of H_2^+ with 6.45-eV photons. This system has been well studied theoretically. The transitions induced are from selected vibrational levels of H_2^+ in its ground state ($X^2\Sigma_g^+$), primarily $v'' = 2$, to the repulsive $2p\sigma_u$ state. The laser is pulsed at 10—20 Hz and the pulse duration is 10 ns, providing a duty factor of only 10^{-7}. The laser light pulse is detected and triggers a time to amplitude converter (TAC). The mass spectrometer is set to $m^* = 1/2$, and the ion signal terminates the TAC. The pulse-height distributions are displayed on a multichannel analyzer. A peak appearing with the expected time delay is evidence of photodissociation. At the present time, it is necessary to scan the kinetic energy spectrum by incrementally resetting the mass spectrometer to nearby nominal masses and mapping out this distribution point by point. Replacing the exit slit and multiplier of the mass spectrometer with a multichannel plate and readout system should increase the rate of data acquisition by at least an order of

magnitude and improve statistics, since the irreproducibility of successive laser pulses will no longer be a factor.

The molecular ions of primary interest to us at the present time are those whose properties are not accessible by PES and most other techniques, such as HeH^+, H_3^+, Li_2Cl^+, and others which have no neutral molecular analogs.

XII. HIGH-RESOLUTION, LASER-RF SPECTROSCOPY WITH ATOMIC AND MOLECULAR BEAMS

INTRODUCTION

The laser-rf double-resonance technique has been used to make extensive high-precision measurements of the spin-rotation and hyperfine interactions in several alkaline-earth monohalides. These radicals can be regarded, to a very good approximation, as consisting of a single electron outside filled p shells in the metal and halogen ions. They are therefore closely analogous to alkali atoms, and should be among the simplest diatomic molecules to understand in detail. Unfortunately, however, even features as basic as the hyperfine structure (hfs) of the molecular ground state are difficult to understand even qualitatively. These molecules are of considerable current interest, and a great deal of research is being done in laboratories around the world to attack these problems.

The molecular-beam, laser-rf, double-resonance technique used here is particularly well suited for such studies because (a) its precision ($\sim$1 kHz) is several thousand times that of the other methods commonly used (Doppler-free Lamb-dip laser spectroscopy, for example), and (b) by focusing on the lower level of an optical transition, it breaks the correlation between upper and lower levels that normally clouds interpretation of the hfs. These advantages have made it possible for us to observe details unseen elsewhere, and generally to obtain data unique in quality for several of these molecules. The work is continuing and is a prerequisite to the kind of ab initio calculations necessary to understand this class of molecule in some detail.

a. High-Precision Laser-rf Double-Resonance Spectroscopy of the $^2\Sigma$ Ground State of CaF

W. J. Childs and L. S. Goodman

This paper[1] describes in detail the work published[2] in 1979 in Physical Review Letters on the $v = 0, X^2\Sigma$ molecular ground state of CaF. The study constitutes the first high-precision systematic investigation of the N dependence of the spin-rotation and hfs interactions in a diatomic molecule.

---

[1] W. J. Childs and L. S. Goodman, Phys. Rev. A 21, 1216 (1980).

[2] W. J. Childs and L. S. Goodman, Phys. Rev. Lett. 44, 316 (1980).

b. Precise Determination of the v and N Dependence of the Spin-Rotation and Hyperfine Interactions in the CaF $X^2\Sigma_{1/2}$ Ground State

W. J. Childs, G. L. Goodman,* and L. S. Goodman

This work[1] extends our earlier study of the v = 0, $X^2\Sigma$ state to higher vibrational levels. Precise measurements of the spin-rotation and hfs splittings are reported for $0 \leq v'' \leq 4$, and $1 \leq N'' \leq 119$, and the results are analyzed in detail with the standard Hamiltonian. The spin-rotation and hyperfine parameters are expanded in Dunham-type double series in powers of $v + \frac{1}{2}$ and $N(N + 1)$ and least-squares-fitted values are found in this way for 14 of the coefficients, more than achieved previously for any other diatomic molecule. The precision of the present technique makes it possible to determine the magnetic Frosch-Foley dipole-dipole hfs parameter c to 1 part in 15 000; this is the first measurement of c for any alkaline-earth monohalide and is an important number for testing the ab initio theory. Included in our paper is an extensive ab initio (self-consistent charge discrete variational Hartree-Fock-Slater, or X_α) calculation. It is shown that although the theory can account for the lower-order [in $v + \frac{1}{2}$ or $N(N + 1)$] coefficients to within about 20%, it is off by large factors for the higher-order coefficients. The state of the existing theory is therefore inadequate and more data on related radicals will be needed as a guide for further development of the theory. Figure XII-1 shows the average hyperfine structure plotted as a function of N for several values of v. The hfs had never been observed in the free molecule before the present work.

*Consultant, Communaissance, Downers Grove, Illinois.

[1]W. J. Childs, G. L. Goodman, and L. S. Goodman, J. Mol. Spectrosc. 86, 365 (1981).

c. Radio-Frequency Optical Double-Resonance Spectroscopy of SrF: The $X^2\Sigma$ State

W. J. Childs, L. S. Goodman, and I. Renhorn

This work,[1] performed at Argonne with the collaboration of I. Renhorn of the University of Stockholm, presents high precision spin-rotational and hfs results for SrF analogous to those achieved earlier for CaF. In addition

[1]W. J. Childs, L. S. Goodman, and I. Renhorn, J. Mol. Spectrosc., in press, 1981.

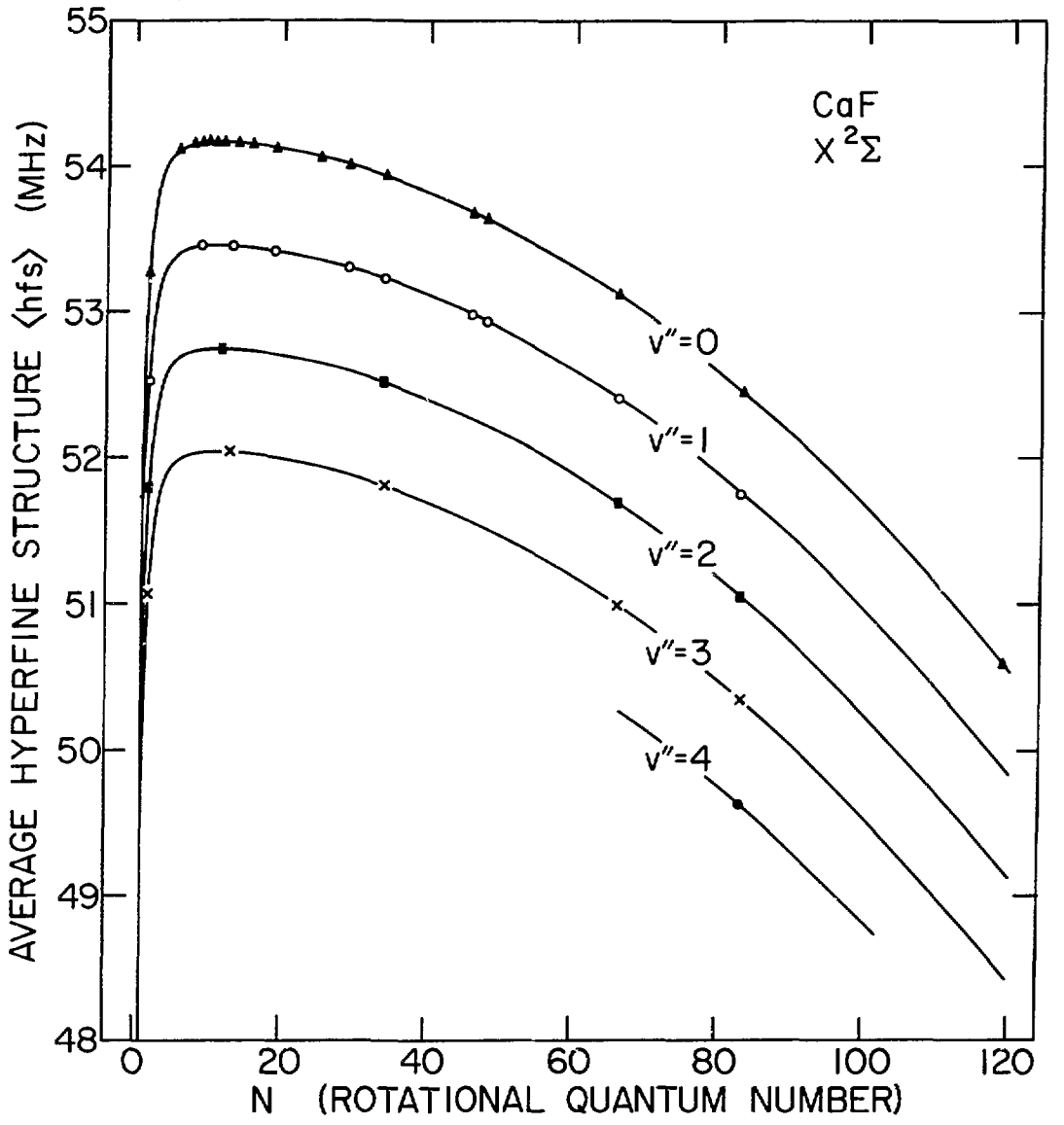

Fig. XII-1. Rotational (N) and vibrational (v) dependence observed for the average hyperfine splitting of the J=N+½ and J=N-½ levels of the $X^2\Sigma^+$ molecular ground state of the CaF radical. No previous observations have been reported for the hfs of the free CaF radical.

to broadening the base of accurate data for alkaline-earth monohalide hfs, the SrF work had two special features. Firstly, measurements were made in both ^{88}SrF and ^{86}SrF, and the observed dependence of the various parameters on isotopic mass was investigated and found to agree closely with the theory. Secondly, by combining the precisely measured hfs splittings in the $X^2\Sigma$ state with the hfs observed in Doppler-free laser-induced $B^2\Sigma$—$X^2\Sigma$ fluorescence lines, rough values for the hfs splittings in the excited B state were obtained.

d. Hyperfine and Spin-Rotational Structure of CaBr $X^2\Sigma$ (v = 0) by Molecular-Beam Laser-rf Double Resonance

W.J. Childs, David R. Cok, G. L. Goodman,* and L. S. Goodman

This work[1] extends the double-resonance studies of the calcium monohalides from CaF to CaBr; precise values are shown in Table XII-I for the spin-rotation and hyperfine parameters in both $Ca^{79}Br$ and $Ca^{81}Br$. The value given for the dipole-dipole Frosch-Foley parameter c is the first such measurement for CaBr, and that for the quadrupole strength eqQ is the first accurate value in any calcium monohalide; the conventional techniques do not have the resolution to measure these quantities. The isotopic dependence of the parameters is in good agreement with the theory. The new values for b, c, and eqQ will be particularly valuable for distinguishing between the two mechanisms suggested for the hfs, namely: (1) configuration-interaction mixing of a little CaBr with the dominant Ca^+Br^- and (2) spin-polarization of the Br^- orbitals by the unpaired outer electron, as suggested by Bernath and Field. New ab initio spin-polarized calculations are in progress here to test mechanism (2) to the extent possible with what little data so far exists. It is planned to make similar studies of other calcium monohalides in order to establish trends to check theoretical predictions. Typical laser-rf, double-resonance spectra are shown in Fig. XII-2.

---

*Consultant, Communaissance, Downers Grove, Illinois.

[1]W. J. Childs, David R. Cok, G. L. Goodman, and L. S. Goodman, accepted by J. Chem. Phys., 1981.

TABLE XII-I. Parameter values determined for the $X^2\Sigma$ state of $Ca^{79}Br$ and $Ca^{81}Br$ from the present research. Columns 2 and 3 give the least-squares fit values for the parameters identified in column 1 when the standard Hamiltonian is fitted to the data. The experimental and theoretical ratios of the parameter values found for $Ca^{79}Br$ to those for $Ca^{81}Br$ are given in columns 4 and 5, while the final column gives the differences between the observed and theoretical ratios in units of one standard deviation.

Parameter	$Ca^{79}Br$ (exp) (MHz)	$Ca^{81}Br$ (exp) (MHz)	79/81 (exp)	79/81 (theor)	diff/σ (exp - theor)
γ_0	90.72452(9)	89.97275(10)	1.008356(2)	1.008354	1.0
γ_1	$-9.111(3) \times 10^{-5}$	$-8.958(4) \times 10^{-5}$	1.0171(6)	1.0168	0.5
γ_2	$-7.12(17) \times 10^{-11}$	$-7.09(28) \times 10^{-11}$	1.00(5)	1.03	-0.6
b_0	95.3286(9)	102.7637(11)	0.92765(2)	0.92765	0.0
b_1	$-2.054(3) \times 10^{-4}$	$-2.197(3) \times 10^{-4}$	0.9349(20)	0.9355	-0.3
c_0	77.620(7)	83.660(9)	0.92780(14)	0.92770	0.7
c_{I_0}	0.0041(2)	0.0044(2)	0.93(7)	0.94	-0.1
$(eqQ)_0$	20.015(7)	16.714(6)	1.1975(6)	1.1971	0.7
$(b + c/3)_0$	121.202(3)	130.650(3)	0.92768(4)	0.92770	-0.5

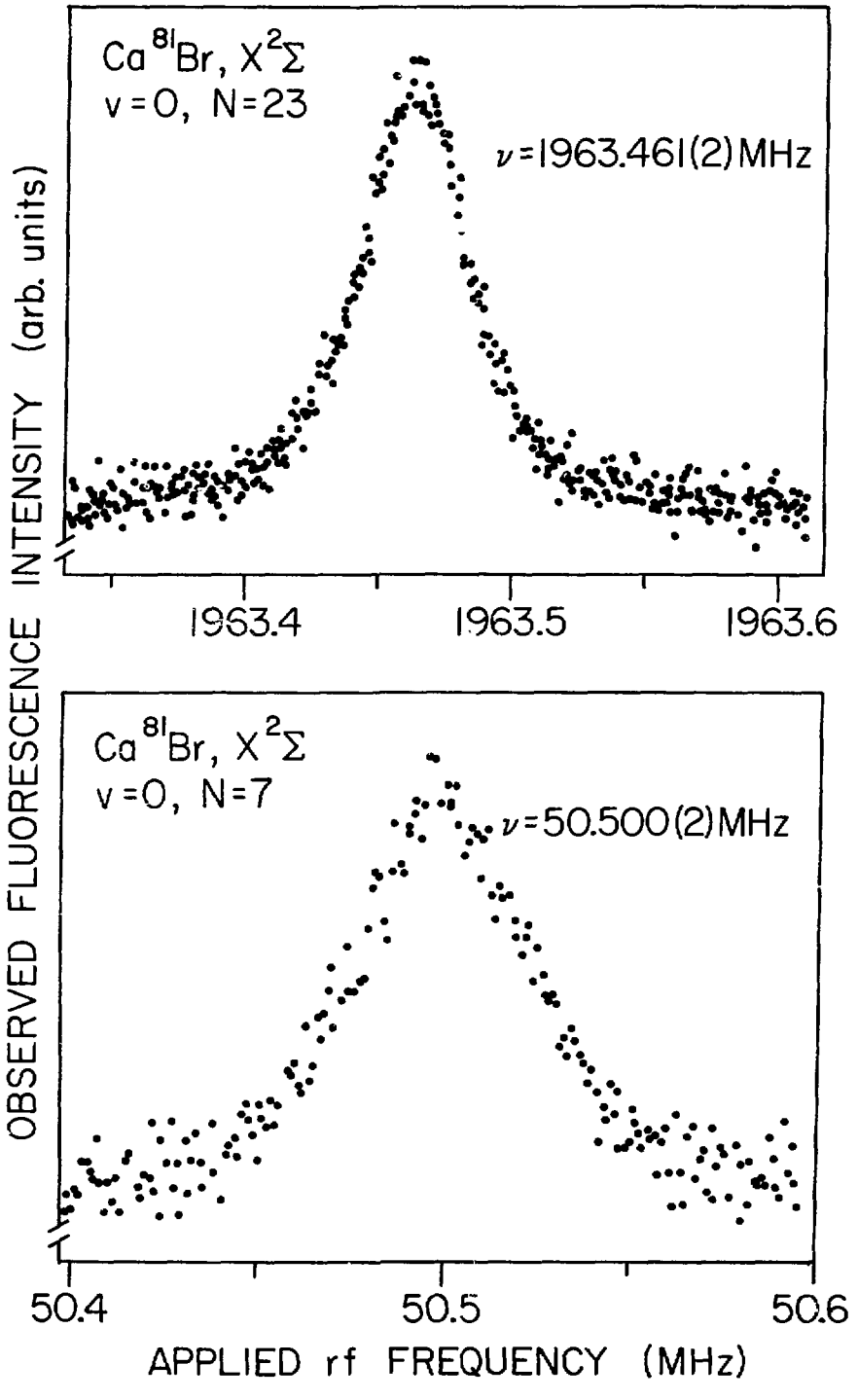

Fig. XII-2. Laser-rf, double-resonance spectra observed in the $X^2\Sigma^+$ (v=0) molecular ground state of $Ca^{81}Br$. For the upper curve, $\Delta F = \Delta J = 1$, and for the lower, $\Delta J = 0$ and $\Delta F = 1$.

e. Determination of Dipole and Quadrupole hfs in the Excited $B^2\Sigma$ State of $Ca^{79}Br$ and $Ca^{81}Br$

W. J. Childs, David R. Cok, and L. S. Goodman

The precise knowledge of the CaBr $X^2\Sigma$ ground-state hfs intervals from double-resonance studies is here supplemented with measurements of the hfs splittings of Doppler-free $B^2\Sigma$—$X^2\Sigma$ optical transitions to obtain[1] the hfs splittings in the excited $B^2\Sigma$ state of CaBr. These intervals are then fitted with the conventional $^2\Sigma$ molecular Hamiltonian to yield the hfs parameters for the B state to about 5%. The value found for the quadrupole hfs parameter eqQ is much larger than that predicted by Bernath and Field on the basis of their spin-polarization model. Nevertheless, a definitive test of the model will require hfs data on other calcium monohalides (in excited as well as ground states), and in addition more sophisticated ab initio calculations.

[1]W. J. Childs, David R. Cok, and L. S. Goodman, accepted by Can. J. Phys., 1981.

f. Double Resonance, Fluorescence Spectroscopy and hfs in Pr I

W. J. Childs and L. S. Goodman

A small amount of additional data was collected in our continuing study of the hfs of low atomic levels of Pr I. A paper describing the present status of the praseodymium work has been prepared.[1]

[1]W. J. Childs and L. S. Goodman, accepted by Phys. Rev. A, 1981.

XIII. MÖSSBAUER EFFECT RESEARCH

INTRODUCTION

The effort during the last year has been mainly the study of gamma-ray quantum beats and their applications. Quantum beats are an individual photon effect, in which the photon amplitude is modulated at a radio frequency. This is obtained by filtering frequency-modulated quanta through a resonant medium. The frequency modulation is produced by vibrating a Mössbauer source piezoelectrically. The amplitude modulation is detected as a periodic alteration in the counting rate. Its harmonic composition is extremely sensitive to the energy difference between the gamma-ray energy and that of the resonance in the medium. This is the basis for application of quantum beats.

During 1980, work was done on the theory of the process and on improvements in the technique.

a. Advances in the Theory of Quantum Beats of Recoil-Free Gamma Radiation

J. E. Monahan, H. E. Stanton, and G. J. Perlow

The theory treats the photon amplitude semiclassically and the absorption as an optical process in a resonant medium. In the 1979 publication of Monahan and Perlow, the intensity $I(\Delta E,t)$ that describes the time and frequency dependence of the count rate was given in terms of a double sum over sideband indices of the product of a time-dependent and an energy-dependent summand. The latter was an infinite series of which the lowest order term was relatively simple and higher terms increased in complexity. It was felt that the essential properties of the theory were contained in the lowest order term and the effect of subsequent terms served to take thickness effects into account. Theoretical work and computer simulation were carried out to test this hypothesis.

b. Improvements in the Techniques of Frequency Modulation

L. E. Campbell and G. J. Perlow

A foil containing a source of Mössbauer radiation is vibrated by transmitting ultrasound from a piezocrystal through glycerine to the active surface of the foil. The velocity spectra of the foil at various frequencies and amplitudes of the rf driving voltage are obtained and analyzed.

A pure Bessel-function dependence of the sideband intensity would represent the ideal case in which all active elements in the foil move in phase. This is not found. Curve fitting is used to determine other components of the motion.

XIV. THEORETICAL ATOMIC PHYSICS

INTRODUCTION

Our studies on the effect of relativity and electron correlation in atomic processes consist of five major parts, three of which involve case studies of atomic processes in the discrete, continuous and autoionizing regions of the spectrum, and two of which deal with development of new relativistic many-body theories for atomic problems.

(1) Atomic Structure of Neutral Atoms and Highly Stripped Ions. In the Be sequence, core-excited $(1s2s2p^2)^5P$ and $(1s2p^3)^5S^0$ states are the lowest quintet states in the spectrum and are metastable against autoionization. They are strongly affected by relativity and correlation effects, and provide important tests of relativistic many-electron atomic theory. The emission line $^5S^0-^5P$ is observed in beam-foil spectra and is in good agreement with theory. Using a multiconfiguration Dirac-Fock (MCDF) technique, we are studying the forbidden transition $(1s2s2p^2)^5P-(1s^22s2p)^3P^0$ as the dominant decay mode of the ^5P states. Preliminary results show that these lines should be observable in beam-foil experiments.

The MCDF technique is also applied to excited states of heavy atoms. These studies can aid in the identification of spectral lines, for example, those in resonance regions of Te and I where precision measurements are available.

Experimental measurements of hyperfine structures in heavy atoms have provided important insight into the dynamics of electron correlation. New experiments on the hyperfine structures of stripped ions are now possible with advances in technique. Our calculations can provide valuable comparisons of the hyperfine integrals with experiment.

(2) Low-Energy Atomic Photoionization. Low-energy atomic photoionizations are known to be sensitive to electron correlations. With advances in experimental technique, relativistic effects also show up in refined details of photoelectron spectroscopy. With the relativistic random phase approximation (RRPA), we can systematically examine effects arising from interchannel couplings, core polarizations, and relativity. The RRPA has been applied to rare gas atoms with great success. We are now studying photoionization of Mg, Zn, Cd, and Hg atoms and inner shell photoionizations of the 4d electron in Xe and Ba. Comparison with experiment will provide further evidence on the validity and limitation of the RRPA.

(3) Rydberg Series and Autoionization Resonances. An ab initio method of analyzing autoionization spectra is achieved by combining the RRPA with the multichannel quantum defect theory (MQDT). Results on Beutler-Fano resonances are in excellent agreement with experiment. We are studying window resonances arising from inner shell excitations $ns \rightarrow n'p$ in rare gas atoms. Extension of this method to the study of Rydberg series in the Ne sequence is also in progress. The main advantage of this approach

is that we can avoid the problem of generating wave functions for high Rydberg states, and obtain accurate ab initio data on energy levels and oscillator strengths for the whole series simultaneously.

(4) Generalization of the Relativistic Random-Phase Approximation. The RRPA is known to include dominant correlation effects in atomic processes and is very successful in dealing with closed shell atoms. Past attempts in extending this method to open shell systems have not been very successful. Starting from the time-dependent variational principle, we arrive at a set of generalized RRPA equations which reduce to the usual multiconfiguration Dirac-Fock equations in the absence of any external field. We are applying this new technique, the multiconfiguration relativistic random-phase approximation (MCRRPA), to the discrete excitation $(2s^2)\,^1S—(2s2p)\,^1P^0$ in Be-like ions. Preliminary results show great improvements over the corresponding RRPA values. More studies of this method will be carried out.

(5) Foundation of the Relativistic Theory of Many-Electron Atoms. In spite of the success of relativistic theories such as the MCDF in calculating relativistic effects in atomic systems, the basic many-electron Dirac-Coulomb Hamiltonian actually has intrinsic theoretical problems. Recently, the difficulty has been partially overcome, mainly through the efforts of Mittleman and Sucher, by deriving a new many-electron Hamiltonian from quantum electrodynamics (QED). Based on this new approach, we are working on a practical way of calculating atomic structure, with the capability of correcting residual errors systematically. Along with advances in experimental measurements of spectral lines, we should be able to make precision tests of atomic theories and QED in few-electron systems.

a. Radiation from the Negative Lithium Ion

R. L. Brooks, J. E. Hardis,* H. G. Berry, L. J. Curtis,† K. T. Cheng, and W. Ray

We confirm that the 3489 Å line observed in beam-foil-excited lithium spectra originates from the $(1s2p^3)\,^5S^0—(1s2s2p^2)\,^5P$ transition as suggested by Bunge. This is the first time that observed line radiation has been ascribed to a negative ion. The transition has also been identified in heavier ions along the isoelectronic sequence.

*Thesis student, University of Chicago, Chicago, Illinois.

†University of Toledo, Toledo, Ohio.

b. Autoionization Resonances in Atomic Tellurium

K. T. Cheng

In the autoionization spectrum of atomic Te observed by Berkowitz and Goodman, there are several series of resonances which are not clearly identified. We have calculated excitation energies and transition amplitudes

for core-excited states of Te and confirmed that these lines are $5s5p^4np$ ($n = 5, 6, 7, \cdots$) resonances converging to the $(5s5p^4)\ ^4P_{5/2}$ threshold. The calculated quantum defects of these lines are in good agreement with experiment.

c. Spin Polarization of Photoelectrons

K. T. Cheng, K.-N. Huang,* and W. R. Johnson†

Spin polarizations of photoelectrons reveal important dynamic effects of photoionization. We calculate spin polarizations of outer ns- and np-shell photoelectrons in rare gas atoms using the RRPA. Results are in excellent agreement with experiment. Our study also shows that totally polarized electrons can be produced from photoionizations of the xenon 5p shell by polarized light. This is potentially a new source for producing polarized electrons.

d. Beutler-Fano Resonances

W. R. Johnson,† K. T. Cheng, K.-N. Huang,* and M. LeDourneuf‡

We employ the MQDT in analyzing Beutler-Fano autoionization resonances in rare gas atoms, with ab initio quantum defect data obtained from the RRPA. Theoretical resonance profiles are in excellent agreement with precision measurements by Berkowitz and Eland. We also calculate angular distributions and spin polarizations of photoelectrons in the resonance region. Studies along the Xe isoelectronic sequence show a decreasing strength in the coupling between open and closed channels.

e. Spectroscopy of Few-Electron Ions

K. T. Cheng, Y.-K. Kim* and J. P. Desclaux§

We have calculated the low-lying spectra of few-electron ions isoelectronic to the first row atoms (up to 9 electrons). Comparison with precision measurements provides important tests of relativistic many-electron

*Radiological and Environmental Research Division, ANL.

†University of Notre Dame, Notre Dame, Indiana.

‡Observatoire de Paris, Mendon, France.

§Centre d'Etudes Nucleaires de Grenoble, Grenoble, France.

theory and QED. Allowed and forbidden transitions between low-lying excited states have also been calculated. These data are urgently needed in controlled-fusion research.

APPLIED PHYSICS

INTRODUCTION

Although the main business of the Physics Division is basic research, we are also conducting a research program that is dedicated primarily to applied research goals. This involves the Interaction of Energetic Particles with Solids (M. Kaminsky). This applied research is carried out in conjunction with the basic research studies from which it evolved.

XV. INTERACTION OF ENERGETIC PARTICLES WITH SOLIDS

INTRODUCTION

This research project is designed to study specific atomic and molecular phenomena that occur when energetic ions (keV—MeV range) interact with both bulk and surfaces of solids. Particularly, fundamental studies of the mechanisms underlying (a) the release of atomic and molecular species from solid surfaces, and (b) the changes in the surface topography and in the microstructure of the implant region under energetic-particle impact are being conducted.

One main goal of these studies is to determine how well-characterized surface regions of lattices with (1) a defined low degree of lattice damage and low gas content, or with (2) a high degree of lattice damage and high gas content caused by trapping of incident ions (e.g., H^+, D^+, $^4He^+$) will affect the basic mechanisms of such fundamental atomic processes as ion/atom reflection, secondary ion and electron emission, atom/molecule release by sputtering, and energy-loss mechanisms and charge states of particles penetrating through a lattice. Information of this type is practically nonexistent for light-ion bombardment of solids. However, such information is of significant importance for (a) a better understanding of atomic collision processes, (b) analysis of older data which showed significant scatter and may have been influenced by lattice damage and incident-ion trapping, and (c) for such practical applications as fusion-plasma-impurity control and accelerator technology.

Furthermore, we are conducting studies in direct support of the national fusion-power development program (supported by OFE/DOE and Princeton University). These studies have the following four goals: (1) To identify and develop a sufficient understanding of the processes leading to plasma contaminant release, surface damage and erosion of candidate beam dump, beam limiter and first-wall materials in order to allow the selection of optimum designs. (2) To generate data on plasma contaminant release yields and the degree of surface damage and erosion of low-Z coatings and medium-Z claddings under irradiation conditions that will be meaningful for an assessment of their use for vacuum vessels, armor plates, beam limiters and calorimeters in both near-term and long-term machines. (3) To search for solutions for the control and reduction of plasma contaminant release and surface damage and erosion processes. (4) To conduct cooperative studies with major plasma laboratories in the USA and abroad in order to help in the identification of some of the major sources for, and types of plasma contaminants and surface erosion in existing plasma devices and in the next generation of devices. Some work in pursuit of these goals was carried out with Princeton's Plasma Physics Laboratory, Lawrence Livermore Laboratory and with the Kurchatov Institute in Moscow.

Finally, experiments will be designed for a search of molecular ions formed by the <u>simultaneous</u> interaction of two independent ion beams

(e.g., H^+ and D^+ in the 10-keV—100-keV range) with solid films. Transmission and backscattering using both monocrystalline and polycrystalline films, will be studied.

The experiments are carried out with well-characterized surfaces of solids which are studied with scanning electron microscopy, transmission electron microscopy, and scanning Auger spectroscopy. The irradiations are being carried out with three different facilities.

One facility is a recently completed novel accelerator system which produces two ion beams simultaneously, and merges them on the same beam axis before permitting them to interact with solid targets at a chosen angle of incidence. This system allows (1) in situ sputtering-yield determination under ultrahigh-vacuum conditions, (2) a search for the formation of molecular species formed by the simultaneous interaction of ions of two different species (e.g., H^+, D^+) with solids, and (3) a search for interactive surface effects on the release of target particles and on target surface damage and erosion.

The second facility consists of a low-energy ion accelerator (1 keV to 15 keV). This system allows in situ determination for low ion energies under ultrahigh-vacuum conditions. Calibrated sputter-depth profiling is used to determine the sputter deposits in situ. The third facility, upgraded during 1977/78, produced high current densities of mass analyzed ions ($\sim$10 mA/cm^2) in the 10-keV to 120-keV energy range and allows target irradiation in the ultrahigh-vacuum range.

1. EXPERIMENTAL AND CALCULATED DEPTH DISTRIBUTIONS OF DAMAGE AND PROJECTED RANGES OF 20-keV ^{4}He IONS IN NICKEL

G. Fenske,* S. K. Das, M. Kaminsky, G. Miley,† B. Terreault,‡ G. Abel,‡ and J. P. Labrie§

Quantitative experimental information on the depth distributions of cavities in helium implanted metals is nonexistent for helium ion energy ranges from 20 keV to 100 keV. Such information is of interest for a better understanding of atomic collision processes, of energy loss mechanisms, and of the blistering process. In addition, this information is of practical interest for such applications as the control of surface erosion of components in fusion devices, the design and operation of high pressure helium gas cooled fast reactors, and accelerator technology.

*Thesis student, University of Illinois, Urbana, Illinois.

†University of Illinois, Urbana, Illinois.

‡Université du Quebec, Varennes, Quebec, Canada.

§Université de Montréal, Montréal, Quebec, Canada.

In this paper we present, for the first time, experimental information on both the depth distribution of cavities and the projected range of 20-keV ^{4}He ions injected into annealed, polycrystalline nickel held at 500°C. We obtained the entire depth distribution of cavities caused by 20-keV ^{4}He ions with a recently improved technique of sectioning irradiated samples parallel to the incident ion beam direction.[1] Transmission electron microscope (TEM) analysis of such sectioned samples allowed us to view the entire depth distribution of cavities (e.g., voids, gas bubbles) [including the region near to the irradiated surface (<0.1 μm)] with an excellent depth resolution (∿10 Å) and with only a small uncertainty (50—100 Å) in locating the irradiated surface. The range distribution of implanted helium was obtained with the elastic recoil detection (ERD) technique[2] with a maximum depth uncertainty of ±120 Å.

Figures XV-1(a), (b), (c), and (d) show a typical microphotograph of the cavities, quantitative data on the average cavity diameter, number density, and volume fraction as functions of the implant depth, respectively. The cavities observed in the plating are believed to be hydrogen bubbles trapped in the plating during the nickel strike application. Examination of unirradiated foils indicates that these do not affect the quantitative analysis.

The helium concentration profile obtained from the ERD analysis is shown in Fig. XV-2 as a function of the implant depth. The depth scale was derived from the ERD data assuming a target density of 8.9 gm/cm^3. The volume swelling profile is also shown in Fig. XV-2; however, the widths of the depth intervals ΔX_c have been corrected to account for the change in target density due to volume swelling $\Delta V/V$ within each interval using the following relation

$$\Delta X_c = \Delta X_{ex} [1 - \Delta V/V], \qquad (1)$$

where ΔX_{ex} was the depth interval initially chosen for the TEM analysis.

Within the limits of the experimental uncertainty in locating the surface, the most-probable range (0.088 μm) agrees quite well with the location of the maximum volume swelling.

---

[1] G. Fenske, S. K. Das, and M. Kaminsky, J. Nucl. Mater. 80, 373 (1979).

[2] B. Terreault, J. G. Martel, R. G. St.-Jacques, and J. L'Ecuyer, J. Vac. Sci. Technol. 14, 294 (1977).

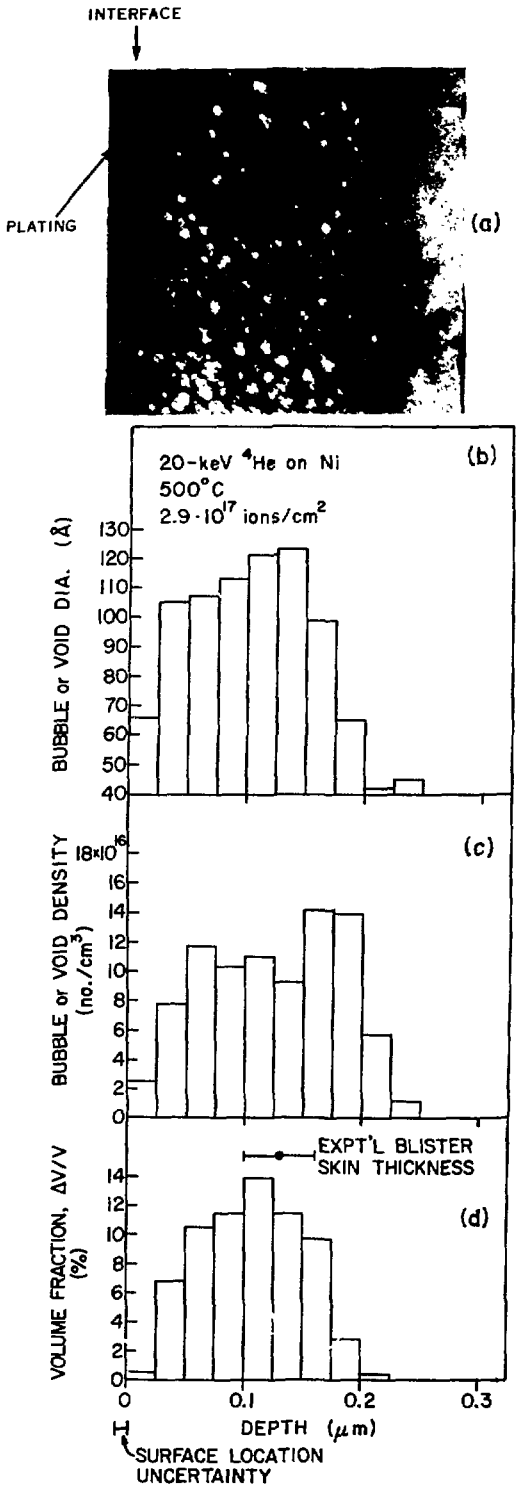

Fig. XV-1. (a) Cavity microstructure of nickel irradiated with 20-keV $^4He^+$ ions at 500°C to a dose density of 2.9×10^{17} ions/cm^2. (b)—(d) Show the average cavity diameter, cavity number density, and the volume fraction of cavities as a function of depth in nickel for the irradiation conditions stated under (a), respectively.

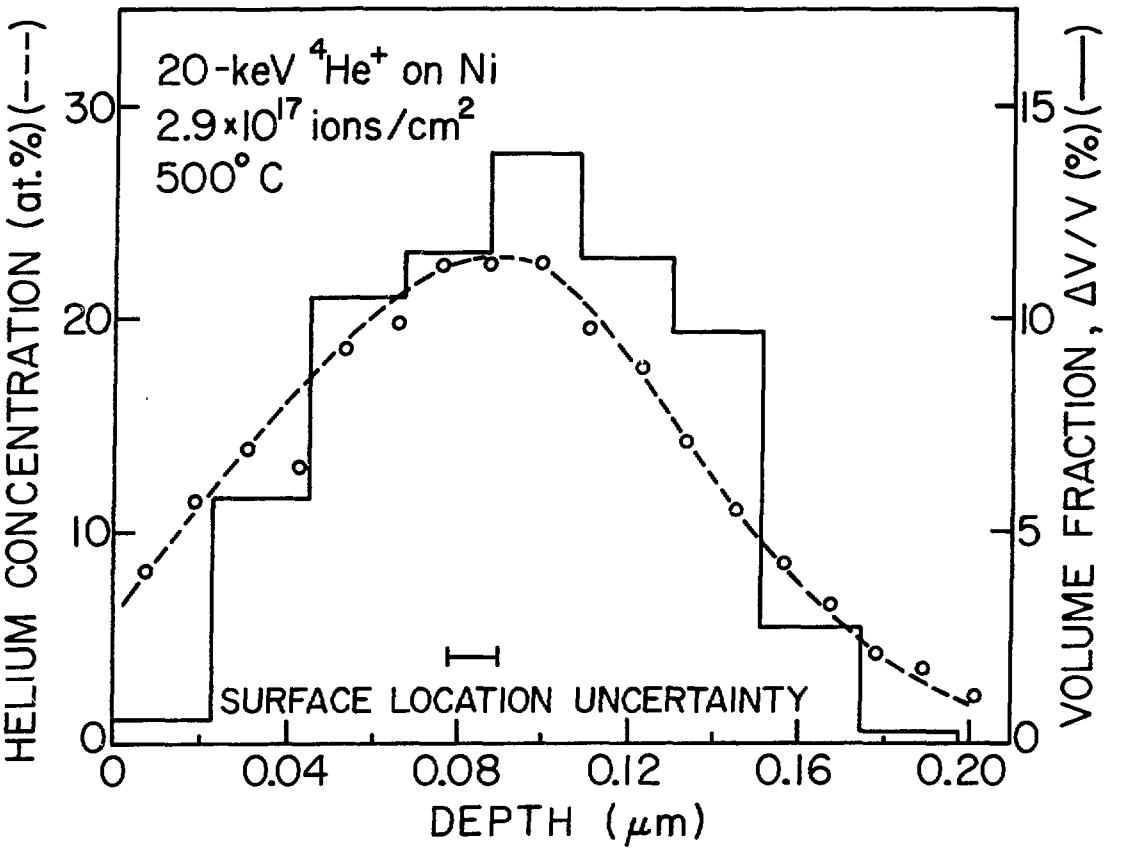

Fig. XV-2. Helium concentration profile obtained from the ERD analysis is shown as a function of the implant depth (dashed lines) for the case of nickel irradiated with 20-keV $^4He^+$ ions at 500°C to a dose density of 2.9×10^{17} ions/cm^2. A histograph of the volume fraction of cavities as a function of depth for the same irradiation conditions is shown for comparison (solid line).

Now we can compare the experimental damage and range distributions with the calculated ones. Figures XV-3(a) and (b) show calculated depth distributions of the energy deposited into displacing atoms (solid curve) and projected range probabilities (dashed curves). The most-probable projected ranges obtained from the TRIM calculation[3] (0.080—0.085 μm) and the Edgeworth expansion[4] (∿0.081 μm) are in good agreement, and differ from the most-probable range obtained from the Gaussian approximation used by Brice[5]

[3] J. P. Biersack and L. G. Haggmark, Nucl. Instrum. Methods 174, 257 (1980).

[4] K. B. Winterbon, Ion Implantation Range and Energy Deposition Distributions, Vol. 2, Low Incident Ion Energies (Plenum, New York, 1975).

[5] D. K. Brice, Ion Implantation Range and Energy Deposition Codes: COREL, RASE4, and DAMG2, SAND 75-0622 (1977).

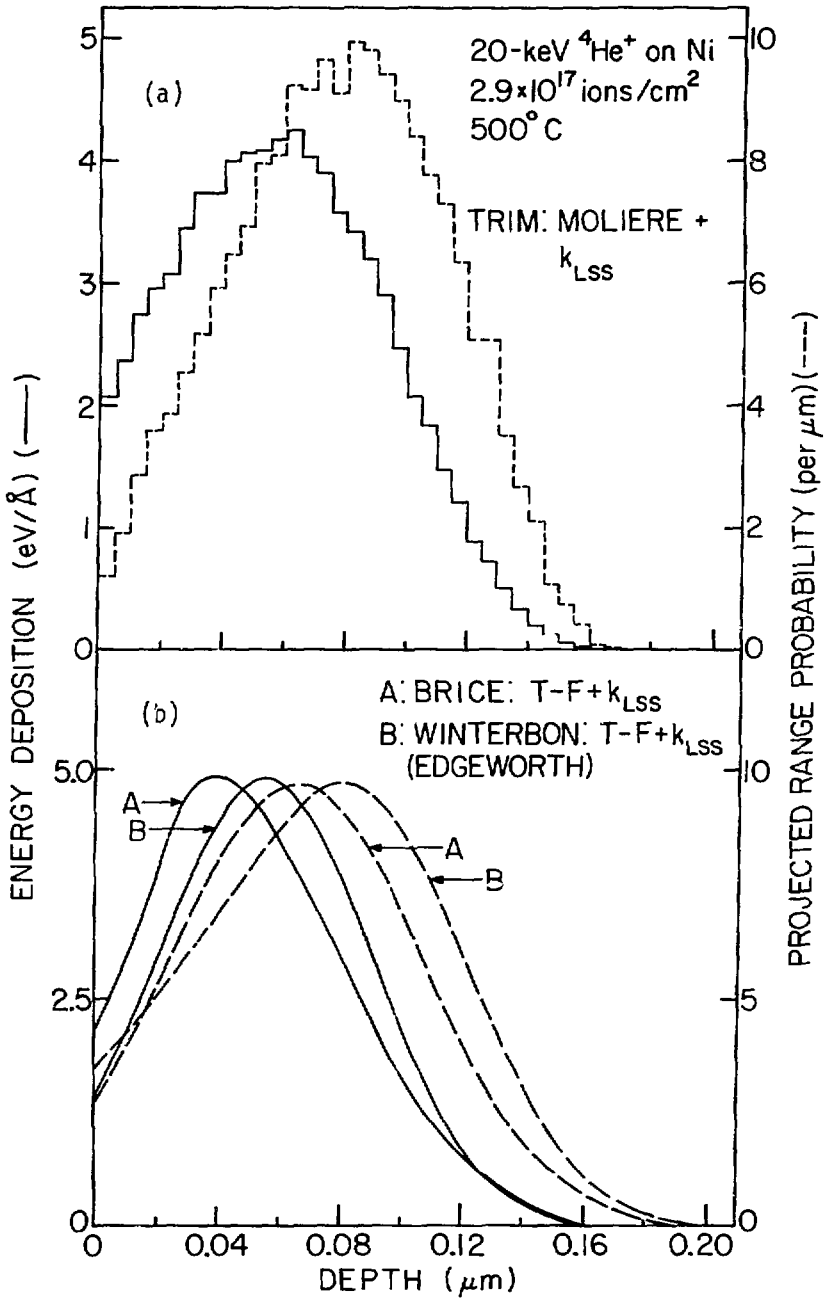

Fig. XV-3. Depth distributions of the energy deposited into displacing atoms (solid line) and the projected range probabilities (dashed line) calculated according to (a) the TRIM code (Ref. 3) and (b) Brice's code [Ref. 5(A)], and Winterbon's method [Ref. 4(B)], for the case of 20-keV $^4He^+$ ion irradiation of nickel.

(∿0.065 μm). In a similar manner, the maxima in the energy deposition profiles obtained from the TRIM calculation and the Edgeworth expansion agree with one another and are located at a depth larger than that calculated according to Brice. The major difference in calculating the profiles in Fig. XV-3(b) is that the Edgeworth expansion uses the skewness and kurtosis to reconstruct the distribution from its spatial moments (in addition to the average range and straggling) while Brice's codes do not. The good agreement between the most-probable ranges for the TRIM profiles (which inherently include the skewness, kurtosis, and higher moments) and the Edgeworth expansion, and the disagreement with the Gaussian approximation, appears to indicate that higher-order moments cannot be neglected for these particular energy and projectile-target combinations.

Other factors that can influence the location of the most-probable range are the electronic and nuclear stopping. However, for 20-keV ^{4}He ions in nickel, differences in nuclear screening functions (e.g., Thomas-Fermi or Bohr screening function) do not significantly affect the values of the straggling or average projected range. While the most-probable projected range determined from the peak in the helium concentration (Fig. XV-2) with the ERD analysis yields a value of (0.088 ± 0.012) μm, the projected range calculated with the aid of the Edgeworth expansion yields a value of only 0.081 μm. This difference is within the experimental accuracy of the ERD technique. However, if we assume that the difference between the experimental and calculated values is real, it is of interest to determine how strongly the selection of the proper electronic stopping can minimize this difference. Previous results[1] for 500-keV ^{4}He ions in nickel indicated that the LSS constant K_{LSS} should be reduced by ∿15% to achieve agreement between theoretical and experimental results. However, a reduction in K_{LSS} of this size will increase the most-probable range to only 0.086 μm for the 20-keV ^{4}He case. Thus, a larger decrease in the K_{LSS} value of ∿20% is required for agreement.

The combined effects of (i) the volumetric swelling within the implanted region, (ii) the difference in the calculated most-probable projected range due to the difference in reconstructing the range distribution, and (iii) errors in the electronic stopping, can be used to clarify the reported discrepancies between calculated average projected ranges and observed blister skin thicknesses of exfoliated blisters on 20-keV ^{4}He

implanted nickel foils. For 20-keV ^4He ions in nickel, the average skin thickness (0.13 ± 0.03 μm) is approximately twice the calculated average projected-range (∿0.065 μm) based on theoretical LSS electronic stopping powers. While it has been common practice to compare the observed thicknesses with the average projected range, it appears more appropriate to use the most-probable range for this comparison. However, as discussed earlier, the use of an Edgeworth expansion, together with the assumption of an error of ∿20% in the electronic stopping for 20-keV $^4He^+$ ions in nickel, shifts the peak in the calculated projected-range profile from 0.065 μm to 0.088 μm. Furthermore, the effect of the volume swelling on the range profile can account for 0.024 to 0.028 μm, when the shift due to swelling is linearly extrapolated with dose from 2.9×10^{17} ions/cm^2 to the critical blister-formation dose of 4 to 5×10^{17} ions/cm^2. Together, these three errors account for a shift in the most-probable projected range of 0.047 to 0.052 μm. If this, and the 0.005 to 0.010 μm thickness lost from the surface in the sample preparation technique are added to the average projected-range (based on theoretical LSS electronic stopping), the result, 0.12 to 0.13 μm, is well within the range of the observed skin thicknesses. More detailed discussions of the results can be found in Ref. 6.

[6] G. Fenske, S. K. Das, M. Kaminsky, G. Miley, B. Terreault, G. Able, and J. P. Labrie, J. Appl. Phys. 52, 3618 (1981).

2. SEARCH FOR MICROSTRUCTURAL INFLUENCES ON THE SPUTTERING OF ANNEALED ALUMINUM AND SINTERED ALUMINUM POWDER (SAP 895) UNDER D^+ AND $^4He^+$ BOMBARDMENT: YIELDS, ANGULAR DISTRIBUTIONS

S. K. Lam and M. Kaminsky

It is the main goal of these studies to determine how the significant differences between the surface microstructure of annealed aluminum (99.99% pure Al, average grain size 300 μm) and that of sintered aluminum powder SAP 895 (89.5% Al, 10.5% Al_2O_3, average grain size 0.5 μm) will influence the sputtering (e.g., yields, angular distribution, chemical composition of sputter deposit) of these solids under D^+ and $^4He^+$ bombardment in the energy range of 3.5 to 9.5 keV. In previous experiments,[1]

[1] S. K. Das and M. Kaminsky, J. Nucl. Mater. 63, 292 (1976).

it was found that the blister erosion yield of SAP 895 due to blister exfoliation was three orders of magnitude lower than that for annealed aluminum under 100-keV helium irradiation at room temperature. This observation was attributed to the difference in the surface microstructure of SAP and annealed Al. The equivalent Al thickness and the chemical composition of the sputter deposits were analyzed by three independent techniques: (1) Rutherford backscattering (RBS), (2) peak-to-peak amplitude measurement using Auger electron spectroscopy (AES), and (3) sputter depth profiling with AES. All of these techniques differ from the weight loss technique used recently by other authors[2] for Al sputtering experiments.

The RBS technique was used with a 1.25-MeV H^+ beam of 0.3 mm diameter striking the deposit. The backscattered protons were detected and energy-analyzed at a laboratory angle of 154°. Figure XV-4 shows an RBS spectrum from a 35 monolayer (ML) thick Al deposit on a 175 $\mu g/cm^2$ thin carbon foil. One can readily distinguish the aluminum peak from the relatively broad carbon peak, typical for the collector, and the oxygen peak due to contamination. The agreement between the calculated and experimental values of the onset energies is very good, as indicated in Fig. XV-4. A quantitative correlation between the area A under the Al peak, and the Al deposit thickness ρt was obtained by calibration with standards. The standards were prepared by vacuum vapor deposition of known amounts of Al (with thicknesses of 1, 2, 5, 10, 25, 50, and 100 ML) on substrates of 175 $\mu g/cm^2$ thick carbon foils. The thicknesses were determined with a Kronos crystal monitor, Model QM321. In general, the deviation in A from the average value obtained from the four repeated runs for a given Al standard was found to be within ±10%. A linear calibration curve of the average values of A vs ρt was obtained with a mean deviation of ±10%. The extrapolation of this curve went through $A = 0$ at $\rho t = 0$.

The yields for sputtered aluminum determined in the present studies with the RBS technique are summarized in Table XV-I, together with the total Al sputtering yield values calculated with (i) the semiempirical formula due to Smith,[3] and (ii) the TRIM code.[4] The major parameters used in these calculations are listed in the footnotes to Table XV-I.

[2] J. Bohdansky, J. Roth, and F. Brossa, J. Nucl. Mater. 85 & 86, 1145 (1979).

[3] D. L. Smith, J. Nucl. Mater. 75, 20 (1978).

[4] J. P. Biersack, private communication.

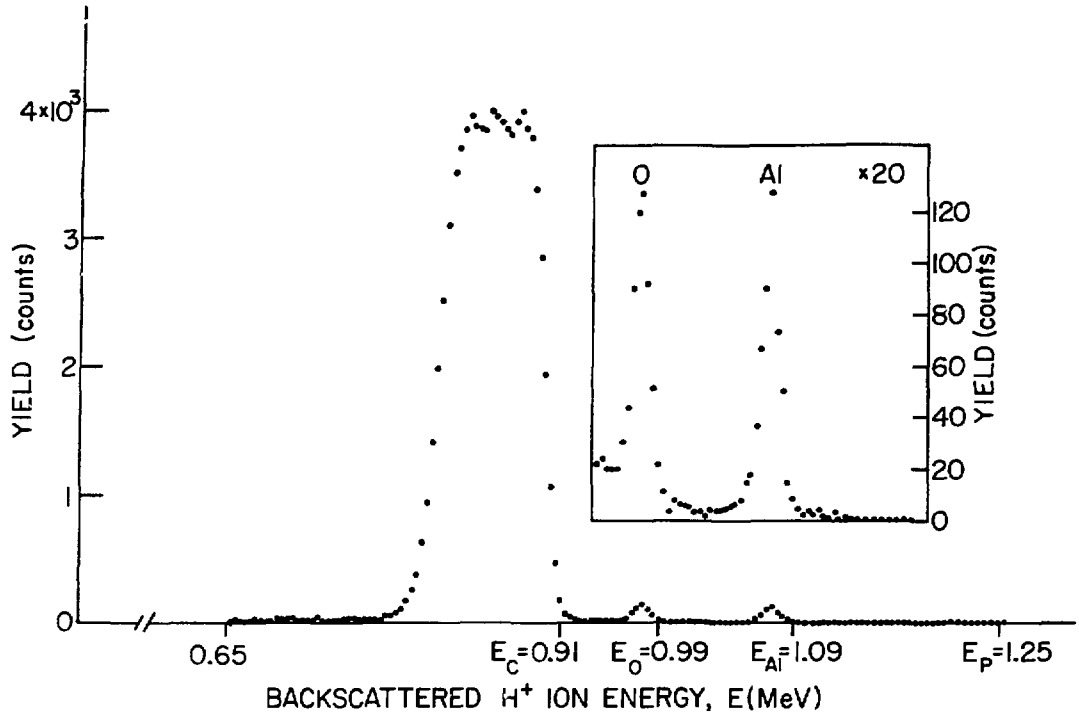

Fig. XV-4. Rutherford backscattering spectrum of a sputter deposit with an equivalent Al thickness of 35 monolayers on a 175 $\mu g/cm^2$ thick carbon substrate (resulting from a 3.5-keV He^+-Al sputtering run), obtained with a 1.25-MeV primary H^+ ion beam and for a laboratory scattering angle of 154°. E_C, E_O, and E_{Al} are the calculated onset energies for carbon, oxygen, and aluminum, respectively.

In Table XV-I, it can be seen that for He^+ ion energies between 3.5 and 9.5 keV the mean yields for sputtered aluminum typical for SAP 895 targets are consistently 5—18% higher than those for annealed Al targets, while no significant difference is observed for the D^+ irradiations for the same energy range. The experimental Al sputtering yields as a function of incident ion energy are plotted in Figs. XV-5 and XV-6 for the D^+ and He^+ irradiations of the Al target, together with the yield values which have been calculated using Smith's expression and the TRIM code. The yield data are, within the experimental accuracy, in reasonable agreement with the predictions of Smith's expression for both D^+ and He^+ irradiations of aluminum with energies varying from 3.5 and 9.5 keV. For an irradiation energy of 20 keV for both D^+ and He^+, the experimentally determined yields for the annealed Al are larger than those calculated according to Smith's

TABLE XV-I. Yields for sputtered aluminum (atoms/ion).

Projectile	Projectile incident energy (keV)	Experimental yield values		Theoretical yield values	
		Annealed Al target	SAP (895) target	Al target	
				TRIM code[a]	Semiempirical expression[b]
D^+	3.5	0.014 ± 0.002	0.014 ± 0.002	0.014	0.014
	5.5	0.012 ± 0.002	0.012 ± 0.002	0.012	0.011
	7.5	0.010 ± 0.002	0.010 ± 0.002	0.008	0.009
	9.5	0.008 ± 0.001	0.008 ± 0.001	. . .	0.007
	20	0.007 ± 0.001	. . .	. . .	0.004
$^4He^+$	3.5	0.089 ± 0.012	0.093 ± 0.012	0.083	0.089
	5.5	0.073 ± 0.010	0.079 ± 0.010	0.072	0.070
	7.5	0.063 ± 0.008	0.070 ± 0.008	0.065	0.057
	9.5	0.056 ± 0.008	0.066 ± 0.008	. . .	0.048
	20	0.049 ± 0.010	. . .	. . .	0.026

[a]For the major parameters the following values were used: binding energy (Frenkelpair) BE = 3.9 eV, surface binding energy SBE = 1.6 eV, correction factor for electronic stopping power C_K = 1, and screening factors CA = 1 and CA2 = 1. For the D^+ irradiations the trajectories of 20 000 incident ions were followed and 11 000 for the $^4He^+$ irradiations.

[b]Equation (7) given in Ref. 3 was used for the calculations. For the surface binding energy a value of U_0 = 3.4 eV, listed in Table 1 of Ref. 3, was used.

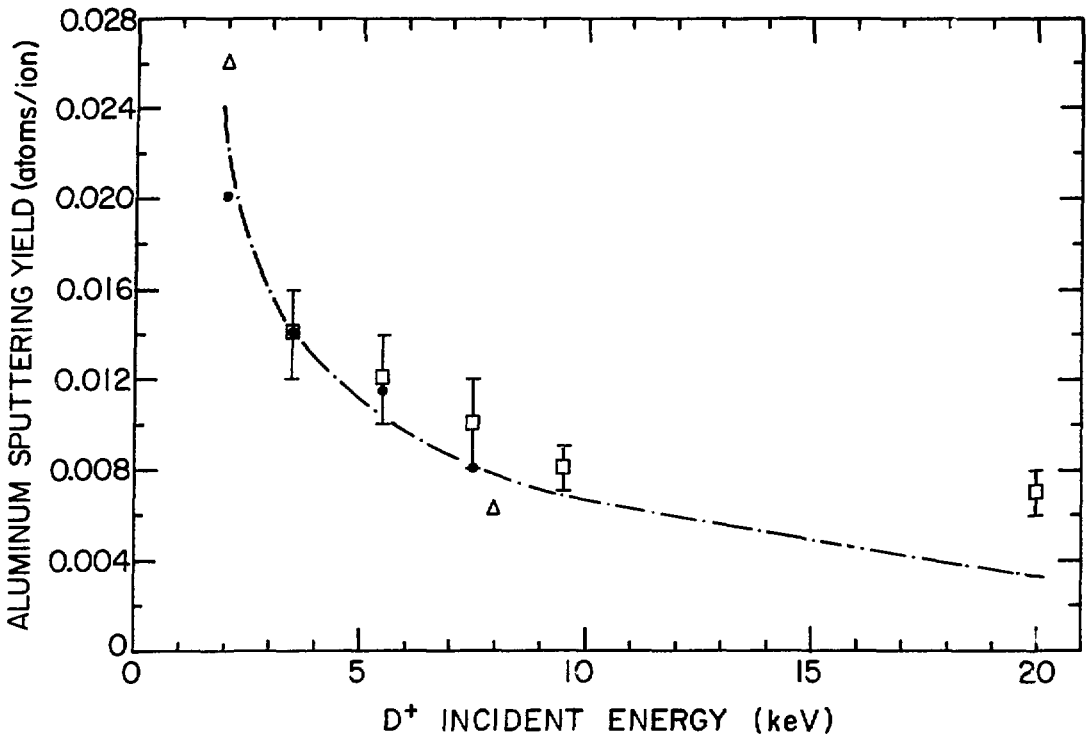

Fig. XV-5. The dependence of the aluminum sputtering yields on the incident deuteron energy for polycrystalline aluminum targets for normal incidence. The values marked □ and Δ have been obtained experimentally in the present work and by Bohdansky et al. (Ref. 2), respectively. The values marked (●) and the curve (—·—·—) have been calculated using the TRIM code (Ref. 4) and Smith's semiempirical formula (Ref. 3), respectively.

expression. A possible reason for this discrepancy is that the measured Al yields have been enhanced by the roughened (and thereby enlarged) target surfaces produced by ion bombardment during the irradiations. Such a yield enhancement by rough surface structures has been observed in our recent yield measurements of TiB_2 coatings under D^+ and $^4He^+$ bombardment and by others. The yields calculated by the TRIM code are also in reasonable agreement with the experimentally determined yields for both D^+ and He^+ irradiations of aluminum with energies varying from 3.5 to 7.5 keV. It should be pointed out that these calculated values have a statistical error of 10% and estimated fluctuations of about 15%.

The recent data on the total sputtering yields of Al obtained by Bohdansky et al. (Ref. 2) with the weight loss method are also shown in

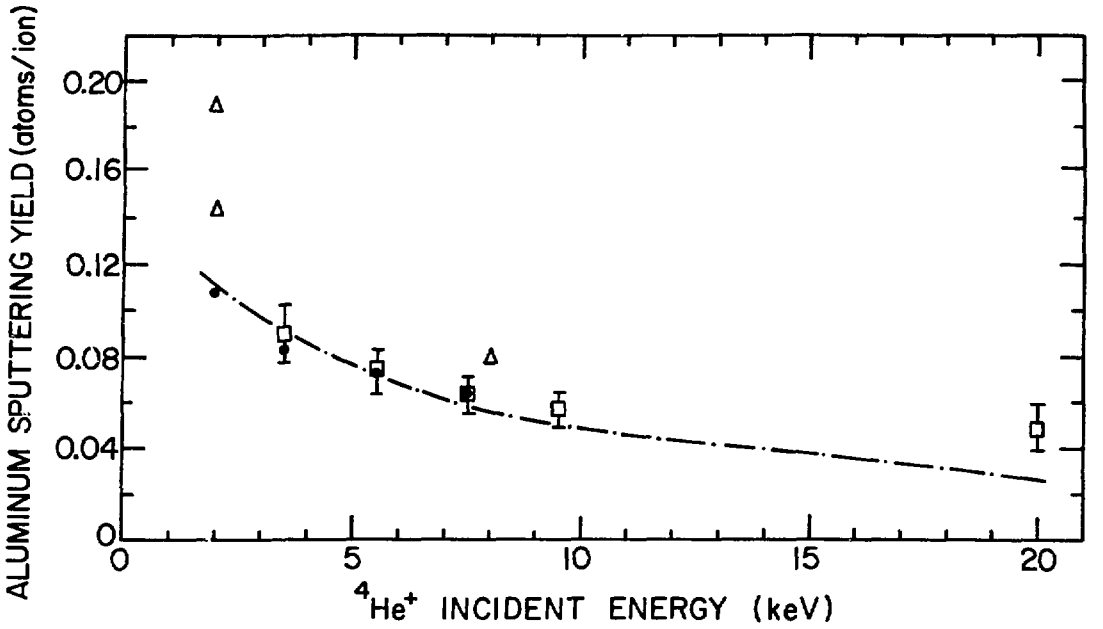

Fig. XV-6. The dependence of the aluminum sputtering yields on the incident $^4He^+$ energy for polycrystalline aluminum targets for normal incidence. Experimental values marked □ and Δ have been obtained experimentally in the present work and by Bohdansky et al. (Ref. 2), respectively. The values marked (●) and the curve (—·—·—) have been calculated using the TRIM code (Ref. 4) and Smith's semiempirical formula (Ref. 3), respectively.

Figs. XV-5 and XV-6 for comparison. It can be seen in Fig. XV-5 that the Al yields reported for 2-keV and 8-keV D^+ irradiations also show reasonable agreement (within 20%) with the values calculated according to Smith's formula. For the case of He^+ ion irradiations, the yield values reported by Bohdansky et al. for 2 keV are significantly higher (30—70%) than those predicted by Smith and by the TRIM calculations. In turn, we find reasonable agreement between our yields typical for Al targets and the yield values calculated according to both Smith's empirical expression and the TRIM code energy regions where a comparison can be made. It should be noted that Bohdansky et al. reported no significant difference in the total sputtering yield values for SAP and Al, for the same incident He^+ ion energy, although no explicit error limits for the values quoted above were given. We, in turn, observe that the mean yields typical for SAP targets are higher than those for the annealed Al by approximately 5—18%. For further details regarding the results, see Ref. 5.

[5] S. K. Lam and M. Kaminsky, J. Nucl. Mater. 89, 205 (1980).

3. SURFACE EFFECTS INDUCED BY SIMULATED PLASMAS

a. Two-Laminar and Three-Laminar Clad Materials for Fusion Applications

M. Kaminsky

In support of the improvement program of the Tokamak Fusion Test Reactor (TFTR) at Princeton University, two different types of clad materials are under study to meet specific requirements. One type is being developed for armor plates to protect the first wall against a single fault condition (e.g., caused by plasma disruption) which could result in a single radiation pulse of high power deposition ($\sim$8 kW/cm^2) for a pulse length of probably less than 0.1 sec. Another type is being developed for fixed and movable limiters, which will be exposed to repeated radiation pulses (1.5 sec pulse length, 300 sec pulse repetition period) with power densities of about 1 to 4 kW/cm^2, respectively, under normal operating conditions.

In view of these different radiation environments for different first wall components the following major considerations are guiding the claddings development program: (a) Clad materials must be able to withstand power densities ranging from $\sim$1 to $\sim$8 kW/cm^2 for specified pulse lengths. (b) Clad materials must be able to tolerate and survive exposures to different types of radiations (e.g., electromagnetic radiations, electrons, ions, atoms, neutrons), in many cases at power densities within the range specified in item (a). (c) Clad materials must exhibit good adhesion, adequate heat shock resistance, acceptable thermal cycling fatigue life, low outgassing rates and vapor pressure at operating temperature, low sputtering yields, and acceptable hydrogen isotope recycling characteristics. (d) Clad materials should preferably be of low to medium atomic number. (e) Effective and inexpensive fabrication processes should be used for the claddings (e.g., hot pressing, explosion bonding).

The choices for the type of clad materials of their thicknesses were made on the basis of heat transfer calculations. Figure XV-7 illustrates the type of result obtained from heat transfer calculations performed for a certain type of clad material (0.05 cm V on 1.27 cm thick OFHC Cu) exposed to a given power density (1.1 kW/cm^2) for a certain pulse length (1.5 sec) and a pulse repetition period of 300 sec.[1] The design

[1] R. Budny, Plasma Physics Laboratory, Princeton University, Report #23, February 1980.

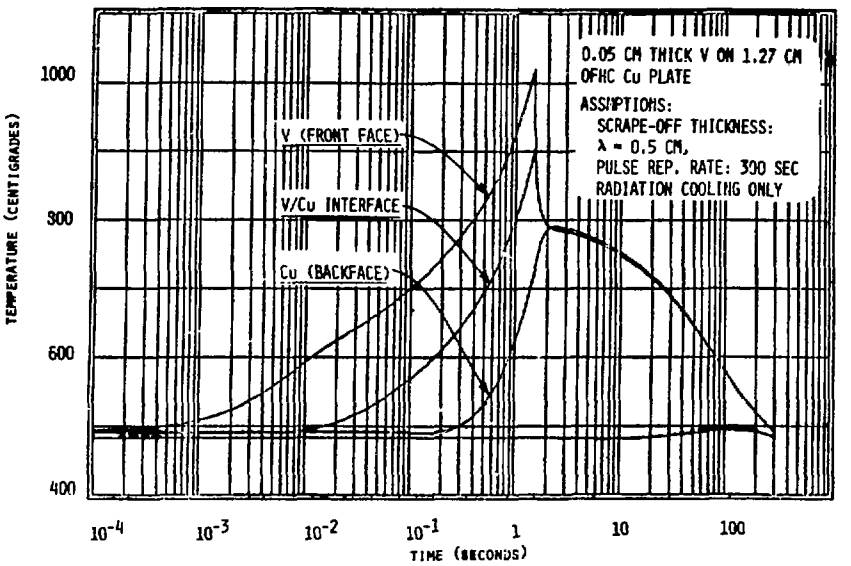

Fig. XV-7. Calculated temperature rise of an explosion clad plate caused by the deposited power density of 1.1 kW/cm^2 for a 105 sec pulse length and a 300 sec pulse repetition period (Ref. 1).

parameters for the claddings (e.g., type of material, thickness) are then chosen such that the peak temperatures for (1) the surface of the refractory metal facing the plasma (front face - Fig. XV-7), and (2) the interface of the refractory metal and copper, stay below the melting temperatures for these materials. For the protection against single fault conditions, however, it is less important that the front face of the refractory metal does not melt than that the copper at the interface does not melt.

In order to meet these specific requirements the following design choices were made.

(1) For protection against the repeated radiation pulses for power densities in the range from 1 to 4 kW/cm^2 a two-laminar clad material was developed. Typically, a 0.05 cm thick sheet of a refractory metal [e.g., Ti, V, V (10% Ti) and V (20% Ti) alloy] was clad to a 1.3 cm thick OFHC copper plate as heat sink.

(2) For protection against a single radiation pulse of high power density (up to 8 kW/cm^2 for 0.1 sec) a three-laminar clad material was developed. Typically, a 0.05 cm thick sheet of V was clad to a 0.25 cm thick Nb,

or Mo, or st. steel plate which, in turn, was clad to a 1.3 cm thick OFHC copper plate as heat sink.

Explosion cladding was used for the bonding of both the two-laminar and three-laminar materials. The cladding of the three plates for a three-laminar material occurred simultaneously.

To achieve good bonding it was necessary that the plates to be bonded had a ductility (elongation) of better than 20% and were flat and free of surface debris.

(i) Characterization of the Bond Interface

The bonded zone region of the clad plates was examined with the aid of optical metallography and scanning electron microscopy with x-ray energy analysis (SEMX).

Optical Metallography. Two metallographic samples were cut from each of the clad plates so that the bonded zones could be examined (after polishing and etching) in two planes at right angles to each other. One of these planes is parallel to the long edge plane of the rectangular clad plate (which is also parallel to the direction of the explosive wave propagation). A metallographic view of this plane is called the longitudinal view. The view of the other plane, at right angles to this one, is called the transverse view. As an example, Fig. XV-8 gives a longitudinal view of the bond interface zones of a three laminar cladding of V/Nb/Cu. This figure reveals two important features: (1) At the Nb/Cu interface the wavy interface with the associated crest formations (the latter features are reminiscent of Helmholtz instabilities). These features support the model for the existence of a fluid (melt) bond zone for a short period during the time of the propagation of the collision zone along the long axis of the plate. The existence of this wavy interface contributes to the high strength of the bond due to the increase in the bond surface area. (2) A solidified melt layer which was generally very thin (≤ 2 μm), with no detectable major brittle intermetallic compound formation. This feature also contributes to the high strength of the bond.

Qualitatively, similar pictures have been obtained for the V/Cu, Nb/Cu, and Mo/Cu bond interfaces. Only one type of the clad materials, the V/Mo/Cu samples, had a serious defect. Optical metallographic examination of the V/Mo and Mo/Cu interfaces showed good bond interfaces. However,

Vanadium

Niobium

Niobium

OFHC Copper

Fig. XV-8. Optical metallograph photomicrographs of the longitudinal view of the bond zones V/Nb and Nb/Cu of an explosion clad three laminar system (0.05 cm V on 0.31 cm Nb on 1.27 cm OFHC Cu).

structural delaminations could be observed in the Mo, occurring in the grain boundaries parallel to the heavily-textured, elongated grains. Various tests of the clad materials revealed encouraging results:

(ii) Heat Shock Resistance and Thermal Cycling Fatigue of Clad Samples

Heat shock tests of such three-laminar materials as V/Mo/Cu, V/Mb/Cu and V/304 st. steel/Cu were performed with electron beam irradiations for power densities ranging up to 8 kW/cm^2 on a target area of 1 cm^2 for a pulse length of 0.7 sec (this pulse length is longer than required) by M. Ulrickson (Princeton Plasma Physics Laboratory). All samples survived the power density of $\sim$8 kW/cm^2, a very encouraging result. Since some of the V/Mo/Cu samples showed delamination in the Mo prior to the heat shock test, it was decided against further tests of this type of material.

Tests of heat shock resistance and of thermal cycling fatigue were performed for such two-laminar materials as V/Cu, Ti/Cu, V (10% Ti)/Cu and V (20% Ti)/Cu. All samples withstood power densities in the range from 4.5 to 5.0 kW/cm^2 on a 1 cm^2 target area for a pulse length of 1 sec. The same types of clad materials were subjected to thermal fatigue tests for 1000 electron beam pulses at a power density of 3.5 kW/cm^2, a pulse length of 0.5 sec and a pulse repetition period of 300 sec. With the exception of the Ti/Cu material, all other materials showed only some light surface cracking in small areas. The Ti/Cu material, in turn, showed severe surface damage due to cracking. This is thought to be due in large part to the Ti phase transformation at $\sim$883°C.

(iii) Shear Strength of Bonds of Clad Materials

Tensile tests were conducted at room temperature on flat samples of clad materials (e.g., V/Cu, V/Nb/Cu, Ti/Cu) to determine the shear strength of the bond. Test specimen were prepared by machining the refractory laminate and the copper to certain thicknesses and by cutting two parallel notches on opposite faces of the specimen to reach the bond surface on both sides of the specimen, as indicated schematically in the footnote to Table XV-II. The shear stress S at the bond surface was calculated from the maximum load P and the expression $S = P/A_3$, where A_3 is the area of the bond surface between the notches. All tests were conducted by T. Kassner

TABLE XV-II. Tests of shear strength of bonds of clad materials. Tests were conducted by T. Kassner and O. K. Chopra, ANL.

Material	Temp. K (°C)	Cross sectional area, mm^2 Laminate (V or V/Nb), A_1	Copper, A2	Bond area mm^2, A_3	Maximum load, kg	Shear stress in bond MPA	(KSI)
V/Cu	298 (25)	5.8	39.3	22.6	458	198.7	(28.8)
V/Nb/Cu	298 (25)	65.9	70.5	46.8	956	200.3 Nb bond to Cu	(29)
Ti/Cu	298 (25)	8.9	47.7	23.1	471	200.0	(29)

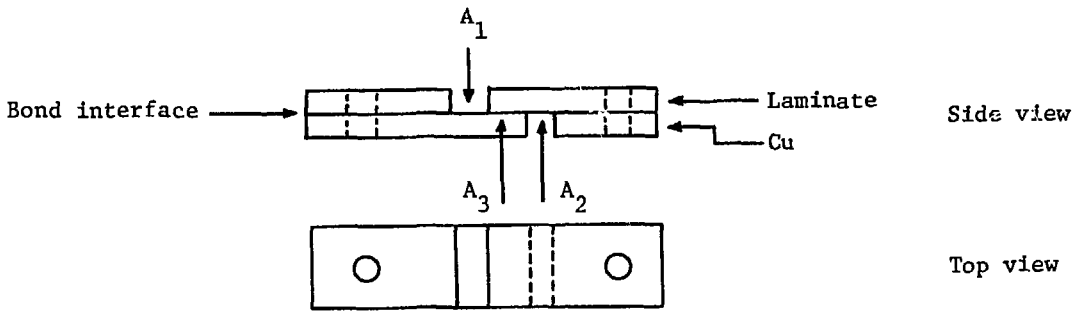

and O. K. Chopra, ANL, with an Instron tensile testing machine at constant crosshead speed of 4 mm/min. The tests revealed the encouraging result that, at the shear stress values listed in the last column of Table XV-II, the bond surfaces did not fail but the laminates fractured. Therefore, the actual bond strength of the clad materials will be at least equal to or larger than the shear stress values listed. For further test results regarding sputtering yields and outgassing rates, see Ref. 1.

[1] M. Kaminsky, Thin Solid Films 73, 117 (1980).

b. Sputtering of TiB_2 Coatings under D^+ and $^4He^+$ Ion Bombardment: Total Yields

M. Kaminsky, S. K. Lam, and K. Moy*

The use of low to medium-Z materials which have low impurity release yields and minimal surface erosion yields appears desirable for plasma device operations. Titanium diboride (TiB_2) is one of the candidate coating materials which has been considered for this purpose. In order to evaluate the suitability of TiB_2 coatings for first-wall component applications, it is important to determine the effects of D^+ and $^4He^+$ irradiations on these coatings. We have recently reported on the surface damage and erosion of TiB_2 coatings under D^+ and $^4He^+$ irradiations for energies ranging from 5 to 120 keV.[1,2] The main aim of the present study is to determine the total sputtering yield for both polished and unpolished TiB_2 coatings for D^+ and $^4He^+$ ion irradiation with energies ranging from 3 to 15 keV. Figures XV-9(a) and XV-9(b) are scanning electron micrographs of surfaces of TiB_2 coatings on Poco graphite in the as-deposited condition and after mechanical polishing, respectively. It can be seen that the as-deposited TiB_2 coating surface is rough and has many nodules. The size and number density of these nodules varied from one region to the other on the same substrate. A crude estimate of the actual surface area (per unit surface area) for this coated sample from the analysis of scanning electron micrographs revealed that this area is more than two orders of magnitude larger

*Graduate student, Illinois Institute of Technology, Chicago, Illinois.

[1] M. Kaminsky and S. K. Das, J. Nucl. Mater. 85 & 86, 1095 (1979).

[2] S. K. Das and M. Kaminsky, Thin Solid Films 63, 269 (1979).

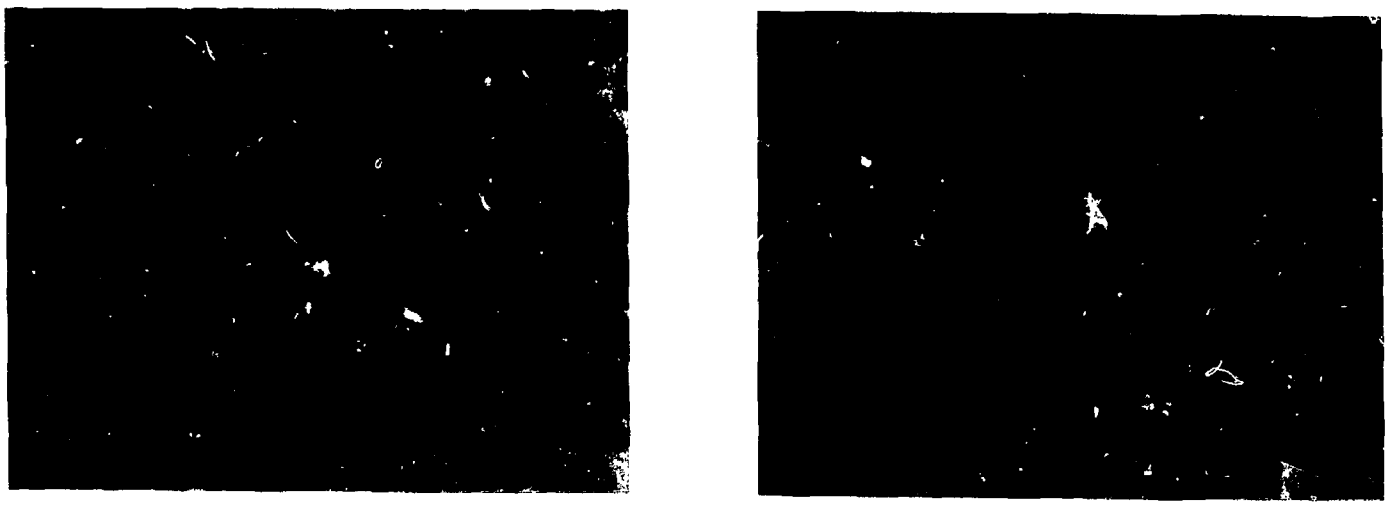

(a) (b)

Fig. XV-9. Scanning electron micrographs of two types of surfaces of chemically vapor-deposited TiB_2 coatings prior to irradiation: (a) as-deposited surface; (b) polished surface.

than that typical for the polished surface. More precise measurements are in progress using Brunauer-Emett-Teller desorption spectroscopy.

The irradiations were carried out with mass-analyzed D^+ and $^4He^+$ ion beams striking the targets at normal incidence. For the collection of sputtered material, physically vapor-deposited aluminum foils were used which had an equivalent thickness of about 50 $\mu g\ cm^{-3}$. Rutherford backscattering spectrometry was used to determine (a) the chemical composition, and (b) the thickness of the sputter deposit. Total sputter yields were determined from the total mass of material which had been sputtered from the irradiated spot for a given incident ion fluence.

The results summarized in Table XV-III reveal the following trends. The yield values decrease with increasing ion energy for the energy range studied. The experimentally determined yield values for the rough TiB_2 surfaces in the as-received state are about 50—65% larger than those for the smoother polished surfaces. This result suggests that for this type of rough surface the enhancement in sputtering (e.g., resulting from angles of incidence other than normal for a large fraction of ions) is on balance larger than the possible reduction (e.g., due to redeposition of sputtered particles). The agreement between the calculated value[3] and those determined for the polished surfaces for He^+ irradiations is good, whereas for the D^+ irradiations the measured values are consistently lower than the semiempirical calculations predicted.

For the operation of plasma devices these sputter yield results for TiB_2 coatings are very encouraging. For example, the yield values for these coatings are significantly lower than those for an uncoated surface of 304 LN stainless steel (the vacuum vessel material for the tokamak fusion test reactor). For the polished TiB_2 target under D^+ irradiations over the energy range from 3 to 15 keV, the yield values are about 250—350% smaller than those for 304 LN stainless steel [e.g., for 5-keV D^+ irradiations $S(TiB_2) = (0.52 \pm 0.05) \times 10^{-2}$ atoms ion^{-1} and S(304 LN stainless steel) $= (1.8 \pm 0.1) \times 10^{-2}$ atoms ion^{-1}]. A comparison of the yield values for these materials for helium irradiations shows for polished TiB_2 coatings a similar decrease by 230—300%. From the point of view of permissible plasma impurity concentration, the gain is even larger because of the

[3] D. L. Smith, J. Nucl. Mater. 75, 20 (1978).

TABLE XV-III. Total sputtering yields (atom ion^{-1}).

Projectile	Projectile incident energy (keV)	Experimental total yield values		Calculated yield values,[a] TiB_2
		As-received TiB_2	Polished TiB_2	
D^+	3	$(1.2 \pm 0.1) \times 10^{-2}$	$(0.72 \pm 0.07) \times 10^{-2}$	$(1.1) \times 10^{-2}$
	5	$(0.81 \pm 0.08) \times 10^{-2}$	$(0.52 \pm 0.05) \times 10^{-2}$	$(0.72) \times 10^{-2}$
	10	$(0.57 \pm 0.06) \times 10^{-2}$	$(0.36 \pm 0.04) \times 10^{-2}$	$(0.42) \times 10^{-2}$
	15	$(0.46 \pm 0.05) \times 10^{-2}$	$(0.27 \pm 0.03) \times 10^{-2}$	$(0.28) \times 10^{-2}$
$^4He^+$	3	$(1.1 \pm 0.1) \times 10^{-1}$	$(0.68 \pm 0.08) \times 10^{-1}$	$(0.66) \times 10^{-1}$
	5	$(0.76 \pm 0.08) \times 10^{-1}$	$(0.52 \pm 0.05) \times 10^{-1}$	$(0.51) \times 10^{-1}$
	10	$(0.55 \pm 0.06) \times 10^{-1}$	$(0.33 \pm 0.04) \times 10^{-1}$	$(0.30) \times 10^{-1}$
	15	$(0.42 \pm 0.04) \times 10^{-1}$	$(0.26 \pm 0.03) \times 10^{-1}$	$(0.21) \times 10^{-1}$

For the calculations the values used for the major parameters were as follows: surface binding energy $U_0 = 4.2$ eV; effective charge $Z_{eff}(TiB_2) = 10.7$; $M_{eff}(TiB_2) = 25.2$.

[a]Reference 3, Eq. (7), was used for these calculations.

difference in the effective atomic numbers of TiB_2 and 304 LN stainless steel. These very encouraging results suggest that the use of TiB_2 coatings on first-wall components may help to decrease plasma radiation losses and to improve plasma stability.

PUBLICATIONS FROM 1 APRIL 1980 THROUGH 31 MARCH 1981

The list of "journal articles and book chapters," is classified by topic; the arrangement is approximately that followed in the Table of Contents of this Annual Review. The "reports at meetings" include abstracts, summaries, and full texts in volumes of proceedings; they are listed chronologically.

A. BOOKS

1. DICTIONARY OF TERMS FOR VACUUM SCIENCE AND TECHNOLOGY, SURFACE SCIENCE, THIN FILM TECHNOLOGY, VACUUM METALLURGY
   edited by Manfred S. Kaminsky and James M. Lafferty*
   American Institute of Physics for the American Vacuum Society, 1980

2. THEORY OF THE NUCLEAR SHELL MODEL
   R. D. Lawson
   Oxford University Press, Oxford, England, 1980

B. PUBLISHED JOURNAL ARTICLES AND BOOK CHAPTERS

1. HOW MANY NUCLEONS ARE INVOLVED IN PION ABSORPTION IN NUCLEI?
   R. D. McKeown, S. J. Sanders, J. P. Schiffer, H. E. Jackson, M. Paul, J. R. Specht, E. J. Stephenson, R. P. Redwine,† and R. E. Segel‡
   Phys. Rev. Lett. 44, 1033-1036 (21 April 1980)

2. COMPARISON OF PION- AND PHOTON-INDUCED REACTIONS ON ^{12}C
   R. D. McKeown, J. P. Schiffer, H. E. Jackson, M. Paul, S. J. Sanders, J. R. Specht, E. J. Stephenson, R. P. Redwine,† R. E. Segel,‡ J. Arends,§ J. Eyink,§ H. Hartmann,§ A. Hegerath,§ B. Mecking,§ G. Nöldeke,§ and H. Rost§
   Phys. Rev. Lett. 45, 2015-2017 (22 December 1980)

---

*General Electric R&D Center, Schenectady, New York.

†Massachusetts Institute of Technology, Cambridge, Massachusetts.

‡Northwestern University, Evanston, Illinois.

§University of Bonn, Bonn, West Germany.

3. INCLUSIVE ($\pi^{\pm}$,π^{0}) REACTIONS IN NUCLEI
   T. J. Bowles, D. F. Geesaman, R. J. Holt, H. E. Jackson, J. Julien, R. M. Laszewski, J. R. Specht, E. J. Stephenson, R. P. Redwine,* L. L. Rutledge, Jr.,† R. E. Segel,† and M. A. Yates‡
   Phys. Rev. C 23, 439-447 (January 1981)

4. THE DESIGN AND CALIBRATION OF A HIGH EFFICIENCY DEUTFRON TENSOR POLARIMETER
   E. J. Stephenson, R. J. Holt, J. R. Specht, J. D. Moses,‡ R. L. Burman,‡ G. D. Crocker,‡ J. S. Frank,‡ M. J. Leitch,‡ and R. M. Laszewski§
   Nucl. Instrum. Methods 178, 345-355 (15 December 1980)

5. ^{24}Mg(^{16}O,^{12}C)^{28}Si AND ^{24}Mg(^{16}O,^{16}O)^{24}Mg REACTIONS AT BACKWARD ANGLES
   M. Paul, S. J. Sanders, D. F. Geesaman, W. Henning, D. G. Kovar, C. Olmer, J. P. Schiffer, J. Barrette,‖ and M. J. LeVine‖
   Phys. Rev. C 21, 1802-1809 (May 1980)

6. RESONANT BEHAVIOR OF THE ^{24}Mg(^{16}O,^{12}C)^{28}Si REACTION
   S. J. Sanders, M. Paul, J. Cseh, D. F. Geesaman, W. Henning, D. G. Kovar, R. Kozub, C. Olmer, and J. P. Schiffer
   Phys. Rev. C 21, 1810-1818 (May 1980)

7. RESONANT BEHAVIOR OF THE ^{24}Mg(^{16}O,^{12}C)^{28}Si* ($6.4 \lesssim E_x \lesssim 10$ MeV) REACTION
   S. J. Sanders, C. Olmer, D. F. Geesaman, W. Henning, D. G. Kovar, M. Paul, and J. P. Schiffer
   Phys. Rev. C 22, 1914-1919 (November 1980)

8. COMPLETE FUSION OF ^{15}N + ^{27}Al
   F. W. Prosser, Jr., R. A. Racca,¶ K. Daneshvar, D. F. Geesaman, W. Henning, D. G. Kovar, K. E. Rehm, and S. L. Tabor
   Phys. Rev. C 21, 1819-1823 (May 1980)

9. TARGET DEFORMATION EFFECTS AT LARGE ANGULAR MOMENTA IN HEAVY-ION FUSION REACTIONS
   B. B. Back,** R. R. Betts,** W. Henning, K. L. Wolf,** A. C. Mignerey,†† and J. M. Lebowitz‡‡
   Phys. Rev. Lett. 45, 1230-1232 (13 October 1980)

---

*Massachusetts Institute of Technology, Cambridge, Massachusetts.

†Northwestern University, Evanston, Illinois.

‡Los Alamos National Laboratory, Los Alamos, New Mexico.

§University of Illinois, Urbana, Illinois.

‖Brookhaven National Laboratory, Upton, New York.

¶University of Kansas, Lawrence, Kansas.

**Chemistry Division, ANL.

††University of Maryland, College Park, Maryland.

‡‡Brooklyn College, Brooklyn, New York.

10. THE $\pi h^{3}_{11/2}$ SPECTRUM IN THE THREE VALENCE PROTON NUCLEUS $^{149}_{67}Ho_{82}$
J. Wilson,* S. R. Faber,* P. J. Daly,* I. Ahmad,† J. Borggreen, P. Chowdhury, T. L. Khoo, R. D. Lawson, R. K. Smither, and J. Blomqvist‡
Z. Phys. A 296, 185-186 (1980)

11. HYDROGEN TRAPPING IN MOLYBDENUM IN THE PRESENCE OF RADIATION DAMAGE
A. L. Hanson,§ D. H. Vincent,§ and C. N. Davids
J. Nucl. Mater. 98, 259-269 (1981)

12. SELF-SUPPORTING BORON FILMS
George E. Thomas
Nucl. Instrum. Methods 177, 591-592 (1980)

13. BETA-ALPHA ANGULAR CORRELATIONS IN MASS 8
R. D. McKeown, G. T. Garvey, and C. A. Gagliardi
Phys. Rev. C 22, 738-749 (August 1980)

14. TEST OF THE ISOBARIC MULTIPLET MASS EQUATION FROM β-DELAYED PROTON DECAY OF ^{24}Si
A. G. Ledebuhr,‖ L. H. Harwood,‖ R. G. H. Robertson,‖ and T. J. Bowles
Phys. Rev. C 22, 1723-1728 (October 1980)

15. CROSS SECTIONS FOR THE $^{6}Li(^{3}He,p)$ REACTION AT ENERGIES BELOW 2 MeV
A. J. Elwyn, R. E. Holland, C. N. Davids, J. E. Monahan, F. P. Mooring, and W. Ray, Jr.
Phys. Rev. C 22, 1406-1419 (October 1980)

16. GAMMA-RAY STUDIES IN ^{45}V
S. A. Gronemeyer, L. Meyer-Schützmeister, A. J. Elwyn, and G. Hardie
Phys. Rev. C 21, 1290-1300 (April 1980)

17. β^{+} DECAY OF ^{67}As
Martin J. Murphy, Cary N. Davids, and Eric B. Norman
Phys. Rev. C 22, 2204-2212 (November 1980)

18. ALPHA PARTICLE CAPTURE THROUGH THE GIANT ELECTRIC RESONANCES IN ^{90}Zr
K. Raghunathan,¶ L. L. Rutledge,¶ R. E. Segel, and L. Meyer-Schützmeister
Phys. Rev. C 22, 2409-2415 (December 1980)

---

*Purdue University, West Lafayette, Indiana.

†Chemistry Division, ANL.

‡Research Institute of Physics, Stockholm, Sweden.

§University of Michigan, Ann Arbor, Michigan.

‖Michigan State University, East Lansing, Michigan.

¶Northwestern University, Evanston, Illinois.

19. MEASUREMENT OF THE ^{32}Si HALF-LIFE VIA ACCELERATOR MASS SPECTROMETRY
W. Kutschera, W. Henning, M. Paul, R. K. Smither, E. J. Stephenson, J. L. Yntema, D. E. Alburger,* J. B. Cumming,* and G. Harbottle*
Phys. Rev. Lett, 45, 592-596 (25 August 1980)

20. MEASUREMENT OF THE $^{26}Mg(p,n)^{26}Al^{g}$ (7.2×10^{5} yr) CROSS SECTION VIA ACCELERATOR MASS SPECTROMETRY
M. Paul, W. Henning, W. Kutschera, E. J. Stephenson, and J. L. Yntema
Phys. Lett. 94B, 303-306 (11 August 1980)

21. NEUTRON INTERACTION WITH CARBON-12 IN THE FEW-MeV REGION
A. Smith,† R. Holt, and J. Whalen†
Nucl. Sci. Eng. 70, 281-293 (1979)

22. PHOTONEUTRON STUDIES OF E1, M1 AND E2 EXCITATIONS IN ^{13}C
R. J. Holt, R. M. Laszewski, H. E. Jackson, J. E. Monahan, and J. R. Specht
Phys. Rev. C 21, 1699-1704 (May 1980)
Erratum; Phys. Rev. C 21, 1841 (1981)

23. TECHNIQUES FOR HEAVY-ION COUPLED-CHANNELS CALCULATIONS. I. LONG-RANGE COULOMB COUPLING
M. Rhoades-Brown, M. H. Macfarlane, and Steven C. Pieper
Phys. Rev. C 21, 2417-2426 (June 1980)

24. TECHNIQUES FOR HEAVY-ION COUPLED-CHANNELS CALCULATIONS. II. ITERATIVE SOLUTION OF THE COUPLED RADIAL EQUATIONS
M. Rhoades-Brown, M. H. Macfarlane, and Steven C. Pieper
Phys. Rev. C 21, 2436-2446 (June 1980)

25. EXCITATION OF NON-NORMAL PARITY STATES BY PION SCATTERING: APPLICATION TO ^{13}C
T.-S. H. Lee and D. Kurath
Phys. Rev. C 22, 1670-1679 (October 1980)

26. A CLOSURE-APPROXIMATION CALCULATION OF A PION DOUBLE-CHARGE-EXCHANGE REACTION
Guang-Lie Li,‡ Chu-Hsia Li,‡ and T.-S. H. Lee
Phys. Lett. 99B, 200-204 (19 February 1981)

---

*Brookhaven National Laboratory, Upton, New York.

†Applied Physics Division, ANL.

‡State University of New York, Stony Brook and Academia Sinica, Beijing, People's Republic of China.

27. COMPARISON OF INELASTIC ELECTRON SCATTERING WITH $[g_{9/2} \otimes (f_{7/2}^{-3})_J]_8$- SHELL-MODEL CALCULATIONS FOR THE T=1 AND T=2, 8^- STATES IN ^{54}Fe
R. A. Lindgren,* J. B. Flanz,* R. S. Hicks,* B. Parker,* G. A. Peterson,* R. D. Lawson, W. Teeters, C. F. Williamson,† S. Kowalski,† and X. K. Maruyama‡
Phys. Rev. Lett. 46, 706-709 (16 March 1981)

28. ON THE POSSIBLE EXISTENCE OF STABLE FOUR-QUARK SCALAR MESONS WITH CHARM AND STRANGENESS
Nathan Isgur§ and Harry J. Lipkin
Phys. Lett. 99B, 151-153 (12 February 1981)

29. WHY MASSES AND MAGNETIC MOMENTS SATISFY NAIVE QUARK MODEL PREDICTIONS
Isaac Cohen‖ and Harry J. Lipkin
Phys. Lett. 93B, 56-60 (2 June 1980)

30. ISOSPIN-VIOLATING MIXING IN MESON NONETS
Nathan Isgur,§ H. R. Rubinstein,¶ A. Schwimmer,¶ and H. J. Lipkin
Phys. Lett. 89B, 79-83 (31 December 1979)

31. SHORT-RANGE CORRELATIONS AND BARYON DECAY
G. Karl** and H. J. Lipkin
Phys. Rev. Lett. 45, 1223-1226 (13 October 1980)

32. SU(5) WITHOUT SU(5): CONSERVATION LAWS IN UNIFIED MODELS OF QUARKS AND LEPTONS
Harry J. Lipkin
Nucl. Phys. B171, 301-315 (1 September 1980)

33. THE MICROSCOPIC STRUCTURE AND GROUP THEORY OF THE INTERACTING BOSON MODEL
Harry J. Lipkin
Nucl. Phys. A350, 16-30 (1980)

34. WHY IS B—L CONSERVED AND BARYON NUMBER NOT IN UNIFIED MODELS OF QUARKS AND LEPTONS?
Harry J. Lipkin
Phys. Rev. Lett. 45, 311-313 (4 August 1980)

---

*University of Massachusetts, Amherst, Massachusetts.

†Massachusetts Institute of Technology, Cambridge, Massachusetts.

‡National Bureau of Standards, Washington, D.C.

§University of Toronto, Toronto, Canada.

‖Weizmann Institute of Science, Rehovot, Israel.

¶Max-Planck-Institut, Munich, Germany, and Weizmann Institute of Science, Rehovot, Israel.

**University of Guelph, Guelph, Ontario, Canada.

35. HYPERNETTED-CHAIN EULER-LAGRANGE EQUATIONS AND THE ELECTRON FLUID
John G. Zabolitzky
Phys. Rev. B 22, 2353-2372 (1 September 1980)

36. PHENOMENOLOGICAL HAMILTONIAN FOR PIONS, NUCLEONS AND Δ ISOBARS: APPLICATIONS TO THE PION-DEUTERON SYSTEM
M. Betz and T.-S. H. Lee
Phys. Rev. C 23, 375-398 (January 1981)

37. (π,d) PICK-UP REACTION
M. Betz and A. K. Kerman*
Nucl. Phys. A345, 493-515 (25 August 1980)

38. PHENOMENOLOGICAL RELATIVISTIC QUANTUM MECHANICS OF THE NNπ SYSTEM
M. Betz and F. Coester
Phys. Rev. C 21, 2505-2510 (June 1980)

39. CLASSICAL-EQUATIONS-OF-MOTION CALCULATIONS OF MULTIPLICITIES FOR HIGH-ENERGY COLLISIONS OF $^{20}Ne + {}^{20}Ne$
A. R. Bodmer and C. N. Panos†
Nucl. Phys. A356, 517-522 (23 March 1981)

40. CLASSICAL-EQUATIONS-OF-MOTION CALCULATIONS OF HIGH-ENERGY HEAVY-ION COLLISIONS
A. R. Bodmer, C. N. Panos, and A. D. MacKellar‡
Phys. Rev. C 22, 1025-1054 (September 1980)

41. FRINGING FIELDS AND CRITICISMS OF THE AHARONOV-BOHM EFFECT
Harry J. Lipkin
Phys. Rev. D 23, 1466-1467 (15 March 1981)

42. AHARONOV-BOHM EFFECT IN BOUND STATES: THEORETICAL AND EXPERIMENTAL STATUS
Murray Peshkin
Phys. Rev. A 23, 360-361 (January 1981)

43. IMPROVED EXTRACTION OF NEGATIVE ION BEAMS FROM THE INVERTED SPUTTER SOURCE
Peter J. Billquist and Jan L. Yntema
Nucl. Instrum. Methods 178, 9-10 (1980)

44. HYPERNUCLEAR PHYSICS AND HYPERNUCLEAR INTERACTIONS
A. R. Bodmer
Encyclopedia of Physics, edited by Rita G. Lerner and George L. Trigg (Addison-Wesley, Reading, Massachusetts, 1981), pp. 427-429

---

*Massachusetts Institute of Technology, Cambridge, Massachusetts.

†University of Ioannina, Greece.

‡University of Kentucky, Lexington, Kentucky.

45. NUCLEAR STATES
J. E. Monahan
Encyclopedia of Physics, edited by Rita G. Lerner and George L. Trigg (Addison-Wesley, Reading, Massachusetts, 1981), pp. 696-697

46. NUCLEAR RADIATION
Dennis G. Kovar
McGraw-Hill Encyclopedia of Energy, 2nd edition, edited by S. P. Parker (McGraw-Hill, Inc., New York, 1981), p. 445

47. NUCLEAR REACTION
Dennis G. Kovar
McGraw-Hill Yearbook of Science and Technology. 1981, edited by S. P. Parker (McGraw-Hill, Inc., New York, 1981), pp. 264-269

48. NUCLEAR REACTIONS
John P. Schiffer
Encyclopedia of Physics, edited by Rita G. Lerner and George L. Trigg (Addison-Wesley, Reading, Massachusetts, 1981), pp. 689-691

49. CONVENIENT NUMERICAL TECHNIQUE FOR SOLVING THE ONE-DIMENSIONAL SCHRÖDINGER EQUATION FOR BOUND STATES
P. J. Cooney, E. P. Kanter, and Z. Vager
Am. J. Phys. 49, 76 (January 1981)

50. TRANSMISSION OF FAST H_2^+ THROUGH THIN FOILS
N. Cue,* N. V. de Castro-Faria,* M. J. Gaillard,* J.-C. Poizat,* J. Remillieux,* D. S. Gemmell, and I. Plesser
Phys. Rev. Lett. 45, 613-617 (25 August 1980)

51. DETERMINING THE STEREOCHEMICAL STRUCTURES OF MOLECULAR IONS BY "COULOMB-EXPLOSION" TECHNIQUES WITH FAST (MeV) MOLECULAR ION BEAMS
Donald S. Gemmell
Chem. Rev. 80, 301-311 (1980)

52. EXPERIMENTAL CONFIRMATION OF THE JAHN-TELLER DISTORTION OF CH_4^+
Donald S. Gemmell, Elliot P. Kanter, and Werner J. Pietsch
J. Chem. Phys. 72, 1402-1404 (15 January 1980)
Reprinted: J. Chem. Phys. 72, 6818-6819 (15 June 1980)

53. WAVELENGTHS AND FINE STRUCTURE OF 2s-2p TRANSITIONS IN TWO- AND THREE-ELECTRON IONS
H. G. Berry, R. DeSerio, and A. E. Livingston
Phys. Rev. A 22, 998-1011 (September 1980)

54. RADIATION FROM THE NEGATIVE LITHIUM ION
R. L. Brooks, J. E. Hardis, H. G. Berry, L. J. Curtis, K. T. Cheng, and W. Ray
Phys. Rev. Lett. 45, 1318-1322 (20 October 1980)

*University of Lyon, Lyon, France.

55. MEASUREMENT OF THE n=2 DENSITY OPERATOR FOR HYDROGEN ATOMS PRODUCED BY PASSING PROTONS THROUGH THIN CARBON TARGETS
Gerald Gabrielse
Phys. Rev. A 23, 775-784 (February 1981)

56. SIGNIFICANCE OF TIME-REVERSAL SYMMETRY FOR TIME-RESOLVED MEASUREMENTS OF HYDROGENIC AND OTHER ATOMIC OBSERVABLES
Gerald Gabrielse
Phys. Rev. A 22, 138-148 (July 1980)

57. LINE IDENTIFICATIONS AND LIFETIME MEASUREMENTS IN SINGLY AND DOUBLY EXCITED C IV AND IN C V
C. Jacques,* E. J. Knystautas,* R. Drouin,* and H. G. Berry
Can. J. Phys. 58(8), 1093-1098 (1980)

58. WAVELENGTH MEASUREMENTS OF 1s2s ^{3}S-1s2p ^{3}P TRANSITIONS IN HELIUM-LIKE $^{28}Si^{12+}$, $^{32}S^{14+}$, AND $^{35}Cl^{15+}$
A. E. Livingston,† S. J. Hinterlong,† J. A. Poirier,† R. DeSerio,‡ and H. G. Berry
J. Phys. B 13, L139-L142 (1980)

59. ORIENTATION AND ALIGNMENT OF THE 3p ^{1}P AND 4d ^{1}D LEVELS OF NEUTRAL HELIUM
R. M. Schectman,§ R. D. Hight,§ C. T. Chen,§ L. J. Curtis,§ H. G. Berry, T. J. Gay, and R. DeSerio
Phys. Rev. A 22, 1591-1599 (October 1980)

60. PHOTOELECTRON SPECTROSCOPY OF AgCl, AgBr AND AgI VAPORS
J. Berkowitz, C. H. Batson, and G. L. Goodman
J. Chem. Phys. 72, 5829-5837 (1 June 1980)

61. PHOTOIONIZATION OF LITHIUM CHLORIDE VAPORS: THE STRUCTURE AND STABILITY OF ALKALI HALIDE MOLECULES AND IONS
J. Berkowitz, C. H. Batson, and G. L. Goodman
J. Chim. Phys. 77(7/8), 631-645 (1980)

62. BRANCHING IN ELECTRONIC AUTOIONIZATION OF CS_2 AND N_2O
J. H. D. Eland
Mol. Phys. 40(4), 917-931 (1980)

63. VIBRATIONAL LEVEL POPULATIONS IN THE AUTOIONIZATION OF OXYGEN
J. H. D. Eland
J. Chem. Phys. 72, 6015-6019 (1 June 1980)

64. MASS SPECTRA AND DOUBLY CHARGED IONS IN PHOTOIONIZATION AT 30.4 nm AND 58.4 nm
Bilin P. Tsai and John H. D. Eland
Int. J. Mass Spectry. Ion Phys. 36, 143-165 (November 1980)

---

*Université Laval, Quebec, Canada.

†University of Notre Dame, Notre Dame, Indiana.

‡University of Chicago, Chicago, Illinois.

§University of Toledo, Toledo, Ohio.

65. HIGH-PRECISION LASER-rf DOUBLE-RESONANCE SPECTROSCOPY OF THE $^2\Sigma$ GROUND STATE OF CaF
W. J. Childs and L. S. Goodman
Phys. Rev. A 21, 1216-1221 (April 1980)

66. PRECISE DETERMINATION OF THE v AND N DEPENDENCE OF THE SPIN-ROTATION AND HYPERFINE INTERACTIONS IN THE CaF $X^2\Sigma_{1/2}$ GROUND STATE
W. J. Childs, G. L. Goodman, and L. S. Goodman
J. Mol. Spectrosc. 86, 365-392 (1981)

67. RADIO-FREQUENCY OPTICAL DOUBLE-RESONANCE SPECTRUM OF SrF: THE $X^2\Sigma^+$ STATE
W. J. Childs, L. S. Goodman, and I. Renhorn
J. Mol. Spectrosc. 87, 522-533 (1981)

68. MÖSSBAUER EFFECT
G. J. Perlow
Encyclopedia of Physics, edited by Rita G. Lerner and George L. Trigg (Addison-Wesley, Reading, Massachusetts, 1981), pp. 607-613

69. A RESONANCE RAMAN/IODINE MÖSSBAUER INVESTIGATION OF THE STARCH-IODINE STRUCTURE. AQUEOUS SOLUTION AND IODINE VAPOR PREPARATIONS
Robert C. Teitelbaum, Stanley L. Ruby, and Tobin J. Marks*
J. Am. Chem. Soc. 102, 3322-3328 (May 1980)

70. THEORETICAL PHOTOIONIZATION PARAMETERS FOR THE NOBLE GASES ARGON, KRYPTON, AND XENON
K.-N. Huang,† W. R. Johnson,† and K. T. Cheng
At. Data Nucl. Data Tables 26, 33-45 (January 1981)

71. CLAD MATERIALS FOR FUSION APPLICATIONS
M. Kaminsky
Thin Solid Films 73, 117-132 (1980)

72. SPUTTERING OF TiB_2 COATINGS UNDER D^+ AND $^4He^+$ ION BOMBARDMENT
M. Kaminsky, S. K. Lam, and K. Moy
Thin Solid Films 73, 91-97 (1980)

73. SPUTTERING OF ANNEALED ALUMINUM AND OF SINTERED ALUMINUM POWDER (SAP 895) UNDER D^+ AND $^4He^+$ BOMBARDMENT: STUDY OF MICROSTRUCTURAL EFFECTS
S. K. Lam and M. Kaminsky
J. Nucl. Mater. 89, 205-220 (1980)

---

*Northwestern University, Evanston, Illinois.

†University of Notre Dame, Notre Dame, Indiana.

C. PUBLISHED REPORTS AT MEETINGS

Proceedings of the 1977 International School of Subnuclear Physics, Erice, Italy, 23 July-10 August 1977

1. WHY IS THERE CHARM, STRANGENESS, COLOUR AND ALL THAT?
   Harry J. Lipkin
   The Whys of Subnuclear Physics, edited by Antonino Zichichi (Plenum, New York/London, 1979), pp. 11-136 + discussion on pp. 137-158

Proceedings of the VII International Conference on Atomic Collisions in Solids, Moscow, USSR, 19-23 September 1977, edited by A. F. Tulinov (Moscow State University Publishing House, 1981)

2. EFFECTS SEEN IN THE INTERACTIONS OF FAST MOLECULAR-ION BEAMS WITH MATTER
   D. S. Gemmell, P. J. Cooney, W. J. Pietsch, A. J. Ratkowski, Z. Vager, B. J. Zabransky, A. Faibis,* G. Goldring,* I. Levine,* and Z. Vager*
   Vol. I, pp. 74-89

3. THE CHANNELING OF POSITIVE AND NEGATIVE PIONS IN A SILICON CRYSTAL
   D. S. Gemmell, R. E. Holland, W. Pietsch, A. J. Ratkowski, J. P. Schiffer, T. P. Wangler, J. N. Worthington, B. Zeidman, C. L. Morris,† and H. A. Thiessen†
   Vol. I, pp. 128-130

4. RADIATION BLISTERING OF Nb IMPLANTED WITH HELIUM IONS OF ENERGIES EXPECTED IN THE FUSION REACTOR
   V. M. Gusev,‡ M. I. Guseva,‡ U. L. Krasulin,‡ U. V. Martinenko,‡ S. K. Das, and M. S. Kaminsky
   Vol. II, pp. 291-294

5. SURFACE EFFECTS IN FUSION DEVICE OPERATION
   M. Kaminsky
   Vol. II, pp. 294-305

Nato Advanced Study Institute/1978 Banff Summer Institute on Nuclear Theory, Banff, Canada, 21 August-1 September 1978

6. A QUASI-NUCLEAR COLOURED QUARK MODEL FOR HADRONS
   H. J. Lipkin
   Common Problems in Low- and Medium-Energy Nuclear Physics, edited by B. Castel, B. Goulard, and F. C. Khanna (Plenum, New York/London, 1979), pp. 173-212

---

*Weizmann Institute of Science, Rehovot, Israel.

†Los Alamos National Laboratory, Los Alamos, New Mexico.

‡Kurchatov Institute of Atomic Energy, Moscow, USSR.

Mathematical Methods and Applications of Scattering Theory (Proceedings of a Conference, Washington, D.C., 21-25 May 1979), edited by J. A. DeSanto, A. W. Sáenz, and W. W. Zachary (Springer-Verlag, Berlin-Heidelberg-New York, 1980)

7. CANONICAL SCATTERING THEORY FOR RELATIVISITC PARTICLES
   F. Coester
   pp. 190-196

The Meson Theory of Nuclear Forces and Nuclear Matter (Proceedings of the Conference, Bad Honnef, Germany, 12-14 June 1979), edited by D. Schütte, K. Holinde, and K. Bleuler (Bibliographisches Institut, Zurich, 1980)

8. NUCLEON-NUCLEON "POTENTIALS" AND TWO-BODY HAMILTONIANS
   F. Coester
   pp. 155-171

9. BRUECKNER-BETHE CALCULATIONS OF NUCLEAR MATTER
   B. D. Day
   pp. 1-36

Nuclear Structure and Heavy-Ion Collisions (Proceedings of the International School of Physics "Enrico Fermi," Varenna, Italy, 9-21 July 1979), Course LXXVII, edited by R. A. Broglia and R. A. Ricci (North-Holland, Amsterdam, 1981)

10. NUCLEAR STRUCTURE AND HEAVY-ION REACTIONS
    J. P. Schiffer
    pp. 205-232

Advances in Mass Spectrometry (Proceedings of the 8th International Mass Spectrometry Conference, Oslo, Norway, 12-18 August 1979), edited by A. Quayle (The Institute of Petroleum, London, 1980)

11. PHOTOELECTRON-PHOTOION COINCIDENCE SPECTROSCOPY
    John H. D. Eland
    Vol. 8A, pp. 17-31

Proceedings of the Tenth International Radiocarbon Conference, Bern/Heidelberg, 19-26 August 1979

12. RADIOISOTOPE DETECTION WITH THE ARGONNE FN TANDEM ACCELERATOR
    Walter Kutschera, Walter Henning, Michael Paul, E. J. Stephenson, and J. L. Yntema
    Radiocarbon 22(3), 807-815 (1980)

1979 Cryogenic Engineering Conference, Madison, Wisconsin, 21-24 August 1979

13. FORCED-CIRCULATION COOLING SYSTEM FOR THE ARGONNE SUPERCONDUCTING HEAVY-ION LINAC
    J. M. Nixon* and L. M. Bollinger
    Advances in Cryogenic Engr. 25, 317-325 (1980)

---

*Chemistry Division, ANL.

Argonne National Laboratory Specialists' Workshop on Basic Research Needs for Nuclear Waste Management, Argonne, Illinois, 5-6 September 1979

14. POSSIBLE APPLICATIONS OF THE MÖSSBAUER TECHNIQUE IN WASTE MANAGEMENT STUDIES
S. L. Ruby
Nuclear Technology 51(2), 178-181 (December 1980)

Proceedings of the Harwell Consultants Symposium on Inert (Rare) Gases in Metals and Ionic Solids, Vol. II, AERE, Harwell, England, 10-14 September 1979, edited by S. F. Pugh, Harwell Report AERE-R9733 (AERE Harwell, Oxfordshire, England, 1980)

15. THE ROLE OF INERT GASES IN FIRST WALL PHENOMENA IN FUSION DEVICES
S. K. Das
pp. 409-421

Sixth International Conference on Atomic Masses, East Lansing, Michigan, 18-21 September 1979

16. MASSES OF NEW ISOTOPES IN THE fp SHELL
C. N. Davids
Atomic Masses and Fundamental Constants 6 (Proceedings of the Conference), edited by J. A. Nolen, Jr., and W. Benenson (Plenum, New York, 1980), pp. 419-430
+ Program of the Conference, Abstracts, Session VI

17. NUCLEAR MASS RELATIONS AND EQUATIONS
J. E. Monahan and F. J. D. Serduke
Atomic Masses and Fundamental Constants 6, pp. 151-159
+ Program of the Conference, Abstracts, Session II

World Conference of the International Nuclear Target Development Society, Boston, Massachusetts, 1-3 October 1979

18. HEAVY ION STRIPPING BY WRINKLED CARBON FOILS
P. K. Den Hartog, J. L. Yntema, G. E. Thomas, and W. Henning
Preparation of Nuclear Targets for Particle Accelerators (Proceedings of the Conference), edited by Jozef Jaklovsky (Plenum, New York, 1981), pp. 29-36
+ Program of the Conference, Abstract D-3

19. LIFETIMES OF CARBON FOILS DEPOSITED ON ETCHED SUBSTRATES
John O. Stoner, Jr.,* Stanley Bashkin,* G. Thomas, J. L. Yntema, and P. Den Hartog
Preparation of Nuclear Targets for Particle Accelerators, pp. 61-63
+ Program of the Conference, Abstract D-5

20. METHODS TO REDUCE CONTAMINATION IN TARGETS PREPARED BY VACUUM DEPOSITION
G. E. Thomas, S. K. Lam, and R. W. Nielsen
Preparation of Nuclear Targets for Particle Accelerators, pp. 277-286
+ Program of the Conference, Abstract C-5

*University of Arizona, Tucson, Arizona.

International Conference on Nuclear Cross Sections for Technology, Knoxville, Tennessee, 22-26 October 1979

21. PHOTONEUTRON LEAKAGE FROM THE W(γ,n) REACTION AT RADIATION THERAPY CENTERS
R. J. Holt, H. E. Jackson, and J. R. Specht
Nuclear Cross Sections for Technology (Proceedings of the Conference), edited by J. L. Fowler, C. H. Johnson, and C. D. Bowman (U.S. Government Printing Office, Washington, D.C., 1980), pp. 427-428
+ Bull. Am. Phys. Soc. 24, 874 (September 1979)

Workshop on Nuclear Structure with Intermediate-Energy Probes, Los Alamos Scientific Laboratory, Los Alamos, New Mexico, 14-16 January 1980, organized by H. Baer et al., Los Alamos Scientific Laboratory Report LA-8303-C (April 1980)

22. MICROSCOPIC ANALYSIS OF PION-NUCLEUS INELASTIC SCATTERING
T.-S. H. Lee
pp. 2-12

Band Structure and Nuclear Dynamics (Proceedings of the International Conference, New Orleans, Louisiana, 28 February-1 March 1980), edited by A. L. Goodman, G. S. Goldhaber, A. Klein, and R. A. Sorensen (North-Holland, Amsterdam, 1980)

23. SOME QUESTIONS ON THE CORIOLIS FORCE, THE STRUCTURE OF ROTATIONAL STATES AND THE IBM
T. L. Khoo
Nucl. Phys. A347, 407-408 (September 1980)

International Conference on Nuclear Behaviour at High Angular Momentum, Strasbourg, France, 22-24 April 1980

24. CONTINUUM γ-RAY SPECTRA AND EXCITATION FUNCTIONS OF YRAST STATES IN ^{152}Dy
I. Ahmad,* J. Borggreen, P. Chowdhury, T. L. Khoo, R. K. Smither, S. R. Faber,† C. L. Dors,† J. Wilson,† and P. J. Daly†
Contributions, organized by F. A. Beck et al. (Centre de Recherches Nucléaires de Strasbourg, 1980), p. 73

25. YRAST SPECTROSCOPY: STATUS OF YRAST ISOMERS, OBLATE SHAPES AND FEEDING OF YRAST STATES
T. L. Khoo
Suppl. J. Phys. (Paris) 41, C10-9—17 (December 1980)

---

*Chemistry Division, ANL.

†Purdue University, West Lafayette, Indiana.

American Physical Society, Washington, D.C., 28 April-1 May 1980

26. EXCITATION FUNCTIONS FOR FISSION INDUCED BY HEAVY ION FUSION REACTIONS
B. B. Back,* R. R. Betts,* W. Henning, K. L. Wolf,* A. C. Mignerey,† and J. M. Lebowitz‡
Bull. Am. Phys. Soc. 25, 482-483 (April 1980)

27. ELASTIC SCATTERING OF $^{32}S + ^{24}Mg$ AT $\theta_{c.m.} = 90°$
R. R. Betts,* B. B. Back,* W. F. Henning, and K. L. Wolf*
Bull. Am. Phys. Soc. 25, 590 (April 1980)

28. STUDY OF CONTINUUM γ-RAY SPECTRA OF ^{152}Dy
J. Borggreen, I. Ahmad,* P. Chowdhury, T. L. Khoo, W. Kutschera, R. K. Smither, P. Daly,§ C. Dors,§ S. R. Faber,§ and J. Wilson§
Bull. Am. Phys. Soc. 25, 605 (April 1980)

29. UNUSUAL EXCITATION FUNCTIONS OF YRAST STATES IN ^{152}Dy
S. R. Faber,§ P. J. Daly,§ C. L. Dors,§ J. Wilson,§ I. Ahmad,* J. Borggreen, P. Chowdhury, T. L. Khoo, W. Kutschera, and R. K. Smither
Bull. Am. Phys. Soc. 25, 604 (April 1980)

30. FISSION MASS AND KINETIC ENERGY DISTRIBUTIONS OF Pt ISOTOPES FORMED BY HEAVY ION FUSION REACTIONS
B. Glagola,* B. B. Back,* R. R. Betts,* K. L. Wolf,* W. Henning, A. C. Mignerey,† and J. M. Lebowitz‡
Bull. Am. Phys. Soc. 25, 482 (April 1980)

31. DISTRIBUTION OF REACTION STRENGTHS IN $^{32}S + ^{40,48}Ca$
W. Henning, B. Back,* D. F. Geesaman, C. M. Jachcinski, D. G. Kovar, C. Olmer, M. Paul, S. J. Sanders, and J. P. Schiffer
Bull. Am. Phys. Soc. 25, 524 (April 1980)

32. MEASUREMENT OF THE $^{26}Mg(p,n)^{26g}Al$ (7.2×10^5 year) CROSS SECTION VIA ACCELERATOR MASS SPECTROMETRY
W. Henning, W. Kutschera, M. Paul, E. J. Stephenson, and J. L. Yntema
Bull. Am. Phys. Soc. 25, 539 (April 1980)

33. FUSION OF $^{24}Mg + ^{24}Mg$
C. M. Jachcinski, D. G. Kovar, D. F. Geesaman, C. Olmer, M. Paul, S. J. Sanders, and J. L. Yntema
Bull. Am. Phys. Soc. 25, 592 (April 1980)

---

*Chemistry Division, ANL.

†University of Maryland, College Park, Maryland.

‡Brooklyn College, Brooklyn, New York.

§Purdue University, West Lafayette, Indiana.

APS, Washington, D.C., April 1980 (cont'd.)

34. FUSION OF $^{16}O + ^{24,26}Mg$ AT HIGHER ENERGIES
D. G. Kovar, C. Jachcinski, C. N. Davids, W. Henning, and S. J. Sanders
Bull. Am. Phys. Soc. 25, 524 (April 1980)

35. ACCELERATOR MASS SPECTROMETRY OF ^{32}Si WITH THE ARGONNE FN TANDEM
W. Kutschera, W. Henning, M. Paul, R. K. Smither, E. J. Stephenson, J. L. Yntema, D. E. Alburger,* J. B. Cumming,* and G. Harbottle*
Bull. Am. Phys. Soc. 25, 539 (April 1980)

36. HOW MANY NUCLEONS ARE INVOLVED IN PION ABSORPTION IN NUCLEI?
R. D. McKeown, S. J. Sanders, J. P. Schiffer, H. E. Jackson, M. Paul, J. R. Specht, E. J. Stephenson, R. P. Redwine,† and R. E. Segel‡
Bull. Am. Phys. Soc. 25, 505 (April 1980)

37. SINGLE NUCLEON TRANSFER INDUCED BY 45 MeV ^{12}C ON A ^{48}Ca TARGET
J. F. Petersen,§ R. J. Ascuitto,§ D. G. Kovar, S. J. Sanders, W. Henning, and M. Paul
Bull. Am. Phys. Soc. 25, 523 (April 1980)

38. SEARCH FOR PARITY NON-CONSERVATION IN ^{6}Li
R. G. H. Robertson,‖ A. B. McDonald,‖ G. C. Ball,‖ W. G. Davies,‖ E. D. Earle,‖ P. L. Dyer,¶ R. C. Melin,¶ and T. J. Bowles
Bull. Am. Phys. Soc. 25, 577 (April 1980)

39. RESONANT BEHAVIOR OF THE $^{24}Mg(^{16}O,^{12}C)^{28}Si$ REACTION
S. J. Sanders
Bull. Am. Phys. Soc. 25, 552 (April 1980)

40. INCLUSIVE PION SCATTERING
S. J. Sanders, R. D. McKeown, J. P. Schiffer, H. E. Jackson, M. Paul, J. R. Specht, E. J. Stephenson, R. P. Redwine,† and R. E. Segel‡
Bull. Am. Phys. Soc. 25, 560 (April 1980)

---

*Brookhaven National Laboratory, Upton, New York.

†Massachusetts Institute of Technology, Cambridge, Massachusetts.

‡Northwestern University, Evanston, Illinois.

§Yale University, New Haven, Connecticut.

‖AECL, Chalk River Nuclear Laboratories, Chalk River, Ontario, Canada.

¶Michigan State University, East Lansing, Michigan.

28th Annual Conference on Mass Spectrometry and Allied Topics, New York, New York, 25-30 May 1980

41. THE STRUCTURE AND STABILITY OF ALKALI HALIDE MOLECULES AND IONS
J. Berkowitz, G. L. Goodman, and C. H. Batson
Proceedings of the Conference, edited by Wade L. Fite (American Society for Mass Spectrometry, 1980), pp. 420-421
+ Program of the Conference, p. 147

42. STEREOCHEMICAL STRUCTURES OF MOLECULAR IONS DETERMINED THROUGH "COULOMB EXPLOSION" TECHNIQUES WITH FAST (MeV) MOLECULAR-ION BEAMS
Donald S. Gemmell
Proceedings of the Conference, pp. 270-273

VI International Conference on Vacuum Ultraviolet Radiation Physics, Charlottesville, Virginia, 2-6 June 1980, R. C. Elton, Conference Secretary (U.S. Naval Research Laboratory, Washington, D.C., 1980)

43. PHOTOIONIZATION OF ATOMIC IODINE AND ATOMIC TELLURIUM
J. Berkowitz, C. H. Batson, and G. L. Goodman
Extended Abstracts, Vol. II, abstract II-9

Proceedings of the Second Workshop on Interacting Boson Models, Erice, Italy, 12-18 June 1980

44. A TEST OF THE INTERACTING BOSON MODEL USING PION-NUCLEUS INELASTIC SCATTERING
T.-S. H. Lee
Interacting Bose-Fermi Systems in Nuclei, edited by F. Iachello (Plenum, New York, 1981), pp. 143-147

Resonant Behavior of Heavy-Ion Systems (Proceedings of the International Conference, Aegean Sea, Greece, 23-26 June 1980), edited by G. Vourvopoulos (National Printing Office, Athens, 1981)

45. STRUCTURES IN FUSION AND ALPHA-TRANSFER CROSS SECTIONS
W. Henning
pp. 232-260

From Nuclei to Particles (Proceedings of the International School of Physics "Enrico Fermi," Varenna, Italy, 23 June-5 July 1980), Course LXXIX, edited by A. Molinari (North-Holland, Amsterdam, 1981)

46. BRUECKNER-BETHE CALCULATIONS OF NUCLEAR MATTER
B. D. Day
pp. 1-71

Proceedings of the Workshop on Plasma Materials, Albuquerque, New Mexico, 24-25 June 1980 (Sandia National Laboratories, Albuquerque, New Mexico, 1980)

47. RESEARCH AND DEVELOPMENT ON COATINGS IN APEX AT ARGONNE NATIONAL LABORATORY
D. M. Gruen,* M. Kaminsky, J. Norem,† M. J. Pellin,* and C. E. Young*
pp. 18.1-18.9

48. CLADDED MATERIALS FOR LIMITERS AND ARMOR PLATES
M. Kaminsky
pp. 13.1-13.9

49. SUMMARY OF WORKSHOP ON SPUTTERING CAUSED BY PLASMA (NEUTRAL BEAM) SURFACE INTERACTION, HELD AT ANL, 9-10 JULY 1979
M. Kaminsky
pp. 1.1-1.11

11th International Conference on High-Energy Accelerators (Proceedings of the Conference, Geneva, Switzerland, 7-11 July 1980), edited by W. S. Newman (Birkhäuser Verlag, Basel, 1980)

50. DESIGN STUDY FOR A 2-GeV DOUBLE-SIDED MICROTRON
Y. Cho,† R. J. Holt, H. E. Jackson, T. K. Khoe,† and G. S. Mavrogenes*
pp. 115-119

Baryon 1980 (Proceedings of the IVth International Conference on Baryon Resonances, Toronto, Canada, 14-16 July 1980), edited by Nathan Isgur (University of Toronto, 1981)

51. WHO NEEDS BARYON SPECTROSCOPY?
Harry J. Lipkin
pp. 461-468

DUMAND-80 (Proceedings of the 1980 International DUMAND Symposium, Honolulu, Hawaii, 24 July-2 August 1980), edited by V. J. Stenger (Hawaii DUMAND Center, University of Hawaii, Honolulu, 1981)

52. SOLAR NEUTRINO CALCULATIONS: AN UPDATE
B. W. Filippone
Vol. II, pp. 115-125

7th International Conference on Atomic Physics, Cambridge, Massachusetts, 4-8 August 1980, organized by B. Bederson et al.

53. ANGULAR DISTRIBUTION AND SPIN POLARIZATION OF PHOTOELECTRONS FROM NOBLE GASES
K.-N. Huang,‡ W. R. Johnson,‡ and K. T. Cheng
Abstracts, pp. 182-183

---

*Chemistry Division, ANL.

†Accelerator Research Facilities Division, ANL.

‡University of Notre Dame, Notre Dame, Indiana.

Conference on Atomic Physics, Cambridge, August 1980 (cont'd.)

54. ANALYSIS OF BEUTLER-FANO AUTOIONIZING RESONANCES IN THE RARE GAS ATOMS USING THE RELATIVISTIC MULTICHANNEL QUANTUM DEFECT THEORY
W. R. Johnson,* K. T. Cheng, K.-N. Huang,* and M. Le Dourneuf†
Abstracts, pp. 68-69

55. PRESENT STATUS OF TESTS OF QED AND RELATIVITY IN 2s-2p TRANSITIONS OF TWO- AND THREE-ELECTRON IONS
A. E. Livingston,* S. J. Hinterlong,* J. A. Poirier,* R. DeSerio, R. L. Brooks, and H. G. Berry
Abstracts, pp. 19-20

Polarization Phenomena in Nuclear Physics - 1980 (Fifth International Symposium, Santa Fe, New Mexico, 11-15 August 1980), edited by G. G. Ohlsen et al. (American Institute of Physics, New York, 1981), AIP Conference Proceedings No. 69

56. A POLARIZED ^{6}Li TARGET TO STUDY PARITY VIOLATION
C. A. Gagliardi, A. R. Davis, G. T. Garvey, R. D. McKeown, B. Myslek-Laurikainen, R. G. H. Robertson, S. J. Freedman,‡ and T. J. Bowles§
Part 2, pp. 939-940

57. MEASUREMENT OF TENSOR POLARIZATION IN PION-DEUTERON ELASTIC SCATTERING
R. J. Holt
Part 2, pp. 1180-1194

Nuclear Structure (Proceedings of the Netherlands Physical Society 1980 International Summer School on Nuclear Structure, Dronten, The Netherlands, 12-23 August 1980), edited by K. Abrahams, K. Allaart, and A. E. L. Dieperink (Plenum, New York, 1981)

58. NUCLEAR STRUCTURE AND HEAVY-ION REACTIONS
John P. Schiffer
pp. 127-163

Proceedings of the International Conference on Nuclear Physics, Berkeley, California, 24-30 August 1980, Vol. 1, Abstracts (Lawrence Berkeley Laboratory, Berkeley, California, 1980), LBL-11118

59. CONTINUUM γ-RAY SPECTRA AND EXCITATION FUNCTIONS OF YRAST STATES IN ^{152}Dy
I. Ahmad,‖ J. Borggreen, P. Chowdhury, T. L. Khoo, R. K. Smither, S. R. Faber,¶ C. L. Dors,¶ J. Wilson,¶ and P. J. Daly¶
p. 354

---

*University of Notre Dame, Notre Dame. Indiana.

†Observatorie de Paris, Meudon, France.

‡Stanford University, Stanford, California.

§Los Alamos National Laboratory, Los Alamos, New Mexico.

‖Chemistry Division, ANL.

¶Purdue University, West Lafayette, Indiana.

Conference on Nuclear Physics, Berkeley, August 1980 (cont'd.)

60. THE SCATTERING OF 162-MeV PIONS BY ^{14}N
D. F. Geesaman, C. Olmer, B. Zeidman, G. C. Morrison,* R. E. Segel,† G. S. Blanpied,‡ G. R. Burleson,‡ L. W. Swenson,§ R. Anderson,‖ R. L. Boudrie,‖ and H. A. Thiessen‖
p. 692

61. THE MEASUREMENT OF NUCLEAR QUANTITIES VIA ACCELERATOR MASS SPECTROMETRY
W. Kutschera, W. Henning, M. Paul, R. K. Smither, E. J. Stephenson, J. L. Yntema, D. E. Alburger,¶ J. B. Cumming,¶ and G. Harbottle¶
p. 745

62. HOW MANY NUCLEONS ARE INVOLVED IN PION ABSORPTION IN NUCLEI?
R. D. McKeown, S. J. Sanders, J. P. Schiffer, H. E. Jackson, M. Paul, J. R. Specht, E. J. Stephenson, R. P. Redwine,** and R. E. Segel†
p. 702

63. CORRELATIONS BETWEEN MOMENTS OF INERTIA AND CLOSED-SHELL MASSES OF GROUND STATE BANDS IN EVEN-Z, EVEN-N NUCLEI
Robert K. Smither
p. 307

64. BAGS, DELTAS AND NUCLEAR MATTER
A. W. Thomas,†† S. Théberge,†† and B. Day
p. 47

The Physics of Ionized Gases [Invited Lectures and Progress Reports of X Summer School and Symposium on the Physics of Ionized Gases (SPIG '80), Dubrovnik, Yugoslavia, 25-30 August 1980], edited by M. Matić (Boris Kidrič Institute of Nuclear Sciences, Beograd, Yugoslavia, 1980)

65. COATINGS AND CLADDINGS FOR THE REDUCTION OF PLASMA CONTAMINATION AND SURFACE EROSION IN FUSION REACTORS
M. Kaminsky
pp. 501-526

---

*University of Birmingham, Birmingham, England.

†Northwestern University, Evanston, Illinois.

‡New Mexico State University, Las Cruces, New Mexico.

§Oregon State University, Corvallis, Oregon.

‖Los Alamos National Laboratory, Los Alamos, New Mexico.

¶Brookhaven National Laboratory, Upton, New York.

**Massachusetts Institute of Technology, Cambridge, Massachusetts.

††TRIUMF, Vancouver, B.C., Canada.

High-Energy Physics with Polarized Beams and Polarized Targets (Proceedings of the 1980 International Symposium, Lausanne, Switzerland, 25 September-1 October 1980), edited by C. Joseph and J. Soffer (Birkhäuser-Verlag, Basel, 1981)

66. PAST LESSONS AND FUTURE IMPORTANCE OF POLARIZATION
Harry J. Lipkin
pp. 408-427

Proceedings of the 1980 Applied Superconductivity Conference, Santa Fe, New Mexico, 29 September-2 October 1980

67. A SIX TESLA ANALYZING MAGNET FOR HEAVY-ION BEAM TRANSPORT
R. P. Smith,* L. Bollinger, J. Erskine, L. Genens,* and J. Hoffman*
IEEE Trans. Magn. MAG-17, 179-181 (January 1981)

Division of Nuclear Physics, American Physical Society, Minneapolis, Minnesota, 9-11 October 1980

68. INVESTIGATION OF HIGH SPIN YRAST STATES IN ^{150}Dy
I. Ahmad,† W. Kutschera, J. Borggreen, T. L. Khoo, R. K. Smither, P. Chowdhury, C. N. Davids, S. Levenson, and S. R. Faber‡
Bull. Am. Phys. Soc. 25, 735 (September 1980)

69. TIME-OF-FLIGHT ENERGY MEASUREMENT OF A PULSED BEAM USING A RESONANT DETECTOR
L. M. Bollinger, R. N. Lewis,§ and R. C. Pardo
Bull. Am. Phys. Soc. 25, 745 (September 1980)

70. BRUECKNER-BETHE CALCULATIONS OF NUCLEAR MATTER
B. D. Day
Bull. Am. Phys. Soc. 25, 726 (September 1980)

71. FRAGMENTATION OF ^{18}O AT E = 72 AND 141 MeV
L. C. Dennis,‖ S. L. Tabor,‖ K. W. Kemper,‖ J. D. Fox,‖ K. Abdo,‖ G. Neuschaefer,‖ D. G. Kovar, H. Ernst, and C. M. Jachcinski
Bull. Am. Phys. Soc. 25, 744 (September 1980)

72. RESONANCE BEHAVIOR OF THE ^{24}Mg(^{16}O,^{12}C)^{28}Si(g.s.) REACTION
W. Henning, S. J. Sanders, H. Ernst, C. Jachcinski, D. G. Kovar, and J. P. Schiffer
Bull. Am. Phys. Soc. 25, 727 (September 1980)

---

*Accelerator Research Facilities Division, ANL.

†Chemistry Division, ANL.

‡Purdue University, West Lafayette, Indiana.

§Electronics Division, ANL.

‖Florida State University, Tallahassee, Florida.

APS, Minneapolis, October 1980 (cont'd.)

73. PARITY MIXING MATRIX ELEMENT IN ^{10}B
D. Kurath and W. Teeters
Bull. Am. Phys. Soc. 25, 722 (September 1980)

74. PION INELASTIC SCATTERING FROM ^{4}He, ^{12}C, ^{58}Ni AND ^{208}Pb
S. M. Levenson, E. P. Colton,* D. F. Geesaman, R. J. Holt, H. E. Jackson, J. P. Schiffer, J. R. Specht, K. E. Stephenson, B. Zeidman, R. E. Segel,† P. A. M. Gram,‡ and C. A. Goulding§
Bull. Am. Phys. Soc. 25, 725 (September 1980)

75. YIELDS OF SPECIFIC RESIDUE NUCLEI FROM THE FUSION OF $^{16,18}O$ + $^{24,26}Mg$
R. A. Racca,‖ F. W. Prosser, Jr.,‖ K. Daneshvar, C. N. Davids, and D. G. Kovar
Bull. Am. Phys. Soc. 25, 733 (September 1980)

76. SPECTROSCOPY OF THE THREE VALENCE PROTON NUCLEUS ^{149}Ho
J. Wilson,¶ S. R. Faber,¶ P. J. Daly,¶ I. Ahmad,** J. Borggreen, P. Chowdhury, T. L. Khoo, R. D. Lawson, R. K. Smither, and J. Blomqvist††
Bull. Am. Phys. Soc. 25, 734-735 (September 1980)

SNEAP 80 (Proceedings of the Symposium of Northeastern Accelerator Personnel, Madison, Wisconsin, 13-15 October 1980), edited by James H. Billen (University of Wisconsin, Madison, 1981)

77. THE PERFORMANCE OF THE CARBON STRIPPING FOILS IN THE ARGONNE FN TANDEM
P. K. Den Hartog, F. Munson, C. Heath, and G. Thomas
pp. 208-218

78. OPERATING EXPERIENCE WITH THE ARGONNE SUPERCONDUCTING BOOSTER
J. L. Yntema
pp. 254-257

79. ARGONNE NATIONAL LABORATORY - 1979-80 TANDEM ACCELERATOR REPORT
J. L. Yntema, P. K. Den Hartog, P. Billquist, and F. Munson
pp. 11-12

---

*Accelerator Research Facilities Division, ANL.

†Northwestern University, Evanston, Illinois.

‡Los Alamos National Laboratory, Los Alamos, New Mexico.

§Florida A & M University, Tallahassee, Florida.

‖University of Kansas, Lawrence, Kansas.

¶Purdue University, West Lafayette, Indiana.

**Chemistry Division, ANL.

††AFI Stockholm, Sweden.

1980 Annual Meeting of the Optical Society of America, Chicago, Illinois, 14-17 October 1980

80. PRECISE DETERMINATION OF THE v AND N DEPENDENCE OF THE SPIN-ROTATION AND HYPERFINE INTERACTIONS IN THE CaF $X^2\Sigma^+_{1/2}$ GROUND STATE
W. J. Childs and L. S. Goodman
J. Opt. Soc. Am. 70, 1587 (December 1980)
+ Optics News 6(3), 38 (1980)
+ Program of the Conference, p. P29

Fourteenth LAMPF Users Group Meeting, Los Alamos, New Mexico, 27-28 October 1980

81. PION SCATTERING RESEARCH AT LAMPF
Benjamin Zeidman
LAMPF Users Group Newsletter 13(1), 91-104
(Los Alamos, New Mexico, February 1981)

Division of Electron and Atomic Physics, American Physical Society, Los Angeles, California, 1-3 December 1980

82. RADIATION FROM THE NEGATIVE LITHIUM ION
R. L. Brooks, J. E. Hardis, H. G. Berry, and L. J. Curtis
Bull. Am. Phys. Soc. 25, 1128 (November 1980)

83. APPLICATIONS OF RELATIVISTIC MULTICONFIGURATION QUANTUM DEFECT THEORY TO XENON-LIKE IONS
K. T. Cheng and W. R. Johnson*
Bull. Am. Phys. Soc. 25, 1133 (November 1980)

84. MOLECULAR EFFECTS IN BEAM-FOIL COLLISION INDUCED ALIGNMENT OF HeI
T. J. Gay, H. G. Berry, and R. DeSerio
Bull. Am. Phys. Soc. 25, 1129 (November 1980)

85. ENERGY DEPENDENCE OF ALIGNMENT IN FOIL COLLISION EXCITED n=3 STATES OF HeI
T. J. Gay, H. G. Berry, R. DeSerio, H. P. Garnir, R. M. Schectman,† N. Schaffel,† R. D. Hight,‡ and D. Burns‡
Bull. Am. Phys. Soc. 25, 1129 (November 1980)

86. MULTICONFIGURATION RELATIVISTIC RANDOM PHASE APPROXIMATION APPLIED TO Be-LIKE IONS
W. R. Johnson,§ K.-N. Huang,§ and K. T. Cheng
Bull. Am. Phys. Soc. 25, 1133 (November 1980)

---

*Radiological and Environmental Research Division, ANL.

†University of Toledo, Toledo, Ohio.

‡University of Nebraska, Lincoln, Nebraska.

§Notre Dame University, Notre Dame, Indiana.

Proceedings of the Workshop on Foundations of the Relativistic Theory of Atomic Structure, Argonne, Illinois, 4-5 December 1980, organized by H. G. Berry, K. T. Cheng, W. R. Johnson, and Y.-K. Kim, Argonne National Laboratory Topical Report ANL-80-126 (March 1981)

87. ATOMIC STRUCTURE CALCULATIONS USING THE RELATIVISTIC RANDOM PHASE APPROXIMATION
K. T. Cheng and W. R. Johnson*
pp. 115-132

88. RECENT RESULTS IN $\Delta n = 0$, $n = 2$ TRANSITIONS OF HELIUM-LIKE SYSTEMS
R. DeSerio, H. G. Berry, and R. L. Brooks
pp. 240-259

Molecular Ions, Molecular Structure and Interaction with Matter (Proceedings of the 38th Bat-Sheva Seminar, Rehovot and Haifa, Israel, 3-12 January 1981), edited by Baruch Rosner (Adam Hilger, Bristol, England and The Israel Physical Society, Ramat-Gan, Israel, 1981)

89. OPTICAL OBSERVATIONS OF MOLECULAR DISSOCIATION IN THIN FOILS
H. G. Berry, T. J. Gay, and R. L. Brooks
pp. 217-220

90. UV-LASER PHOTOFRAGMENTATION OF A 2-MeV H_2^+ BEAM
N. Cue, A. K. Edwards, D. S. Gemmell, E. P. Kanter, and R. Kutina
pp. 194-197

91. USING AN ELECTROSTATIC ACCELERATOR TO DETERMINE THE STEREOCHEMICAL STRUCTURES OF MOLECULAR IONS
Donald S. Gemmell
pp. 25-49

92. MEASUREMENTS ON THE EXTENDED RANGE OF THE WAKE
G. J. Kumbartzki,† G. Krösing,† H. Neuburger,† W. Pietsch,‡ and D. S. Gemmell
pp. 163-167

Recent Progress in Many-Body Theories (Proceedings of the Second International Conference, Oaxtepec, Mexico, 12-17 January 1981), edited by J. G. Zabolitzky et al. (Springer-Verlag, Berlin-Heidelberg, 1981)

93. NUCLEAR FORCES AND NUCLEAR MATTER INCLUDING PIONS AND ISOBARS
F. Coester
pp. 35-41

94. BRUECKNER-BETHE CALCULATIONS OF NUCLEAR MATTER
B. D. Day
pp. 169-176

---

*University of Notre Dame, Notre Dame, Indiana.

†University of Bonn, Bonn, Germany.

‡University of Cologne, Cologne, Germany.

Recent Progress in Many-Body Theories, Oaxtepec, January 1981 (cont'd.)

95. COUPLED CLUSTER DESCRIPTION OF RELATIVISTIC MANY BODY SYSTEMS
H. Kümmel
pp. 177-185

Gauge Theories, Massive Neutrinos, and Proton Decay (Proceedings of Orbis Scientiae 1981, Coral Gables, Florida, 19-22 January 1981), edited by A. Perlmutter (Plenum, New York, 1981)

96. MAGNETIC MOMENTS OF COMPOSITE FERMIONS
Harry J. Lipkin
p. 359

D. PHYSICS DIVISION REPORTS

1. PROCEEDINGS OF THE WORKSHOP ON FOUNDATIONS OF THE RELATIVISTIC THEORY OF ATOMIC STRUCTURE, Argonne National Laboratory, Argonne, Illinois, 4-5 December 1980
organized by H. G. Berry, K. T. Cheng, W. R. Johnson,* and Y.-K. Kim*
Argonne National Laboratory Topical Report ANL-80-126 (March 1981)

2. STUDY OF A NATIONAL 2 GeV CONTINUOUS BEAM ELECTRON ACCELERATOR
Y. Cho,† R.J. Holt, H. E. Jackson, T. K. Khoe,† and G. S. Mavrogenes‡
Physics Division Informal Report ANL-PHY-79-2 (Revision 1) (August 1980)

---

*Radiological and Environmental Research Division, ANL.

†Accelerator Research Facilities Division, ANL.

‡Chemistry Division, ANL.

STAFF MEMBERS OF THE PHYSICS DIVISION

Listed below are the permanent staff of the Physics Division for the year ending 31 March 1981. The program heading indicates only the individual's current primary activity.

EXPERIMENTAL NUCLEAR PHYSICS

Scientific Staff

[*] Lowell M. Bollinger, Ph.D., Cornell University, 1951

Cary N. Davids, Ph.D., California Institute of Technology, 1967

[**] Alexander J. Elwyn, Ph.D., Washington University, 1956

[†] John R. Erskine, Ph.D., University of Notre Dame, 1960

[††] Gerald T. Garvey, Ph.D., Yale University, 1962

Donald F. Geesaman, Ph.D., State University of New York, Stony Brook, 1976

Walter Henning, Ph.D., Technical University, Munich, 1968

Robert E. Holland, Ph.D., University of Iowa, 1950

Roy J. Holt, Ph.D., Yale University, 1972

Harold E. Jackson, Jr., Ph.D., Cornell University, 1959

Teng Lek Khoo, Ph.D., McMaster University, 1972

[‡] Dennis G. Kovar, Ph.D., Yale University, 1971

Victor E. Krohn, Ph.D., Case Western Reserve University, 1952

[‡‡] Walter Kutschera, Ph.D., University of Graz, Austria, 1965

[§] Alexander Langsdorf, Jr., Ph.D., Massachusetts Institute of Technology, 1937

[§] John J. Livingood, Ph.D., Princeton University, 1929

---

[*] In charge of Superconducting Linac Project.

[**] In charge of Dynamitron accelerator operations.

[†] No longer at Argonne as of August 1980. Present address: U.S.D.O.E., Washington, D.C.

[††] Joint appointment with the University of Chicago; Associate Laboratory Director for Physical Research through November 30, 1980.

[‡] Temporarily assigned to Hahn-Meitner-Institüt für Kernforschung, Berlin, Germany (September 1980—August 1981).

[‡‡] Visiting Scientist through June 1980.

[§] Retired-consultant.

*Robert D. McKeown, Ph.D., Princeton University, 1979

**Luise Meyer-Schützmeister, Ph.D., Technical University of Berlin, 1943

Richard C. Pardo, Ph.D., University of Texas, 1976

G. Roy Ringo, Ph.D., University of Chicago, 1940

†John P. Schiffer, Ph.D., Yale University, 1954

Kenneth W. Shepard, Ph.D., Stanford University, 1970

††Robert K. Smither, Ph.D., Yale University, 1956

‡J. L. Yntema, Ph.D., Free University of Amsterdam, 1952

Benjamin Zeidman, Ph.D., Washington University, 1957

Technical and Engineering Staff

Ralph Benaroya

John J. Bicek

Peter J. Billquist

Patric K. Den Hartog

William F. Evans

Walter A. Huston

Joseph E. Kulaga

Bruce G. Nardi

James R. Specht

James L. Stadelmann

George E. Thomas, Jr.

James N. Worthington

Jerome R. Wrobel

Gary P. Zinkann

---

*No longer at Argonne as of December 1980. Present address: California Institute of Technology, Pasadena, California.

**Temporarily assigned to Max Planck Institute, Heidelberg, Germany (October 1979—September 1980). Deceased January 1981.

†Director of the Physics Division. Joint appointment with the University of Chicago.

††Joint appointment as Associate Editor of Applied Physics Letters. Transferred to Chemical Engineering Division, February 1981.

‡In charge of Tandem accelerator operations.

THEORETICAL PHYSICS

Scientific Staff

*Arnold R. Bodmer, Ph.D., Manchester University, 1953
Kwok-tsang Cheng, Ph.D., University of Notre Dame, 1977
Fritz Coester, Ph.D., University of Zurich, 1944
Benjamin Day, Ph.D., Cornell University, 1963
Dieter Kurath, Ph.D., University of Chicago, 1951
Robert D. Lawson, Ph.D., Stanford University, 1953
Tsung-Shung Harry Lee, Ph.D., University of Pittsburgh, 1973
**Malcolm H. Macfarlane, Ph.D., University of Rochester, 1959
James E. Monahan, Ph.D., St. Louis University, 1953
†Murray Peshkin, Ph.D., Cornell University, 1951
Steven C. Pieper, Ph.D., University of Illinois, 1970

ATOMIC AND MOLECULAR PHYSICS

Scientific Staff

Joseph Berkowitz, Ph.D., Harvard University, 1955
H. Gordon Berry, Ph.D., University of Wisconsin, 1967
Kwok-tsang Cheng, Ph.D., University of Notre Dame, 1977
William J. Childs, Ph.D., University of Michigan, 1956
††Donald S. Gemmell, Ph.D., Australian National University, 1960
Leonard S. Goodman, Ph.D., University of Chicago, 1952
Manfred S. Kaminsky, Ph.D., University of Marburg, 1957
Elliot P. Kanter, Ph.D., Rutgers University, 1977
‡Gilbert J. Perlow, Ph.D., University of Chicago, 1940
‡‡Stanley L. Ruby, B.A., Columbia University, 1947

---

*Joint appointment with the University of Illinois, Chicago Circle Campus.

**Joint appointment with the University of Chicago. No longer at Argonne as of August 1980. Present address: Indiana University, Bloomington, Indiana.

†Deputy Director of the Physics Division.

††Associate Director of the Physics Division.

‡Joint appointment as Editor of the Applied Physics Letters.

‡‡Transferred to Environmental Impact Studies Division, December 1980.

Technical and Engineering Staff

Charles H. Batson
*John A. Dalman
Robert W. Nielsen
Walter J. Ray
Bruce J. Zabransky

ADMINISTRATIVE STAFF

**Albert J. Hatch, M.S., University of Illinois, 1947
**F. Paul Mooring, Ph.D., University of Wisconsin, 1951

From 1 April 1980 through 31 March 1981 there were 46 temporary staff members and visitors (including 14 postdoctoral appointees), 14 graduate students, and 9 undergraduates. These temporary appointments in the Physics Division are listed below.

TEMPORARY APPOINTMENTS

Postdoctoral Appointees

Robert L. Brooks (from University of Alberta, Alberta, Canada): Fast ion spectroscopy. (August 1979—)

Partha Chowdhury (from State University of New York, Stony Brook, New York): Studies of high-spin states of nuclei. (November 1979—)

David R. Cok (from Harvard University, Cambridge, Massachusetts): RF laser spectroscopy. (September 1980—)

Hartmut J. H. Ernst (Technical University of Munich, Munich, Germany): Heavy-ion reaction studies. (Feodor-Lynen Fellowship of the Alexander v. Humboldt Foundation.) (January 1980—)

*No longer at Argonne as of December 1980.
**Assistant Director of the Physics Division.

William S. Freeman (from State University of New York, Stony Brook, New York): Experimental heavy-ion and charged-particle nuclear physics. (December 1980—)

Thomas J. Humanic (from University of Pittsburgh, Pittsburgh, Pennsylvania): Heavy-ion nuclear physics. (August 1980—)

Christopher M. Jachcinski (from State University of New York, Stony Brook, New York): Heavy-ion reactions: particularly, $^{16}O + ^{24,26}Mg$ and $^{24}Mg + ^{24}Mg$ fusion. (October 1979—August 1980)

Raymond E. Kutina (from University of Toronto, Toronto, Canada): Photo-ionization of free radicals. (March 1980—)

John A. Parmentola (from Massachusetts Institute of Technology, Cambridge, Massachusetts): Quark bag models; multiple scattering theory. (August 1980—)

Appajosula S. Rao (from University of Liverpool, Liverpool, England): Surface erosion studies related to plasma wall interactions. (April 1980—)

Mark J. Rhoades-Brown (from University of Surrey, England): Heavy-ion direct reaction studies with particular emphasis on developing mathematical techniques to enable large scale coupled-channel calculations to be carried out. (October 1977—August 1980)

Stephen J. Sanders (from Yale University, New Haven, Connecticut): Experimental medium-energy and heavy-ion physics research. (September 1977—July 1980)

Kenneth E. Stephenson (from University of Wisconsin, Madison, Wisconsin): Pion-nucleus reaction experiments. (September 1979—)

Robert B. Wiringa (from Los Alamos National Laboratory, Los Alamos, New Mexico): Many-body theory for nuclear matter and its implications for the nucleon-nucleon interaction, especially as influenced by isobar degrees of freedom. (January 1981—)

Long-Term Visitors (at Argonne more than 4 months)

Ademola Amusa (University of Ife, Ile-Ife, Nigeria, Africa): Shell-model calculations in some nuclei (e.g., ^{20}O). (May 1980—)

Daniel Ashery (Tel Aviv University, Ramat Aviv, Israel): Pion-nucleus reactions. (August 1980—)

Jørn Borggreen (Niels Bohr Institute, Copenhagen, Denmark): Gamma-ray studies at the ANL superconducting linac. (August 1979—May 1980)

*Thomas W. Dombeck (University of Maryland, College Park, Maryland): Search for the neutron electric dipole moment. (October 1980—)

Steven R. Faber (Purdue University, West Lafayette, Indiana): High-spin physics by gamma-ray spectroscopy. (September 1979—)

Stuart J. Freedman (Standord University, Stanford, California): Weak interactions research. (Alfred P. Sloan Fellow.) (January 1981—)

Zbigniew W. Grabowski (Purdue University, West Lafayette, Indiana): Heavy-ion nuclear physics. (September 1980—)

Mitsuji Kawai (Kyushu University, Fukuoka, Japan): Coupled channel theory of nuclear reactions. (October 1980—)

**Harry J. Lipkin (Weizmann Institute of Science, Rehovot, Israel): Theoretical nuclear and particle physics. (June 1979—)

Bogumila Myslek-Laurikainen (Institute of Nuclear Research, Swierk, Poland): Parity violation in the 5.1-MeV J=2 doublet of ^{10}B. (December 1978—December 1980)

Itzhak Plesser (Weizmann Institute of Science, Rehovot, Israel): Interaction of fast molecular ions with solid target: (1) molecular structure gained through this interaction; (2) various aspects of the interaction itself—wake, multiple scattering, transmission, etc. (August 1979—August 1980)

R. G. Hamish Robertson (Michigan State University, East Lansing, Michigan): Experimental studies of parity violation in ^{10}B and ^{6}Li. (Alfred P. Sloan Fellow) (January 1980—July 1980)

Malcolm F. Steuer (University of Georgia, Athens, Georgia): Studies of stopping powers of molecular ions in amorphous solids and the channeling of molecular ions in thin gold crystals. (August 1980—)

Resident Graduate Students

Lambros Arnellos (University of Illinois, Chicago Circle Campus, Chicago, Illinois): Theoretical work in relativistic heavy-ion collisions and in quark models of baryon-baryon interactions. (June 1979—December 1980)

Alexandra R. Davis (University of Chicago, Chicago, Illinois): Heavy-ion research. (January 1979—)

Robert DeSerio (University of Chicago, Chicago, Illinois): Measurement of $\Delta n=0$, $n=2$ transitions in medium-Z ions. (July 1980—January 1981) Ph.D., University of Chicago, 1981

---

*Joint appointment with Los Alamos National Laboratory, Los Alamos, New Mexico.

**Joint appointment with the Fermi National Accelerator Laboratory, Batavia, Illinois.

Rollin Evans (Iowa State University, Ames, Iowa): On-line laser spectroscopy of radioactive atoms using the superconducting linac. (March 1981—)

Bradley W. Filippone (University of Chicago, Chicago, Illinois): Experimental nuclear astrophysics. (June 1979—)

Carl A. Gagliardi (Princeton University, Princeton, New Jersey): Weak interactions in nuclear physics. (July 1977—)

Timothy J. Gay (University of Chicago, Chicago, Illinois): Polarization effects in the beam-foil interaction. (April 1978—July 1980) Ph.D., University of Chicago, 1981

Jonathan E. Hardis (University of Chicago, Chicago, Illinois): Ion-ion and ion-atom collisions. (October 1979—)

Samuel M. Levenson (University of Chicago, Chicago, Illinois): Nuclear physics research. (January 1979—)

Short-Term Visitors (at Argonne less than 4 months)

A. Faculty

Larry E. Campbell (Hobart & William Smith Colleges, Geneva, New York): Experimental program to develop a photovoltaic cell. (June 1980—August 1980)

John W. Clark (Washington University, St. Louis, Missouri): Studies in nuclear matter theory. (June 1980—August 1980)

Patrick J. Cooney (Middlebury College, Middlebury, Vermont): Interaction of fast (MeV) molecular ions with matter. (June 1980—July 1980)

Nelson Cue (State University of New York, Albany, New York): Transmission and breakup of fast molecules in thin foils; breakup of fast molecules in a gas and in a laser field. (June 1980—August 1980)

Larry J. Curtis (University of Toledo, Toledo, Ohio): In-beam atomic spectroscopy of light ions. (June 1980—July 1980)

Alan K. Edwards (University of Georgia, Athens, Georgia): Laser excitation of fast molecular beams and dissociation of molecular beams by foils. (June 1980—September 1980)

Anthony D. Frawley (Florida State University, Tallahassee, Florida): Resonator development for the heavy-ion linac project, specifically, to develop a technique for measuring the transverse (or steering) field. (November 1980—December 1980)

Morton Hamermesh (University of Minnesota, Minneapolis, Minnesota): Group theory in quantum mechanics. (July 1980—August 1980)

Hermann G. Kümmel (Ruhr Universität, Bochum, Germany): Application of coupled cluster methods in quantum field theory. (August 1980—November 1980)

David A. Lewis (Iowa State University, Ames, Iowa): On-line laser spectroscopy of radioactive atoms using the superconducting linac.

A. Eugene Livingston (University of Notre Dame, Notre Dame, Indiana): Beam-foil spectroscopy of neutral and ionized atoms.

Jeffrey W. Lynn (University of Maryland, College Park, Maryland): Electric dipole moment of the neutron.

Michael Paul (Hebrew University of Jerusalem, Israel): Heavy-ion nuclear reactions. (June 1980—September 1980)

Ingemar G. Renhorn (Institute of Physics, University of Stockholm, Sweden): Laser spectroscopy. (May 1980)

Ralph E. Segel (Northwestern University, Evanston, Illinois): Nuclear physics research. (June 1980—September 1980)

Arvind K. Srivastava (University of Missouri, Rolla, Missouri): Surface damage of fusion reactor materials. (August 1980—September 1980)

William D. Teeters (Chicago State University, Chicago, Illinois): Nuclear shell theory.

Zeev Vager (Weizmann Institute of Science, Rehovot, Israel): Dissociation of molecules in foil targets. (April 1980—May 1980)

James L. Whitton (University of Copenhagen, Copenhagen, Denmark): Study of light-ion bombardment induced damage in Inconel 625. (July 1980—September 1980)

B. Graduate Students

Jordan B. Camp (University of Chicago, Chicago, Illinois) (March 1981—)

Tsewei Chen (Northwestern University, Evanston, Illinois): Inclusive charged-particle spectrum from the interaction of nuclei with intermediate energy proton.

Keith A. Inglis (State University of New York, Albany, New York): Breakup of molecules in foils. (June 1980—August 1980)

Michael J. Politano (Loyola University, Chicago, Illinois): Fast tuner system for linac resonators. (June 1980—July 1980)

James A. Rothstein (University of Chicago, Chicago, Illinois): Study of fast molecular ions and interaction with thin foils; ion and laser interactions. (May 1980—October 1980)

C. Undergraduate Students

Domenico Delli Carpini (Fordham College, Bronx, New York). (January 1980—May 1980)

Richard W. Chamberlin, Jr. (Illinois Institute of Technology, Chicago, Illinois).

Thomas E. Harrington III (Louisiana State University, Baton Rouge, Louisiana). (June 1980—August 1980)

Daniel T. Holslin (Concordia College, Moorhead, Minnesota). (June 1980—August 1980)

Edward A. Johnson (Washington & Lee University, Lexington, Virginia). (January 1981—)

William O. Perkins (North Carolina State University, Raleigh, North Carolina).

Vincent F. Streif (Beloit College, Beloit, Wisconsin). (September 1980—December 1980)

Linas Vepstas (University of Chicago, Chicago, Illinois).

Paul R. Zschack (Illinois Institute of Technology, Chicago, Illinois).